Journal of Polymer Science

Part A-1: Polymer Chemistry

Contents

(continued inside)

Journal of Polymer Science: Part A-1: Polymer Chemistry

Contents (continued), Vol. 8

Poly[tris(diorganophosphinato)alanes]

EDWARD E. FLAGG and DONALD L. SCHMIDT, *The Dow Chemical Company, Midland, Michigan 48640*

Synopsis

Poly[tris(diorganophosphinato)alanes], $[Al(OPRR'O)_3]_n$, were synthesized in which the organic moieties (R,R') contained from one to eighteen carbon atoms. Polymeric properties depended upon the organic moieties; polymers were fusible, tractable, and flexible when the organic moieties contained six or more carbon atoms. Soluble polymers were prepared by using mixtures of symmetrical and unsymmetrical phosphinates. One polymer, poly{bis[n-butyl(benzyl)phosphinato]di-n-octylphosphinatoalane}, exhibited a degree of polymerization greater than 1000 and an exceptionally high intrinsic viscosity of 37 dl/g. The properties of the different polymers are discussed, and feasible structures are proposed.

INTRODUCTION

Metal phosphinates, $M(OPRR'O)_n$,[1–5] have been the subject of recent investigations for several reasons: (1) the phosphinato ligand is an excellent bridging moiety; (2) the metal–oxygen bonds are strong and the metal phosphinates are often resistant to oxidation and hydrolysis; (3) the skeletal structures of the polymers are completely inorganic; (4) a large range of polymeric properties results from the dependence upon metal, M, and phosphorus substituents, R; (5) the multi-coordinate metals present a variable number of bridging sites and often the chemistry is uniquely different from other polymer chemistry.

Bis(phosphinate) chemistry has been emphasized because triple-bridged structures were predicted for tris(phosphinates) and it was reasonable to assume that the resultant polymers would be insoluble, infusible, and intractable. The literature[6,7] supports this hypothesis, and only recently have tractable tris(phosphinates) of aluminum[1] and chromium[7] been prepared. Poly(phosphinato)alanes have been studied extensively in our laboratory.* Earlier reports concerned monophosphinates[8] and bis(phosphinates);[9] this report describes the preparation and characterization of poly[tris-(phosphinato)alanes]. Although there are earlier reports of poly[tris-(phosphinato)alanes],[6,10] the restricted choice of diorganophosphinato ligands prevented a thorough characterization of the polymers.

---

* The substituted alane (AlH₃) nomenclature is used for these tris(phosphinates) of aluminum(III); e.g., $\{[C_4H_9(C_6H_5CH_2)PO_2]Al[(O_2P(C_8H_{17}))_2]\}_n$ is poly{bis[n-butyl(benzyl)phosphinato]di-n-octylphosphinatoalane}.

1

Poly[tris(diorganophosphinato)alanes] were prepared by reacting etherated alane, $AlH_3 \cdot 0.3[O(C_2H_5)_2]$, or triethylalane, $(C_2H_5)_3Al$, with three equivalents of phosphinic acid.   The Brönsted acid–base

$$3nR_2P(O)OH + nR_3'Al \xrightarrow[-70°C]{THF} \{Al[OPR_2O]_3\}_n + 3nR'H \qquad (1)$$

reaction [eq. (1)] was exothermic and aluminum-oxygen-phosphorus valence bonds formed at low temperatures.   Polymerization resulted from coordinate bonds between phosphoryl moieties ($-P=O$) and additional bonding sites on aluminum.

EXPERIMENTAL

All reactions were carried out in an inert atmosphere dry box or under a stream of dry nitrogen.   Tetrahydrofuran (THF) was distilled from sodium-biphenyl complex and stored with the strict exclusion of oxygen and water. Triethylalane was purchased from Texas Alkyls, Inc. and distilled in a dry box before use.   Etherated alane was prepared by a reported procedure.[11] With the exception of di-n-(3,3,3-trifluoropropyl)phosphinic acid, $(CF_3CH_2CH_2)_2P(O)OH$, the phosphinic acids were prepared and purified by previously described procedures.[8]   R. E. Ridenour, of our laboratory, prepared $(CF_3CH_2CH_2)_2P(O)OH$ by oxidizing the dialkylhydrogenphosphine oxide intermediate from the Grignard reaction of $CF_3CH_2CH_2MgBr$ and di-n-butylhydrogenphosphonate.[8]

ANAL.   Calcd for $C_6H_9F_6O_2P$:   C, 27.92%; H, 3.51%; P, 12.00%; eq. wt., 258. Found: C, 27.95%; H, 3.50%; P, 12.10%; eq. wt. 267; crystalline white solid, mp 69.5–70.0°C.

An American Optical, Spencer polarized microscope was equipped with a Polaroid camera and Kofler hot stage.   Infrared spectra, x-ray powder diffraction patterns, gel-permeation chromatographs, differential thermal analysis (DTA), and molecular weight and intrinsic viscosity determinations were performed by published procedures.[1,8]   Thermogravimetric analyses (TGA) were carried out in air or nitrogen at 10°C/min.[8]   Elemental analyses, performed in our Analytical Laboratory, are reported in Table I.

Only three examples of the experimental procedures will be given because of the basic similarity of the syntheses.

Preparation of $\{Al[O_2P(C_6H_{13})_2]_3\}_n$, Poly{tris(di-$n$-hexylphosphinato)alane}

Di-n-hexylphosphinic acid (2.5467 g, 0.01087 mole) was dissolved in THF (250 ml) and added to a stirred solution of etherated alane (0.003623 mole) in THF (500 ml) at Dry Ice temperature.   Evolution of hydrogen indicated a fast reaction near $-70°C$.   The heterogeneous solution was allowed to warm slowly to ambient temperature ($\sim25°C$), then heated under re-

TABLE I

Properties and Analyses of Poly{tris(diorganophosphinato)alanes},
$\{[OR'R''PO]_m Al(OPR_2O)_{3-m}\}_n$

Polymer	m	R	R'	R''	C, % found (calcd.)	H, %	Al, %	P, %	Mp, °C	Solubility, MW, DP in THF[b]	Other properties[c]
I	0	CH_3	—	—	23.50 (23.55)	5.60 (5.92)	8.65 (8.81)	30.20 (30.36)	Inf.	Insol.	Hard, brittle
II	0	$CF_3(CH_2)_2$	—	—	27.60 (27.08)	3.06 (3.03)	3.19 (3.38)	11.40 (11.64)	355 (dec)	Insol.	Hard, friable, very crystalline
III	0	C_6H_{11}	—	—	55.80 (56.06)	10.28 (10.35)	— (4.20)	— (14.46)	390–415	Insol.	Hard, brittle
IV	0	C_6H_{13}	—	—	59.30 (59.48)	10.73 (10.82)	3.68 (3.71)	12.60 (12.78)	380–410	~Insol. (sl. sol.)	Film-forming, semiflexible
V	1.5	C_5H_{11}	C_7H_{15}	—	59.18 (59.48)	10.85 (10.82)	— (3.71)	— (12.78)	335(400)	Sl. sol.	Film-forming, semiflexible
VI	1.5	C_6H_{13}	C_8H_{17}	—	62.05 (62.22)	10.80 (11.19)	3.12 (3.33)	11.85 (11.47)	300–310	Sl. sol.	Film-forming, semiflexible
VII	0	C_8H_{17}	—	—	64.30 (64.40)	11.50 (11.49)	3.00 (3.01)	10.10 (10.38)	385–410	Sl. sol.	Film-forming, soft, flexible
VIII	2	C_7H_{15}	C_4H_9	$C_6H_5CH_2$	60.90 (60.83)	8.77 (8.79)	3.67 (3.80)	— (13.08)	285–300	2–5×10^5, $270 < n \leq 670$	Film-forming, semiflexible, $10 < [\eta] \leq 30$
IX	2	C_8H_{17}	C_4H_9	$C_6H_5CH_2$	61.15 (61.77)	9.04 (9.01)	3.03 (3.65)	— (12.58)	300–320	1.8×10^4–7.8×10^5, $23 < n \leq 1650$	Film-forming, semiflexible, $15 \leq [\eta] \leq 37$
X	1.5	C_8H_{17}	$C_{18}H_{37}$	$C_{18}H_{37}$	70.70 (71.19)	12.50 (12.41)	2.04 (2.05)	6.97 (7.06)	330–370	1.64×10^4–3.8×10^4, $12.5 < n \leq 29$	Film-forming, soft, flexible, $8.2 < [\eta] \leq 31$
XI	2	C_8H_{17}	$C_{18}H_{37}$	$C_{18}H_{37}$	71.50 (72.58)	12.50 (12.60)	1.84 (1.85)	6.00 (6.38)	~335–350	1.58×10^4, $n \approx 11$	Film-forming, soft, flexible, $\eta_{inh} = 4.12$

[a] P substituent = substituent groups on phosphinato moieties.

[b] Solubility and molecular weight in THF; DP or n, degree of polymerization.

[c] $[\eta]$, intrinsic viscosity in THF at 25°C; inherent viscosity, η_{inh} at 0.100 g/100 ml, 25°C.

fluxing solvent for 16 hr. The product was collected on a filter, washed several times with THF, and dried under vacuum for 12 hr.

Preparation of $\{[(C_6H_{13})_2PO_2]_{1\cdot5}Al[O_2P(C_8H_{17})_2]_{1\cdot5}\}_n$, Poly$\{$ses-qui[di-*n*-hexylphosphinato]sesqui[di-*n*-octylphosphinato]alane$\}$

An approximate equimolar excess (5%) of di-*n*-hexylphosphinic acid (12.150 g, 0.0518 mole) and di-*n*-octylphosphinic acid (14.883 g, 0.0512 mole) was dissolved in THF (500 ml). A stirred solution of etherated alane (0.0326 mole) in THF ($\sim$3000 ml) was cooled to $-70°$C and the acids were slowly added. After the acid addition, the heterogeneous solution was allowed to warm to ambient temperature, then heated under refluxing solvent for 24 hr. A resilient, colorless film was collected on a filter, washed several times with THF, then dried under vacuum for 24 hr. The dried product formed a clear, flexible film upon molding at 50°C and 5000 psi pressure.

Preparation of $\{[C_4H_9(C_6H_5CH_2)PO_2]_2Al[O_2P(C_8H_{17})_2]\}_n$, Poly$\{$bis-[*n*-butyl(benzyl)phosphinato]di-*n*-octylphosphinatoalane$\}$

Etherated alane (0.00503 mole) was dissolved in THF (1200 ml) and cooled to $-70°$C. A stoichiometric 1:2 ratio of di-*n*-octyl-phosphinic acid (1.4523$_4$ g, $\sim$0.0050 mole) and *n*-butyl(benzyl)-phosphinic acid (2.1242$_5$ g, 0.0100 mole) was added to the stirred alane solution. A clear, viscous solution was observed after warming to ambient temperature and stirring overnight (16 hr). Samples were taken for analysis, and the remaining solution was heated under reflux for 4 hr. After sampling again, the polymer was isolated by evaporating the solvent under reduced pressure. During the desolvation process, the product began to form a clear, coherent film upon the reaction vessel wall. This solid could be redissolved before the desolvation was complete by adding solvent and heating gently. The nonsolvated film was essentially insoluble in THF and resistant to swelling by common solvents. Chemical and physical analyses indicated the film was the desired polymer; there was no evidence for solvolysis, i.e., no solvated products or polytetrahydrofuran. Polymer slowly precipitated from the sampled solutions (2.16 mg/ml) upon standing at ambient temperature for 8 months.

RESULTS AND DISCUSSION

The very fast reaction of alanes and phosphinic acids provides a very convenient method for preparing poly[tris(diorganophosphinato)alanes]. In this reaction, the alanes serve dual roles as Brönsted bases, i.e., proton acceptors, and typical Lewis acids or electron acceptors. Tetrahydrofuran is an excellent solvent because it is an aprotic Lewis base. The additions of acids to alanes are carried out near $-70°$C to minimize side reactions such as the reduction of phosphoryl ($\diagdown$P$=$O) moieties by temporary ex-

cesses of alanes.* Purity of reagents can not be overemphasized espe-
cially when etherated alane is used; any traces of acids or oxidizing agents
result in significant loss of active hydride. (This is normally observed as
an insoluble, white oxo-bridged alane, Al-O-Al .) The success of the re-
actions depends upon pure active alanes; although exact stoichiometry is
desirable in most cases, excess phosphinic acid can be used when the final
product is insoluble in THF.

The polymeric properties of poly{tris(diorganophosphinato)alanes}
depend upon the organic substituents; brittle, friable polymers are ob-
tained from the phenyl moiety[6] and n-alkyl moieties with less than six
carbon atoms. In general, the melting points decrease and the solubilities
increase with the alkyl chain length. Poly{tris(di-n-hexylphosphinato)-
alane} and higher homologs (polymers IV–XI) form coherent films.
Pressed films of polymers IV–XI are somewhat resilient; preliminary test-
ing of mechanical properties gave a maximum per cent elongation of 68%
for polymer VI.[12]

Mixtures of diorganophosphinato ligands give polymers which are lower
melting, more flexible, and more soluble than the corresponding homo-
polymers. This is clearly illustrated by the properties of poly{sesqui[di-
n-pentylphosphinato]sesqui[di-n-heptylphosphinato]alane} (V) and poly-
{tris(di-n-pentylphosphinato)-alane} (III). When the mixture contained
unsymmetrical n-butyl(benzyl)phosphinate (VIII and IX), the solubility
increased without a corresponding increase in flexibility. Although the
reference to solubility implied THF, the general trend was the same for
other solvents. The following relative solubilities were normally observed:
THF > 50% THF–toluene > toluene ≥ 50% THF–heptane > heptane >
50% THF–methylene chloride > methylene chloride. It was also observed
that polymers VIII and IX became virtually insoluble in THF after the
polymers were desolvated. The contrary was true for polymers X and XI,
thus emphasizing the importance of organic moieties in determining solu-
tion properties.

The general dependency upon organic moieties reflects several factors:
(1) the relative ability of the organic moieties to interact with solvents,
thus allowing structural modifications in solution; (2) the effect of bulky
groups on the extent of interchain linking; and (3) the reduction in intra-
molecular order, with subsequent reduction in overall crystallinity. The
morphology of the polymers has not been studied in detail, but some
correlations were observed between minor phase changes and melting points
by DTA and polarized microscopy. The general features of the DTA
graphs were weak endotherms at 40–100°C and 180–220°C, moderate
exotherms at 225–250°C, and strong endotherms at the melting points.
Phase changes were observed optically as local decreases or increases in
polymer crystallinity. Some birefringence was observed above the incipi-

* Inverse addition can be used but the solubility of the acids in THF decreases rapidly
as the temperature is lowered.
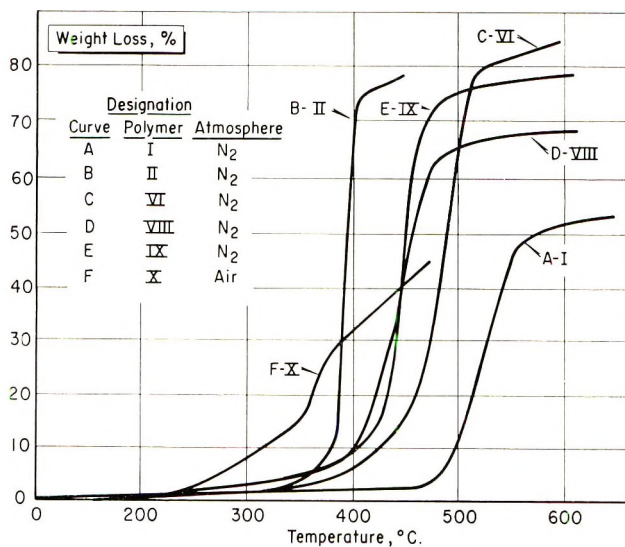
Fig. 1. TGA curves for some poly[tris(diorganophosphinato)alanes].

ent melting point in certain cases; additional observations above the melting point were usually obscured by some discoloration in air. Rapid quenching with liquid nitrogen reduced but did not completely eliminate crystallinity; the samples were often more crystalline after fusion.

All of the polymers were partially crystalline on the basis of polarized microscopy and x-ray diffraction powder patterns. The diffraction bands decreased in number and sharpness as the size of the organic moieties increased. More bands were observed for homopolymers (I–IV, VII) than polymers with mixtures of phosphinato ligands. For example, polymer III has thirteen bands (13.5–2.90 Å) but polymer V has four bands (16–4.5 Å); polymer VII has six bands (18–4.15 Å) but polymer VIII has four (15–3.9 Å). The diffraction patterns were the same before and after fusing the polymers.* It should be noted that the powder patterns of poly[tris-(di-organophosphinato)alanes] and poly[bis(di-organophosphinato)fluoro-alanes] are quite similar,[9] although more bands are normally observed for the latter polymers.

Figure 1 gives typical TGA curves for six polymers. These data are generally consistent with earlier work[8,9] where the thermal stability decreased with the length and weight per cent of alkyl moieties. The thermal stability of poly{tris(di-n-3,3,3-trifluoropropylphosphinato)alane}, II, was disappointing because a logical mechanism for thermal decomposition involved initial chain degradation at a terminal site. A comparison of bond energies[13] indicates that the P—C bond is thermodynamically the weakest

* The x-ray diffraction powder patterns will be submitted to the ASTM X-Ray Powder Diffraction File, Department of Geophysical Sciences, University of Chicago, Chicago, Illinois.

of the interatomic bonds; therefore, unsaturated hydrocarbons are probably the initial thermal decomposition products. The approximate bond energies are E(P—C), 63 kcal; E(P—H), ~77 kcal; E(P—O) bridged, 80 kcal; E(C—C), 82 kcal; E(C—H), ~99 kcal; E(Al—O) single, 102 kcal (JANAF Table); and E(P$\rightarrow$O), 120 kcal.[13] It should be noted that the relative thermal stabilities of triorganophosphine oxides, R_3O=P, are methyl $\geqq$ phenyl $\gg$ ethyl.[14]

The polymers are resistant to aqueous solutions of strong acids and bases (<100°C), and surprisingly stable to hydrolysis by water above 100°C. The polymers will "dissolve" in 50% ethanol–aqueous potassium hydroxide upon prolonged exposure. Polymer VI gave no indication of hydrolysis when heated under pressure in water at 150°C for 24 hr. Although there must be considerable ionic character in the Al—O bonds, the organic moieties apparently shield the coordinate sites from attack, and the extensive phosphoryl bridging increases the energy requirements for intersphere coordination and replacements by attacking ligands.

Increased solubilities permitted molecular weight determinations for polymers VIII through XI. The results were very significant for polymers VIII and IX because the molecular weights exceeded 400 000 in both cases, and very high intrinsic viscosities were observed. Of the two polymers, poly{bis[n-butyl(benzyl)phosphinato]-di-n-octylphosphinatoalane}, IX, was studied in more detail.* A solution of IX, containing 2.16 mg of polymer per milliliter of THF, gave a molecular weight of 440 000 ($n \approx 590$) after several hours at ambient temperature. After heating under refluxing solvent for 4 hr, the molecular weight increased to 460 000 ($n \approx 620$). The same solution was stored at ambient temperature for four months, then subjected to additional molecular weight and intrinsic viscosity determinations. The molecular weight had increased to 780 000 ($n \approx 1050$) and an unusually high intrinsic viscosity of 37 dl/g (THF, 25°C) was obtained. After standing another 4 months at ambient temperature, the polymer had partially precipitated from solution. These data give clear evidence that the polymer grows in solution.[1,8,9] No molecular weight distribution was obtained because the high viscosity interfered with the equilibration in the gel permeation chromatography columns, and further dilution prevented proper detection of the polymer.

The intrinsic viscosity (37 dl/g) of IX is much larger than reported values for other metal phosphinates and it is comparable to reported values for certain polyelectrolytes.[15] The viscosity of polymer VIII is of similar magnitude, thus suggesting that both polymers form partially rigid rodlike molecules in solution with large effective hydrodynamic volumes. The Al—O—P—O— backbones provide structural integrity; the principal role of alkyl moieties is to form an effective organic layer around the inorganic skeletal structure and to interact with the solvent.

Additional data were obtained for polymer IX when a small fraction of

---

* This polymer was discussed briefly in an earlier communication.[1]

etherated alane was partially hydrolyzed before acid addition.* The molecular weight was only 1400 (n, based on polymer only ≈ 2) before heating; after heating under refluxing solvent for ~ 72 hr, the molecular weight increased to 17 600 ($n \approx 23$), clearly much lower than earlier work. The gel-permeation chromatograph (GPC) of this solution (1.94 mg/ml) indicated a broad molecular weight distribution with weak peaks near ~ 400–500 and $\sim 50\ 000$. (The quoted values are based on precise THF–polystyrene calibration curves, but for these polymers the numbers must be considered as only rough estimates because of the geometry of the chains.)

These data strongly suggest that the partially hydrolyzed, soluble species, probably oxo-bridged bis(phosphinato)alanes, grow at a much slower rate than the normal tris(diorganophosphinato)alane molecules, and exchange reactions take place between polymer molecules and free acid remaining in solution. Despite the relatively low molecular weight, a surprisingly high intrinsic viscosity of 15.4 dl/g was observed for the solution.

Molecular weight determinations for polymers X and XI gave 16 400 ($n \approx 12$) and 15 800 ($n \approx 11$), respectively. Although the low degrees of polymerization and high solubilities can be attributed to bulky n-octadecyl moieties, partial hydrolysis of alane was indicated by some opaqueness in the solutions, diffusion in the osmometer, and the similarity of the GPC curves of low molecular weight IX and polymer X. Again, a wide distribution of molecular weights was observed with the strongest peaks near ~ 400–500 and $\sim 40\ 000$–50 000.

Polymer X was prepared with no evidence for partial hydrolysis of alane; after heating 36 hr, the molecular weight was 38 000 ($n \approx 29$) and the intrinsic viscosity (THF, 25°C) was 31 dl/g. The molecular weight is still low in comparison with polymers VIII and IX; it is consistent with steric hindrance to interatomic bridging by the bulky octadecyl moieties. The intrinsic viscosity is surprisingly high but clearly consistent with rod-like molecules in solution.

It is obvious that a condensation reaction is necessary for formation of primary Al—O—P valence bonds, i.e., the Brönsted acid–base, oxidation–reduction reaction of protons and hydride (or ethide) ion. This is not sufficient to insure the actual reaction mechanism proceeds in two distinct steps: the "condensation" reaction [eq. (2)] and subsequent "addition" polymerization by coordinate bond formation [eq (3)]:

$$\text{AlR}_3 + 3\text{HO}-\text{P}\overset{\displaystyle O}{\diagdown} \rightarrow 3\text{RH} + \text{Al}\left(\text{O}-\text{P}\overset{\displaystyle O}{\diagdown}\right)_3 \qquad (2)$$

$$n\text{S}_x\cdot\text{Al}\left(\text{O}-\text{P}\overset{\displaystyle O}{\diagdown}\right)_3 \rightarrow \left[\diagdown\text{Al}(\text{O}-\overset{|}{\underset{|}{\text{P}}}-\text{O})_3\ \text{Al}(\text{O}-\overset{|}{\underset{|}{\text{P}}}=\text{O})_3\right]_{n-1} + xn\text{S} \qquad (3)$$

---
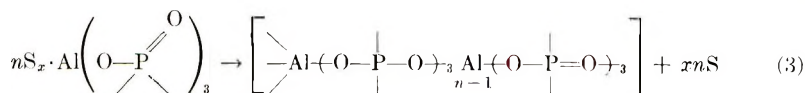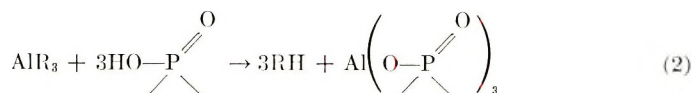
* The interaction involved a faulty stirring bar, but otherwise oxidizing agents and water were excluded.

where S is a solvent molecule, normally THF. The polymer will have active sites for further polymerization; this will be discussed later in more detail. No tris(diorganophosphinato)alane monomers have been isolated and some coordination bonding between phosphoryl ($-\overset{\diagdown}{\underset{\diagup}{P}}=O$) moieties and alanes would be expected at low temperatures. If a small amount of oligomer formation is accepted during the condensation step, the basic two-step reaction sequence or "mechanism" is very probable. It is consistent with high molecular weights at ambient temperature despite the moderately strong THF-alane coordinate bonds,[8] the observed polymer growth in solution, and the lower molecular weights when the bulkier octadecyl moieties are present. It is clear from the data that the initial condensation reaction is fast and very important for a high degree of polymerization. Although condensation can take place with oxo-bridged or less reactive alanes, polymer growth is slow or inhibited:

$$\overset{\diagdown}{\underset{\diagup}{Al}}-O-\overset{\diagup}{\underset{\diagdown}{Al}} + HO\overset{O}{\underset{|\diagdown}{\overset{\parallel}{P}}} \rightarrow \overset{\diagdown}{\underset{\diagup}{Al}}-O-\overset{O}{\underset{\diagup\diagdown}{\overset{\parallel}{P}}} + HO-\overset{\diagup}{\underset{\diagdown}{Al}} \qquad (4)$$

$$\overset{\diagdown}{\underset{\diagup}{Al}}-X + HO-\overset{O}{\underset{|\diagdown}{\overset{\parallel}{P}}} \rightleftharpoons HX + \overset{\diagdown}{\underset{\diagup}{Al}}-O-\overset{O}{\underset{\diagup\diagdown}{\overset{\parallel}{P}}} \qquad (5)$$
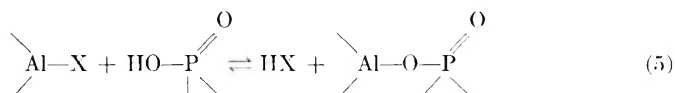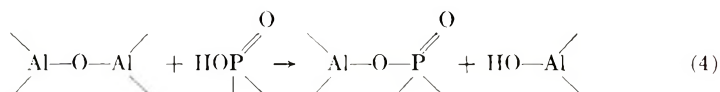
where X denotes OH, halogen, phosphinato moiety.

In the absence of undesirable side reactions, the data support growth by the addition of polymer molecules rather than polymer and monomer units.* Nonbridged aluminum sites are undoubtedly coordinated with THF,[8] and bridging requires the replacement of a THF molecule by a phosphoryl ($-\overset{\diagdown}{\underset{\diagup}{P}}=O$) moiety. The exact mechanism is not known, but it is reasonable to assume the step is bimolecular and dependent upon the number of non-bridging phosphinato moieties remaining in solution.

$$(6)$$
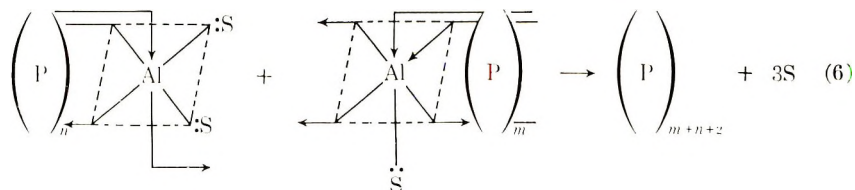
Linear growth can be envisioned by a "tail-head" reaction at two faces; this reaction has low probability when the degree of polymerization is large.

* The probability of monomer units remaining in solution is very low because the monomer is potentially hexa-functional, i.e., $Al[OP(R)_2O]_3$ has three bridging ligands and three coordinating sites on aluminum. Coordination by solvent molecules does not change the basic functionality.

A line representation for octahedral faces is given in eq. (6), where the arrow represents a phosphinato moiety and S represents a solvent molecule.

Several factors determine the structure and stereochemistry of the polymers: (1) the cumulative effects of organic moiety size and the geometry at aluminum sites; (2) the relative amounts of uncoordinate phosphinato moieties, bis(phosphinato) bridging, and tris(phosphinato) bridging; (3) the extent of intra-atomic (chelating) versus interatomic phosphinato bridging; and (4) overall polymer geometry, i.e., linear chains, two-dimensional layers with or without interlayer bridging, and three-dimensional networks. The literature[16] leaves little doubt that the site geometry at the phosphorus atoms will be basically tetrahedral, but aluminum can have tetrahedral (4-coordinate), trigonal bipyramid or tetragonal pyramid (5-coordinate), and octahedral (6-coordinate) site geometry.[9,17-20] The polymeric nature of the tris(diorganosphosphinato)alanes indicates a minimum coordination of four; if 4-coordinate, free phosphinato ($-O-P=O$) moieties would be twice as abundant as bridging moieties. Free phosphoryl moieties are not observed in the infrared spectra ($\sim$1200 cm^{-1}) and strong bands near 1130 and 1040 cm^{-1} can be most readily interpreted in terms of symmetrical and asymmetrical modes of approximately equivalent moieties.[21,22] Infrared spectra will be discussed in detail in a separate communication.[22] The 6-coordinate state is favored over the 5-coordinate state because it will utilize all of the phosphinato bridging potential; the 3d orbitals are available for the stronger sp^3d^2 octahedral bonding[23] which maximizes the coordination number without a large increase in the electrostatic repulsion energy between coordinating ligands.[24]
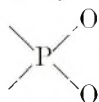
The evidence in the literature strongly supports interatomic phosphinato bridging in preference to intra-atomic (chelate) bridging.[1,25-27] If chelate formation was favored, chain termination would take place rapidly in solution. The fact that the polymers continue to grow in solutions with excess acid indicates that chelate formation is thermodynamically less stable than interatomic bridging.* With the exception of terminal moieties, it has been concluded that virtually all of the phosphinato moieties are utilized in interatomic bridging between 6-coordinate aluminum.

Possible 6-coordinate aluminum structures are given in Figure 2. The important features of structure A are out-of-plane bis(phosphinato) bridging and chelating. If the third phosphinato moiety does not bridge or chelate, the last site will be occupied by a solvent molecule. Likewise, if the third phosphinato moiety bridges after structure A is formed, a three-

---

* With the exception of some novel diorganotin bis(diorganophosphinates),[28] no evidence can be found in the literature for chelating phosphinato moieties. A clear distinction has been made between phosphinato, R(R')PO$_2$, and phosphinothioato, R(R')-PSO, or phosphinodithioato, R(R')PS$_2$, ligands.[6]
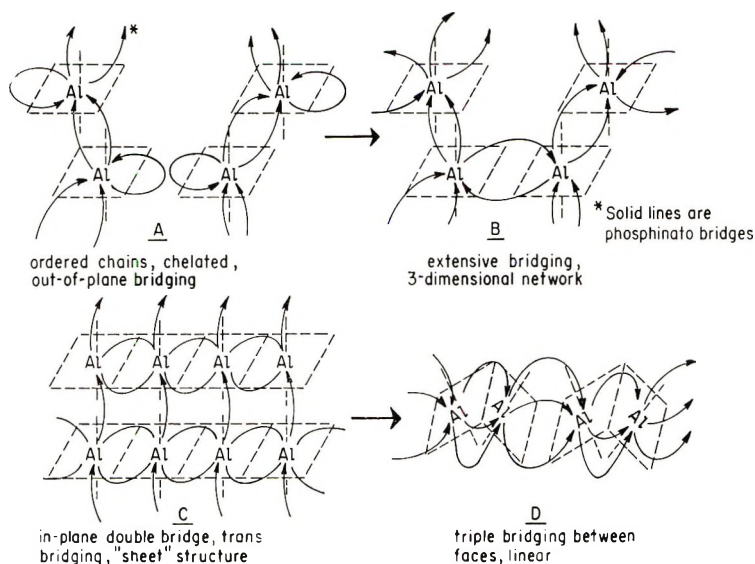
Fig. 2. Possible structures for poly[tris(diorganophosphinato)alanes].

dimensional network such as structure B should result. Polymers with structure B will tend to be brittle, insoluble, and intractable. The data for polymers I–III and poly{tris(diphenylphosphinato)alane}[6] are consistent with structure B, although structure C will give similar properties. Structure C has the third phosphinato moiety *trans* to the bis(phosphinato) bridging plane; the "sheet" network is a direct consequence of extensive interplane bridging. The simplest modification is less interplane bridging, i.e., free phosphinato moieties and intersphere solvation. Evidence presented earlier suggests that this modification is thermodynamically less favorable than bridging. It is obvious that a third intraplane bridge leads to a less crosslinked structure and ultimately to structure D. The tricyclic, eight-member rings of D will be less rigid than smaller tricyclic rings. Structure D should be more flexible than structures B and C, but less flexible than structure A. Structure D is clearly consistent with solubility and viscosity data for polymers VIII through XI. The relatively linear polymer chains should be partially rigid and rodlike in solution; the cylindrical structures with long pendant groups should have large effective hydrodynamic volumes. Finally, the data for polymers IV through VII are consistent with intermediate C and D structures.

The physical and chemical properties of poly{tris[diorganosphosphinato]-alanes} compare favorably with polymeric mono(diorganophosphinato)-alanes* and bis(diorganophosphinato)alanes.[9] This reflects several important features of (phosphinato)alanes: (1) the strong tendency to form extensively bridged, polymeric structures; (2) the use of higher coordinate

* Poly{[diorganophosphinato]difluoroalanes} have been discussed briefly in an earlier report,[29] a more detailed report is planned.

states (predominantly six) especially in solids with Al—O and Al—F bonds; (3) the use of higher energy $3d$ orbitals; (4) the role of phosphorus substituents in structure modifications; and (5) the inherent difficulty in establishing structural constraints based upon the number of phosphinato moieties. The complexity of this alane chemistry is directly related to the small, highly charged Al^{+++} ion, and $3s$, $3p$, $3d$ hybridized orbitals. Beryllium(II) and zinc(II) phosphinates[25-27] have simpler sp^3 tetrahedral bonding because the energy of the $3d$ orbitals is too high in beryllium(II) and the orbitals ($3d^{10}$) are filled in zinc(II). Tetrahedral cobalt(II) has four paired and three unpaired electrons in the $3d$ orbitals; therefore, it utilizes sp^3 hybridized orbitals.[30] Some similarities are expected between chromium(III) phosphinates[29] and (phosphinato)alanes, but the role of the d orbitals constitutes a major difference. The Cr^{+++} ion has a d^3 configuration;[10] the remaining $3d$ orbitals, the $4s$ and $4p$ orbitals are available for comparatively low energy, closed shell bonding ($3d^2 4s 4p^3$) with essentially octahedral geometry. The basic 6-coordinate structure is fixed, although different stereochemical configurations are expected.

In general, (phosphinato)alanes should be more ionic and have greater structural complexity than the corresponding chromium(III) phosphinates; this report and earlier work support this conclusion.[7-9]

SUMMARY AND CONCLUSIONS

The properties of poly[tris(diorganophosphinato)alanes] were modified significantly by changing the organic moieties. Alkyl moieties with six or more carbon atoms gave film-forming, flexible polymers. Mixtures of symmetrical and unsymmetrical phosphinates gave more tractable and normally less crystalline polymers than the corresponding homopolymers. Soluble polymers were prepared which exhibited high degrees of polymerization and exceptionally high intrinsic viscosities. Solutions of poly{bis[n-butyl(benzyl)phosphinato]di-n-octylphosphinatoalane} were studied in considerable detail. Polymer growth in solution was verified by determining the degree of polymerization before heating ($n \approx 590$), after heating ($n \approx 620$), and upon prolonged standing at ambient temperature ($n \approx 1050$). The intrinsic viscosity of 37 dl/g was consistent with partially rigid, rodlike molecules in solution. Some insight into the mechanism of growth was obtained from reactions with partially hydrolyzed alanes. If stoichiometric amounts of Al—R bonds were present, primary Al—O—P valence bonds formed in a fast "condensation" step; this was followed by slower "addition" or coordinate bond-formation steps. With less reactive substituted alanes, the condensation step was apparently slow and reversible. Supporting data were obtained from soluble polymers with octadecyl moieties; these data also supported the concept that steric requirements of organic moieties modify the structure and degree of polymerization of poly[tris(diorganophosphinato)alanes].

Physical and chemical properties of the polymers were discussed and related to possible structural modifications. It was concluded that virtually all of the phosphinato moieties are utilized in interatomic bridging between 6-coordinate, octahedral aluminum. A linear, triple-bridged structure was proposed for the soluble polymers; related bridging structures were proposed for the other polymers.

References

1. E. E. Flagg and D. L. Schmidt, *J. Amer. Chem. Soc.*, **90**, 4173 (1968).

2. S. H. Rose and B. P. Block, *J. Polym. Sci. A-1*, **4**, 573, 583 (1966).

3. A. J. Saraceno and B. P. Block, *J. Amer. Chem. Soc.*, **85**, 2018 (1963).

4. G. E. Coates and D. S. Golighly, *J. Chem. Soc.*, **1962**, 2523.

5. G. H. Dahl and B. P. Block, *Inorg. Chem.*, **6**, 1439 (1967).

6. J. J. Pitts, M. A. Robinson, and S. I. Trotz, *J. Inorg. Nucl. Chem.*, **30**, 1299 (1968).

7. A. J. Saraceno, J. P. King, and B. P. Block, *J. Polym. Sci. B*, **6**, 15 (1968).

8. D. L. Schmidt and E. E. Flagg, *J. Polym. Sci.*, *A-1*, **6**, 3235 (1968).

9. D. L. Schmidt and E. E. Flagg, *J. Polym. Sci.*, *A-1*, **7**, 865 (1969).

10. R. A. Sutton and J. Wood, Brit. Pat. 1,018,456 (1966); *Chem. Abstr.*, **64**, 17748f (1966).

11. A. E. Finholt, A. C. Bond, and H. I. Schlesinger, *J. Amer. Chem. Soc.*, **69**, 1199 (1947).

12. H. A. Smith, E. E. Flagg, and D. L. Schmidt, to be published.

13. T. L. Cottrell, *The Strengths of Chemical Bonds*, 2nd ed., Butterworths, London, 1958.

14. W. J. Bailey, W. M. Muir, and F. Marktscheffel, *J. Org. Chem.*, **27**, 4404 (1962).

15. C. Tanford, *Physical Chemistry of Macromolecules*, Wiley, New York, 1965, pp. 489–512.

16. D. E. C. Corbridge, in *Topics in Phosphorus Chemistry*, Vol. 3, E. J. Griffith and M. Grayson, Ed., Interscience, New York, 1966, pp. 57–437.

17. K. J. Palmer and N. Elliott, *J. Amer. Chem. Soc.*, **60**, 1852 (1938).

18. C. W. Heitsch, E. C. Nordman, and R. W. Parry, *Inorg. Chem.*, **2**, 508 (1963).

19. C. Ercolani, A. Camilii, and G. Satori, *J. Chem. Soc. A* **1966**, 606.

20. J. A. A. Ketelaar, *Z. Krist.*, **85**, 119 (1933).

21. R. A. Nyquist, *J. Mol. Structure*, **2**, 111, 123 (1968).

22. R. A. Nyquist, D. L. Schmidt, E. E. Flagg, and R. E. Ridenour, in preparation.

23. L. Pauling, *The Nature of the Chemical Bond*, 3rd ed., Cornell Univ. Press, Ithaca, N. Y., 1960.

24. J. D. Dunitz and L. E. Orgel, in *Advances in Inorganic Chemistry and Radiochemistry*, Vol. 2, H. J. Emeléus and A. G. Sharpe, Eds., Academic Press, New York, 1960, pp. 1–60.

25. V. Giancotti, F. Giordano, L. Randaccio, and A. Ripamonti, *J. Chem. Soc. A*, **1968**, 757.

26. F. Giordano, L. Randaccio, and A. Ripamonti, *Chem. Commun.*, **1**, 19, 1239 (1967).

27. F. Gemiti, V. Giancotti, and A. Ripamonti, *J. Chem. Soc. A*, **1968**, 763.

28. R. E. Ridenour and E. E. Flagg, *J. Organometal. Chem.*, **16,** 393 (1969).

29. E. E. Flagg and D. L. Schmidt, paper presented at the 154th National Meeting, American Chemical Society, Chicago, Illinois, September 1967; Abstract 0-123.

30. C. J. Ballhausen, *Introduction to Ligand Theory*, McGraw-Hill, New York, 1962, pp. 235–245, 255–261.

Ketone-Zinc Chloride Combination as an Initiator of Polymerization

PRABIR K. DUTT and SANTI R. PALIT, *Department of Physical Chemistry, Indian Association for the Cultivation of Science, Jadavpur, Calcutta, India*

Synopsis

Dihydrocivetone, a macrocyclic ketone, has been found to be a weak initiator of vinyl polymerization. Anhydrous zinc chloride strongly promotes this to form a novel initiating system. Monomers tried successfully are methyl methacrylate, acrylonitrile and α-methylstyrene. The characteristic feature of polymerization of α-methylstyrene differs greatly from those of other monomers and those have been discussed and compared.

A preliminary note[1] reports that the dihydrocivetone (DHC)–$ZnCl_2$ combination is a good initiator of polymerization of methyl methacrylate, acrylonitrile and α-methylstyrene and fails with styrene and vinyl acetate. This may be due to the fact that, in the case of styrene, $ZnCl_2$ is insoluble in the monomer; and in the case of vinyl acetate, $ZnCl_2$ probably reacts resulting in deacetylation of the monomer. The methyl methacrylate and acrylonitrile are almost the same in behavior but very different from α-methylstyrene, and hence we report our results in two separate sections.

EXPERIMENTAL

Purification of Monomers

The stabilized monomers namely, methyl methacrylate, acrylonitrile, and α-methylstyrene, were purified by conventional methods.

Purification of Dihydrocivetone

Dihydrocivetone is purified by repeated crystallization from methyl alcohol. The colorless crystalline solid, m.p. 63°C, was found to be peroxide-free by iodimetric methods.[2,3]

Treatment of Anhydrous Zinc Chloride

A. R. grade anhydrous zinc chloride has been used after heating at 300°C for about 15 min under vacuum.

Polymerization Procedure

Polymerization was carried out in the dark in sealed glass ampoules. The tubes were frozen in liquid air, degassed several times, and sealed under

15

vacuum, and polymerization was carried out at the desired temperature in a thermostatted bath. The polymerization product was extracted with acetone to keep the $ZnCl_2$ in solution and then precipitated with methyl alcohol.

RESULTS

Methyl Methacrylate–Dihydrocivetone
(with or without Promoters)

Of a good number of ketones tried,[4] such as, acetone, methyl ethyl ketone, cyclohexanone, C-11 ketone, C-12 ketone, exaltone and dihydrocivetone (DHC) it has been found that DHC is the most active, and even then the yield of polymer is rather poor (Table I). $[\eta]$ values (Table I) are quite high and almost reach those obtained by thermal polymerization.

TABLE I
Polymerization of Methyl Methacrylate in Bulk at 60°C with DHC as Initiator

[DHC], mole/l.	Yield (in 7 hr), %	$[\eta]$ (30°C, benzene), dl/g
0.40	4.0	5.5
0.20	1.4	
0.10	0.75	
0.05	0.66	6.1

Different types of additives such as oxidants, hydrogen abstractors, Lewis acids, and weak bases, etc., were tried as promoters (Table II) under the same polymerization conditions, and only anhydrous $ZnCl_2$ was found to have the desired property to a considerable extent; further work was therefore carried out with a combination of DHC and $ZnCl_2$.

TABLE II
Effect of Additives in DHC-Initiated Polymerization ([DHC] = 0.40 mole/l.)

Additive	Temperature, °C	Remarks
Oxygen	60	No polymerization
Benzoyl peroxide	30	No improvement of rate
Chloramine-T	60	"
Bromine	60	"
Sulfur	60	"
Benzaldehyde	60	No polymerization
tert-Amines	60	"
Anhydrous $AlCl_3$	60	"
Anhydrous $ZnCl_2$	60	Rate of polymerization markedly increased

Optimum Ratio of DHC and $ZnCl_2$. It was observed that a 1:1 molar ratio of DHC and $ZnCl_2$ is the best initiating system. Addition of excess of DHC above this 1:1 ratio has a very negligible effect on the rate. The rate, however, falls with excess of $ZnCl_2$.
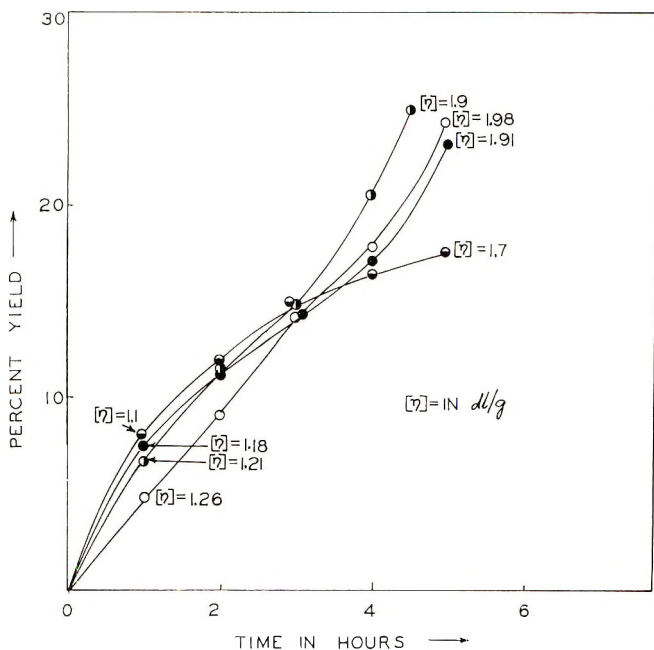
Fig. 1. MMA–DHC–ZnCl₂ system at 50°C in bulk at various [ZnCl₂]: (O) 0.075 mole/l.; (◑) 0.145 mole/l.; (●) 0.29 mole/l.; (◒) 0.44 mole/l. [DHC] = 0.4 mole/l; [η] in dl/g.

Effect of Temperature. The optimal rate of polymerization reached at about 50°C; the rate is quite slow below 50°C.

Yield–Time Curves and Degree of Polymerization. The yield–time curves are of the following two types: (1) an autoaccelerated type (Fig. 1) which is typical with a [DHC]/[ZnCl₂] value greater than unity, and (2) a logarithmic type in which the yield tends to reach a limit (Fig. 1), and which occurs at [ZnCl₂]/[DHC] values greater than unity.

Intrinsic viscosities of polymer samples in benzene solution have been used as an indication of molecular weights. The molecular weights are on the high side, considering the high initiator concentration, and increase appreciably with time (Figs. 1 and 2). Variation of [ZnCl₂] has very little effect on molecular weight, perhaps due to the poor chain transfer capacity of ZnCl₂. On the other hand, an increase in [DHC] produces a decrease in molecular weight, and this may be due to the transfer through the methylenic hydrogen of DHC.

Effect of Inhibitors. Typical radical scavengers such as oxygen and 2,2'-diphenyl-1-picryl hydrazyl inhibit the polymerization reaction. However, hydroquinone acts as an activator at low concentration, but when present in high concentration it inhibits very efficiently.

Effect of Solvents. Solvents in general appear to have either a retarding or inhibiting effect (Fig. 3). For polar solvents this may be due to the fact that the DHC–ZnCl₂ complex, the real initiator, tends to dissociate in
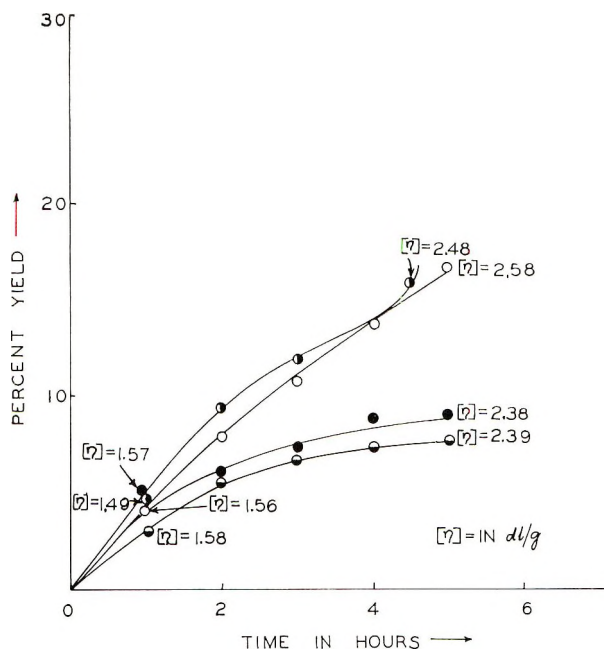
Fig. 2. MMA–DHC–ZnCl₂ system at 50°C in bulk at various [ZnCl₂]: (○) 0.075 mole/ l.; (◑) 0.145 mole/l.; (●) 0.29 mole/l.; (◒) 0.44 mole/l. [DHC] = 0.10 mole/l.; [η] in dl/g.

those solvents. Inhibition in DMF is attributed to the fact that DMF forms a stronger complex with ZnCl₂ than the ketone. The retardation in nonpolar solvents, such as benzene, may be due to dilution effect

Endgroups and Crystallinity. No Zn, OH or Cl endgroup is found in the polymer. The polymer was ignited and the ash tested for Zn. A dye technique was employed to detect OH or Cl group, and the result was negative.[5,6]

The polymer samples were tested for crystallinity by x-ray diffraction and found to be totally amorphous.

Acrylonitrile–DHC–ZnCl₂ System

The results of polymerization are more or less similar to the case of methyl methacrylate but differ in one very important respect, viz., the polyacrylonitrile polymers obtained are insoluble in solvent (dimethyl-formamide, etc.).

Ketones Other Than DHC as Initiator Components

A combination of ketone and ZnCl₂ in a 1:1 molar ratio is an initiator of polymerization. The initiating power is more pronounced with the higher members of the series (Fig. 4); DHC has the best initiating power among the ketones tried. Nevertheless, even the simplest ketone, acetone, when in combination with ZnCl₂ can initiate the polymerization of methyl methacrylate.
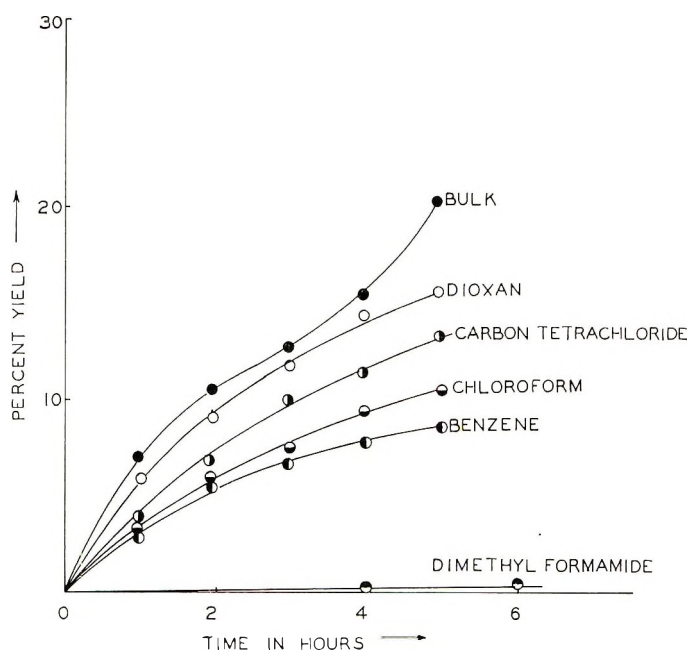
Fig. 3. Effect of solvents on MMA–DHC–ZnCl₂ system at 50°C. Solvent:monomer = 1:1 (v/v); [ZnCl₂] = 0.29 mole/l.; [DHC] = 0.20 mole/l.

α-Methylstyrene

Yield-Time Curves. The polymerization of α-methylstyrene initiated by dihydrocivetone–zinc chloride system is usually characterized by an initial slow rate of polymerization followed by a fast polymerization almost of autoaccelerated nature except when both zinc chloride and dihydrocivetone concentrations are low. This is illustrated by a few typical yield–time plots as shown in Figures 5 and 6. Yields as high as 30% are reached, after which the rates tend to level off.

Optimum Ratio of DHC and ZnCl₂. The rate of polymerization increases continuously with increase in ZnCl₂ at a fixed concentration of dihydrocivetone. On the other hand, at a fixed concentration of ZnCl₂ the rate of polymerization increases and tends to attain a limiting value at a ratio of DHC:ZnCl₂ (about 1:4).

Effect of Temperature. The optimum temperature of polymerization of this monomer (which has a ceiling temperature at 60°C) with the present initiator system is in the room temperature region, i.e., about 30°C. At low temperatures such as −5°C, the rate of polymerization is rather slow and at still lower temperature there is hardly any polymerization.

Inhibition Experiments and the Role of Oxygen. The polymerization of α-methylstyrene is not inhibited by free-radical scavengers like 2,2'-diphenyl-1-picryl hydrazyl and quinone. Oxygen, however, retards the polymerization but cannot suppress it completely (Fig. 7).

Effect of Solvents. A large number of solvents of varied nature has been
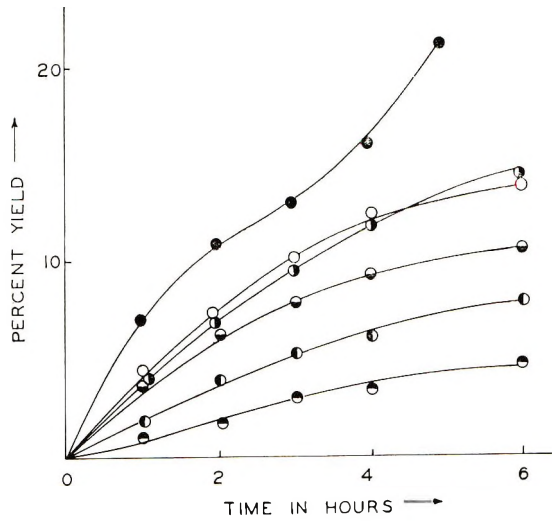
Fig. 4.   Effect of different ketones on MMA–ketone–$ZnCl_2$ system at 50°C in bulk:
(●) DHC (C-17); (◐) 5,5-dimethylcyclohexanedione; (○) C-14 ketone; (◔) cyclohexa-
none; (◑) C-12 ketone; (◕) acetone. $[ZnCl_2]$ = 0.3 mole/l.; ketone concentration =
0.3 mole/l.
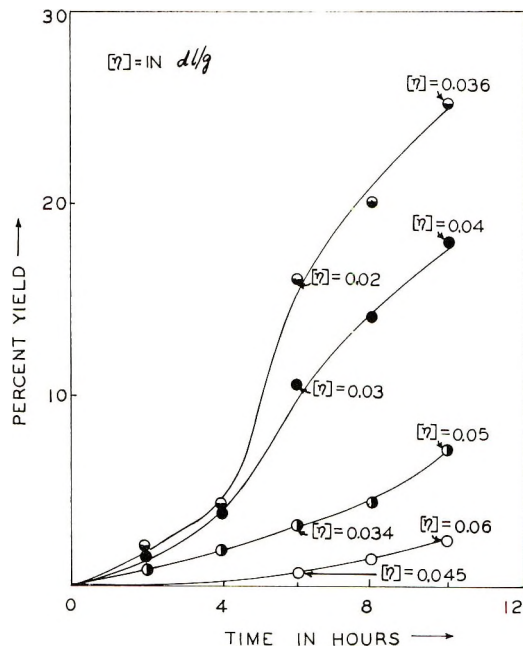
Fig. 5. α-Methylstyrene–DHC–$ZnCl_2$ system at 30°C in bulk at various $[ZnCl_2]$:
(○) 0.10 mole/l.; (◑) 0.20 mole/l.; (●) 0.40 mole/l.; (◕) 0.80 mole/l.   [DHC] = 0.10
mole/l.; $[\eta]$ in dl/g.
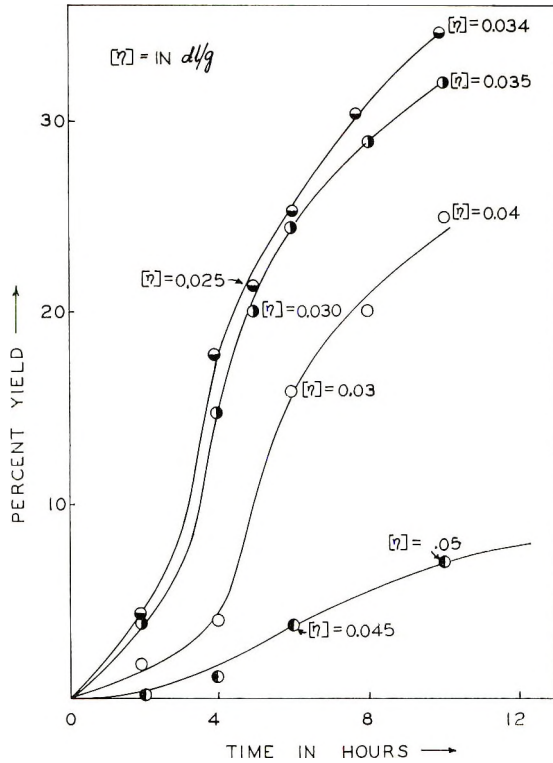
Fig. 6. α-Methylstyrene–DHC–ZnCl$_2$ system at 30°C in bulk at various DHC: (◐) 0.05 mole/l.; (○) 0.10 mole/l.; (◑) 0.20 mole/l.; (◒) 0.40 mole/l. [ZnCl$_2$] = 0.80 mole/l.; [η] in dl/g.

tried as the medium for polymerization at a 1:1 monomer:solvent ratio under the same experimental conditions. The polymerization is completely inhibited in the presence of oxygenated solvents such as dioxane, dimethyl-formamide, acetone, cyclohexanone, etc. This is perhaps due to the fact that tertiary oxonium ions R$_3$O$^+$ are more stable than most carbonium ions and this greater stability perhaps accounts partly for the inhibiting effect of oxygenated solvents. The inhibition or retardation by benzene, a nonpolar solvent, is attributed to dilution effect.

Endgroups. Endgroup analysis by the dye technique indicates that the polymers do not contain any chlorine endgroup.[6] Testing the ash for zinc after igniting a polymer sample shows the polymers to be free of zinc. The endgroup analysis, however, indicates the presence of hydroxyl end-groups[5] in the final polymer which are presumed to have resulted from the hydrolysis of the organozinc compound by moist methyl alcohol during the precipitation of the polymer.

Degree of Polymerization. The poly-α-methylstyrene prepared by this initiator system is of very low molecular weight as indicated by the low [η] values (Figs. 5, 6). The [η] increases a little with time during poly-merization but is not much affected by the variation of initiator concentra-
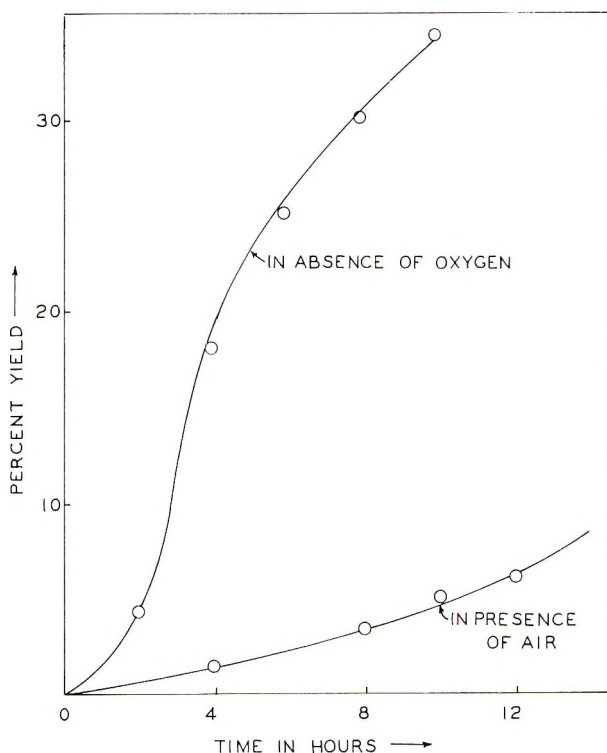
Fig. 7. Effect of oxygen on α-methylstyrene–DHC–ZnCl₂ system at 30°C in bulk.

tions.   Further, $[\eta]$ increases, but not appreciably, if the polymerization is carried out at a lower temperature, say $-5°C$, as shown in Table III.

TABLE III
Effect of Temperature on the Degree of Polymerization
in α-Methylstyrene Polymerization

[DHC], mole/l.	[ZnCl₂], mole/l.	Temperature, °C	$[\eta]$ (30°C, benzene), dl/g
0.10	0.40	30	0.049
0.10	0.40	−5	0.071

DISCUSSION

Methyl Methacrylate Polymerization

It is known that anhydrous ZnCl₂ goes into solution in ketonic solvents with the formation of a very weak complex of the type:

$$\diagdown C\cdots O\cdots ZnCl_2$$
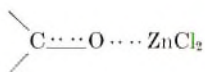
Therefore, when anhydrous ZnCl$_2$ is added to the system containing methyl methacrylate and DHC it can form complexes with both DHC or the carboxyl group of the monomer. The formation of a complex of ZnCl$_2$ with methyl methacrylate activates the monomer to some extent.[7] Since ZnCl$_2$ alone fails to initiate the polymerization, the possibility of a ZnCl$_2$–monomer complex as the initiating species has been excluded and it is presumed that DHC-ZnCl$_2$ complex is the actual initiating species.

From evidence of inhibition by radical scavengers and the observed ease of polymerization with methyl methacrylate one can exclude the possibility of any ionic mechanism. It is also difficult to draw a coordination mechanism even if a DHC–ZnCl$_2$ complex is presumed to initiate polymerization, because there is no labile group here like the alkyl group in Ziegler-Nata catalysts.[8] Again, the possibility of a radical mechanism is not supported by results of copolymerization studies. Polymerization of 1:1 (v/v) methyl methacrylate and styrene with this initiator system was attempted. Microanalysis as well as studies of ultraviolet spectra[4] showed that the product was a homopolymer of methyl methacrylate rather than a copolymer of methyl methacrylate and styrene. The rate of polymerization was lower than that observed with methyl methacrylate alone. This is consistent with the effect of solvents in the methyl methacrylate polymerization discussed earlier.

Therefore, it is rather difficult to draw a mechanism of the observed polymerization on standard lines.

α-Methylstyrene Polymerization

The polymerization of α-methylstyrene with this catalyst combination, on the other hand, is quite different from that of methyl methacrylate. The most important point is that in case of methyl methacrylate DHC has a weak but definite initiating action and anhydrous ZnCl$_2$ promotes this, but with α-methylstyrene ZnCl$_2$ has a very feeble initiating effect, and DHC promotes this enormously. The experimentally observed facts lead us to believe that the mechanism of polymerization for α-methyl styrene is a cationic one, and the mechanism shown in eq. (1) is suggested:

$$>C{=}O\cdots ZnCl_2 \rightarrow >\overset{+}{C}{-}O{-}ZnCl\ Cl^- \text{ (gegenion)} \xrightarrow{\text{Monomer}} \overset{\displaystyle C\!\sim\!\!\!\!\sim^+(Cl^-)}{\underset{}{\overset{|}{O}}}\cdots ZnCl \qquad (1)$$
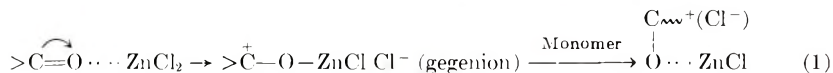
It is presumed that DHC forms a complex of the type $C \overset{...}{=} O{-}ZnCl_2$ on the surface of ZnCl$_2$ and polymerization starts at this surface; in systems in which ZnCl$_2$ is present in solution there is no polymerization because of absence of this interface. This is the reason why liquid ketones fail to form an initiator for this monomer.

The labile organozinc compound is decomposed when the polymer is precipitated with methyl alcohol containing acid, and this results in the incorporation of hydroxyl groups in the polymer and thereby rendering the polymer free of zinc.

TABLE IV

α-Methylstyrene	Methyl methacrylate
Polymerization is not inhibited by radical scavengers, such as 2,2'-diphenyl-1-picrylhydrazyl, quinone, etc.; oxygen acts as a retarder.	Polymerization is inhibited by radical scavengers.
Measurable rate of polymerization is observed in the temperature range 0–50°C	The optimum temperature for polymerization is 50°C
Molecular weights are rather low ($[\eta] = 0.05$)	The molecular weights are relatively high ($[\eta] = 1.8$).
Polymerization is totally inhibited by oxygenated solvents.	Solvents in general have either an inhibiting or a retarding effect.
Combination of simple ketones (e.g., acetone) with $ZnCl_2$ fails to initiate the polymerization.	Simple ketones in combination with $ZnCl_2$ initiates the polymerization.
Polymerization starts at the surface of the insoluble $ZnCl_2$ present in the system.	In this case $ZnCl_2$ is soluble to form a homogeneous system
No halogen endgroup is found. Hydroxyl endgroup is incorporated in the final polymer.	There is neither hydroxyl nor halogen endgroup in the polymer.
A cationic mechanism is suggested.	No definite mechanism is suggested.

To conclude, the polymerization of α-methylstyrene differs fundamentally from that of methyl methacrylate, the only common feature being that in both the instances combination of dihydrocivetone and $ZnCl_2$ gives a good initiator system for polymerization. The characteristic features of polymerization of α-methylstyrene and methyl methacrylate with the present initiator system are compared in Table IV.

References

1. P. K. Dutt and S. R. Palit, *J. Polym. Sci. B*, **3**, 801 (1965).

2. F. E. Critchfield, *Organic Function Group Analysis*, Pergamon Press, London, 1963, p. 159.

3. K. Nozaki, *Ind. Eng. Chem. Anal. Ed.*, **18**, 583 (1946).

4. P. K. Dutt, Doctoral Thesis, Calcutta University, 1966.

5. P. Ghosh, P. Sengupta, and A. Pramanick, *J. Polym. Sci. A*, **3**, 1725 (1965).

6. M. Kumarsaha, P. Ghosh, and S. R. Palit, *J. Polym. Sci. A*, **2**, 1365 (1964).

7. M. Imoto, T. Otsu, and Y. Harada, *Makromol. Chem.*, **65**, 180 (1963).

8. N. G. Gaylord and H. F. Mark, *Linear and Stereoregular Addition Polymers*, Interscience, New York, 1959.

9. A. V. Tobolsky, A. Eisenberg, and K. F. O'Driscoll, *Anal. Chem.*, **31**, 203 (1959).

Gel-Permeation Chromatography and Cellulose. I. Effect of Degree of Nitration of Cellulose on Molecular Weight Distribution Data

LEON SEGAL, J. D. TIMPA, and J. I. WADSWORTH,
Southern Regional Research Laboratory, Southern Utilization Research and Development Division, Agricultural Research Service, United States Department of Agriculture, New Orleans, Louisiana 70119

Synopsis

Consideration is given to the effect on gel-permeation chromatographic (GPC) data of the extent of substitution in nitrated cellulose. GPC parameters for samples containing 13.55–13.81% nitrogen (14.14% corresponds to complete substitution, DS = 3) were hardly affected by this variation in substitution. Variations that were observed are considered to arise within the samples themselves. Experiments with low molecular weight organic iodides, nitrates, and hydroxyl compounds indicate longer chain lengths than actual; this is attributed to extensive solvation of the substituent groups. The very long chain lengths obtained for cellulose nitrate by the present GPC procedure may arise from such an affect.

INTRODUCTION

Because cellulose is insoluble in organic solvents, determination of the molecular weight distributions of cellulosic materials by gel-permeation chromatography (GPC) requires the preparation of a cellulose derivative which is soluble in the solvent used in the gel-permeation chromatograph. The derivative of choice is cellulose trinitrate;[1] the solvent is tetrahydrofuran (THF). The polymers that have been studied by means of GPC are directly soluble in organic solvents without further chemical treatments. However, the required esterification of cellulose introduces a factor which does not appear with the usual polymers. This factor is that of extent and uniformity of substitution of the hydroxyl groups of the cellulose chain molecule. Incomplete nitration of the cellulose molecule usually gives a compound which contains many polar nitrate groups and a small but variable number of hydroxyl groups (Fig. 1).

Complete esterification to the theoretical trinitrate stage (degree of substitution 3, 14.14% N) is the desired goal, but this is very difficult to achieve in practice. The cellulose trinitrate normally obtained has a degree of substitution ranging between 2.79 and 2.88 (13.59–13.81% N). This deficiency in substitution introduces two deleterious effects in the usual molecular weight determinations. The first effect is that the weight of the anhydroglucose unit after nitration is less than the theoretical 297.14.
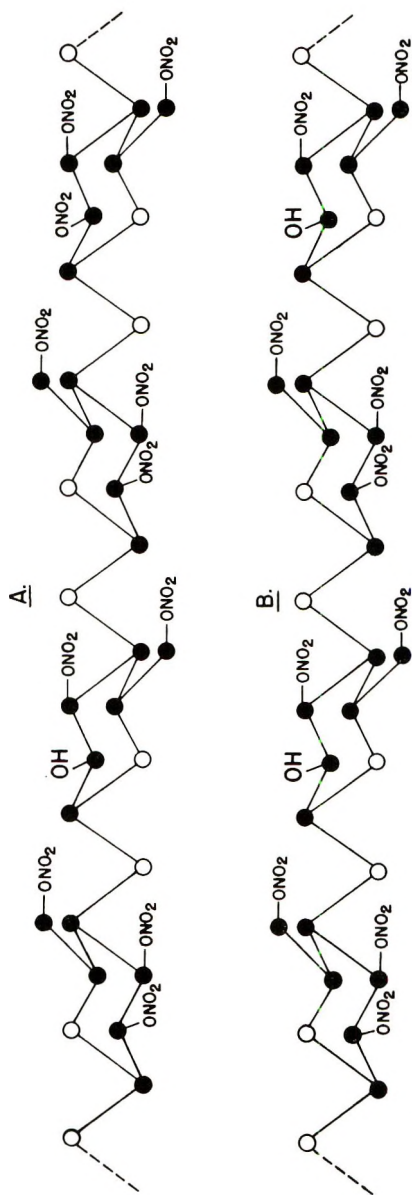
Fig. 1. Illustration of incomplete nitration: (A) partially nitrated cellulose, nitrogen content 13.20%, degree of substitution 2.75; (B) partially nitrated cellulose, nitrogen content 12.50%, degree of substitution 2.50.

The second effect concerns the extent of solute–solvent interaction between the incompletely nitrated cellulose chain and the solvent. This second effect markedly affects measurements of the intrinsic viscosity of solutions of cellulose trinitrate[2−4] and is undoubtedly important in GPC work.

Hendrickson and Moore[5] have shown that alcohol, phenol, and nitrobenzene are eluted much sooner than would be expected because of strong hydrogen bonding with the solvent. This behavior of the alcohols in particular and the above-mentioned aspects of incompletely nitrated cellulose aroused speculation concerning the possible consequences of incomplete nitration of cellulose upon the molecular weight distribution curves obtained by GPC. This paper reports the findings of a study aimed at resolving this question.

EXPERIMENTAL

The cellulose used in this study was a purified cotton yarn with a degree of polymerization (DP) of 5000 (by viscometry in cadoxen solvent). Nitration of 1-g samples and subsequent storage of the products were the same as described in an earlier publication.[6] Variations in the degree of nitration were achieved by diluting the Alexander and Mitchell nitrating acid[7] in the manner described by Lindsley and Frank.[2]

Four concentrations of nitrating acid were used: 100%, 90%, 80%, and 75%. The nitrogen contents of the products, determined by a special semimicro Kjeldahl method of $\pm 0.2\%$ average accuracy,[8] did not correlate with these concentrations, being 13.81, 13.55, 13.59, and 13.54%, respectively. This trend is similar to one for similar data given by Timell.[3] In spite of a nitrogen content of 13.54%, the cellulose nitrated by the 75% acid was only 88–90% soluble, an example, perhaps, of nonuniform substitution.

The values of the Q factor (molecular weight per unit Angstrom length), the soluble samples were adjusted in view of the different values for the weights of the nitrated anhydroglucose units. For 13.5% N, $Q = 55.9$; for 13.6% N, $Q = 56.3$; for 13.8% N, $Q = 56.9$. As all of the GPC fractionations were carried out with only the three 1-g nitrated samples, variations in the distribution curves and the DP data reflect, therefore, the range of experimental error for this technique.

The GPC instrumentation and experimental procedure were the same as those used earlier,[1] except that an analog-to-digital converter was incorporated to provide a punched-tape output of GPC data. This punched tape was used for direct processing of data by computer; thus, all of the calculations to obtain weight-average and number-average DP's and polymolecularity ratios, as well as the plots of the normalized integral and differential molecular weight distribution curves, were performed by computer. The computer program is available on request.

The low molecular weight compounds used to test the effect of substituent groups on the location of peak count were all Eastman White Label grade and were used without further purification.
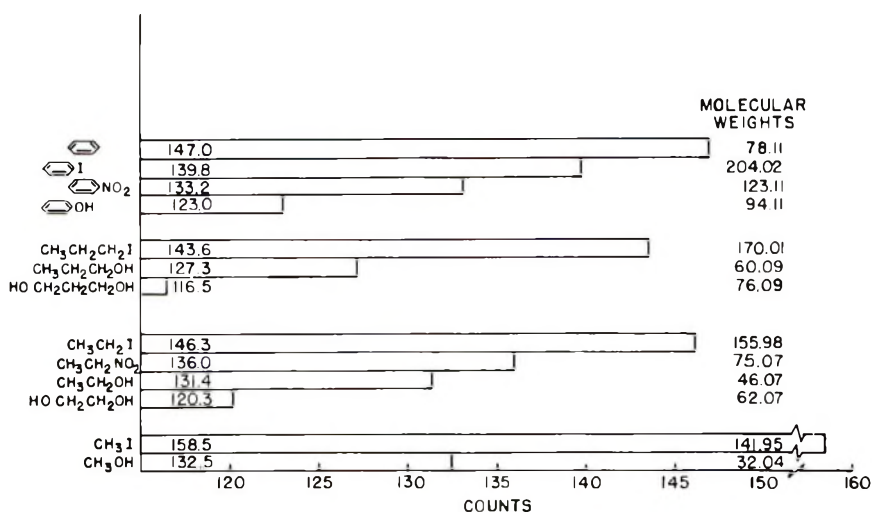
Fig. 2. Effect of substituent groups on location of peak count of low molecular weight monomeric compounds;[5] numbers within the bars are peak counts.

RESULTS AND DISCUSSION

The findings reported by Hendrickson and Moore[5] (Fig. 2) indicate very clearly that molecular weight and chain length of the monomeric compounds studied were not factors of importance insofar as the location of the peak count was concerned; compounds bearing the small hydroxyl group were eluted far sooner than those with the large, electronegative iodine substituent. Furthermore, those compounds with a hydroxyl group at each end of the chain eluted still earlier than did the monohydroxy compounds. Findings of this sort led Hendrickson and Moore to conclude that there was present a very strong solute–solvent interaction (hydrogen bonding) for the hydroxylic compounds dissolved in THF. Because of this interaction, these compounds were highly solvated; they behaved in the GPC columns as if they were very large molecules, far larger in size than their molecular weights or structures would indicate. No consideration whatever is being given here towards relating counts with molecular weights or chain length. Within each series, molecular weight obviously is varying, but chain lengths are not differing greatly. It may well be that Benoit's[9,10] considerations of the effects of the hydrodynamic volume of the dissolved molecule apply to this situation, but these aspects are not within the subject area of the present paper.

Hendrickson and Moore[5] did not include organic nitrates in their study. However, their data on iodobenzene, nitrobenzene, and phenol (Fig. 2) are highly suggestive of what might be expected of the nitrates, i.e., that they would also elute much sooner than their chain lengths or molecular weights would intimate. Experiments with ethanol and n-propanol and their iodide and nitrate derivatives confirm this assumption. The data presented
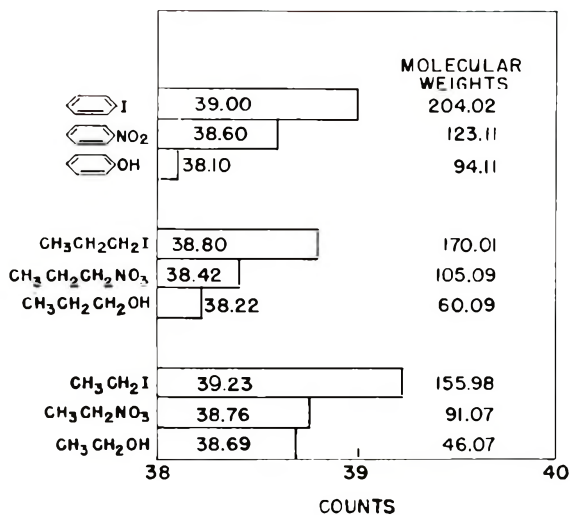
Fig. 3. Effect of substituent groups on location of peak count of low molecular weight monomeric compounds; numbers within the bars are peak counts.

in Figure 3 show that with the present set of four GPC columns (10^7, 1.5×10^6, 10^5, and 3×10^4 Å permeability limits), both the alcohols and the nitrates were eluted much sooner than the iodides, which are of higher molecular weight and larger unsolvated size. It also shows that the alcohols were eluted sooner than the nitrates. Because the permeability limits of the present columns were chosen for polymers of high molecular weight, the differences in elution volumes between these two types of low molecular-weight compounds, the alcohols and the nitrates, are not as clearly defined as would have been achieved by Hendrikson and Moore, whose columns, of course, were chosen specifically for such compounds.

From the data in Figure 3, one might anticipate differences in peak count as the number of hydroxyl groups in partially nitrated cellulose is increased; the data also suggest that the differences in peak count between two samples of different degrees of substitution might be small. In partially nitrated celluloses, hydroxyl groups and nitrate groups are present on the same molecule (see Fig. 1); the effect of a few more or a few less hydroxyl groups may be overwhelmed by the influence of the large number of nitrate groups to be found within the range of 13.6–13.8% N.

One may also deduce from the data of Figure 3 that partially, as well as completely, nitrated cellulose may be eluting much sooner than expected because of high solvation of the polar groups present. The implications of this effect, which may be closely connected to Benoit's[9,10] observations, will be the subject of another paper.

Normalized chromatograms of the celluloses treated with 80–100% nitrating acid are presented in Figure 4; these are arranged in descending order of nitrogen content. Averages of locations of the peak counts also arranged in the same descending order in Figure 5 cannot be described as
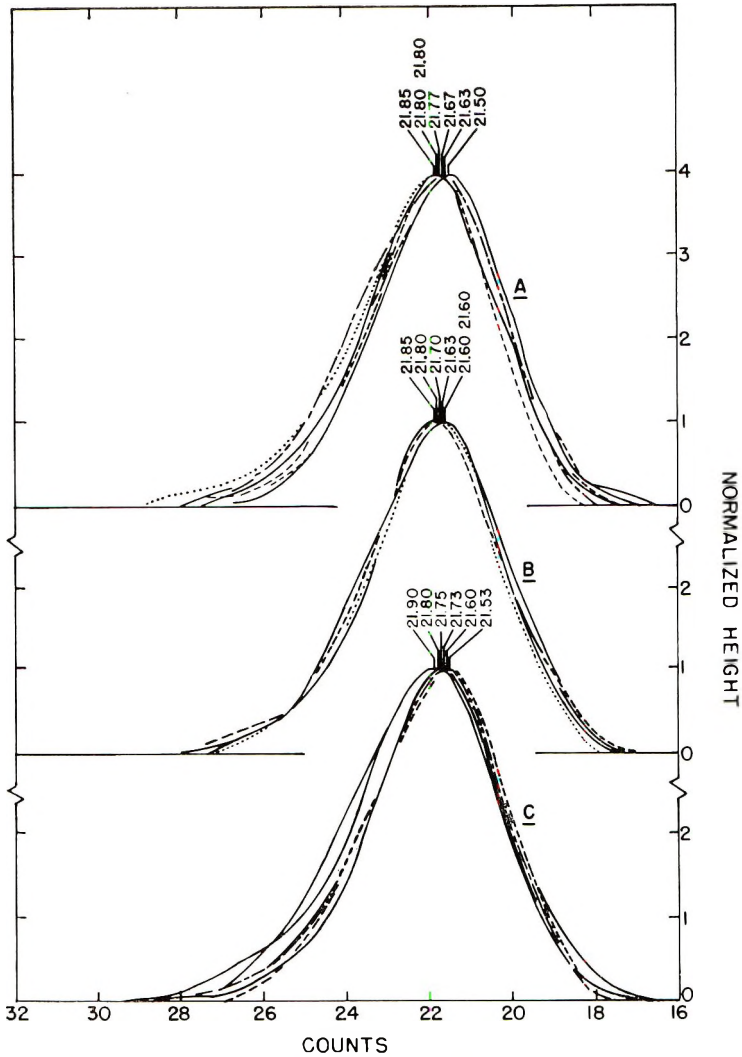
Fig. 4. Normalized chromatograms of nitrated cotton cellulose; (.1) 13.81% N, from 100% nitrating acid; (B) 13.59% N, from 80% nitrating acid; (C) 13.55% N, from 90% nitrating acid.

being different. The standard deviations (0.15, 0.10, 0.12) and the coefficients of variation (0.68, 0.44, 0.56) indicate that there are no significant differences or trends within the range of nitrogen contents of these samples. The spreads of the peak counts for each set are almost identical, and the maximum spread which encompasses all the peak counts for all three sets of curves is only 0.4 count (Fig. 6B).

Although the locations of the peak counts have been found unaffected by the variations in nitrogen content of the samples, one might expect nitrogen content to influence the distribution curves. For example, perhaps the chromatogram for the sample with less nitrogen (and hence more hydroxyl
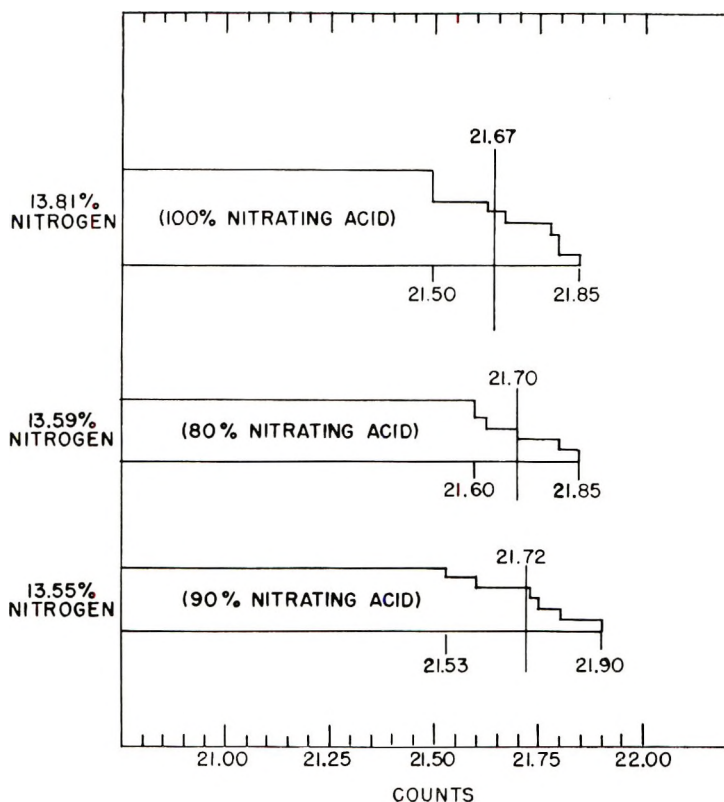
Fig. 5. Location of peak counts for samples of different nitrogen contents. Width of the bars indicates the number of replicates.

groups) would show a shift toward lower counts. This does not seem to be borne out by the curves in Figure 4, at least not with the present range of nitrogen content. Superposition of curves A, B, and C of Figure 4 results in the envelope shown in Figure 6B. Most of the envelope, particularly the portion on the low-count side, is actually developed by the nine curves (Fig. 6A) from the sample with the highest nitrogen content, 13.81% (also shown in Fig. 4A). One can hardly say, then, that increased hydroxyl content on the less highly substituted samples caused any shift toward lower counts.

These findings confirm the conclusions of Bennett and Timell,[11] who reported on the effect of the degree of substitution on the precipitation fractionation of cellulose nitrates. These workers prepared eight nitrates (nitrogen contents of 13.52, 13.64, 13.70, 13.76, 13.82, 13.86, 13.94, and 14.14%) and subjected their acetone solutions to fractional precipitation (diluents: acetone–water, acetone–hexane). The resulting integral DP distribution curves obtained from viscometric data showed that the chain-length distributions of the partially nitrated samples were almost identical with that obtained with the completely nitrated product. From this came the conclusion that the influence of the nonuniformity on distribution
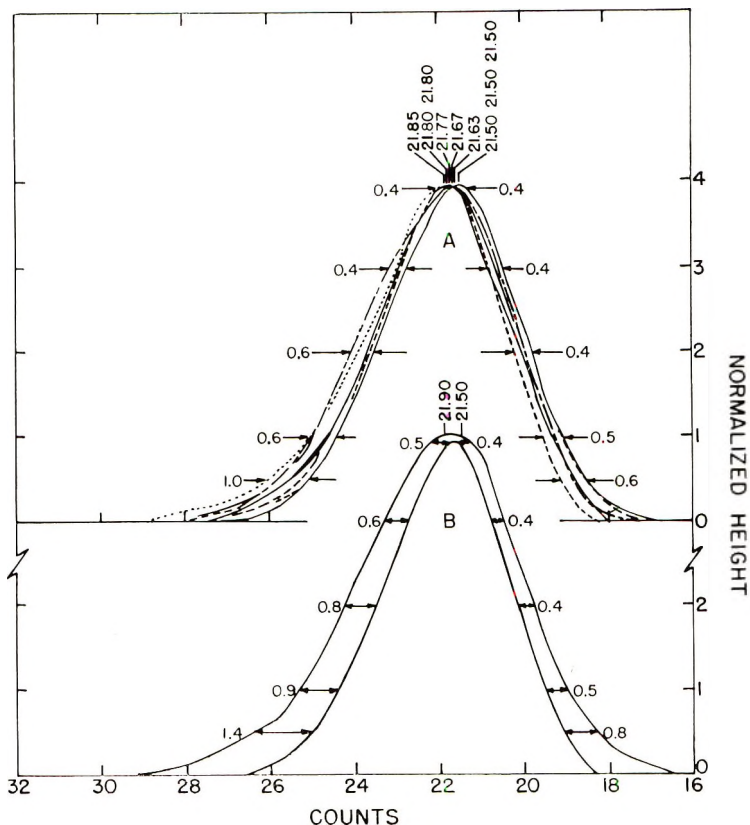
Fig. 6. Variations in the spread of the chromatograms: (A) normalized chromatograms for sample with 13.81% N; (B) envelope of all chromatograms of Fig. 4. Numbers adjacent to the curves give the amount of spread in terms of counts.

results is negligible provided the average nitrogen content is not below 13.5%.

The sample of cotton treated with 75% nitrating acid, containing 13.54% N, was only 88–90% soluble in THF. Such behavior (high substitution but limited solubility in the solvent) can be attributed to nonuniform substitution;[12] this is not at all uncommon in the preparation of cellulose esters and ethers, particularly in heterogeneous reactions such as that of nitration.[12,13] However, the chromatograms of the soluble portion of this sample (Fig. 7) might be considered surprising in that no shifts of the distribution curves relative to those of the first three samples can be detected. The implications of this "partial solution fractionation" of the bulk sample prior to the GPC separation could well be the subject of further investigations on the fine structure of cellulose.

Statistical analysis of the weight-average and number-average DP data (Table I) for these samples indicates that these data were not highly affected by the variations within the present range of nitration. Only in one case did the t test indicate a difference at the 5% level, a difference which was of

TABLE I

Weight-Average and Number-Average Degrees of Polymerization and Polymolecularity Ratios of Samples with Different Nitrogen Contents

	$\overline{DP}_w{}^a$			$\overline{DP}_n{}^a$			DP_w/DP_n		
	13.81% N	13.59% N	13.55% N	13.81% N	13.59% N	13.55% N	13.81%	13.59%	13.55%
	24 130	24 450	24 880	15 860	15 560	15 060	1.52	1.57	1.65
	22 630	23 890	23 850	15 100	15 150	16 060	1.50	1.58	1.49
	22 330	23 590	23 470	15 000	15 720	15 340	1.49	1.50	1.53
	22 120	23 380	22 210	14 260	15 480	14 290	1.55	1.51	1.55
	22 070	22 830	21 330	14 710	15 150	13 040	1.50	1.51	1.63
	21 520	22 400	20 820	12 670	15 300	12 240	1.70	1.46	1.70
	21 420			14 390			1.49		
	21 340			14 240			1.50		
	21 270			14 880			1.43		
Mean	22 090	23 420	22 760	14 570	15 390	14 340	1.52	1.52	1.59
Standard deviation	850	670	1 430	820	210	1 330	0.07	0.04	0.07
Coefficient of variation	3.85	2.85	6.28	5.65	1.39	9.26	4.62	2.72	4.62

a Based on Angstrom length calibration (polystyrene standards), and the appropriate values of Q and molecular weights of the nitrated anhydro-glucose unit according to nitrogen contents in the range 13.5–13.8% N.
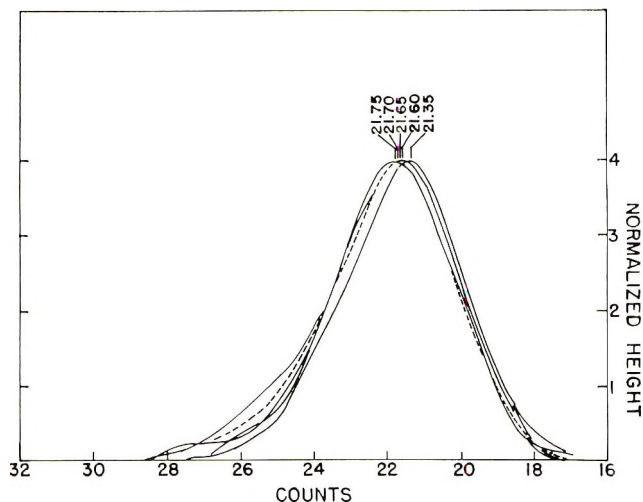
Fig. 7. Normalized chromatograms of nitrated cotton cellulose of 13.54%% N (from 75% nitrating acid).

borderline significance.   This occurs with the two samples of 13.81% and 13.59% nitrogen contents.   At the risk, perhaps, of reading into these data more than may be truly present, one could consider the higher DP values of the latter samples to be a reflection of a higher hydroxyl content.   A high hydroxyl content would afford more sites for increased solvation of the molecule, which then would appear to be larger than it really is.   Comparison of the normalized chromatograms, of course, did not disclose anything like this.

The low variability in the data for the sample of 13.59% N content strongly suggests fairly uniform substitution along the cellulose molecule. Because of the much greater variability in the data for the sample of 13.55% N, one could conclude that a less uniform substitution is present there.   This latter conclusion seems valid if one considers that the sample treated with 75% nitrating acid contains 13.54% N and was only 88–90% soluble in THF.   Uniformity of substitution may play a role, then, in the GPC.   In general, however, what may be extensive solvation of the cellulose nitrate molecule by THF may account for what seems to be very long molecular chains found by the present GPC procedure in cellulosic materials. Because this solvation effect or solute–solvent interaction is of real importance for cellulose studies, and in view of the findings of Benoit and co-workers[9,10] concerning a universal calibration for GPC, further studies are being conducted along these lines.   The results of these studies will be the subject of the second paper in this series.

CONCLUSIONS

The locations of peak counts in the chromatograms of nitrates cotton cellulose with nitrogen contents ranging from 13.55% to 13.81% are not

significantly different. The relatively narrow spread of the chromatograms obtained with these samples suggests that the indicated differential molecular weight distribution of the cellulose is hardly affected by variations in nitrogen content within this range of substitution. The same is true of the average DP data calculated from the chromatograms.

Variations that are observed are considered to be variations arising from within the samples, reflecting, perhaps, some degree of non-uniformity in substitution.

Experiments with low molecular weight organic iodides, nitrates, and hydroxy compounds point to the probability that the cellulose nitrate molecule may be extensively solvated by THF. This may account for the indications of very long, molecular chain lengths in cellulosic materials by the present GPC procedure. Further studies of this factor are in progress.

References

1. L. Segal, in *Analytical Gel Permeation* (*J. Polym. Sci. C*, **21**), J. F. Johnson and R. S. Porter, Eds., Interscience, New York, 1968, p. 267.

2. C. H. Lindsley and M. B. Frank, *Ind. Eng. Chem.*, **45**, 913 (1954).

3. T. E. Timell, *Svensk Papperstid.*, **57**, 913 (1954).

4. M. Marx-Figini, *Makromol. Chem.*, **52**, 133 (1962).

5. J. G. Hendrickson and J. C. Moore, *J. Polym. Sci. A-1*, **4**, 167 (1966).

6. L. Segal, *J. Polymer Sci. B*, **4**, 101 (1966).

7. W. J. Alexander and R. L. Mitchell, *Anal. Chem.*, **21**, 1497 (1949).

8. T. E. Timell and C. B. Purves, *Svensk Papperstid.*, **54**, 303 (1951).

9. H. Benoit, Z. Grubsic, P. Rempp, D. Decker, and J. G. Zilliox, *J. Chim. Phys.*, **63**, 1507 (1966).

10. Z. Grubsic, P. Rempp, and H. Benoit, *J. Polym. Sci. B*, **5**, 753 (1967).

11. C. F. Bennett and T. E. Timell, *Svensk Papperstid.*, **59**, 73 (1956).

12. T. E. Timell, *Svensk Papperstid.*, **58**, 234 (1955).

13. B. Miller and T. E. Timell, *Text. Res. J.*, **26**, 255 (1956).

Thermal Degradation of Poly(vinyl Chloride).
I. Structural Effects in the Initiation and
Decomposition Chain Lengths

V. P. GUPTA and L. E. ST. PIERRE, *Department of Chemistry,*
McGill University, Montreal, Canada

Synopsis

Four poly(vinyl chloride) samples containing different structural irregularities were thermally decomposed. The rates of HCl evolution were compared to the rates of radical generation in the samples. Orders of stabilities related to the structural entities for the initiation of decomposition and for the chain lengths of HCl evolution were established.

INTRODUCTION

Poly(vinyl chloride) has been an important commercial polymer for more than forty years and, as a consequence, it has been the subject of a vast amount of research aimed at the complete spectrum of synthesis, structure, and property problems. Among these problems, a prime area of investigation has been that of thermal stability. Poly(vinyl chloride) exhibits a T_g of 81°C,[1] and during processing, and often in use, it is subjected to elevated temperatures which cause it to undergo a chemical degradation. The degradation is a complex one which has been extensively discussed[2–9] and which can generally be described as a dehydrohalogenation which is accompanied by the formation of a series of conjugated double bonds. These absorb in the visible light range and thus the degraded material can be highly coloured.

Two aspects of the decomposition are important to the contents of this paper. The first is that the dehydrohalogenation is a chain reaction[4] and the second that the initiation of the chains has been shown to be associated with the presence of "structural defects" in the polymer. These defects have been variously identified as endgroups,[4,10–12] branches,[10] olefins, and oxygenated segments.[13,14] The difficulties of positively identifying and quantitatively measuring small numbers of such groups in a macromolecule are obvious. Consequently, recent work has been directed toward the identification of the primary degradation steps by the utilization of model compounds.

Asahina and Onozuka[15] have studied the rates of decomposition of a series of low molecular weight alkyl chlorides which they consider to represent all of the possible structural variations that can be present in poly(vinyl chloride). They have established the rate constants and the energetics for

the degradation of each of these compounds.   If their data are accepted as being representative of the behavior of the macromolecule, the rates and energetics of initiation are now defined, and the primary problem which confronts us has to do with the chain lengths of the dehydrohalogenation chains which begin at these structural irregularities.   The present study is directed to this end.

We have synthesized copolymers which contain the structures studied by Asahina and Onozuka and have then degraded them in the core of an ESR machine.   By simultaneously following the rates of dehydrohalogenation and radical generation, we have established the degradation chain lengths which are associated with each type of structural irregularity.

EXPERIMENTAL

Materials and Preparation

Four types of poly(vinyl chloride) were used in the current study.   They are designated PVC-A, PVC-B, PVC-C, and PVC-D.

PVC-A.   PVC-A was a commercial sample supplied by Shawinigan Chemicals Limited.   The vinyl chloride monomer was polymerized by using benzoyl peroxide as an initiator at 50°C.   The polymer was isolated by drying the reaction mixture under nitrogen gas.   Before using the sample in degradation studies, it was shaken and washed with methanol, filtered, and dried in a vacuum desiccator.

This sample contained no additives and was used in powder form.

PVC-B.   PVC-B was a linear syndiotactic polymer prepared at low temperature, with the use of triisobutylboron as an initiator.   To prepare it, a Pyrex ampoule was connected to a vacuum line and a calculated amount of vinyl chloride was distilled into it under vacuum.   After distillation of the monomer, the ampoule was disconnected from the system, cooled in a Dry Ice–methanol mixture, swept with helium, and the desired amount of initiator was added.   A small amount of air was also introduced in order to accelerate the polymerization reaction.   Finally, the ampoule was sealed and kept at ≈ -43°C for 9.5 days.

The polymer was isolated by pouring the reaction mixture into ice-cold methanol.   It was then filtered, washed, and dried in a vacuum desiccator. The yield was 6%.

The purification of the sample was done by swelling the polymer in 1,2-dichloroethane and precipitating it with petroleum ether.   After a second precipitation it was dried in a vacuum desiccator.

Polyvinyl chloride prepared by this method has been shown to be more linear and syndiotactic than the sample prepared at 50°C by benzoyl peroxide,[16] i.e., PVC-A.   The ratio of syndiotactic to isotactic units in the polymers is given by the ratio of absorbance at 635 cm^{-1} to that at 692 cm^{-1} in the infrared spectra.[16]   These ratios were calculated for PVC-A and PVC-B and are given in Table I.   These ratios suggest that the latter is more crystalline than PVC-A.[16]

TABLE I

Properties of Experimental Poly(vinyl Chlorides)

Sample	Analyses			Propenyl chloride in copolymer, mole-%	$A_{635\ cm^{-1}}$ / $A_{692\ cm^{-1}}$	Sequence length[d] —$(VC)_x$—$(PC)_y$—		T_g, °C[a]	$\bar{M}_n$[b]	Relative crystallinity[c]	Structure
	C, %	H, %	Cl, %			x	y				
A	37.96	4.95	56.44	—	2.1	—	—	86	54,196	1	Regular
B	39.37	5.10	55.09	—	3.6	—	—	87	75,666	1.7	Linear
C	40.00	5.03	54.14	9	—	4.33	1.08	84	27,909	2.2	Tertiary H
D	40.23	4.81	54.43	6	—	7.40	1.06	84	36,776	1.3	Tertiary Cl

a Measured by differential scanning calorimeter, Perkin-Elmer Model DSC1-B.

b Measured by Hewlett Packard high-speed membrane osmometer, Model 502, in cyclohexanone at 60°C.

c Measured by S.R. x-ray diffractometer. The area under the peaks was measured and the per cent crystallinity obtained in the usual way.[19]

d Calculation based on feed ratios and r_1, r_2.[22]

PVC-C. PVC-C was a poly(vinyl chloride) sample having a tertiary hydrogen.

This group was introduced by copolymerizing vinyl chloride with 1-chloropropene.

The methods of preparation, isolation, and purification were the same as for PVC-B. The ampoule was kept at $-43°C$ for 21.5 days and the yield was 2%. The structural defect introduced is shown in structure I.

$$
\begin{array}{c}
\quad\quad\quad\quad\quad H \\
\quad\quad\quad\quad\quad | \\
-CH_2-CHCl-CHCl-CH_2- \\
\quad\quad\quad\quad\quad | \\
\quad\quad\quad\quad\quad CH_3 \\
\quad\quad\quad\quad\quad I
\end{array}
$$
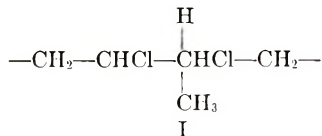
PVC-D. PVC-D was a poly(vinyl chloride) having tertiary chlorine atoms and was prepared by copolymerizing vinyl chloride with 2-chloropropene.

The methods of polymerization, isolation, and purification were the same as mentioned for PVC-B and PVC-C. The reaction mixture was kept at $-43°C$ for 16.5 days and the yield was again 2%. Based on the literature,[17] structure II is to be expected.

$$
\begin{array}{c}
\quad\quad\quad\quad\quad Cl \\
\quad\quad\quad\quad\quad | \\
-CH_2-CHCl-CH_2-CH_2-CHCl- \\
\quad\quad\quad\quad\quad | \\
\quad\quad\quad\quad\quad CH_3 \\
\quad\quad\quad\quad\quad II
\end{array}
$$
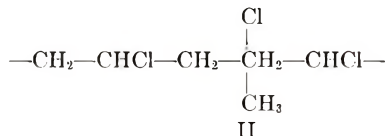
The sequence lengths of the monomers in the copolymer C and D were calculated according to the method of Goldfinger et al.[18] and are shown in Table I along with other properties of the systems studied.

ESR and HCl Measurements

The ESR measurements were performed on a standard Varian model 4500 EPR spectrometer. The powdered polymer samples were placed in a tube and heated inside the cavity of the instrument. The samples were degraded in a nitrogen stream which also acted as a carrier gas for HCl generated from the polymer. The exit gas, carrying the HCl, was then bubbled through conductivity water contained in a conductivity cell. Conductivity measurements were made at $25°C$ on an Industrial Instrument RC-18 conductivity bridge and were used to define the rate of the HCl evolution.

In order to get a uniform packing of the sample in the tube, the polymer was first heated, for a very short time, above the glass transition temperature and then cooled to room temperature. The sample temperature was then increased to the desired decomposition temperature. The spin formation and HCl generation were determined by the ESR signal of the instrument and conductivity measurement respectively.

Thermogravimetric Measurement

Thermogravimetric measurements were performed on a Cahn electro-balance, Model RG. These measurements were made at reduced pressure in a stream of pure nitrogen at a heating rate of 5°C/min. The sample weight was recorded on a 1-mv L and N recorder. The temperatures were measured by using a chromal–alumel thermocouple placed near the sample pan.

A correction for the weight in reduced pressure and weight in air was applied.

The thermogravimetric measurements of all the samples were carried out under identical conditions (heating rate, flow of nitrogen, etc.).

RESULTS AND DISCUSSION

The thermograms from the decomposition of all four polymers studied are shown in Figure 1. From the shapes of the curves, it is apparent that the branched species C and D are considerably less stable than the linear polymer B or the slightly branched (one branch every 400 units[20]) commercial sample A. The enhanced rate for the tertiary chlorine copolymer D is in agreement with the observations of Asahina and Onozuka[15] (Table II). Using model compounds, they observed tertiary chlorides to
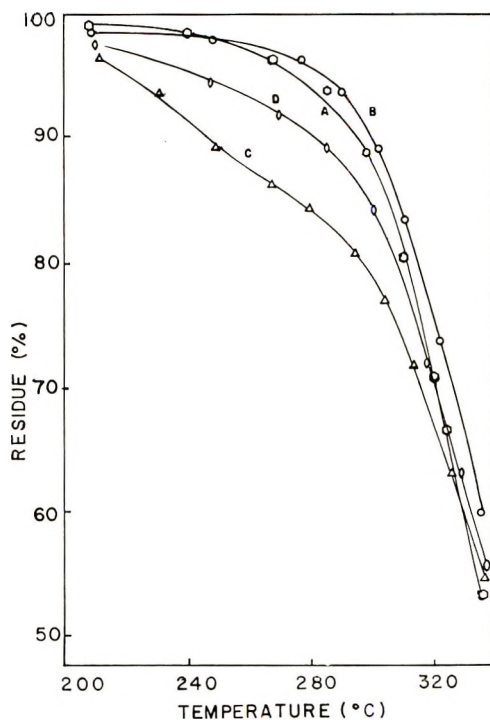
Fig. 1. Relative thermal stability of poly(vinyl chloride) samples by dynamic thermogravimetry: (○) PVC-A; (○) PVC-B; (△) PVC-C; (◊) PVC-D.

TABLE II
Activation Energies for the Dehydrohalogenation of Model Compounds[a]

Compound	E_a, kcal/mole
2-Chloropropane	42.4
2,4-Dichloropentane	69.9
2-Methyl-2-chloropropane	41.6

[a] Data of Asahina and Onozuka.[15]

undergo more rapid thermal degradation than the secondary and to exhibit an activation energy for degradation of about 30 kcal/mole less than that for the secondary structures.

This thermodynamic stability comparison, while useful, does not shed a great deal of light on the degradation when one considers the complexity of the processes involved in the polymer breakdown. Simple HCl evolution rates give little information concerning the rates of initiation and termination of degradation and no information whatsoever on the chain lengths for the HCl ejection. A more complete understanding is possible if the number of propagating chains is monitored during the course of the HCl evolution. Accordingly, isothermal measurements were made where the total HCl evolution and the ESR signal on the decomposing sample were measured simultaneously. These results are shown in Figures 2 and 3.
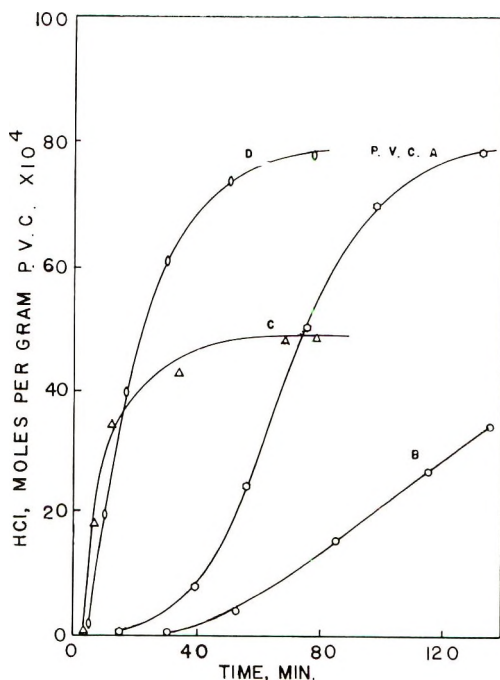
Fig. 2. HCl evolution with time at 224°C: (○) PVC-A; (○) PVC-B; (△) PVC-C; (◊) PVC-D.

TABLE III
Rates of Degradation at Various Temperatures of Poly(vinyl Chloride) Samples

Sample	Temperature, °C	$-d(\text{HCl})/dt \times 10^8$, mole/g/sec[a]	$d(\text{spin})/dt \times 10^{12}$, mole/g/sec[a]	Chain length $\nu \times 10^{-4}$ $\left[= \dfrac{d(\text{HCl})/dt}{d(\text{spin})/dt} \right]$
PVC-A	215	130.5	10.5	12.3
	224	197.9	25.1	7.8
	233	338.8	94.0	3.6
PVC-B	215	30.7	1.7	17.6
	224	57.9	4.3	13.4
	233	335.7	39.2	8.5
	243	772.2	442.7	1.7
PVC-C	188.5	95.2	1.4	65.6
	206	458.3	13.0	35.2
	224	916.6	233.2	3.9
PVC-D	188.5	215.2	11.7	18.3
	206	262.8	54.4	4.8
	215	392.8	89.9	4.3
	224	468.0	210.3	2.2

[a] Rates measured at 10% of total theoretical decomposition.
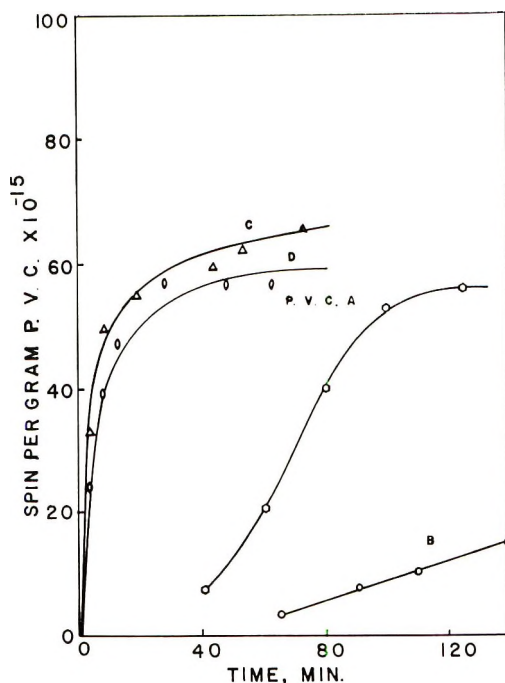
Fig. 3. Spin generation with time at 224°C: (C) PVC-A; (O) PVC-B; (△) PVC-C;
(◊) PVC-D.

In every case both the rates of HCl evolution and the rates of spin genera-
tion underwent a slow initial phase, followed by a rapid first order degrada-
tion and then a leveling off where no further reaction was evident.   It is
interesting to note that the spin concentration increases throughout the
degradation and then persists, thus bringing into question termination
mechanisms based solely on radical coupling.[9]   Indeed, in the present
treatment, we see no alternative but to assume that some terminations
occur when a radical on the polymer chain ends up at some structural point,
such as a crosslink, which does not allow a continued propagation and the
radical then persists in its immobilized matrix.

Since the rates of spin generation parallel the rates of HCl evolution over
the major portion of the decomposition, comparison between them can be
made at any time or degree of degradation.   The data in Table III are the
rates when 10% of the theoretical HCl had evolved.   The temperature
coefficients of the rates, at this same degree of degradation, were used in
calculating activation energies.   (A more detailed kinetic analysis will
appear in a following paper.)

The rates of HCl evolution and spin concentration increase are shown in
Table III and the activation energies associated with these rates are given
in Table IV.

Two activation energies were compared to the model compound data,

TABLE IV
Activation Energies for the Dehydrohalogenation
of Poly(vinyl Chloride) Samples

Sample	E_a (HCl), kcal/mole	E_a (spin), kcal/mole
PVC-A	26 ± 1	56 ± 3
PVC-B	61 ± 5	107 ± 8[a]
PVC-C	29 ± 3	61 ± 3
PVC-D	16 ± 4	34 ± 1

[a] The unduly high E_a (spin) for PVC-B is thought to be related to crystal melting in the decomposition temperature range.

E_a(HCl) the activation energy for HCl evolution and E_a (spin), that for spin generation.

The activation energies for the overall degradation, $-d(HCl)/dt$, are, as one would expect, lower for all structures than are those for spin generation which would be associated with the initiation step. The values are also below the values on the model compounds and the tertiary-halogen-containing polymer, PVC-D, exhibits an exceedingly low E_a(HCl), about half of that for the others.

On the other hand, the energetics of spin generation, $d(spin)/dt$, which are thought to be associated with the initiation of decomposition, were higher than those of the model compounds with one exception, PVC-D. This compound, which contains tertiary halogen groups exhibited the lowest E_a for spin generation and, while the value is somewhat lower than that observed for the tertiary halogen containing model compound, there is a consistency in that both are very low compared to the classical PVC structures. The very high value for the linear polymer further points to branch points as the source of degradation initiation.

Additional insight to the total decomposition process can be obtained by taking the ratio, over the linear portion once again, of $-d(HCl)/dt$, to $d(spin)/dt$. The result yields $d(HCl)/d$ (spin) which, when considered in the usual steady-state manner, is a measure of the relative chain lengths of the propagation step in the degradations. Table III illustrates these comparisons and from it several firm conclusions can be drawn.

Since the manner of preparation of polymers B, C, and D were identical, endgroup effects can be discounted, and one can assume that the polymer structures differ only in relation to the entities introduced by inclusion of comonomers and the regular branching observed in polymers such as PVC-A. On this basis it is seen that measurable decomposition commences at lower temperatures in polymers having the larger number of branch points and the most rapidly decomposing species, at the low temperature, is that containing the tertiary chlorine. Furthermore, the rapidity of the HCl evolution in that system is associated with the higher number of chains rather than the length of the chains. At 224°C (Table V) the branched polymers are markedly less stable than the linear in terms of their rates of

TABLE V
Rates of Degradation at 224°C

	PVC-A	PVC-B	PVC-C	PVC-D
$-d(\text{HCl})/dt \times 10^8$, mole/g/sec	197.9	57.9	916.6	468.0
$d(\text{spin})/dt \times 10^{12}$, mole/g/sec	25.1	4.3	233.2	210.3
Chain length $\nu \times 10^{-4}$ $\left[= \dfrac{d(\text{HCl})/dt}{d(\text{spin})/dt} \right]$	7.8	13.4	3.9	2.2

HCl evolution, and the instability is again associated with the number of propagating chains rather than the chain lengths. The ratios of decomposition rates and chain lengths, $d(\text{HCl})/d$ (spin) are given in Table VI.

TABLE VI

Polymer	Structure	$-d(\text{HCl})/dt$	$d(\text{spin})/dt$	$d(\text{HCl})/d(\text{spin})$
PVC-A	Regular	1	1	1
PVC-B	Linear	0.29	0.17	1.7
PVC-C	Tertiary H	4.6	9.3	0.49
PVC-D	Tertiary Cl	2.3	8.4	0.28

Thus, despite the difference in their E_a (spin), the instabilities of PVC-C and PVC-D, as measured by $-d$ (HCl)/dt, are both due to high initiation rates, which in turn are related to the structural elements in the polymers. However, should the stability be measured in terms of chain length of the HCl evolution, it is also clear that the least stable polymer, once initiation has occurred, is the linear PVC-B.

Returning to the branched polymers, one can analyze them for an order of stability related to the types of branches present. Commercial PVC's will probably have both tertiary hydrogen and tertiary chlorine, but the relative amounts are difficult to define. However, in the PVC-C and the PVC-D polymers, even though both types of defect may be present, the predominant species are the tertiary hydrogen and tertiary chlorine respectively.

Table VII compares their behavior at the two lower temperatures studied. At 188.5°C the PVC-D is decomposing more than twice as fast as PVC-C because it has a very large number of propagating chains. The efficiency of propagation of the tertiary hydrogen containing species is, however, almost four times that of the tertiary halogen polymer. Thus, while the PVC-D is actually the more unstable at 188°C, the higher chain length shows PVC-C to be potentially worse, since it would perform very badly if it contained impurity fragments initiating decomposition. This particular point is manifested most markedly in the comparison of the decomposition rates at 206°C. Here the number of propagating chains

TABLE VII
Rates of Degradation at 188.5 and 206°C

	188.5°C		206°C	
	C	D	C	D
$-d(\text{HCl})/dt \times 10^8$, mole/g/sec	95.2	215.2	458.3	262.8
$d(\text{spin})/dt \times 10^{12}$, mole/g/sec	1.4	11.7	13.0	54.4
Chain length $(\nu) \times 10^{-4}$ $\left[= \dfrac{d(\text{HCl})/dt}{d(\text{spin})/dt} \right]$	65.6	18.3	35.2	4.8

has now increased in both polymers, but the greater chain length in PVC-C results in its rate of decomposition being now twice that of the PVC-D.

It is apparent from their behavior that while the tertiary halogen provides more facile initiation of degradation, it also provides a more rapid termination. The former aspect is undesirable and the latter beneficial in terms of overall stability.

CONCLUSIONS

Three factors are important in establishing the stability of poly(vinyl chloride): The rate of chain initiation, the length of the resultant chain, and the rate of termination. By measuring the spin concentrations in four polymers of defined structure while simultaneously measuring decomposition rate, the following general statements relating structures to stabilities can be made.

Branching in PVC's results in both rapid initiation and termination.

Among the branch types, tertiary halogens initiate and terminate more rapidly than tertiary hydrogens (smaller chain lengths).

Linear polymers do not initiate chains easily but, having been initiated, they have exceedingly long chain lengths for their decompositions.

The chain lengths for HCl evolution, based on the relative rates of generation of HCl to residual spins, are one to two orders of magnitude greater than those previously reported.[21] These values are undoubtedly higher than the actual chain lengths but can be expected to reflect relative stabilities among the polymers studied.

References

1. F. D. Reding, E. R. Walter, and F. J. Welch, *J. Polym. Sci.*, **56**, 225 (1962).

2. A. S. Kenyon, *Symposium on Polymer Degradation Mechanism* (Circ. 525), Natl. Bur. Stand., Washington, D. C., 1953, p. 81.

3. D. Druesedow and C. F. Gibbs, *Symposium on Polymer Degradation* (Circ. 525), Natl. Bur. Stand., Washington, D. C., 1953, p. 69.

4. E. J. Arlman, *J. Polym. Sci.*, **12**, 547 (1954).

5. E. J. Arlman, *J. Polym. Sci.*, **12**, 543 (1954).

6. L. H. Wartman, *Ind. Eng. Chem.*, **47**, 1013 (1955).

7. B. Baum and L. H. Wartman, *J. Polym. Sci.*, **28**, 537 (1958).

8. D. E. Winkler, *J. Polym. Sci.*, **35**, 3 (1959).

9. R. R. Stromberg, S. Straus, and G. B. Achhammer, *J. Res. Nat. Bur. Stand.*, **60**, 481 (1958); *J. Polym. Sci.*, **35**, 355 (1959).

10. W. I. Bengough and H. M. Sharpe, *Makromol. Chem.*, **66**, 31 (1963).

11. A. Crosato-Arnaldi, G. Palma, E. Peggion, and G. Talamini, *J. Appl. Polym. Sci.*, **8**, 747 (1964).

12. G. Talamini and G. Pezzin, *Makromol. Chem.*, **39**, 26 (1960).

13. P. Berticat and G. Vallet, *C. R. Acad. Sci.* (Paris), **261**, 2102 (1965).

14. Z. V. Popova, N. V. Tikhova, and G. A. Razuvaev, *Vysomolekul. Soedin.*, **7**, 731 (1965).

15. M. Asahina and M. Onozuka, *J. Polym. Sci. A*, **2**, 3305, 3315 (1964).

16. J. W. L. Fordham, P. H. Burleigh, and C. L. Sturm, *J. Polym. Sci.*, **41**, 73 (1959).

17. A. Caraculacu, *J. Polym. Sci. A-2*, **4**, 1829 (1966).

18. G. Goldfinger and T. Kane, *J. Polym. Sci.*, **3**, 462 (1948).

19. P. H. Hermans and A. Weidinger, *J. Polym. Sci.*, **4**, 135 (1949).

20. A. Nakajima and K. Kato, *Makromol. Chem.*, **95**, 52 (1966).

21. B. Loy, *J. Polym. Sci.*, **50**, 245 (1961).

22. G. V. Tkachenko, P. H. Khomikovskii, A. D. Abkin, and S. S. Medvedev, *Zh. Fiz. Khim.*, **31**, 242 (1957).

Molecular Weight Distributions in Radiation-Induced Polymerization. III. γ-Ray-Induced Polymerization of Styrene at Low Temperatures

ROBERT Y. M. HUANG and JOHN F. WESTLAKE, *Department of Chemical Engineering, University of Waterloo, Waterloo, Ontario, Canada*

Synopsis

The kinetics of the γ-radiation-induced polymerization of styrene was studied at radiation intensities of 8×10^4, 2.4×10^5, 3.1×10^5, and 8.3×10^5 rad/hr over a temperature range of $-10°C$ to $30°C$. The water content of the irradiated samples varied from 1.0×10^{-3} to 7.5×10^{-3} mole/l. The power dependence of the rate of polymerization on the dose rate at $-10°C$ varied from 0.53 to 0.71 as the water content of the sample varied from 7.5×10^{-3} to 1.0×10^{-3} mole/l. A value of 3.1 kcal/mole was determined for the overall activation energy. Molecular weight distribution studies by gel-permeation chromatography indicated the presence of two distinct peaks. The contribution of each peak was dependent on specific experimental parameters. Kinetic data and molecular weight distribution data indicate the coexistence of two propagating species. Analysis of the data strongly suggests that a free-radical mechanism and a cationic mechanism are involved.

INTRODUCTION

The radiation-induced polymerization of vinyl monomers, in particular styrene, has been the subject of numerous experimental investigations during the last two decades. During this period considerable data were amassed which supported the theory that the radiation-induced polymerization of liquid styrene proceeded via a free-radical mechanism. However, several recent studies by Okamura et al.[1-4] and Metz et al.[5,6] indicated that if styrene was exhaustively purified and dried before irradiation, the subsequent polymerization gave strong indications of proceeding by a cationic mechanism, even at high temperatures. Okamura et al.[2] reported that, at 16°C, a water concentration of approximately $1-2 \times 10^{-3}$ mole/l. suppressed the ionic mechanism to a large degree. In a preliminary communication from this laboratory [7] the coexistence of free-radical and cationic reaction mechanisms in the γ-ray-induced polymerization of styrene in a transition region of water concentration (approximately 2×10^{-3} mole/l.) was reported. The existence of two reaction mechanisms gave rise to a bimodal molecular weight distribution of the polystyrene.

The present series of studies is concerned with the kinetics and the molecular weight distributions of the γ-ray-induced polymerization of vinyl

49

monomers in the liquid and solid states. In previous papers[7-9] the polymerization kinetics and the molecular weight distributions of the γ-ray-induced polymerization of styrene in the liquid state over a temperature range of 0-50°C were reported. The purpose of the present study is to conduct similar investigations at lower temperatures in both the liquid and solid states and to determine the effect of water concentration on the polymerization kinetics and the resulting molecular weight distributions.

EXPERIMENTAL

Materials

Monomer. Styrene (Eastman Organic Chemicals) was washed three times with 6% sodium hydroxide solution and three times with distilled water to remove the inhibitor, then dried over anhydrous calcium chloride for one day in a refrigerator. The styrene was distilled at 36-40°C and 13-16 mm Hg absolute pressure. The middle fraction was tested for the presence of polystyrene and then stored in a refrigerator until used in the preparation of ampoules for irradiation (within 16 hr).

Methanol. (ACS grade, Fisher Scientific Company) containing the free-radical inhibitor hydroquinone (purified, Fisher Scientific Company) was used for the precipitation of polystyrene from the reaction mixture after irradiation.

Polystyrene Standards. Eleven standard monodisperse ($\bar{M}_w/\bar{M}_n = 1.04-1.20$) polystyrene samples with molecular weights of 900, 2100, 4800, 10 300, 19 800, 51 000, 97 200, 16×10^4, 41.1×10^4, 86×10^4, and 18×10^5 were obtained from the Pressure Chemical Company of Pittsburgh, Pennsylvania, and used for the calibration of the gel-permeation chromatograph.

Equipment

Radiation Facility. The irradiation source used in the present study was a Gammacell 220 ^{60}Co γ-ray irradiation facility, designed and built by the Commercial Products Division, Atomic Energy of Canada Limited, Ottawa, Ontario. By using a series of lead attenuators, four radiation intensities ranging from 7.4×10^4 to 8.5×10^5 rad/hr are obtainable in the sample chamber.

Temperature Control. Ampoules containing the reaction mixture were maintained at the desired temperature during irradiation by placing them in a reaction cell through which the coolant (methanol) was circulated. Temperature control was maintained by using a Lauda UK80DW Ultra Kryostat, Model 1967. Temperature in the cell was monitored by using a sensitive thermistor detector. The temperature in the cell for all runs was maintained to within ±0.05°C of the desired value.

Monomer Purity Analysis. An analysis of monomer purity was made on one ampoule from each set of runs. The monomer was analyzed for

water content and organic impurities on a Hewlett Packard 5754B gas
chromatograph. The concentration of water in the sample was determined
by temperature-programming the sample from 100°C to 225°C on a 4-ft
column (Porapak Q) with the use of a thermal conductivity detector at
250°C. Organic impurities were determined by temperature program-
ming the sample from 30°C to 250°C on a 6 foot column (UC-W98) using a
flame ionization detector. Monomer purity ranged from 99.82 to 99.86%
and the water content of the sample varied from 1.0×10^{-3} to 7.5×10^{-3}
mole/l.

Gel-Permeation Chromatography. The molecular weight distribution
of the product polystyrene was determined by using gel-permeation
chromatography. A Waters GPC unit, Model 200, fitted with four ana-
lytical columns of designated size 10^7, 10^5, 10^4, and 10^3 A° was used.
Tetrahydrofuran (Fisher Certified ACS Grade) was used as the eluting
solvent. The flow rate was maintained at 1.0 ml/min and the oven
temperature was kept at $25 \pm 0.5°C$. Sample injection time was 60 sec,
corresponding to a sample injection of 1.0 ml. The effect of sample con-
centration was corrected for using the method proposed by Cantow.[10]
Calibration with the eleven standard samples followed the universal cali-
bration concept proposed by Boni,[11] assuming the effective separation
parameter to be the equivalent hydrodynamic volume.

Procedure

The polymerizations were carried out in 10-ml glass ampoules. Ap-
proximately 300 ml of previously distilled styrene was degassed by suc-
cessive freeze-thaw cycles while under continuous pumping. Four or five
cycles were sufficient to degas the monomer, which was then placed under a
nitrogen atmosphere. The monomer was transferred to a filling vessel
and the individual ampoules (also under a nitrogen atmosphere) were
filled. The ampoules were flame-sealed under vacuum at a pressure of
10^{-3} mm Hg. The weight of each sample was determined gravimetrically
and the ampoules were then stored at $-30°C$ until irradiated. Irradia-
tions were conducted at the desired dose rate and temperature for time
intervals such that the conversion for most samples was less than 5%.
Following irradiation the contents of the ampoule were precipitated in a
50–60-fold excess of rapidly stirred methanol containing hydroquinone.
The precipitated polystyrene was filtered on sintered glass Gooch crucibles
containing #42 Whatman filter paper and then dried to constant weight at
58–60°C in a vacuum oven. The per cent conversion was determined
gravimetrically. Polymerization runs were carried out at -10, 0, 15, and
30°C. Runs at $-10°C$ were performed at radiation dose rates of 7.5×10^4, 2.4×10^5, 3.1×10^5, and 8.3×10^5 rad/hr. Runs at 0, 15, and 30°C
were conducted at a radiation dose rate of 8.2×10^5 rad/hr. The maxi-
mum reaction time for various runs ranged from 5 to $37^1/_2$ hr, depending
on the dose rate and temperature.

The molecular weights and the molecular weight distribution were de-

termined by gel-permeation chromatography. In order to ensure that the
distribution obtained was representative of the molecular distribution of
the polymer formed, the entire sample was dissolved in THF. An aliquot
was then taken and diluted to give a 0.25 wt-% solution. Sample in-
jection time was 60 sec, corresponding to 1.0 ml of polymer solution. The
number-average ($\bar{M}_n$) and weight-average ($\bar{M}_w$) molecular weights were
calculated from the gel-permeation chromatogram and calibration data
according to the method recommended by Waters. Correction for im-
perfect resolution was made by using the Hermite polynomial expansion
method of Tung.[12]

RESULTS

Experimental data for the per cent polymerization versus reaction time
at $-10°C$ for various dose rate and water concentrations are plotted in
Figures 1–3. In most cases the per cent conversion was maintained below
5% to avoid the Trommsdorff effect. The polymerization rates calculated
from the kinetic data (method of least squares) indicate that the rate of
polymerization is dependent upon the water content of the irradiated
sample, and that this dependency increases as the dose rate increases.
Figure 4 illustrates the polymerization rate dependence upon reaction
temperature. The overall activation energy calculated from an Arrhenius
plot of polymerization rate versus $1/T$ was 3.1 kcal/mole. This value lies
between the values obtained for purely ionic and purely free-radical
polymerization (see Table I). Another interesting result is the variation
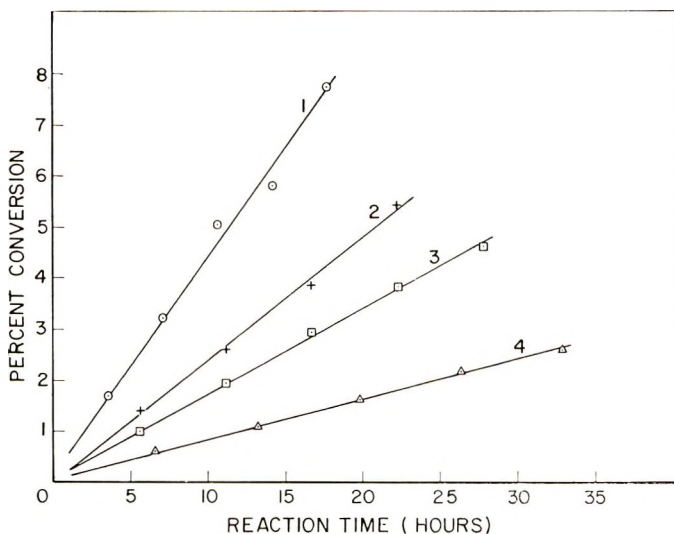
Fig. 1. Kinetic data, conversion vs. reaction time: (1) dose rate 0.842 Mrad/hr, slope
0.421%/hr; (2) 0.318 Mrad/hr, 0.236%/hr; (3) 0.246 Mrad/hr, slope 0.165%/hr; (4)
0.075 Mrad/hr, slope 0.078%/hr. Water content 1.0×10^{-3} mole/l.; temperature
$-10.0°C$.
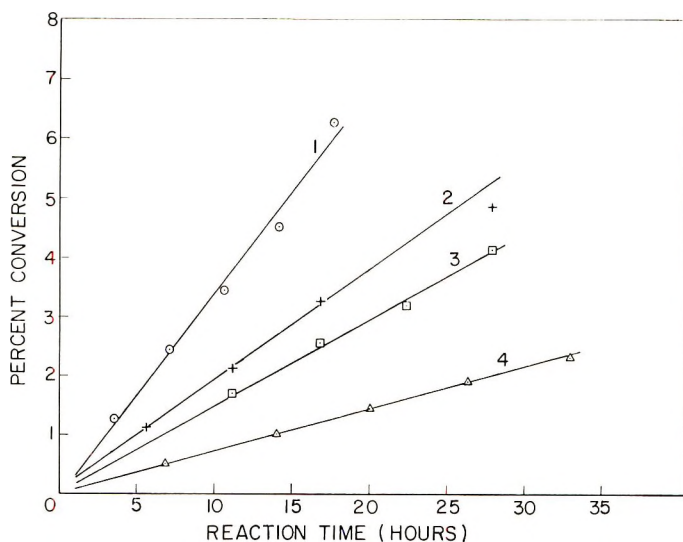
Fig. 2. Kinetic data, conversion vs. reaction time: (*1*) dose rate 0.833 Mrad/hr, slope 0.323%/hr; (*2*) 0.314 Mrad/hr, 0.176%/hr; (*3*) 0.244 Mrad/hr, 0.138%/hr; (*4*)0.075 Mrad/hr, 0.067%/hr. Water content 2.5×10^{-3} mole/l.; temperature $-10.0°C$.
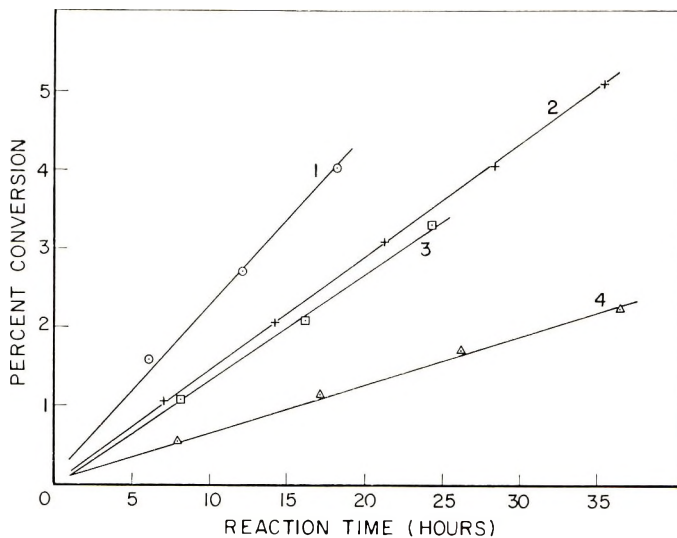
Fig. 3. Kinetic data, conversion vs. reaction time: (*1*) dose rate 0.824 Mrad/hr, slope 0.218%/hr; (*2*) 0.311 Mrad/hr, 0.144%/hr; (*3*) 0.241 Mrad/hr, 0.135%/hr; (*4*) 0.074 Mrad/hr, 0.061% hr. Water content 7.5×10^{-3} mole/l.; temperature $-10.0°C$.

of the dependence of the rate of polymerization upon dose rate with the water content of the sample. The data of Table II show that the polymerization rate dependence on dose rate increases from 0.53 at a water concentration of 7.5×10^{-3} mole/l. to 0.71 at a water concentration of 1.0×10^{-3} mole/l.
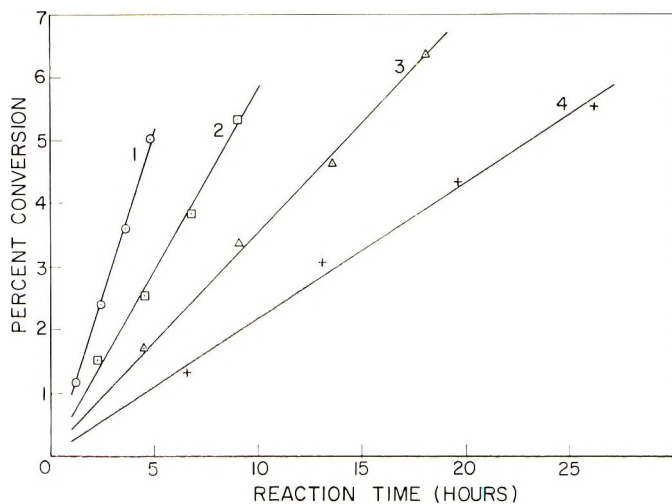
Fig. 4. Kinetic data, conversion vs. reaction time: *(1)* +30.0°C, slope 1.031%/hr; *(2)* +15.0°C, 0.574%/hr; *(3)* 0°C, 0.345%/hr; *(4)* −10.0°C, 0.214%/hr. Water content 5.2 × 10⁻³ mole/l.; dose rate 0.815 Mrad/hr.

By far the most interesting aspect of the results obtained is the effect of temperature, conversion, dose rate, and water concentration on the molecular weight distributions.

Figure 5 depicts the effect of polymerization temperature on the molecular weight distribution. Related results at different experimental conditions have been reported in a previous communication.[7] The molecular weight distribution of the sample polymerized at 30°C (curve 1) is unimodal and quite narrow. However, as the polymerization temperature is

TABLE I
Overall Activation Energy of γ-Ray-Induced Polymerization of Styrene

Overall activation energy, kcal/mole	Polymerization mechanism	Investigator
7.15	Free-radical	Ballantine et al.[13] (Corrected value by Chapiro[16])
6.0–6.3	Free-radical	Huang et al.[8]
3.1	Free-radical and cationic	Present work
∼0	Cationic	Okamura et al.[2]
Small negative value	Cationic	Metz et al.[6]

TABLE II
Dependence of Polymerization Rate on Dose Rate

Water concentration, mole/l.	Power dependence ($R_p \propto I^n$)
7.5 × 10⁻³	0.53
2.5 × 10⁻³	0.66
1.0 × 10⁻³	0.71
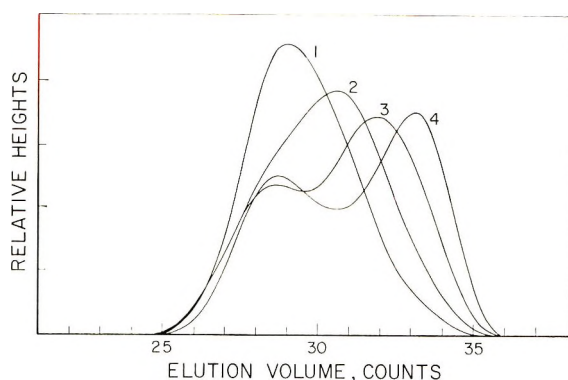
Fig. 5. GPC Chromatogram, effect of temperature on the molecular weight distribution: (1) +30.0°C, 4.98% conversion; (2) +15.0°C, 5.47%; (3) 0.0°C, 5.30%; (4) −10.0°C, 4.59%. Water content 5.2 × 10⁻³ mole/l.; dose rate 0.815 Mrad/hr.

decreased, the distribution broadens (15°C), and a second peak (hereafter referred to as the secondary peak) appears in the distribution (0°C) and contributes significantly to the overall distribution at −10°C. Thus a decrease in the polymerization temperature from 30°C to −10°C has resulted in changing the molecular weight distribution from a relatively narrow, unimodal distribution to a broad, bimodal distribution. The values of $\bar{M}_n$, $\bar{M}_w$, and $\bar{M}_w/\bar{M}_n$ for the temperature studies conducted at a dose rate of 8.2×10^5 rad/hr and a water concentration of 5.2×10^{-3} mole/l. are presented in Table III. The values obtained at 30°C are in good agree-

TABLE III
Molecular Weight and Molecular Weight Distribution Data
at Radiation Dose Rate 8.15×10^5 rad/hr.

Polymerization temperature, °C	Conversion, %	$\bar{M}_w$	$\bar{M}_n$	$\bar{M}_w/\bar{M}_n$
30.0	1.15	54 500	30 400	1.79
	2.36	49 500	26 200	1.89
	3.56	49 000	25 600	1.91
	4.98	44 000	23 600	1.86
15.0	1.49	41 400	17 600	2.36
	2.52	36 600	17 100	2.14
	3.81	36 300	16 300	2.23
	5.30	36 800	15 500	2.38
0.0	1.69	36 100	13 400	2.69
	3.34	35 900	11 900	3.03
	4.59	32 800	10 200	3.21
	6.32	33 400	10 400	3.23
−10.0	1.29	27 000	9 400	2.86
	3.02	31 000	8 500	3.62
	4.28	28 600	7 200	3.96
	5.47	28 400	6 900	4.15
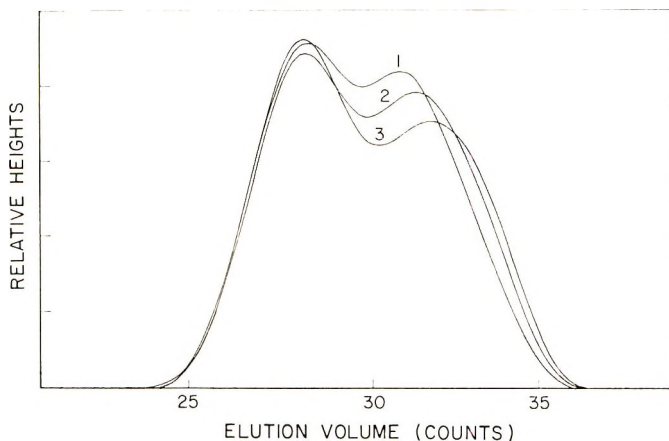
Fig. 6. GPC chromatogram, effect of per cent conversion on the molecular weight distribution at $-10°C$: (1) 1.36% conversion; (2) 2.52%; (3) 5.29%. Dose rate, 0.318 Mrad/hr; water content 1.0×10^{-3} mole/l.; temperature $-10.0°C$.

ment with previously reported values for the radiation-induced free-radical polymerization of styrene.[8]   An overall shift of the molecular weight distribution in the direction of decreasing molecular weight with decreasing temperature (Fig. 5) is reflected by a decrease in the values of $\bar{M}_w$ and $\bar{M}_n$.   This decrease becomes less apparent as the temperature decreases because of distribution broadening and the subsequent appearance of a second, high molecular weight peak in addition to the primary (original) peak.   Also, the value of the polydispersity ratio $(\bar{M}_w/\bar{M}_n)$ increases considerably as the polymerization temperature decreases.   This is a result of distribution broadening caused by the appearance of the secondary peak.

The effect of the second variable, conversion, on the molecular weight distribution is illustrated in Figure 6.   Three features of this graph are worth noting.   For the bimodal distributions, the contribution of the secondary peak to the overall molecular weight distribution increases as the sample conversion increases.   The position of the secondary peak remains essentially constant as conversion increases.   On the other hand, the primary peak shifts in the direction of decreasing molecular weight.   Figure 7 illustrates the effect of dose rate on the molecular weight distribution: For the lowest dose rate (curve 4), the molecular weight distribution is unimodal.   As the dose rate increases the secondary peak appears and becomes predominant at the highest dose rate (curve 1).   Note also that both peaks shift as the dose rate increases.   The secondary peak shifts in the direction of increasing molecular weight and the primary peak shifts in the direction of decreasing molecular weight.

The effect of the water content of the sample on the molecular weight distribution is perhaps the most interesting.   This is illustrated in Figure 8.   Two aspects of this graph are noteworthy.   In the case of the bimodal distribution, the amount that each peak contributes to the overall molecular
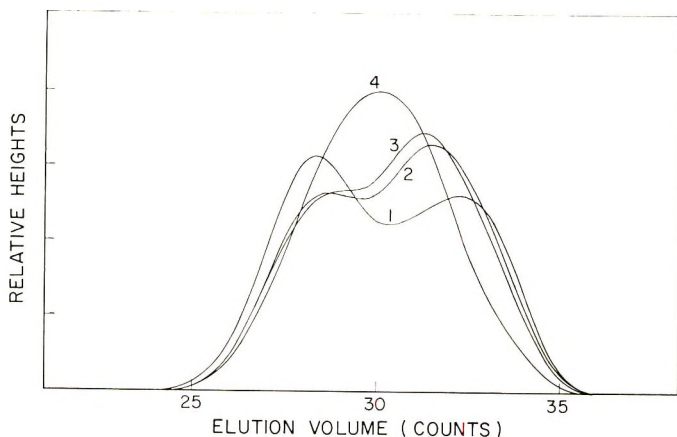
Fig. 7. GPC chromatogram, effect of dose rate on the molecular weight distribution at $-10°C$: (1) dose rate 0.833 Mrad/hr, 2.27% conversion; (2) 0.314 Mrad/hr, 1.97%; (3) 0.244 Mrad/hr, 2.38%; (4) 0.075 Mrad/hr, 2.16%. Water content 2.5×10^{-3} mole/l.
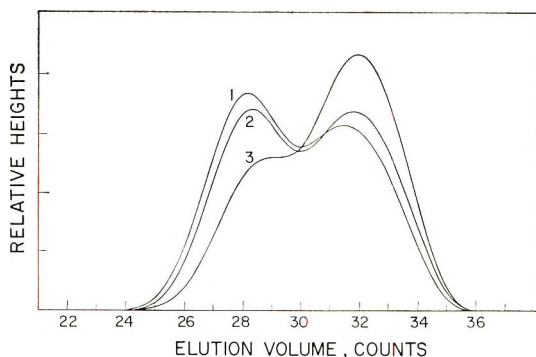
Fig. 8. GPC chromatogram, effect of water concentration on the molecular weight distribution at $-10°C$: (1) water concentration 1.0×10^{-3} mole/l., 3.75% conversion; (2) 2.5×10^{-3} mole/l., 3.04%; (3) 7.5×10^{-3} mole/l., 3.04%. Dose rate 0.314 Mrad/hr; temperature $-10.0°C$.

weight distribution is determined, to a large degree, by the water content of the sample. The second interesting feature is that both peaks shift in the direction of decreasing molecular weight as the water content of the sample is increased.

DISCUSSION

The results presented in the preceding section cannot be explained in terms of an exclusively free-radical mechanism. The power dependence of the polymerization rate upon the dose rate, the magnitude of the activation energy, and in particular the molecular weight distributions strongly indicate the presence of two distinct reaction mechanisms. In a recent

publication, Okamura et al.[2] reported that a water concentration of approximately $1-2 \times 10^{-3}$ mole/l. was sufficient to suppress any ionic contribution to the polymerization mechanism at 16°C. Therefore, the radiation-induced polymerization of styrene proceeds by a free-radical mechanism in a "wet" system and a cationic mechanism in a "dry" system. The present study was conducted at $-10°C$ with water concentrations ranging from 1.0×10^{-3} to 7.5×10^{-3} mole/l. It is plausible that the experimental conditions of the present study, where the styrene monomer purity lies between the wet and dry systems, would lead to a polymerization process in which both a free-radical and an ionic mechanism (specifically a cationic mechanism) are operative simultaneously. The discussion to follow supports this postulate.

The experimentally determined value for the overall activation energy, 3.1 kcal/mole, is approximately half of those previously reported for the free-radical polymerization of styrene. Recent studies of styrene polymerization in a dry system via a cationic mechanism indicate that the overall activation energy for this process is approximately 0 kcal/mole (see Table I). An intermediate value would suggest that polymerization by both mechanisms is occurring. The variation in the dependence of the polymerization rate on dose rate (Table II) can readily be explained in terms of the above postulate. For radiation-induced cationic polymerization in dry systems, the dependence of the polymerization rate on the dose rate has been reported to be 1.0 for samples of high purity samples and decreases to values near 0.5 for "ultra pure and dry" samples.[2-4,6,14] It is also well known that the polymerization rate for the radiation-induced free-radical polymerization of styrene in a wet system exhibits the classical 0.5-power dependence on the dose rate. In the present study the sample purity lies between the wet and dry, high purity regions, and hence the experimentally determined values for the polymerization rate-dose rate power dependence which lie between 0.5 (free-radical mechanism) and 1.0 (cationic mechanism) could be attributed to the co-existence of two propagating species. The data of Figures 1–3 indicate that the rate of polymerization increase as the water content of the sample decreases. This effect has been observed for cationic polymerization in a dry system[2,5,6] and suggests that, in our system, one of the propagating species is ionic in nature. As mentioned previously, it has been reported by Okamura et al.[2] that the reaction mechanism becomes predominantly free-radical if the water concentration is increased above a value of approximately $1-2 \times 10^{-3}$ mole/l. This explains the reduction in the polymerization rates and the approach of the polymerization rate–dose rate power dependence to a value of 0.5 as the water content of the sample increases from 1.0×10^{-3} to 7.5×10^{-3} mole/l.

Additional evidence for the hypothesis of two propagating species may be found by examining the effect of temperature, conversion, dose rate and water concentration on the molecular weight distributions. In the following discussion, an attempt will be made to attribute each peak of the bi-

modal distributions to a specific reaction mechanism by analyzing the effect of the previously mentioned variables on the molecular weight distributions.

Figure 5 illustrates the effect of reaction temperature on the molecular weight distribution. The secondary peak begins to contribute to the molecular weight distribution as the polymerization temperature decreases, becoming quite prominent at $0°C$. Since a cationic mechanism is favored at lower temperatures, the secondary peak is tentatively attributed to a cationic mechanism and the primary peak to a free-radical mechanism. The secondary peak does not contribute significantly to the molecular weight distribution at $15°C$ (curve 2), but it is quite prominent at $0°C$ (curve 3). This increase in the proportion of cationic polymerization at $0°C$ could be the result of a decrease in the 'effective' inhibitor concentration of the sample due to partial 'freezing out' of the water. Considering now the two curves for which the secondary peak is reasonably prominent (curves 3 and 4), it is evident that, as the polymerization temperature increases, the primary peak shifts considerably in the direction of increasing molecular weight while the secondary peak does so only to a small degree. The kinetics of free-radical polymerization predict an increase in the number-average molecular weight with increasing temperature, while experimentally determined values[2,14] of $\bar{M}_n$ and $\bar{M}_v$ for the radiation-induced cationic polymerization of styrene indicate a slight decrease in molecular weight with increasing temperature. It is felt that the tentative peak-reaction mechanism assignment is still valid. The preceding evidence, however, is somewhat inconclusive.

It is apparent from Figure 6 that the secondary peak becomes more predominant as conversion increases. This can be explained if the secondary peak is attributed to a cationic mechanism. In the early stages of polymerization, the growing cationic chains may be terminated by small amounts of water present in the sample. However, the inhibitor concentration decreases with time due to continued freezing out of the water, and hence the amount of cationic polymerization increases with increasing conversion. Figure 6 illustrates another interesting point. The position of the secondary peak remains constant as conversion increases. Okamura et al.[2] have reported that the molecular weight is independent of conversion for the cationic polymerization of styrene. On the other hand, the primary peak shifts slightly in the direction of decreasing molecular weight. This is in agreement with the molecular weight distribution theory of free-radical polymerization.[15] Although it is experimentally impossible to resolve completely the two contributing peaks of the bimodal distributions, it has been established that the secondary peak is insensitive to changes in conversion, and as shown later, relatively insensitive to dose rate. Therefore, a calculation of the average peak molecular weight for the secondary peak of all reasonably developed bimodal distributions is of considerable interest. The average peak molecular weight was 58 000 with a standard deviation of 5700. Since the number-average molecular weight $\bar{M}_n$ is

somewhat lower than this value, the present results agree reasonably well with the values of approximately 47 000 for $\bar{M}_n$ obtained by Okamura et al.[2] and also with the viscosity-average molecular weights $\bar{M}_v$ of approximately 75 000 determined by Metz et al.[5]

Figure 7 shows the effect of dose rate on the molecular weight distribution. The secondary peak becomes more predominant as the dose rate increases. If the polymerization process is proceeding via two reaction mechanisms, as postulated, the mechanism having the higher dose rate dependence will become more prominent with increasing dose rate. Since the polymerization rate-dose rate dependence of free-radical and cationic polymerizations are 0.5 and 1.0, respectively (for our system), it is concluded that the secondary peak is the result of cationic polymerization. Curves 1, 2, and 3 indicate a shift of the secondary peak in the direction of increasing molecular weight with increasing dose rate while the reverse is true of the primary peak. The latter observation is consistent with free-radical kinetics.[15] For cationic polymerization, Okamura et al.[2] reported a slight increase in molecular weight with increasing dose rate which is consistent with the present results. The molecular weight data of Potter[14] at 0°C agree with these findings.

Consider now the effect of the fourth variable, water concentration, on the molecular weight distribution. Figure 8 illustrates that the amount that each peak contributes to the overall molecular weight distribution is a strong function of the water concentration, especially at high dose rates.[7] The contribution of the secondary peak increases substantially as the water concentration decreases from 7.5×10^{-3} to 1.0×10^{-3} mole/l. This increase in the amount of cationic polymerization with decreasing water content coincides with the findings of Okamura et al.[1,2] and Metz et al.[5,6,14] for the polymerization of liquid styrene.

The preceding discussions present strong evidence for the postulate of the coexistence of two propagating species, one free-radical and the other cationic. It is apparent from consideration of the experimental parameters involved and the results of other workers that the water content of the sample is the key factor responsible for this occurrence. Since ionic and free radical polymerizations occur in "dry" and "wet" systems, respectively, the present results strongly indicate the existence of a transition region (with respect to water concentration) in which a novel combination of polymerization mechanisms occurs. In a previous paper it was reported that the value of the polydispersity ratio for the free-radical polymerization of styrene over a temperature range of 0°C to 50°C was 1.80–2.00.[8] At that time the high polydispersity ratios were thought to be a result of chain transfer to monomer, termination by disproportionation, graft copolymerization, or chain branching. In view of the present results, however, it is felt that the high ratios resulted from a slight broadening of the molecular weight distribution due to a small contribution of ionic polymerization in addition to the free-radical polymerization.

The GPC data presented in this paper indicate that the molecular weight

distribution is a very sensitive indicator for the effect of various experimental parameters such as dose rate, temperature, conversion and water concentration on the reaction kinetics. Thus, the study of the molecular weight distribution of the polymerization products provides valuable information with regard to the reaction mechanism, or mechanisms, involved.

References

1. K. Ueno, K. Hayashi, and S. Okamura, *J. Polym. Sci. B*, **3**, 363 (1965).

2. K. Ueno, K. Hayashi, and S. Okamura, *Polymer*, **7**, 431 (1966).

3. K. Ueno, F. Williams, K. Hayashi, and S. Okamura, *Trans. Faraday Soc.*, **63**, 1478 (1967).

4. K. Ueno, K. Hayashi, and S. Okamura, *Polymer*, **7**, 451 (1966).

5. R. C. Potter, C. L. Johnson, D. J. Metz, and R. H. Bretton, *J. Polym. Sci. A-1*, **4**, 419 (1966).

6. R. C. Potter, R. H. Bretton, and D. J. Metz, *J. Polym. Sci. A-1*, **4**, 2295 (1956).

7. R. Y. M. Huang and J. F. Westlake, *J. Polym. Sci. B*, **7**, 713 (1969).

8. R. Y. M. Huang, J. F. Westlake, and S. C. Sharma, *J. Polym. Sci. A-1*, **7**, 1729 (1969).

9. R. Y. M. Huang and P. Chandramouli, *J. Polym. Sci. B*, **7**, 245 (1969).

10. M. J. R. Cantow, R. S. Porter, and J. F. Johnson, *J. Polym. Sci. B*, **4**, 707 (1966).

11. K. A. Boni, F. A. Sliemers, and P. B. Stickney, *J. Polym. Sci. A-2*, **6**, 1579 (1968).

12. L. H. Tung, *J. Appl. Polym. Sci.*, **10**, 375 (1966).

13. D. S. Ballantine, P. Colombo, A. Glines, and B. Manowitz, *Chem. Eng. Progr. Sympos. Ser.*, **50**, 267 (1954).

14. R. C. Potter, Ph.D. Thesis, Yale University, New Haven, Conn., 1966.

15. C. H. Bamford, W. G. Barb, A. D. Jenkins, and P. F. Onyon, *The Kinetics of Vinyl Polymerization by Radical Mechanisms*, Butterworths, London, 1958, Chap. 7.

16. A. Chapiro, *Radiation Chemistry of Polymeric Systems*, Interscience, New York 1962.

Synthesis of a Spirobenzothiazoline Polymer and its Thermal Rearrangement to a Polydihydrobenzothiazine

J. M. AUGL and W. J. WRASIDLO, *U. S. Naval Ordnance Laboratory, White Oak, Silver Spring, Maryland 20910*

Synopsis

The reaction of 3,3'-dimercaptobenzidine with 1,4-cyclohexanedione leads to a soluble, high molecular weight, spirobenzothiazoline polymer. Above 200°C the spirolinks of this polymer rearrange into a ladder structure leading to a polydihydrobenzothiazine.

The synthesis of benzothiazolines by reacting o-aminothiophenols with ketones has been described in the literature.[1-3] We have reported the preparation and characterization of two stereoisomers of hexahydrophenothiazine.[4-6] Hackmack and Krastinat[7] reported that one of the isomers of hexahydrophenothiazine (II) can also be obtained by a thermal rearrangement of 2,2-spiropentamethylenebenzothiazoline (I). The reaction takes place as shown in eq. (1).
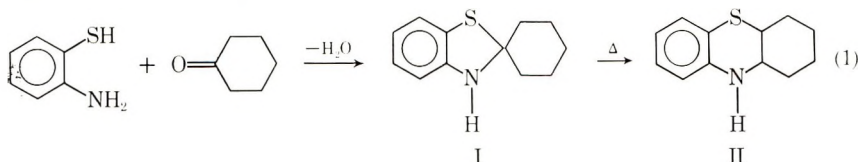
Adapting this route and using bifunctional reagents, we prepared a spirobenzothiazoline polymer and its thermally rearranged product, a polydihydrobenzothiazine.

RESULTS AND DISCUSSIONS

The reaction of 1,4-cyclohexanedione with 3,3'-dimercaptobenzidine dihydrochloride leads to a high molecular weight polymer (III) ($\eta_{inh} = 1.01$ dl/g), as shown in eq (2).

63
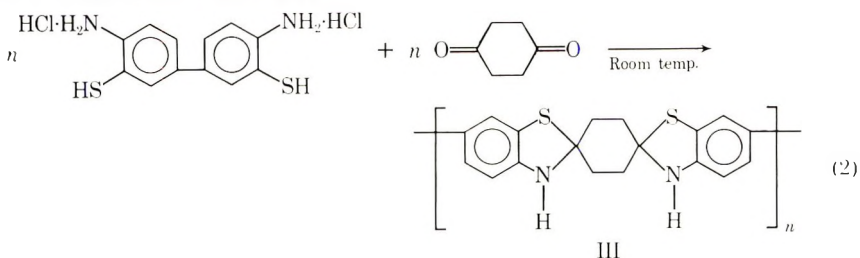
The feasibility of this reaction was first studied on model compounds
IV and V.

IV   V
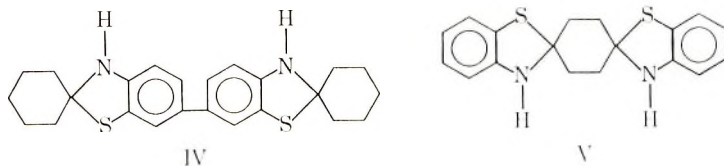
Both model compounds were obtained in near-quantitative yields. The
infrared spectra of IV and V were different and could not be matched with
that of polymer III. However, all bands found in the spectrum of the
polymer were also present in one or the other model compound. Polymer
III undergoes thermal rearrangement from a spiro to a ladder structure
(probably through the formation of a nonclassical sulfonium ion), as shown
in eq. (3).
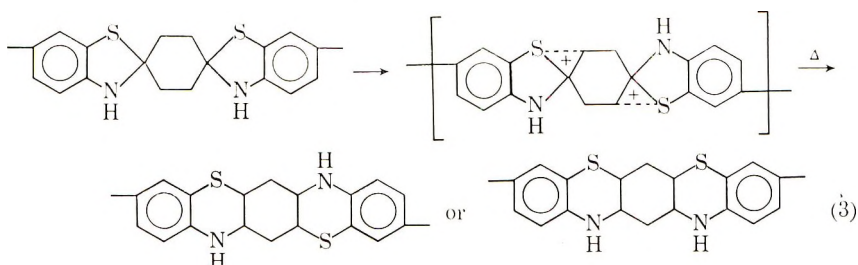
The rate of conversion was followed in the infrared by the disappearance
of a NH band at 3200 cm^{-1}, which is characteristic for the spiro structure,
and by the appearance of a band at 3340 cm^{-1} in the spectrum of the ladder
structure. Periodic infrared examination of a 1-mil thick polymer film
after heat treatment under reduced pressure showed that rearrangement was
complete after $7^{1}/_{2}$ hr at 200°C or after 3 min at 250°C.

The thermal decomposition temperature of polymer VI, determined by
thermogravimetric analysis (TGA) in vacuum at a heating rate of 5°C/
min, was 350°C. The TGA curve for the spiro polymer (III) was, as ex-
pected, identical to that of polymer VI, since rearrangement took place
during the heat-up period prior to decomposition. Polymer VI exhibited
a glass transition* at 210°C. An attempt to measure the glass transition
for polymer III gave erratic results. Apparently some thermal rearrange-
ment occurs prior to attainment of the glass transition temperature. Both
polymers were readily soluble in aprotic solvents, such as dimethyl acetam-
ide (DMAC), pyridine, or dimethyl sulfoxide. Films of both polymers
were very sensitive to a combination of light and oxygen and upon exposure
to it, the films changed their color from light yellow to purple within min-

* Determined by dielectric loss measurements of polymer film in vacuum at a heating
rate of 5°C/min. The relatively low glass transition of polymer VI is due to the chain-
flexibilizing cycloaliphatic portion of the ladder structure.

utes. When stored in the dark in pure oxygen or in nitrogen in the presence of light, the films remained unchanged. No change was observed in the infrared spectrum during the darkening of exposed films, and it seems that coloration is due to minor localized photo-oxidation leading to the formation of some quinoid structures.

EXPERIMENTAL

Model Compounds

Bis(2,2′-pentamethylene-spiro-benzothiazoline), IV. A mixture of 0.5 g (1.6 mmole) of 3,3′-dimercaptobenzidine dihydrochloride, 1.2 g (10 mmole) of cyclohexanone, 2 ml of pyridine, and 20 ml of ethanol were refluxed under nitrogen for $1/2$ hr. The solution was poured into 10 ml of water and the precipitate was filtered, dried, and redissolved in 5 ml of benzene. Reprecipitation from hexane gave 0.634 g (89% of theory), mp 203–206°C.

ANAL. Calcd for $C_{24}H_{28}N_2S_2$: C, 70.54%; H, 6.91%; N, 6.85%; S, 15.69%. Found: C, 70.52%; H, 6.95%; N, 6.84%; S, 15.62%.

1″,4″-Dispiro-cyclohexane-6,6′-bis(benzothiazoline), V. A solution of 2.40 g (0.02 mole) of o-aminothiophenol and 1.12 g (0.01 mole) of 1,4-cyclohexanedione in 25 ml of ethanol was refluxed for 45 min. The precipitated white solid was filtered, washed with ethanol, and dried. The yield was 3.13 g (98% of theory), mp 245–247°C (lit.[1] mp, 243°C).

Polymerization

Poly-[2,2′-(1″,4″-dispiro-cyclohexane)-6,6′-bis(benzothiazoline)], III. A mixture of 0.867 g (0.003 mole) of 3,3′-dimercaptobenzidine, 0.336 g (0.003 mole) of 1,4-cyclohexanedione and 8.4 ml of DMAc was stirred at ambient temperature for 1 hr. To the highly viscous solution was then added 0.3 ml of pyridine and stirring was continued for one additional hour. The polymer was precipitated and washed with deoxygenated ethanol in a Waring Blendor. The inherent viscosity of a 0.5% DMAc solution was 1.01 dl/g. Films of the polymer were cast from a 10% DMAc solution.

ANAL. Calcd for $C_{18}H_{16}N_2S_2$: C, 66.63%; H, 4.97%; N, 8.63%; S, 19.76%. Found: C, 66.48%; H, 5.05%; N, 8.70%; S, 19.94%.

Ladder Polymer. Conversion of III to the ladder structure VI, poly-7,7′-[1″,4″-dihydro (2,3H) benzothiazino (2′,3′-b) hexahydro (1,2,3,4H)-phenothiazine], was accomplished by heating 1-mil films either for $7^1/_2$ hr at 200°C or for 3 min at 250°C under reduced pressure.

ANAL. Calcd: same as for III. Found: C, 65.60%; H, 4.90%; N, 8.12%; S, 19.20%.

References

1. A. I. Kiprianov and V. A. Portnyagnia, *J. Gen. Chem. USSR* (Eng. Ed.), **25**, 2223 (1955).

2. H. J. Teuber and H. Waider, *Chem. Ber.*, **91**, 2341 (1958).

3. R. C. Elderfield and E. C. McClenachan, *J. Amer. Chem. Soc.*, **82**, 1982 (1960).

4. O. Hromatka, J. Augl, M. Vaculny, and H. Petrousek, *Monatsh.*, **89**, 517 (1958).

5. O. Hromatka, R. Klink, J. Augl, and R. Kirchmayr, *Monatsh.*, **92**, 96 (1961).

6. O. Hromatka, J. Augl, E. Flieder, and R. Klink, *Monatsh.*, **92**, 107 (1961).

7. G. Hackmack and W. Krastinat, German Pat. 1,151,802 (1963).

Vinyl Polymerization with Fe(III)–Thiourea as Initiator System. Part II. Kinetics: Predominant Primary Radical Termination*

B. M. MANDAL, U. S. NANDI, and S. R. PALIT, *Department of Physical Chemistry, Indian Association for the Cultivation of Science, Jadavpur, Calcutta 32, India*

Synopsis

The rate of polymerization R_p of methyl methacrylate initiated by $Fe(ClO_4)_3$ and thiourea (TU) in *tert*-butyl alcohol is independent of [Fe(III)] and [TU] in the concentration range studied. In contrast to R_p, the degree of polymerization DP changes markedly with the change in the initiator concentration. DP is overwhelmingly lower than is expected in a standard radical polymerization at the same R_p. Further, R_p is proportional to the square of the monomer concentration. Initiation efficiency is less than one. Independent experiments proved that in the azobisisobutyronitrile-initiated polymerization the R_p and DP are negligibly affected by [$Fe(ClO_4)_3$] or [TU], though high [TU] brings about high induction periods. The results of Fe(III)–TU-initiated polymerization have been interpreted in terms of the predominant termination of polymer radicals by primary radicals.

INTRODUCTION

In Part I we discussed the general features of the Fe(III)–TU-initiated polymerization reaction and the kinetics of the $Fe(ClO_4)_3$ and thiourea (TU) reaction.[1] For the kinetic study of the polymerization reaction, the homogeneous polymerization of methyl methacrylate (MMA) in *tert*-butyl alcohol (TBA) with the use of the $Fe(ClO_4)_3$–TU initiator system was selected for the reasons mentioned in Part I. In a short communication[2] the salient features of this reaction have been reported.

EXPERIMENTAL

The preparation and purification of materials and experimental techniques were described in Part I.[1] All polymerization experiments were carried out with the use of $Fe(ClO_4)_3$ solution from the same stock. Stock solutions of $Fe(ClO_4)_3$ in TBA were prepared (the strength being determined by gravimetry), allowed to stand for about 15 days at room temperature, and then stored in a refrigerator. With such stock solutions about 10% variation in rates was noted after more than 3 months.

---

* Presented in part at the International Symposium of Macromolecular Chemistry, Tokyo–Kyoto, Japan, 1966.

Isolation and Purification of Polymers

The polymer solution was poured into acidified methanol (4–5 drops of concentrated HCl in about 100 ml of methanol) to remove the adsorbed Fe(III) from the polymer. The precipitated polymer was washed with methanol and dried at 45°C for about 20 hr.

Degree of Polymerization

The degree of polymerization (DP) was determined viscometrically from $[\eta]$ in benzene solution at 30°C by using the relation:[3]

$$[\eta] = 8.69 \times 10^{-5} \bar{M}_n^{0.76}$$

RESULTS AND DISCUSSION

Effect of TU or Fe(ClO₄)₃ in the Radical Polymerization of MMA

An essential prerequisite to the quantitative study of the Fe(ClO₄)₃–TU-initiated polymerization is a knowledge of the extent to which TU or Fe-(ClO₄)₃ affects the radical polymerization reaction.

Table I and Figure 1 show that TU, when present in an azobisisobutyronitrile (AIBN)-initiated polymerization system, brings about unusually high induction periods almost proportional to its concentration. Following the induction period the rate of polymerization R_p is almost the same as that of the control without TU. Also, the polymers formed in the absence or presence of TU have almost the same intrinsic viscosity. Table I also includes the inhibitor concentrations as calculated from the induction period and the rate of initiation. This calculation was based on the assumption that a molecule of inhibitor is consumed by every polymer radical. The value of the rate of initiation R_i necessary for the calculation was obtained from eq. (1):

$$R_i = 2fk_d[\text{AIBN}] \tag{1}$$

where f is the efficiency of initiation, and k_d is the rate constant for the first-order decomposition of AIBN. The value of f was taken[4] as 0.5, and k_d is 5.2×10^{-7} sec^{-1} at 40°C, as computed from the equation given by Talât-Erben and Bywater.[5] On the average, the calculated inhibitor concentration amounts to 0.48 mole-% of TU. The reason for such inhibition is

TABLE I
Effect of TU in AIBN-Catalyzed Polymerization of MMA[a]

[TU], mole/l. $\times 10^2$	Induction period, hr	$R_p \times 10^5$, mole/l.-sec	$[\eta]$, dl/g	Inhibitor concn, calculated from induction period, mole/l. $\times 10^5$
0	Negligible	2.58	1.93	—
0.5	1.5	2.58	1.93	2.64
1.5	4.0	2.54	1.96	7.0
3.0	7.75	2.50	1.98	13.6

[a] [MMA] = 3.92 mole/l.; [AIBN] = 1 $\times$ 10^{-2} mole/l.; 40°C.
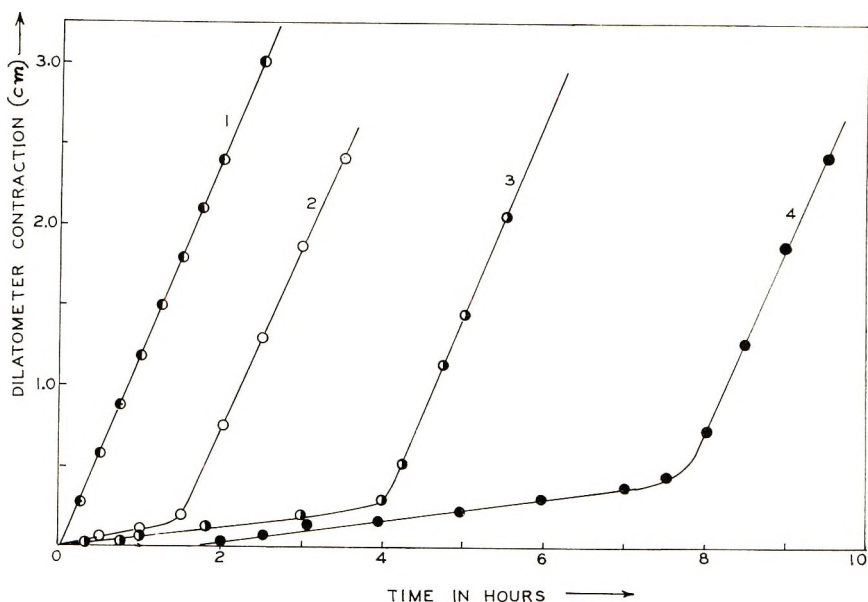
Fig. 1. Inhibition of MMA polymerization by TU: (1) [TU] = 0; (2) [TU] = 5 mmole/l.; (3) 15 mmole/l.; (4) 30 mmole/l. [MMA] = 3.92 mole/l. in TBA; [AIBN] = 1×10^{-2} mole/l.; 40°C.

obscure; it is probably not due to any impurity, as the TU used in this work was sufficiently purified by repeated crystallization (mp 180°C, see Part I[1]). $Fe(ClO_4)_3$ does not affect significantly the AIBN-catalyzed polymerization of MMA as is evident from Table II. This observation is in agreement with the results of Entwistle.[6] The slight increase in R_p observed in the presence of $Fe(ClO_4)_3$ might be due to the synergistic effect of $Fe(ClO_4)_3$ on the decomposition of AIBN. It is noteworthy that the decomposition of AIBN was accelerated also in the presence of silver perchlorate[7] or organo-aluminium compounds;[8] the possibility of enhanced decomposition of 4,4′-azobis(4-cyanopentanoic acid) in the presence of $Fe(ClO_4)_3$ was also indicated by Cavell et al.[9]

Induction Periods

It has been established above that TU contains 0.48 mole-% inhibitor. Figure 2 of Part I showed that short induction periods precede the Fe-

TABLE II
Effect of $Fe(ClO_4)_3$ in AIBN-Catalyzed Polymerization of MMA[a]

$[Fe(ClO_4)_3]$, mole/l. $\times 10^3$	$R_p \times 10^5$, mole/l-sec	$[\eta]$, dl/g	$\bar{P} \times 10^2$
0	2.58	1.93	52.5
4.22	2.75	1.71	44.7
7.03	—	1.64	42.3
12.67	2.80	1.64	42.3
16.9	—	1.60	40.8
17.4	2.84	1.55	39.3

$(ClO_4)_3$-TU initiated polymerization reaction. The length of the induction period varies from 5 to 40 min, depending on the concentrations of Fe(III) and TU used in this work. For the same concentration of TU used, the induction period (a few minutes) in the Fe(III)–TU initiated reaction is much less than that (hours, Table I) in the AIBN initiated system. The shorter induction period in the former system may be due to the higher rate of generation of primary radicals from the redox reaction (2), in comparison to that from the decomposition of AIBN [eq. (1)] in the latter system at 40°C.

$$\text{Fe(III)} + \text{S=C} \overset{\text{NH}_2}{\underset{\text{NH}_2}{\diagdown}} \rightarrow \text{Fe(II)} + \dot{\text{S}}-\text{C} \overset{\overset{+}{\text{N}}\text{H}_2}{\underset{\text{NH}_2}{\diagdown}} \qquad (2)$$
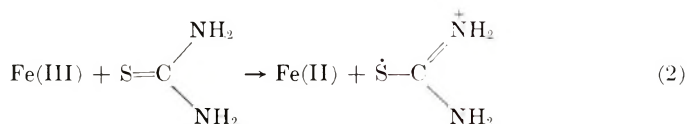
The value of the second-order rate constant for reaction (2) is 0.03 l./mole-min at 40°C (Part 1[1]), and details for Eq. (1) are given in the previous section.

Dependence of the Rate R_p and the Degree of Polymerization DP on the Initiator Concentration

It is evident from Table III that R_p is almost independent of the Fe-$(ClO_4)_3$ concentration over the range 1.74×10^{-3} mole/l. to 1.74×10^{-2} mole/l. at a fixed TU concentration of 3.33×10^{-2} mole./l. Rates of polymerization at fairly low concentration of $Fe(ClO_4)_3$, e.g., $[Fe(ClO_4)_3]$ of 1×10^{-3}–5×10^{-3} mole/l., at a fixed [TU] of 2.5×10^{-3} mole/l. exhibit changes which are insignificant compared to the extent of changes in the catalyst concentration. Thus, R_p can be considered to be independent over a wide range of $Fe(ClO_4)_3$, concentration especially in the high region. From the trend of R_p values it may appear that at extremely low concentrations of $Fe(ClO_4)_3$ a marked degree of dependence of R_p on [Fe(III)] could be observed. Unfortunately, such a study could not be carried out because $Fe(ClO_4)_3$ precipitates out below about 8×10^{-4} mole/l. in TBA.

TABLE III
Dependence of Rate and Degree of Polymerization on $Fe(ClO_4)_3$ Concentration[a]

$[Fe(ClO_4)_3]$, mole/l. $\times 10^3$	[TU], mole/l. $\times 10^3$	$R_p \times 10^5$, mole/l.-sec	$\bar{P} \times 10^2$ Measured	$\bar{P} \times 10^2$ Expected[b]
17.40	33.3	1.95	3.7	69
8.70	33.3	1.90	6.4	70
4.35	33.3	1.95	8.6	69
1.74	33.3	1.93	13.6	70
0.87	33.3	1.51	24.7	89
5.0	2.5	1.46	25.0	92
2.5	2.5	1.21	48.8	114
1.0	2.5	1.14	74.6	122

[a] [MMA] = 3.92 mole/l.; 40°C.

[b] Estimated from a plot of $1/\bar{P}$ vs. $R_p/[M]^2$ for the AIBN initiated system at 40°C in TBA.

The effect of the variation of TU concentration on R_p is similar as is evident from Table IV; R_p is found to be insensitive to changes in the TU concentration over the range 2.1×10^{-3}–3.3×10^{-2} mole/l. at a fixed $Fe(ClO_4)_3$ concentration of 8.7×10^{-3} mole/l.

A further important feature is that the DP of the polymers changes markedly with a change in concentration of either ferric perchlorate or thiourea at a fixed concentration of the other, though R_p remains sensibly constant under identical conditions. The variation in DP at constant R_p in the absence of the particularly rapid chain transfer reactions is incompatible with a radical mechanism involving mutual bimolecular termination of polymer radicals. Moreover, the DP of the polymers obtained in the polymerization reaction effected by $Fe(ClO_4)_3$ and TU is much lower (Tables III–IV) than that expected in a radical polymerization involving mutual bimolecular termination of polymer radicals (cf. AIBN-initiated polymerization) at identical rates of polymerization. To illustrate this point, the expected degree of polymerization in AIBN initiated system at the same rates of polymerization as achieved in the $Fe(ClO_4)_3$–thiourea-initiated reaction is included in Tables III and IV.

Since neither $Fe(ClO_4)_3$ nor TU has any significant influence on the DP in the radical polymerization of MMA (cf. AIBN-initiated polymerization, Tables I–II), the low DP of the polymers formed in the Fe(III)–TU-initiated reaction is not attributable to the presence of either of them singly. Again, the low DP is not due to the interaction of the polymer radical with products like Fe(II) or formamidine disulfide of the $Fe(ClO_4)_3$–TU reaction.[1] This is evident from the fact that DP increases slightly with the progress of the reaction, whereas the interaction with the products necessitates a decrease in DP with progress of the reaction.

Rate Dependence on Monomer Concentration

Figure 2 illustrates the dependence of the rate of polymerization on monomer concentration at two different catalyst concentrations. From Figure 2 it is evident that the rate of polymerization is proportional to the square of the monomer concentration.

TABLE IV
Dependence of Rate and Degree of Polymerization on TU Concentration[a]

[TU], mole/l. $\times 10^3$	$R_p \times 10^5$, mole/l. sec	$\bar{P} \times 10^2$	
		Measured	Expected[b]
33.3	1.89	6.4	71.4
16.6	1.72	6.7	76.0
8.3	1.86	9.3	71.8
4.15	1.63	17.5	83.3
2.05	1.46	20.0	90.5

[a] $[Fe(ClO_4)_3] = 8.70 \times 10^{-3}$ mole/l. in all cases; $[MMA] = 3.92$ mole/l.; 40°C.
[b] Estimated from a plot of $1/P$ vs. $R_p/[M]^2$ for the AIBN-initiated system at 40°C in TBA.
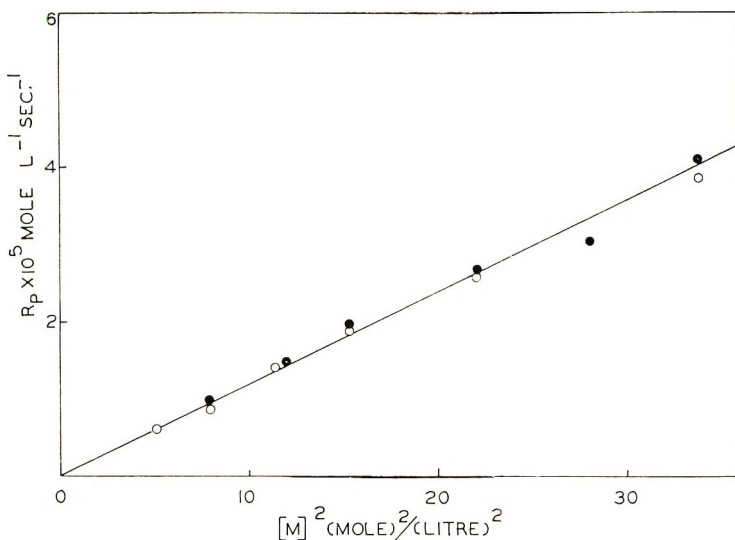
Fig. 2. Dependence of R_p on monomer concentrations: ($\bullet$) [Fe(ClO$_4$)$_3$] = 1.2 × 10^{-2} mole/l., [TU] = 0.75 × 10^{-2} mole/l.; (O) [Fe(ClO$_4$)$_3$] = [TU] = 1 × 10^{-2} mole/l.

Efficiency of Initiation

The efficiency of initiation in the present system is less than one, varying from 20 to 60% depending on the catalyst concentrations, as shown in Table V.   Our previously reported values[2] for the efficiency of initiation proved to be largely in error, and the new values reported here should be used instead.   Efficiency was calculated from the ratio

$$f = \text{Rate of initiation } (R_i)/\text{Rate of Fe(II) formation } (R_{Fe(II)})$$

$R_{Fe(II)}$ was considered equivalent to the rate of primary radical generation based on the assumption that a radical is generated for the generation of every Fe(II) according to the reaction (2). R_i was obtained from the relation $\nu = R_p/R_i$. ν was taken approximately equivalent to DP, since the termination in this reaction is predominantly by primary radical.   (It is noteworthy that the other alternative processes of termination as by Fe(III) complex or through disproportionation also leads to ν = DP. Moreover, perturbation in DP through radical reactions with substrates like tert-butyl alcohol, TU, and Fe(ClO$_4$)$_3$ present in the system is small at 40°C.)

Mechanism

So far it is evident that R_p is independent of Fe(ClO$_4$)$_3$ or thiourea concentration over a wide range and exhibits a proportionality with the square of the monomer concentration.   Again, the particularly low DP of the polymers (Tables III and IV) indicates that the polymer radicals are terminated overwhelmingly by processes other than the mutual bimolecular reaction.   Two possible ways of termination that can account for the present results are (a) termination of polymer radicals by primary radicals;

TABLE V
Efficiency of Initiation[a]

$[Fe(ClO_4)_3]$, mole/l. $\times 10^3$	$[TU]$, mole/l. $\times 10^3$	$R_p \times 10^5$, mole/l.-sec	$1/\bar{P} \times 10^3$	$R_i \times 10^8$, mole/l.-sec.	$R_{Fe(II)} \times 10^8$, mole/l.-sec	f
17.4	33.3	1.95	2.69	5.33	27.1	0.19
8.7	33.3	1.90	1.56	3.0	13.4	0.22
1.74	33.3	1.93	0.73	1.44	2.7	0.53
8.7	8.33	1.86	1.07	1.93	3.33	0.60

[a] $[MMA] = 3.92$ mole/l.; solvent, TBA; 40°C.

(b) initiation of polymerization and termination of polymer radicals by a complex formed out of Fe(III) and TU.

Primary Radical Termination. Effect of this mode of termination in polymerization reactions has been discussed.[10-16] Very high catalyst concentration,[11] very low monomer concentration,[14] and use of comparatively stable radicals[15,16] for chain initiation are shown to affect the kinetics and the degree of polymerization and these have been accounted for by assuming primary radical termination. Exclusive primary radical termination leads to the kinetic expression (3):[10]

$$R_p = k_i k_p [M]^2 / k_{t'} \tag{3}$$

where k_i is the rate constant for the addition of the initiator radical to the monomer, k_p the propagation rate constant, and $k_{t'}$ the rate constant for the termination of the polymer radical by the primary radical. The present results conform well to the kinetic expression (3).

Termination by Fe(III) Species. As an alternative way to account for the results, we assumed that a complex is formed between Fe(III) and TU as in other Fe(III) and mercaptide systems,[17,18] and that the complex is responsible for the initiation as well as the termination reactions. Such a scheme gives rise to the kinetic expression (4):

$$R_p = (\text{constant}) f[M] \tag{4}$$

This equation can account for our experimental results only if f is proportional to [M], which is not generally observed except at too low monomer concentrations.[19]

Termination of radicals by metal salts is, however, very complex, being highly susceptible to the nature of the anion with which the metal ion is associated.[20] Such terminations are classified broadly in two types, viz., ligand transfer and electron transfer. Metal ions associated with anions like Cl^-, Br^-, CN^-, CNS^- are claimed to favor termination via the ligand-transfer mechanism, while association with anions like acetate or carboxylates, perchlorate, etc., effects the termination reaction via the electron-transfer mechanism. Quite a number of ferric salts of the later type have been shown to be incapable of terminating the poly(methyl methacrylate) radical.[6] In this perspective it is very difficult to foretell the oxidative chain-terminating efficiency of the complex assumed to be formed from Fe(III) and TU. The experimental evidence for the occurrence of such termination would have been the direct demonstration of any Fe(II) generated from the postulated reaction (5).

$$R_x^\cdot + \text{Fe(III)-TU complex} \rightarrow P_x + \text{Fe(II)} \tag{5}$$
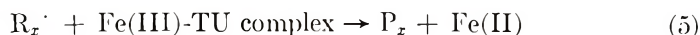
Though the rate of Fe(II) generation in the Fe(III)–TU reaction in TBA was increased due to the addition of MMA, such an increase may well be attributed to the solvent effect, as a more pronounced increase in the rate was observed on the addition of a comparable ester solvent (ethyl acetate) instead of MMA under otherwise identical conditions[1] (Table II, Part 1).

Of the two alternatives, we are in favor of primary radical termination due to the following considerations.

(1) The efficiency of initiation is very low. In the estimation of the efficiency of initiation, the rate of formation of Fe(II) was taken equivalent to the rate of primary radical generation. The efficiency, therefore, accounts for those radicals that are in the bulk of the solution and not in the cage. The "geminate recombination" theory,[21] usually used to account for efficiency less than unity[19] in the case of initiation with dissociative initiators yielding two radicals at each occurrence of decomposition, is therefore not applicable. Thus, a large percentage of the primary radicals are wasted by reactions other than the initiation. One such side reaction may be the primary radical termination.

(2) Existence of the assumed complex in the solution is not supported by spectral study. No new peak appears on mixing $Fe(ClO_4)_3$ and TU in TBA. Moreover, application of the continuous variation technique[22,23] using with the use of a 1.5 mM (1 cm cells) or 13 mM (1 mm cells) solution of each of Fe(III) and TU at 380, 400, and 420 mμ does not point definitely to the existence of a well defined complex. The slight increase in optical density of $Fe(ClO_4)_3$ solution on mixing TU however, is indicative of weak interaction. This is not unexpected, in view of the already prevalent strong alcohol complexes in the solution of $Fe(ClO_4)_3$ in TBA. The formation of strong complexes with ferric salts and alcohol is well known. A coordination number of 2 has been assigned in case of $FeCl_3$ and various alcohols.[24]

(3) The rate of radical generation in the present polymerization reaction is high, and this is known to perturb the kinetics of polymerization.[11]
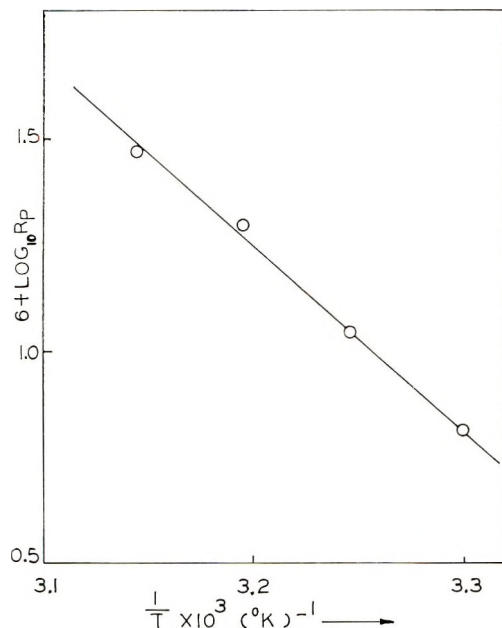
Fig. 3. Arrhenius plot for MMA polymerization. [MMA] = 3.92 mole/l.; [Fe(ClO₄)₃] = 8.7 × 10⁻³ mole/l.; [TU] = 3.33 × 10⁻² mole/l.

On the basis of the above considerations we conclude that this is possibly a case of primary radical termination.

Energy of Activation

Arrhenius plot of $\log R_p$ versus $1/T$ as shown in Figure 3 leads to a value of 19.9 kcal/mole for the activation energy of the overall polymerization reaction. On the assumption that primary radical termination is the chief terminating process, the kinetic expression (3) leads to

$$E_{\text{polymerization}} = E_i + E_p - E_{t'} = 19.9 \text{ kcal/mole}$$

and subsequently to $E_i - E_{t'} = 13.6$ kcal/mole as E_p is 6.3 kcal/mole.[25] On assuming further that $E_{t'}$ approximates E_t (the mutual bimolecular termination activation energy[25]), E_i is about 10.8 kcal/mole, which is quite large compared to E_p.

References

1. B. M. Mandal, U. S. Nandi, and S. R. Palit, *J. Polym. Sci.*, *A-1*, **7**, 1407 (1969) (Part I).

2. B. M. Mandal, U. S. Nandi, and S. R. Palit, *J. Polym. Sci. B*, **5**, 677 (1967).

3. T. G. Fox, J. B. Kinsinger, H. F. Mason, and E. M. Schuele, *Polymer*, **3**, 71 (1962).

4. G. Ayrey and C. G. Moore, *J. Polym. Sci.*, **36**, 41 (1959).

5. M. Talât-Erben and S. Bywater, *J. Amer. Chem. Soc.*, **77**, 3712 (1955).

6. E. R. Entwistle, *Trans. Faraday Soc.*, **56**, 284 (1960).

7. C. H. Bamford, R. Denyer, and J. Hobbs, *Polymer*, **8**, 493 (1967).

8. T. Hirano, T. Miki, and T. Tsuruta, *Makromol. Chem.*, **104**, 230 (1967).

9. E. A. S. Cavell, I. T. Gilson, and A. C. Meeks, *Makromol. Chem.*, **73**, 145 (1964).

10. E. Collinson and F. S. Dainton, *Discussions Faraday Soc.*, **51**, 1392 (1955).

11. C. H. Bamford, A. D. Jenkins, and R. Johnston, *Trans. Faraday Soc.*, **55**, 1451 (1959).

12. P. E. M. Allen and C. R. Patrick, *Makromol. Chem.*, **48**, 89 (1961).

13. G. Henrici-Olivé and S. Olivé, *Makromol. Chem.*, **37**, 71 (1960).

14. M. G. Baldwin, *J. Polym. Sci. A*, **1**, 3209 (1963).

15. G. S. Misra, A. Hafeez, and K. S. Sharma, *Makromol. Chem.*, **51**, 123 (1962).

16. S. G. Cohen and C. H. Wang, *J. Amer. Chem. Soc.*, **77**, 2457 (1955).

17. D. L. Leussing and I. M. Kolthoff, *J. Amer. Chem. Soc.*, **75**, 3904 (1953).

18. N. Tanaka, I. M. Kolthoff, and W. Stricks, *J. Amer. Chem. Soc.*, **77**, 1996 (1955).

19. J. C. Bevington, *Trans. Faraday Soc.*, **51**, 1392 (1959).

20. J. K. Kochi, *Rec. Chem. Progr.*, **27**, 207 (1966); *Science*, **155**, 415 (1967).

21. R. M. Noyes, *J. Amer. Chem. Soc.*, **77**, 2042 (1955).

22. P. Job, *Ann Chim.* [10], **9**, 113 (1928).

23. W. C. Vosburgh and G. R. Cooper, *J. Am. Chem. Soc.*, **63**, 437 (1941).

24. R. K. Multani, *Indian J. Chem.*, **2**, 506 (1964).

25. M. S. Matheson, E. E. Auer, E. B. Bevilacqua, and E. J. Hart, *J. Amer. Chem Soc.*, **71**, 497 (1949).

ESR Studies of Vinyl Polymerization. II. Initial Reactions of Vinyl Esters with Redox Systems in Aqueous Media

KOICHI TAKAKURA* and BENGT RÅNBY, *Department of Polymer Technology, The Royal Institute of Technology, Stockholm 70, Sweden*

Synopsis

ESR measurements of transient radicals during redox polymerization of various vinyl esters in aqueous solutions have been made by using the rapid-mixing flow method. The initiation was by means of hydroxyl and amino radicals from the systems titanous chloride–hydrogen peroxide and titanous chloride–hydroxylamine, respectively. The well resolved hyperfine structures obtained at monomer concentrations of about 0.05 mole/l. are unambiguously assigned to the monomer radicals formed by addition of initiator radicals to monomers. At higher monomer concentrations, additional weak signals attributed to the growing polymer radicals were observed. The effect of reaction conditions on the signal intensity has been studied in particular for vinyl acetate. The coupling constants of monomer radicals from various vinyl esters (acetate, propionate, butyrate, crotonate, and isopropenyl acetate) were obtained and the spin densities calculated. From the ESR spectra, the monomer radicals have a conformation with the substituent R (R = HO or NH$_2$) of R—CH$_2$—ĊH(OCOR') locked in a position above or below the radical plane. This is tentatively interpreted as due to formation of intramolecular hydrogen bonds to ring structures or complexes with titanium ions. In addition, hydrogen abstraction reactions of some model compounds for poly(vinyl acetate) have been briefly studied in relation to chain transfer and grafting reactions.

INTRODUCTION

The flow technique developed by Dixon and Norman[1,2] has made it possible to obtain well resolved ESR spectra of short-lived (transient) free radicals in aqueous solutions by using rapid redox reactions. This method has been successfully applied to radical polymerization in aqueous solution of a variety of vinyl monomers. Fischer et al.[3–7] have extensively studied transient radicals of mainly acrylic and methacrylic monomers, while vinyl esters and butadiene were studied in this laboratory.[8] Our work has been extended to copolymerization studies of binary monomer systems in which the initial monomer and copolymer radicals could be observed and identified and their relative amounts measured.[9,10] Griffiths et al.[11] have observed ESR spectra of radicals formed by addition reactions to various

---

alkenes including vinyl chloride and vinyl fluoride, using the flow tech-
nique. As a new approach, the flow method is particularly useful for
studies of radical polymerization in solution. The reaction conditions in
the flow system, however, are not the same as those of the usual solution
polymerization; the concentration of initiator is much higher, and the
turbulent flow on mixing may affect the reaction conditions significantly.
Nevertheless, the observed hyperfine structures of the ESR spectra can
provide straightforward information on the structure, the concentration,
and even on the steric conformation of the transient radicals.

As an extension of previous work,[8] this paper describes more detailed
studies of transient radicals, particularly in the initial processes of poly-
merization of various vinyl esters, initiated by hydroxyl and amino radicals.
From the ESR spectra, detailed information on the structure and conforma-
tion of the radicals is derived. In addition, hydrogen abstraction from
some model substances for poly(vinylacetate) has been briefly studied in
relation to chain-transfer reactions.

EXPERIMENTAL

The ESR measurements were carried out by using an X-band ESR
spectrometer (Japan Electron Optics Laboratory Co., Ltd., Model JES-
3B) in a flow apparatus as previously described.[8-10] The initiators used
were hydroxyl radicals from the redox reaction of hydrogen peroxide with
titanium trichloride, and amino radicals from the redox reaction of hydrox-
ylamine and titanium trichloride. Two aqueous solutions, i.e., one oxidant
solution of H_2O_2 or NH_2OH containing monomers (usually about 1.0×10^{-1}
mole/l.), and one reductant solution of $TiCl_3$, both containing sulfuric acid
$(2.2 \times 10^{-2}$ mole/l.), were rapidly mixed immediately before they entered
the flat cell inserted in the ESR cavity. To obtain high concentrations,
monomers with limited solubility in water were often dissolved in both
solutions. The free-radical spectra were usually observed at room temper-
ature $(22 \pm 2°C)$ when the reacting solutions flowed through the flat cell.
The intensity of the ESR signal is related to the flow rate of the solutions.
To retain steady-state conditions, the flow rate of the reacting solutions was
kept constant (usually about 4 ml/sec), giving a time lag from mixing to
measurement of about 0.02 sec. The magnetic field was calibrated with
the proton magnetic resonance signals. The g values were measured with
reference to the ESR spectrum of 1,1-diphenyl-2-picryl hydrazyl in meth-
anol solution as a standard.

The following reagents, all of analytical grade, were used: 15% titanium
trichloride in aqueous solution (iron free), 30% hydrogen peroxide in water,
hydroxylamine hydrochloride, and concentrated sulfuric acid. The mo-
nomers were of the purest grade commercially available: vinyl acetate
(Kebo AB, Stockholm, Sweden), vinyl propionate (provided by Mr. S.
Porrvik of Fosfatbolaget AB, Stockviksverken, Sweden), isopropenyl
acetate (Eastman Organic Chemicals, New York, N.Y., USA), vinyl

butyrate and vinyl crotonate (K & K Laboratories, Inc., New York, N.Y., USA). The monomers were further purified by distillation under reduced pressure to remove stabilizers. Ethyl acetate (Mallinckrodt Chemical Works, New York, N.Y., USA) and isopropyl acetate (Kebo AB, Stockholm, Sweden) were of reagent grade, and were used without further purification.

RESULTS AND DISCUSSION

Addition of Hydroxyl Radicals to Vinyl Acetate (VAc)

In the reaction of titanium (III) ions with hydrogen peroxide (H_2O_2) in acidified aqueous solutions, two ESR signals are generally observed, i.e. a main peak (peak 1, P_1) at low field and a minor peak (peak 2, P_2) at high field. As reported elsewhere,[12] we have assigned peaks 1 and 2 to $HO_2\cdot$ and $HO\cdot$ radicals, respectively, both radicals coordinated with $Ti(IV)$ ions or $Ti(IV)$–H_2O_2 complexes. On addition of VAc monomer to this reaction system, the ESR spectrum of peak 1 and 2 is replaced by that of VAc radicals formed by addition of $HO\cdot$ radicals to the monomer.[8–10] As shown in Figure 1.4, the spectrum obtained at ordinary monomer concentrations (about 5×10^{-2} mole/l.), can be described as a doublet of triplets of narrow quartets (g value 2.0031), assigned unambiguously to monomer radicals (HO—$VAc\cdot$). The spectrum in Figure 1B is discussed later. The intensity of the observed spectrum of VAc radicals is related to the reaction conditions. The effects of some variables were examined in order to obtain as intense and well resolved a spectrum as possible. The signal intensities in Figures 2–5 were measured from the peak height (amplitude) of the main signal component in the ESR spectra of the VAc monomer radicals. The line width of these spectra did not vary appreciably under the experimental conditions used.

Effect of H_2O_2/$TiCl_3$ Ratio. The H_2O_2/$TiCl_3$ ratio r affected the ESR signal intensity significantly (Fig. 2). The maximum intensity was obtained for molar ratios close to $r = 15$. As the ratio was decreased from the value of 10, either by increasing $TiCl_3$ concentration or by decreasing H_2O_2 concentration, the signal intensity decreased rapidly. This is not caused by asymmetry in the flow to and mixing in the flat cell, since reversion of the flow connections did not affect this result at all. It is interesting to note that very low signal intensities were obtained for r values about unity, although on the basis of simple kinetics the highest intensity should be expected. This discrepancy seems to arise mainly from radical-scavenging property of titanium ions, probably the predominant $Ti(IV)$ ions in the reaction system. The intensity of VAc radical spectra decreased appreciably when $TiCl_4$ was added to the reaction system. Furthermore, analogous effects were observed with small amounts of ferric chloride added (0.004 mole/l.), which is known to act as a strong radical scavenger.[13,14] With this reagent, the intensity decreased markedly down to noise level
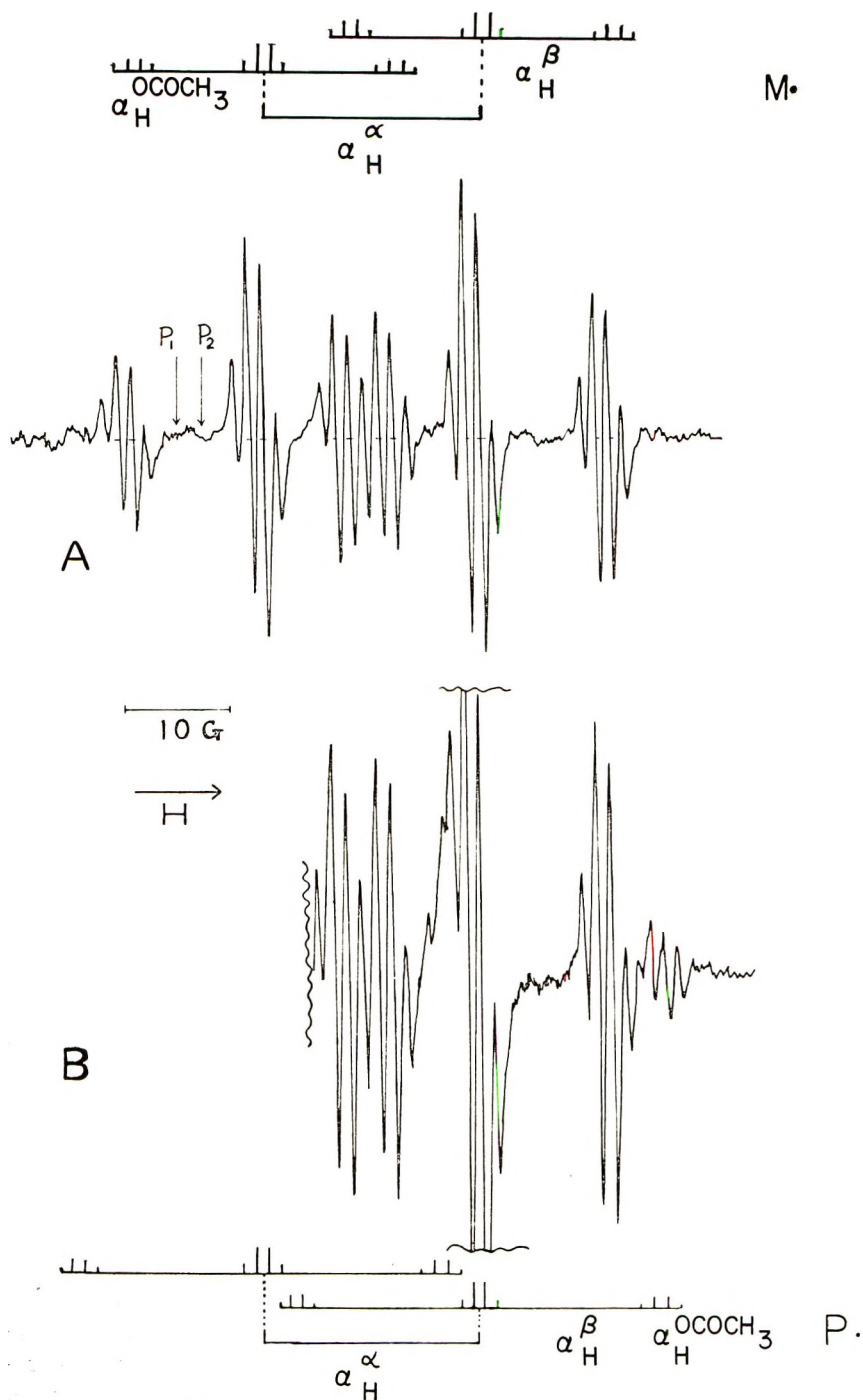
Fig. 1. ESR spectra from vinyl acetate (VAc) in the system of H_2O_2 and $TiCl_3$: (A) Monomer radicals, [VAc] = 5.5×10^{-2} mole/l., P_1 and P_2 indicate the position of peaks 1 and 2, respectively, which appear in the absence of the monomer; (B) Monomer (VAc) and polymer (PVAc) radicals, [VAc] = 3.2×10^{-1} mole/l; the stick spectrum shows the hyperfine lines for the radicals attributed to the polymer radicals. [H_2O_2] = 1.1×10^{-1} mole/l.; [$TiCl_3$] = 7×10^{-3} mole/l. [H_2SO_4] = 2.2×10^{-2} mole/l.
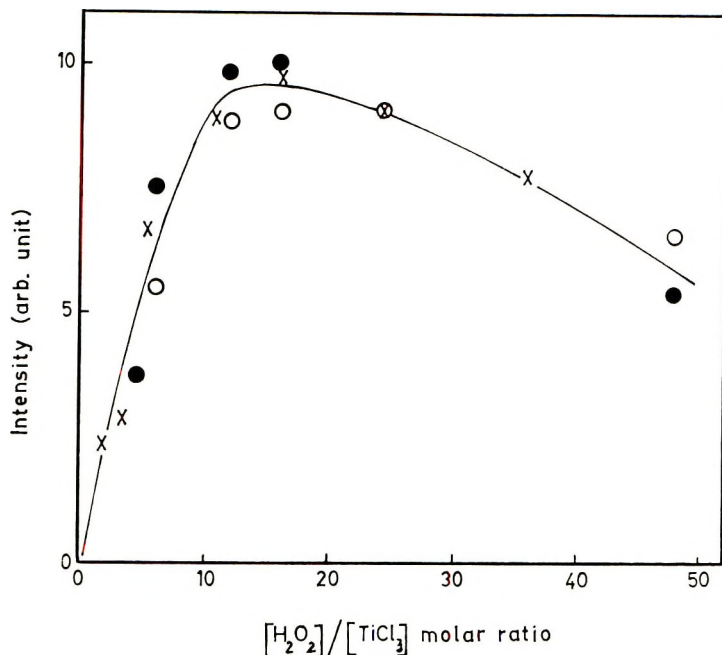
Fig. 2. Effect of molar ratio of $H_2O_2/TiCl_3$ on the signal intensity of VAc monomer radicals: (O) series A, H_2O_2 concentration kept constant at 0.17 mole/l., [TiCl$_3$] varied; (●) series B, TiCl$_3$ concentration kept constant at 0.007 mole/l., [H$_2$O$_2$] varied; (×) series C, same conditions as for series B except that the connections of inlet tubes to the mixing chamber were reversed. [VAc] = 4.1×10^{-2} mole/l.; [H$_2$SO$_4$] = 2.2×10^{-2} mole/l.; flow rate 4 ml/sec.

even when the measurements were carried out under conditions which otherwise were optimal ([H$_2$O$_2$] = 1.1×10^{-1} mole/l., [TiCl$_3$] = 7×10^{-3} mole/l., [VAc] = 4.1×10^{-2} mole/l.). Therefore, these observations may be interpreted as due to termination reactions of Ti(IV) and Fe(III) ions with the VAc radicals through a process of electron transfer or ligand transfer as proposed by Bamford et al.[14] and by Kochi.[15] Such scavenging effect of metal halides seems to be enhanced for reactive radicals having negative e values, e.g., VAc radicals.

Effect of Initiator Concentration. The variation of signal intensity of VAc monomer radical as a function of the initiator concentration is shown in Figure 3, where the H$_2$O$_2$/TiCl$_3$ molar ratio was kept constant at $r = 16$. With increasing initiator concentration the signal intensities reach a maximum value and then decrease. Also this behavior suggests that some species derived from the redox process, e.g., Ti(IV) ions, may be involved in chain termination reactions with VAc radicals.

Effect of Sulfuric Acid. Addition of H$_2$SO$_4$ generally reduced the signal intensity of VAc radicals, as shown in Figure 4. With no H$_2$SO$_4$ added, the initial signals from the redox system (peak 1 and 2) remained in the spectrum of VAc radicals, but they disappeared at an H$_2$SO$_4$ concentration above 0.01 mole/l.
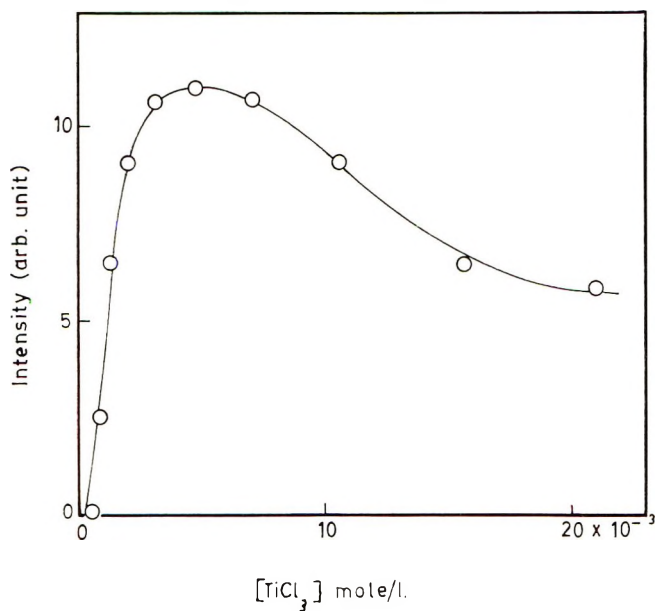
Fig. 3. Effect of initiator concentration on the signal intensity of VAc monomer radicals. Molar ratio of $H_2O_2/TiCl_3$ was kept constant at 16; [TiCl$_3$] varied; [VAc] = 4.1 × 10^{-2} mole/l.; [H$_2$SO$_4$] = 2.2 × 10^{-2} mole/l.
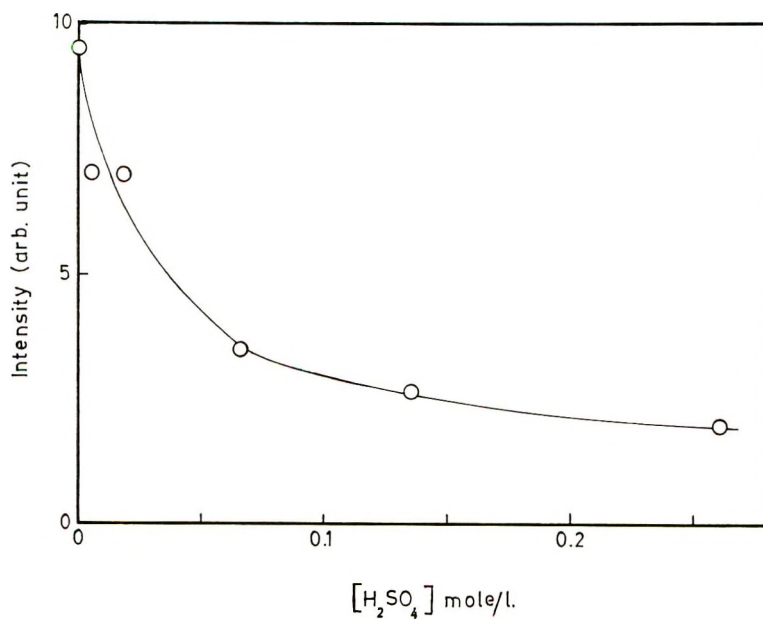
Fig. 4. Effect of H_2SO_4 concentration on the signal intensity of VAc monomer radicals. [H$_2$O$_2$] = 0.15 mole/l.; [TiCl$_3$] = 7 × 10^{-3} mole/l.; [VAc] = 5.5 × 10^{-2} mole/l.

Effect of VAc Monomer Concentration. Under optimum conditions, the effect of monomer concentration was examined within the concentration range of 2×10^{-3} to 3.2×10^{-1} mole/l. As the concentration increased, the signal intensity of VAc monomer radicals increased, passed through a maximum, and then tended to decrease. At saturated monomer concentration (ca. 3×10^{-1} mole/l.), additional weak signals were superimposed on the signals of the monomer radical, as shown in Figure 1B, containing half a spectrum obtained at higher magnetic field. These new signals are tentatively assigned to growing VAc chain radicals, $HO\text{-}(VAc)_n\text{-}VAc\cdot$. Due to the limited solubility of the monomer, the intensity of this spectrum cannot be further increased under these conditions. The coupling constants for the secondary spectrum were $a_H{}^\alpha = 20.3$ gauss, $a_H{}^\beta = 17.5$ gauss, and $a_{OCOCH_3}{}^H = 1.3$ gauss. The intensities of the two spectral components ($M\cdot$ and $P\cdot$ respectively) at increasing monomer concentration are shown in Figure 5. Up to a monomer concentration of about 1×10^{-1} mole/l., no definite ESR signals due to VAc polymer radicals could be observed, and no polymerlike substance could actually be detected in the reaction streams immediately after mixing the two solutions.

The low intensity of VAc polymer radicals is in marked contrast to the results for acrylic monomers,[3-7] where intense and well resolved spectra due to polymer radicals are easily observed, even at monomer concentrations as low as 5×10^{-2} mole/l. These observations suggest that the highly reactive VAc radicals preferentially terminate with species such as $HO\cdot$ radicals, VAc monomer radicals or Ti(IV) ions rather than undergo propagation.
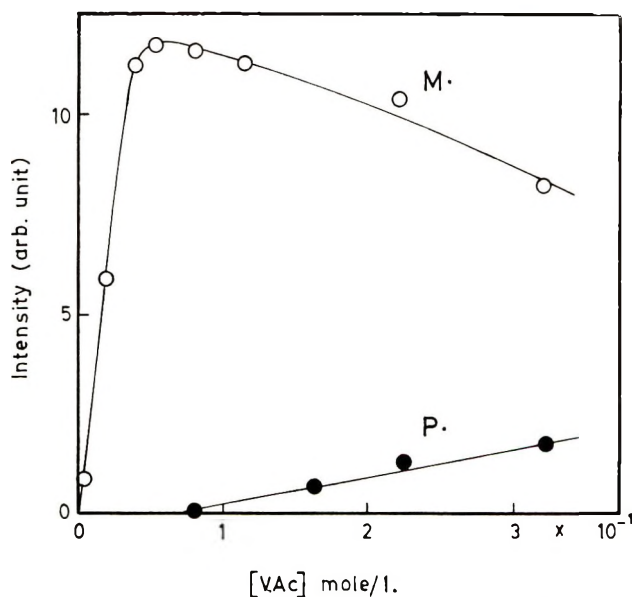
Fig. 5. Effect of VAc monomer concentration on signal intensity of VAc monomer radicals ($M\cdot$) and polymer radicals ($P\cdot$). $[H_2O_2] = 0.10$ mole/l.; $[TiCl_3] = 6.0 \times 10^{-2}$ mole/l.; $[H_2SO_4] = 2.0 \times 10^{-2}$ mole/l.

VAc is a monomer of low reactivity, expected to show a low rate of addition to VAc radicals. As previously reported,[9,10] however, introduction of small amounts of a more reactive second monomer (M), such as acrylonitrile or fumaric acid into the VAc system, has given ESR spectra assigned to initial copolymer radicals of the general structure VAc-M·.

ESR Spectra of Radicals Obtained by the Addition of Hydroxyl and Amino Radicals to Various Vinyl Esters

ESR spectra for radicals of isopropenyl acetate (IPAc), vinyl propionate (VPr),[8] vinyl butyrate (VBu), and vinyl crotonate (VCr) were measured after initiation with HO· radicals at monomer concentrations below 0.1 mole/l. The ESR spectrum of IPAc was an expected quartet of triplets, as shown in Figure 6. Each spectral line was further split into a narrow quartet due to the expected very weak coupling with the three protons in the acetate group. VPr and VBu gave similar spectra as VAc, except for the narrow triplet due to the two protons next to the carbonyl in the ester group. The spectrum of VBu is shown in Figure 7 (compare Fig. 14). The spectrum from VCr was rather weak, and the narrow splittings due to
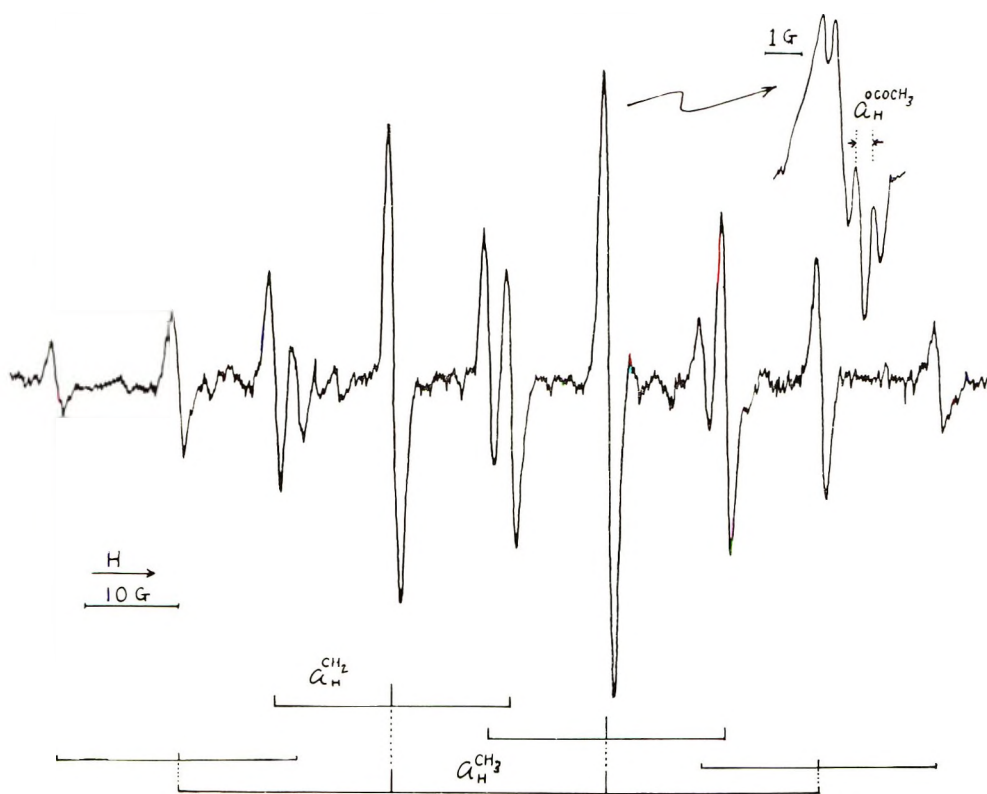
Fig. 6. ESR spectrum from isopropenyl acetate in the system H_2O_2–$TiCl_3$. [IPAc] = 4.6×10^{-2} mole/l.; (H_2O_2) = 1.5×10^{-1} mole/l.; [$TiCl_3$] = 7×10^{-3} mole/l.; [H_2SO_4] = 2.2×10^{-2} mole/l.
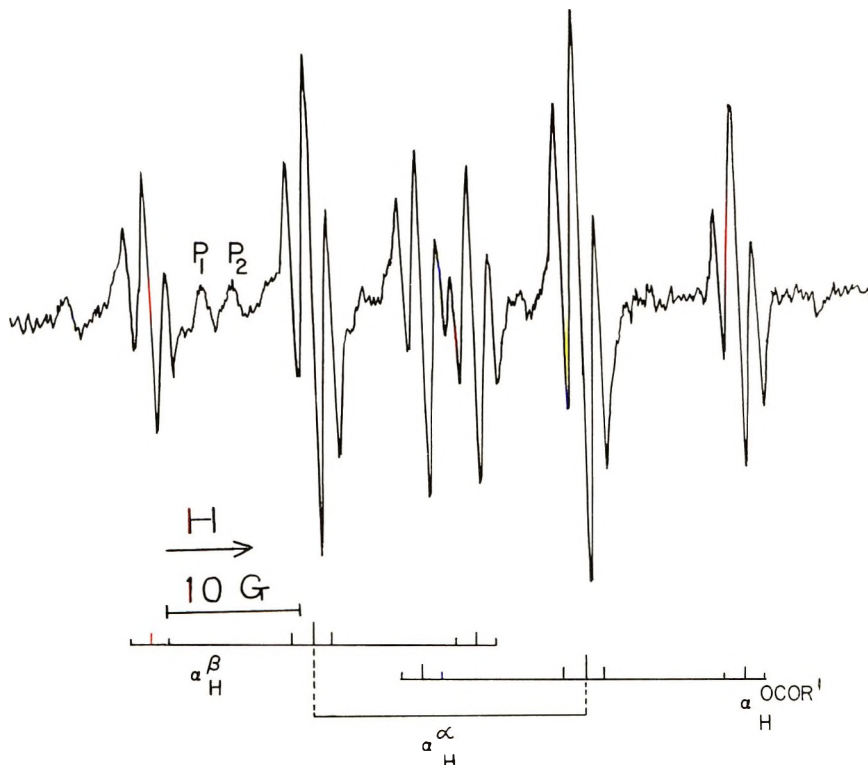
Fig. 7. ESR spectrum from vinyl butyrate in the system of H_2O_2–$TiCl_3$. [VBu] = 3.5×10^{-2} mole/l.; [H_2O_2] = 1.5×10^{-1} mole/l.; [$TiCl_3$] = 7×10^{-3} mole/l.; [H_2SO_4] = 2.2×10^{-2} mole/l.

the protons in the ester group could not be resolved in the spectrum. The coupling constants obtained for the five monomer radicals are given in Table I.

The assignment of the observed spectra to vinyl ester monomer radicals is unambiguous when the following information is considered. With the use of $H_2N \cdot$ radicals as initiator in the same manner as reported by Corvaja et al.[5] for other monomers, spectra for the monomer radicals were observed. These spectra showed the expected coupling with the nitrogen atom of the H_2N group attached to the β-carbon, and almost the same coupling with the β-protons as observed for the corresponding HO adduct radicals. For VAc a poorly resolved spectrum of low intensity was obtained, probably because of its low reactivity towards $H_2N \cdot$ radicals, as expected from the very low Q value (0.026) of VAc in the Q,e chart for copolymerization.[16] The Q values can be taken as a measure of the average reactivity of the monomers in free radical addition reactions. Consequently, IPAc and VPr, both having somewhat higher Q values than VAc (0.045 and 0.052, respectively[16]) showed well resolved spectra. Typical spectra obtained from IPAc and VPr with NH_2 radical initiation are shown in Figures 8 and 9, respectively, where the triplets with lines of the same intensity due to

TABLE I
Coupling Constants and Spin Densities for Various Vinyl Ester Monomer Radicals

Substrate	Initiator	Radicals	Coupling constants, gauss[a]					Spin density ρ_α
			a_H^α	$a_H^{CH_3}$	a_H^β	$a_H^{OCOR'}$	$a_H^{NH_2}$	
VAc	HO·	HO—CH$_2$—ĊH(OCOCH$_3$)	20.3 ± 0.1	—	12.2 ± 0.1	1.30 ± 0.04	—	0.836
IPAc	HO·	{HO—CH$_2$—Ċ(CH$_3$)(OCOCH$_3$)	—	22.5 ± 0.1	12.5 ± 0.1	0.40 ± 0.03	—	0.768[b]
	H$_2$N·	{H$_2$N—CH$_2$—Ċ(CH$_3$)(OCOCH$_3$)[c]	—	23.0 ± 0.1	13.1 ± 0.1	unresolved	8.2 ± 0.1	0.785[b]
VPr	HO·	{HO—CH$_2$—ĊH(OCOCH$_2$CH$_3$)	20.2 ± 0.1	—	12.3 ± 0.1	1.61 ± 0.05	—	0.836[d]
	H$_2$N·	{H$_2$N—CH$_2$—ĊH(OCOCH$_2$CH$_3$)[c]	20.5 ± 0.1	—	14.2 ± 0.1	1.62 ± 0.05	8.3 ± 0.1	0.855[d]
VBu	HO·	HO—CH$_2$—ĊH(OCOCH$_2$C$_2$H$_5$)	20.1 ± 0.1	—	12.1 ± 0.2	1.34 ± 0.04	—	0.836[d]
VCr	HO·	HO—CH$_2$—ĊH(OCOCH=CHCH$_3$)	20.4 ± 0.3	—	12.3 ± 0.3	unresolved	—	0.836[d]
EAc[e]	HO·	CH$_3$—ĊH(OCOCH$_3$)	18.8 ± 0.7	—	24.0 ± 0.9	1.44 ± 0.18	—	0.819

[a] The designations α and β refer to the position relative to the carbon which bears the unpaired electron.

[b] Obtained from the $a_H^{CH_3}$-values. The average value of Δ(OCOCH$_3$) obtained from the ρ_α values was 0.104, which agrees well with the value 0.109 calculated from the data for ethyl acetate.

[c] In acid media, these radicals are protonated, i.e., H$_3^+$N—CH$_2$—ĊH(OCOR').

[d] Δ(OCOR') is assumed to be 0.104, irrespective of R' group.

[e] Ethyl acetate, data of Smith et al.[17]
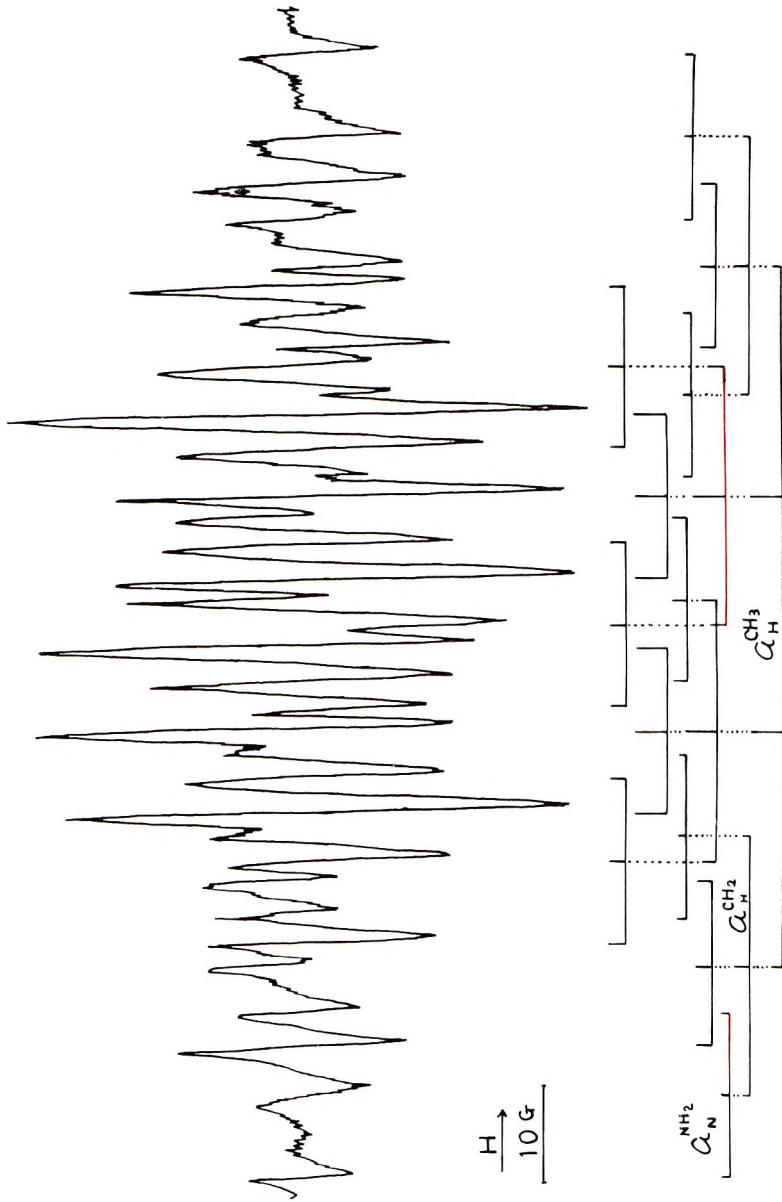
Fig. 8.   ESR spectrum from IPAc in the system of NH₂OH–TiCl₃.   [IPAc] = 6.9 × 10⁻² mole/l.; [NH₂OH] = 2.5 × 10⁻¹ mole/l.; [TiCl₃] = 7 × 10⁻³ mole/l.

Fig. 9. ESR spectrum from vinyl propionate in the system of NH_2OH–$TiCl_3$. [VPr] $= 5.6 \times 10^{-2}$ mole/l.; $[NH_2OH] = 2.5 \times 10^{-1}$ mole/l.; $[TiCl_3] = 7 \times 10^{-3}$ mole/l.; $[H_2SO_4] = 2.2 \times 10^{-2}$ mole/l.

coupling with the nitrogen atom are clearly observed. The coupling constants obtained are listed in Table I, together with those for HO adduct radicals. For comparison, literature data for $CH_3\overset{\cdot}{C}HOCOCH_3$ radicals[17] obtained by hydrogen abstraction from ethyl acetate with HO· radicals in a flow system are also included in Table I.

In this investigation, the vinyl esters show a strong selectivity towards different species in free-radical addition. Hydroxyl radicals are electrophilic in character, and they add easily to the negatively polarized double bond of vinyl esters and form monomer radicals. Methyl radicals, on the other hand, do not give detectable amounts of monomer radicals under identical conditions. Vinyl ester monomers in general show low reactivity towards methyl radical addition. Acrylic monomers, however, react rather easily with methyl radicals according to Fischer et al.[6,7] These combined results are in reasonably good agreement with methyl affinity data of Szwarc.[18] He reported the reactivity of VAc monomer towards methyl radicals to be about forty times lower than those of acrylonitrile and methyl methacrylate.

As seen in Table I, the observed radicals resulting from the addition of R· to vinyl esters have all the structure $R—CH_2—\overset{\cdot}{C}(X_1)(X_2)$. No radicals $R—C(X_1)(X_2)—\overset{\cdot}{C}H_2$ have been observed. Therefore, all our results agree with the general concept that the methylene group of a vinyl monomer $CH_2{=}C(X_1)(X_2)$ is normally more reactive than the substituted carbon

atom towards free radical addition.   It should be noted that all the vinyl esters studied gave almost the same, very small β-hydrogen coupling constants (cf., a_H^β-values in Table I) regardless of the structure of the ester group.   The coupling with the three protons in the acetate group of IPAc was much weaker than for other vinyl esters.   This seems to be an effect of the methyl group attached to the α-carbon atom.   It is also interesting to note that the coupling with the nitrogen atom in the H_2N adduct radicals gave considerably higher value, $(a_N^{NH_2} = 8.3$ gauss) than the nitrogen atom in the H_2N adduct radicals of acrylic acid $(a_N^{NH_2} = 3.4$ gauss).[5] The former, however, is similar to that for the radicals H_2N—CH_2—$\dot{C}H(OH)$ produced by hydrogen abstraction from ethanolamine $(a_N^{NH_2} = 10.3$ gauss), as reported by Norman et al.[2]

The coupling constants of the protons of free rotating methyl groups are proportional to the spin density ρ_α in the $2P_z$ orbital of the trigonal carbon to which the methyl group is bonded, i.e., $a_H^{CH_3} = Q_H^{CH_3} \rho_\alpha$, where $Q_H^{CH_3}$ is 29.3 gauss for aliphatic radicals.[9]   Therefore, the ρ_α value for the IPAc monomer radicals can be determined directly from the observed value of $a_H^{CH_3}$.   Extending the original ideas of Fessenden and Schuler,[19] Fischer[20] proposed that the ρ_α value at the carbon atom in the radical $(X_1)(X_2)(X_3)$-C· is generally given by the equation $\rho_\alpha = \psi [1 - \Delta (X_i)]$ where $\Delta(X_i)$ is a constant for each substituent.   The $\Delta(X_1)$ values are fractions of the spin density withdrawing power of substituents attached to the tervalent carbon atom.   Using the values given by Fischer,[20] $\Delta(H) = 0$, $\Delta(CH_3) = 0.081$, $\Delta(CH_2OH) = 0.079$, $\Delta(CH_2NH_2) = 0.034$, as well as the value obtained in this study, $\Delta(OCOCH_3) = 0.104$, we calculated the ρ_α values for the vinyl ester monomer radicals.   They are also given in Table I.

Steric Conformation of Vinyl Ester Monomer Radicals as Studied from Their β-Hydrogen Coupling Constants

As seen from Table I, all the a_H^β-values are considerably smaller than those for other types of vinyl monomers, e.g., acrylic acid, which gives an HO adduct radical with $a_H^\beta = 27.58$ gauss.[4]   When the a_H^β-value for $CH_3\dot{C}H(OCOCH_3)$ radicals is compared with those of these vinyl ester radicals, a surprisingly great decrease in the a_H^β value occurs when one of the hydrogens of the β-methyl group is replaced with a substituent, i.e., an HO or H_2N group.   There is only a very slight variation with temperature in the a_H^β values for the various VAc monomer radicals, e.g., 12.0 gauss ($8°C$), 12.2 gauss ($20°C$), and 12.8 gauss (about $50°C$).   As previously reported,[8] these results indicate that the studied radicals have a conformation of strongly restricted rotation around the C^α—C^β axis.

For aliphatic radicals, the a_H^β values are known to be strongly dependent on the steric conformation of the radicals, as given by the relationship,[21]

$$a_H^\beta = B_H^\beta \rho_\alpha \cos^2\theta$$

where θ is the angle between the axis of the $2P_z$ orbital of the unpaired electron and the direction of the C^β—H bond, projected on a plane perpendicu-
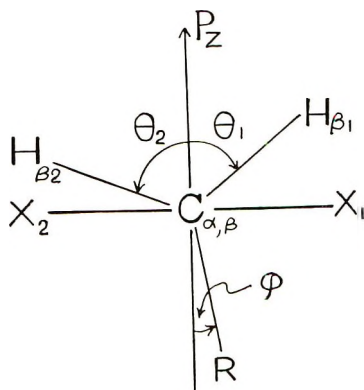
Fig. 10. Steric conformation of free radical of the type $R = CH_2 - C \times_1 \times_2$ with the $C^\alpha - C^\beta$ axis perpendicular to the plane of the paper.

lar to the direction of the C^α—C^β bond. If the two β-protons are equivalent, $a_H{}^\beta$ can be calculated by the equation,[4]

$$a_H{}^\beta = B_H{}^\beta \rho_\alpha \, {}^1/_4(3 - 2\cos^2\phi) = B_{H\beta}\rho_\alpha \cdot \overline{\cos^2\theta}$$

where ϕ is the angle of free rotation between the projection of the C^α—R bond and the axis of the $2P_z$ orbital. The angle ϕ represents the average position of the substituent R projected on a plane perpendicular to the C^α—C^β bond, as illustrated in Figure 10, $\overline{\cos^2\theta}$ is an average for all angles θ attained, and $B_{H\beta}$ is a quantity reported by Fessenden and Schuler (58.6 gauss).[19]

The ϕ values calculated from $a_H{}^\beta$ values for vinyl ester radicals are listed in Table II. For comparison, ϕ values for other radicals obtained by vari-

TABLE II
Values of $a_H{}^\beta$ and Free Rotation Angle ϕ

Radical	$a_H{}^\beta$, gauss	ϕ	Reference
HO—VAc·	12.2	0°	This work
HO—IPAc·	12.5	14°	" "
H$_2$N—IPAc·	13.1	15°	" "
HO—VPr·	12.3	0°	" "
H$_2$N—VBr·	14.2	15°	" "
EAc·	24.0	45°	Smith[16]
HO—AA·[a]	27.58	51.3°	Fischer[4,5]
HO—MAA·[b]	19.98	37.3°	"
H$_2$N—MAA·	16.75	26.3°	"
H$_2$N—CH$_2$—ĊH	11.8	0°	Norman[2]
| OH			
CH$_3$—CH$_2$—ĊH	21.4	42.2°	Livingston[22]
| OH			

[a] HO—AA· refers to HO—CH$_2$—ĊH(COOH).
[b] HO—MAA· refers to HO—CH$_2$—Ċ(CH$_3$)(COOH).

ous workers are also listed.   As seen from Table II, the small values of $a_H{}^\beta$ may be accounted for by assuming an equilibrium conformation in which the angle θ is nearly $60°$ for both methylene hydrogens.   Under these conditions the group R (HO- or H_2N-group) of $R—CH_2—\dot{C}H(OCOR')$ is locked above or below the radical plane.   In general, as the bulkiness of the β substituent of the methylene group is increased, the radicals tend to have a conformation which would maximize the distance between the bulky β substituent group and the group attached to the α-carbon atom.   This would lead gradually to smaller angles ϕ of free rotation.   Such an effect has been nicely demonstrated by Fischer et al.[5,6] by using acrylic type monomer radicals with different initiators.   In our copolymerization studies[9,10] we obtained smaller $a_H{}^\beta$ values for copolymer radicals than for the corresponding monomer radicals.   These data were satisfactorily interpreted as due to the increased bulkiness of the substituents attached to the β-carbon atom.   In the case of vinyl ester monomer radicals, however, this interpretation seems improbable.   It may be suggested that some specific intramolecular interaction is operative between the two polar groups, i.e., the OH or H_2N group on the methylene group and the ester group attached to the α-carbon.   The observed temperature independence of $a_H{}^\beta$ values is consistent with the presence of some intramolecular forces, which strongly hinder the rotation.   As shown in Table II, the situation for β-substituted ethanolic radicals is very similar to this case.   In $CH_3CH_2—$ $\dot{C}HOH$ radicals, free rotation of the CH_3CH_2 group may occur with respect to the $\dot{C}H—OH$; however, if the β-methyl groups are replaced by a polar H_2N group, the angle ϕ of free rotation is very much decreased (to zero). At this moment a reasonable interpretation for the anomalous conformation of the vinyl ester radicals is the formation of an intramolecular hydrogen bond between the OH or H_2N group and the carbonyl oxygen of the ester group attached to the α-carbon, giving a seven-membered ring structure. From studies of a molecular model, this conformation seems to be feasible, although the ring structure is not planar.   This type of hydrogen bond might exist also in aqueous media, as recently proposed by Jellinek[23] for poly(methacrylic acid).   Another possibility is a titanium chelate of the vinyl ester monomer radicals in which Ti(IV) might be coordinated with the two polar groups.   In fact, ethanolamine is known to form a water-soluble chelate compound of titanium.[24]   In the case of vinyl ester compounds, there is, however, no evidence for such titanium complexes.

Hydrogen Abstraction from Ethyl Acetate and Isopropyl Acetate by HO· Radicals

The chain transfer reactions during VAc polymerization and graft copolymerization to PVAc have been extensively studied.   It has been established in some cases that the transfer to polymers occurs preferentially on the hydrogen atoms of the acetyl group.[25]   Some workers reported, however, that most transfer reactions occurred at the α- or β-hydrogens, leading to nonhydrolyzable branches.[26,27]
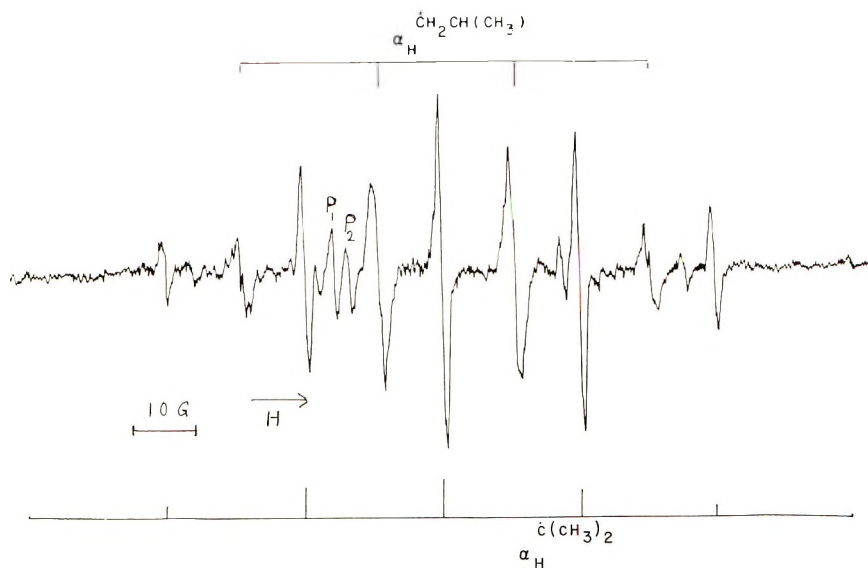
Fig. 11.   ESR spectrum from isopropyl acetate in the system H_2O_2–$TiCl_3$.   [Isopropyl acetate] $= 1.3 \times 10^{-1}$ mole/l.;   [H_2O_2] $= 1.5 \times 10^{-1}$ mole/l.;   [$TiCl_4$] $= 7 \times 10^{-3}$ mole/l.;   [H_2SO_4] $= 2.2 \times 10^{-2}$ mole/l.

In relation to this controversy on the transfer and grafting reactions, the ESR method offers a new method to study the radicals actually involved. In this work, the radicals formed by hydrogen abstraction from model compounds for VAc, e.g., ethyl acetate and isopropyl acetate, have been studied. As previously reported by Smith et al.,[17] ethyl acetate reacted with HO· radicals, and the predominant spectrum of a doublet of quartets with each component split further into a narrow quartet was observed.   The spectrum was attributed to $CH_3\dot{C}H(OCOCH_3)$ radicals.   ESR signals due to ·$CH_2CH_2(OCOCH_3)$ formed by removal of a hydrogen atom from the terminal methyl group was also observed.   However, no product of hydrogen abstraction from the acetyl group was observed.

Isopropyl acetate gave a septet ($a_H = 22.2 \pm 0.1$ gauss), assigned to $CH_3\dot{C}(CH_3)(OCOCH_3)$, formed by abstraction of the secondary hydrogen, on which a quartet was superimposed ($a_H = 2.17 \pm 0.3$ gauss) as shown in Figure 11.   The quartet is attributed to ·$CH_2CH(CH_3)(OCOCH_3)$, formed by abstraction of hydrogen from a terminal methyl.   Although two of the three hydrogens, which couple with the unpaired electron, are in a different location than the third, the observed coupling constants of α- and β-protons are very similar, as previously found for other alkyl radicals. The line-broadening of the quartet is caused by slight differences in the coupling constants.   The splitting of each component of the septet, due to acetyl hydrogens was not observed, probably because there are two α-methyl groups.   Here again, no product of hydrogen abstraction from the acetyl group was obtained.   The absence of this radical in the spectrum is

not due to its instability since a similar radical $HOCO\dot{C}H_2$ was actually observed as a result of hydrogen abstraction of acetic acid with $HO\cdot$ radicals.[2]

It was demonstrated in this paper that the electrophilic hydroxyl radicals attack predominantly the α- and β-hydrogens of the model substances. Instead of $HO\cdot$ radicals an attempt was made to use methyl radicals, which are similar in nature to growing chain radicals of VAc. The quartet spectrum of methyl radicals was obtained but no spectra from the substrates were observed. The possibilities of having hydrogen abstraction is directly dependent upon the character of the attacking radicals. On the basis of these results, it is suggested that graft polymerization onto PVAc, initiated by $HO\cdot$ radicals, may take place mainly at the α- or β-hydrogen positions of the polymer chain. In the case of vinyl ester polymerization, unhydrolyzable branches may, therefore, be formed to some extent on the resulting polymer chain, particularly when an excess of $HO\cdot$ radicals is used as initiator.

References

1. W. T. Dixon and R. O. C. Norman, *Nature*, **196**, 891 (1962); *J. Chem. Soc.*, **1963**, 3119.

2. W. T. Dixon, R. O. C. Norman, and A. L. Buley, *J. Chem. Soc.*, **1963**, 3625.

3. H. Fischer, *Z. Naturforsch.*, **18a**, 1142 (1963); *ibid.*, **19a**, 267 (1964); *J. Polym. Sci. B*, **2**, 529 (1964).

4. H. Fischer, *Z. Naturforsch.*, **19a**, 866 (1964).

5. C. Corvaja, H. Fischer, and G. Giacometti, *Z. Physik. Chem.* (Frankfurt), **45**, 1 (1965).

6. H. Fischer and G. Giacometti, in *Macromolecular Chemistry, Prague 1965 (J. Polym. Sci. C*, **16**), O. Wichterle and B. Sedláček, Eds., Interscience, New York, 1967, p. 2763.

7. H. Fischer, *Makromol. Chem.*, **98**, 179 (1966).

8. H. Yoshida and B. Rånby, in *Macromolecular Chemistry, Prague 1965 (J. Polym. Sci. C*, **16**), O. Wichterle and B. Sedláček, Eds., Interscience, New York, 1967, p. 1333 (Part I).

9. K. Takakura and B. Rånby, *J. Polymer Sci. B*, **5**, 83 (1967).

10. K. Takakura and B. Rånby, paper presented at the IUPAC Symposium on Macromolecular Chemistry, Brussels-Louvain 1967; *J. Polym. Sci. C*, **22**, 939 (1969).

11. W. E. Griffiths, G. F. Longster, J. Myatt, and P. F. Todd, *J. Chem. Soc., B*, **1967**, 530.

12. K. Takakura and B. Rånby, *J. Phys. Chem.*, **72**, 164 (1968).

13. E. Collinson, F. Dainton, and R. McNaughton, *J. Chim. Phys.*, **52**, 556 (1955).

14. C. H. Bamford, A. D. Jenkins, and R. Johnston, *Proc. Roy. Soc.* (London), **A239**, 214 (1957); *J. Polym. Sci.*, **29**, 355 (1958).

15. J. K. Kochi, *J. Amer. Chem. Soc.*, **78**, 4815 (1956); *ibid.*, **79**, 2942 (1957); *ibid.*, **84**, 2121 (1962).

16. G. E. Ham, Ed., *Copolymerization*, Interscience, New York, 1964, p. 845.

17. P. Smith, J. T. Pearson, P. B. Wood, and T. C. Smith, *J. Chem. Phys.*, **43**, 1535 (1965).

18. M. Szware, *J. Polym. Sci.*, **16**, 367 (1955).

19. R. W. Fessenden and R. H. Schuler, *J. Chem. Phys.*, **39**, 2147 (1963).

20. H. Fischer, *Z. Naturforsch.*, **20a**, 428 (1965).

21. C. Heller and H. M. McConnell, *J. Chem. Phys.*, **32**, 1535 (1960).

22. R. Livingston and H. Zeldes, *J. Chem. Phys.*, **44**, 1245 (1966).

23. H. H. G. Jellinek and S. N. Lipovac, *J. Macromol. Chem.*, **1**, 773 (1966).

24. R. Feld and P. L. Cowe, *The Organic Chemistry of Titanium*, Butterworths, London, 1965, p. 64.

25. S. Imoto, J. Ukida, and T. Kominami, *Kobunshi Kagaku*, **14**, 101, 127, 384 (1957).

26. R. O. Howard, Ph.D. thesis, Mass. Inst. Technology, Cambridge, Mass., 1952.

27. J. Roland and L. Ricards, *J. Polym. Sci.*, **9**, 61 (1952).

Reformulation of the General Theory of Ionic Polymerization. II. Rate of Change of Degree of Polymerization with Time

Th. DELEANU and M. DIMONIE, *Institutul de Chimie Fizica al Academiei R. S. Romania, Bucuresti, Romania*

Synopsis

By means of the kinetic equations of polymerization some approximate relations were deduced by using the concomitant rate of change of intrinsic viscosity in many concrete cases. These relations were easy to handle and were sufficiently precise for direct calculation of the rate constants of polymerization.

A detailed mathematical study was carried out to improve the suggested approximations as well as the extension of these considerations.

I. INTRODUCTION

The discussion in the previous paper[1] indicates the possibility of characterizing the polymerization kinetics by the monomer consumption in time and by the arithmetic or weight average of the degree of polymerization obtained by osmotic-pressure or light-scattering measurements.

We suggest in the present paper the use of viscometric data for the same purpose. We assumed that the deactivation of active macromolecules is irreversible. At the end of Section II we then compute a first approximation for the case in which reactivation of deactivated macromolecules would be possible. The deactivation is assumed to be a first-order reaction only in relation with the active polymer concentration. Our computations refer to the deactivation by charge transfer.

This last development, compared to Coleman's paper[2] is possible because we cannot make any hypothesis regarding the speed of the initiation process or the mechanism, but we assume that the active polymers are monofunctional.

For the calculation of the polymer polydispersity in the case of complex polymerization processes in which the initiation reaction is fast, Nanda[3] starts from the hypothesis that the instantaneously initiated active polymers are monodisperse and the length of the macromolecular chain is a continuous quantity.

In Section II we suggest a rigorous method of computing the moments of fractional orders of degrees of polymerization under very general conditions of the initiation process. These moments are used in computing the rate

95

constants of polymerization by means of experimentally determined intrinsic viscosities.

Such computations were made for conditions of radical polymerization[4] in the case of rapid initiation by using the Laplace transform, which was applied for the first time by Bamford[5] studying polymerization kinetics. This method used by Chiang and Hermans[6,7] for the computation of arithmetic and gravimetric molecular weight averages was not of use for the fractional average computation under the conditions studied by us. The slow initiation polymerization was studied by Gold[8] and Nanda[9] as a simple bimolecular process.

In Section III the equations of immediate applicability in the experimental studies are presented.

II. AVERAGES OF A FRACTIONAL ORDER

For the formulation of the various equations which characterize the polymerization process, we shall use the following notations. G_r and $\mathcal{K}_r$ are the number of active and deactivated polymer molecules, respectively, with r mers per unit volume; ρ_ν is the total number of polymer molecules; $\bar{r}$ is the arithmetic average of the degree of polymerization, g is the weight average of the degree of polymerization; ρ_ν is defined by eq. (2); A is the number of initiator molecules per unit volume at $t = 0$; M and M_0 are the number of monomer molecules per unit volume at time t and initially ($t = 0$), respectively; $P.S.Q$ are the rate constants of polymerization, deactivation, and reactivation, respectively; H, ϵ are constants defined by eqs. (4) and (4'); $[\eta]$ is intrinsic viscosity, and p is molecular weight of monomer. Conversion Ω is defined as

$$\Omega = (M_0 - M)/M_0 \qquad\qquad 0 < \Omega < 1$$

t, τ and θ are different notation of time, used in the computation of some integrals in relation with time.

We define:

$$\omega = \omega_t = \int_0^t PM\,dt$$

$$\sigma = \sigma_t = \int_0^t S\,dt$$

$$\omega_{\tau_t} = \omega_t - \omega_\tau = \int_\tau^t PM\,dt$$

$$\sigma_{\tau_t} = \int_\tau^t S\,dt = \sigma_t - \sigma_\tau$$

$$R_\nu(\omega) = \sum_{r=1}^{\infty} \frac{r^\nu \omega^{r-1}}{(r-1)!} e^{-\omega}$$

where ν is the moment order and ρ_ν/ρ_0 is the moment of ν order.

The equations of polymerization kinetics are as follows:

Propagation:

$$d\mathcal{G}_{r+1}/dt = PM(\mathcal{G}_r - \mathcal{G}_{r+1}) - S\mathcal{G}_{r+1} + Q\mathcal{K}_{r+1} \tag{1}$$

Termination:

$$d\mathcal{K}_r/dt = S\mathcal{G}_r - Q\mathcal{K}_r \qquad r = 1,2,3,...$$

We assume $Q = 0$ and introduce the function:

$$\rho_\nu = \sum_{r=1}^{\infty} r^\nu(\mathcal{G}_r + \mathcal{K}_r) \tag{2}$$

for $\nu = 0,1,2,$

$$\rho_0 = (M_0 - M)/\bar{r}$$

$$\rho_1 = M_0 - M;$$

$$\rho_2 = g(M_0 - M) \tag{3}$$

For a certain value of ν ($\nu = \epsilon + 1$) the function ρ_ν depends on the intrinsic viscosity.

We recall the well known relation for the case of the monodisperse polymers:

$$[\eta] = Hp^\epsilon r^\epsilon \tag{4}$$

For the case of polydisperse polymers we substitute the gravimetric average or $\bar{r}^\epsilon$; r^ϵ to r^ϵ $\bar{r}^\epsilon$.[10]

$$[\eta] = Hp^\epsilon \frac{\displaystyle\sum_{r=1}^{\infty} r(\mathcal{G}_r + \mathcal{K}_r)r^\epsilon}{\displaystyle\sum_{r=1}^{\infty} r(\mathcal{G}_r + \mathcal{K}_r)} = \left[Hp^\epsilon \frac{\rho_1 + \epsilon}{\rho_1} \right] \tag{4'}$$

where, in general, $0.5 < \epsilon < 0.9$, and then $1 < 1 + \epsilon < 2$.

System (1) of differential equations admits the particular solution:[2]

$$\mathcal{G}_r = X \frac{\omega^{r-1}}{(r-1)!} e^{-(\omega+\sigma)}$$

$$\mathcal{K}_r = X \int_{\tau=0}^{\tau=t} \frac{\omega_\tau^{r-1}}{(r-1)!} e^{-(\omega_\tau+\sigma_\tau)} d\sigma_\tau \tag{5}$$

X is an integration constant. By computing the total quantity, ρ_0, of polymer from eq. (5) we find that it is a constant, namely $\rho_0 = X = A$. Consequently solution (5) corresponds to the case of instantaneous initiation at time $t = 0$. If the initiation process is not instantaneous, but at the instant τ a quantity $d\rho_0(\tau)$ of polymer is formed, the fact that the system of eqs. (1) is linear entitles us to superpose the solutions corresponding to the

initiation at various instants τ of the quantities $d\rho_0(\tau)$ of polymer, and therefore:

$$\mathcal{G}_r = \int_{\tau=0}^{\tau=t} \frac{\omega_{\tau t}^{r-1}}{(r-1)!} e^{-(\omega_{\tau t}+\sigma_{\tau t})} d\rho_0(\tau)$$

$$\mathcal{K}_r = \int_{\tau=0}^{\tau=t} d\rho_0(\tau) \int_{\theta=\tau}^{\theta=t} \frac{\omega_{\tau\theta}^{r-1}}{(r-1)!} e^{-(\omega_{\tau\theta}+\sigma_{\tau\theta})} d\sigma_\theta \tag{6}$$

In the Appendix we have developed a computation permitting ρ_ν to be estimated by using eq. (5). In the case of instantaneous initiation:[2]

$$\rho_\nu = A + A \int_{\theta=0}^{\theta=t} e^{-\sigma_\theta} d[R_\nu(\omega_\theta)] \tag{7}$$

And if at the instant τ the quantity $d\rho_0(\tau)$ of polymer is initiated we shall obtain, in analogy with eq. (6),

$$\rho_\nu = \int_{\tau=0}^{\tau=t} d\rho_0(\tau) \left\{ 1 + \int_{\theta=\tau}^{\theta=t} e^{-\sigma_{\tau\theta}} d_\theta[R_\nu(\omega_{\tau\theta})] \right\} \tag{8}$$

For ν as positive integer, $R_\nu(\omega)$ are polynomials of degree ν:[2]

$$R_0(\omega) = 1$$

$$R_1(\omega) = 1 + \omega$$

$$R_2(\omega) = 1 + 3\omega + \omega^2$$

$$R_3(\omega) = 1 + 7\omega + 6\omega^2 + \omega^3 \tag{9}$$

If a 0.5% accuracy is satisfactory, then the function $R_\nu(\omega)$ may be approximated by:

$$\bar{R}_\nu(\omega) = \begin{cases} 1 + (2^\nu - 1)\omega + (3^\nu - 2 \times 2^\nu + 1)(\omega^2/2) & \text{if } \omega \leqslant 1 \\ \omega^\nu + \dfrac{\nu(\nu+1)}{2}\omega^{\nu-1} + \dfrac{\nu(\nu+1)(\nu-1)(3\nu-2)}{24}\omega^{\nu-1} & \text{if } \omega \geqslant 1 \end{cases} \tag{10}$$

for $1 \leqslant \nu < 2$. The accuracy is improved without limit when $\omega \to 0$ or $\omega \to \infty$. We shall use the following approximation of function $R_\nu(\omega)$:

$$\bar{\bar{R}}_\nu(\omega) = \omega^\nu \tag{11}$$

This is justified since, in the general study of polymerization $\omega \gg 1$, and we aim to prove this statement. We have introduced the function $\omega_{\tau t}$ for exclusively formal considerations. The physical significance of $\omega_{\tau t}$, as mean degree of polymerization (arithmetic mean) of the polymer initiated at time τ and which remains active at instant t, may be obtained from the kinetic equations of monomer consumption

$$- dM/dt = PM\mathcal{G}$$

with

$$G = \sum_{n=1}^{\infty} G_r \qquad (12)$$

If we denote by $G^{(\tau t)}$ the number of polymer molecules initiated at the time τ which remain active at least till time $t > \tau$ and by $M_{\tau t}$ the quantity of monomer consumed in the process of polymerization of $G^{(\tau t)}$ macromolecules from moment τ to t, then:

$$M_{\tau t} = G^{(\tau t)} \int_{\tau}^{t} PM dt = G^{(\tau t)} \omega_{\tau t} \qquad (13)$$

Here $G^{(\tau t)}$ is a constant magnitude depending on the two extreme moments τ and t.

Therefore, in the case of "living" polymers initiated practically instantaneously at $t = 0$, ω_t represents the mean degree of polymerization, regardless of whether or not the system receives monomer from the outside during polymerization, or of whether or not the rate constant P changes with time, for example due to temperature changes. Equation (7) becomes, in the case of living polymers initiated at $t = 0$:

$$\rho_\nu = A R_\nu(\omega) \qquad (13')$$

then $[R_\nu(\omega)]^{1/\nu}$ also represents a degree of polymerization. On reasoning as before for the case $S \neq 0$, $[R_\nu(\omega)]^{1/\nu}$ will represent a mean degree of polymerization of the polymer which has been initiated at instant τ and which has remained active at instant $t > \tau$.*

We notice that in approximation (11), $[R_\nu(\omega)]^{1/\nu}$ does not depend on ν, i.e., the active polymers behave as if they were monodisperse. Approximation (10) does not account for the errors in the mean, if we consider that the active polymers are not monodisperse.

If we do not assume that the initiation is made instantaneously, we then use, in the case of living polymers, the expression proved in the Appendix:

$$\rho_\nu = - \int_{\tau=0}^{\tau=t} R'_\nu(\omega_{\tau t}) \, dM(\tau)$$

where

$$R'_\nu(\omega) = \partial R_\nu(\omega)/\partial \omega \qquad (14)$$

For $S \neq 0$, the more general equation

$$\rho_\nu = (2^\nu - 1)(M_0 - M) - \int_{\theta=0}^{\theta=t} d\omega_\theta \int_{\tau=0}^{\tau=\theta} R_\nu''(\omega_{\tau\theta}) e^{-\sigma_{\tau\theta}} dM(\tau) \qquad (14')$$

is valid.

* We mention that the magnitude ω was used by Nanda[3] under the name, maximum possible chain length, for the computation of polydispersity. In eq. (5) one can see that $G_r \simeq 0$ except for the value of r for which $\omega \simeq r + 1$.[11]

According to eq. (13) one could interpret that ω is the mean degree of polymerization whereas according to eq. (13') for $\nu = 1$ the polymerization degree is $1 + \omega$.[7] This distinction remains superfluous for $\omega \gg 1$.

The same computing procedure allows us to deduce, from eq. (6), the following expressions for $\mathcal{G}_r$ and $\mathcal{K}_r$, by using only the monomer consumption in time and the rate constant P and S:

$$\mathcal{G}_r + \mathcal{K}_r = -\int_{\theta=0}^{\theta=t} d\omega_\theta \int_{\tau=0}^{\tau=\theta} e^{-\sigma_{\tau\theta}} \frac{d^2}{d\omega_{\tau\theta}^2}\left[\frac{\omega_{\tau\theta}^{r-1}}{(r-1)!}e^{-\omega_{\tau\theta}}\right] d_\tau M \text{ for } r > 2$$

$$(14'')$$

Here the quantity $\rho_0(\tau)$ of polymer no longer appears explicitly.

The study of the initial phases of polymerization is advantageous due to the certainty of the absence of any degradation phenomena and of the absence of insoluble fractions.

Relations (11) and (14) lead to:

$$\rho_\nu = P^{\nu-1}J_\nu(t)$$

where

$$J_\nu(t) = -\nu\int_{\tau=0}^{\tau=t}\left[\int_\tau^t M(\theta)d\theta\right]^{\nu-1} dM(\tau) \tag{15}$$

and, in a first approximation:

$$-J_\nu(t) = M_0^{\nu-1} M_1 t^\nu$$

Hence

$$[\eta] = Hp^\epsilon P^\epsilon M_0^\epsilon t^\epsilon \tag{16}$$

where

$$M = M_0 + M_1 t + (M_2/2) t^2 + ... \tag{17}$$

M_0, M_1, and M_2 are coefficients which represent successive derivatives of M for $t = 0$. A more exact evaluation of ρ_ν according to eq. (A-20) in the Appendix leads to the development:

$$-J_\nu(t) = M_0^{\nu-1} M_1 t^\nu + \left[\frac{M_1}{2 M_0}\left(1 - \frac{2}{\nu(\nu+1)}\right)\right.$$

$$\left. + \frac{M_2}{M_1\nu(\nu+1)} + S(0)\right] M_0^{\nu-1} M_1 t^{\nu+1} \tag{18}$$

It is noticed that $S(0)$, the rate of the deactivation constant at $t = 0$, appears only in the second term of eq. (18), hence eq. (16) is also valid for the case $S \neq 0$ for small t. The computation of S from eq. (18) is practically possible only when M_1/M_0, M_2/M_1, are small or compared with S.

To determine the values of S and P we shall use the graphical method. We shall represent $[\eta]$ in the ordinate, and the time t^ϵ in the abscissa. By extrapolation of the curve to its intersection with the ordinate, we find from eq. (16) the value of P and from the slope the value of S according to eq. (18). This extrapolation must be made at the same value of t when the

polymerization degree $\bar{r} > 10$. When $\bar{r} < 10$, eqs. (16) and (18) are no longer valid. The condition $\bar{r} > 10$ is practically always met. The estimation of P from advanced states of the polymerization process is easy when the initiation rate constant is larger than that of polymerization, i.e., when the initiation may be considered finished after a time $t = a$ (relatively small) and if $S = 0$. In this case the monomer consumption follows the rule:

$$\ln (M_0/M) = APt \tag{19}$$

and the conversion expression at a given instant t will be

$$\Omega = 1 - e^{-APt}$$

Under these conditions, eq. (4) becomes:

$$[\eta] = Hp^\epsilon \, \Omega^\epsilon M_0^\epsilon / A^\epsilon \tag{20}$$

valid for any t. We shall put $[\eta]$ in the abscissa and Ω^ϵ in the ordinate, and from the slope of the straight line we find the concentration A of the polymer, while from the knowledge of the product given by the experimental relation (19) we can find P.

If, however, the initiation is sufficiently fast and we have a very small concentration of initiators, so that $PA \ll S$, then there results:

$$\rho_1 = M_0 - M = M_0\Omega$$

where

$$\Omega \simeq (AP/S) \, (1 - e^{-St}) \qquad \text{for any } t \tag{21}$$

hence $\sigma \simeq M_0 Pt$ and thus:

$$[\eta] = Hp^\epsilon \frac{SM_0^\epsilon P^\epsilon t^\epsilon}{1 - e^{-St}} \left[1 - \frac{St}{1!} \frac{1 + \epsilon}{2 + \epsilon} + \frac{(St)^2}{2!} \frac{1 + \epsilon}{3 + \epsilon} + \cdots \right] \tag{22}$$

For large t it is more suitable to use the relation

$$[\eta] = Hp^\epsilon \frac{PM_0^\epsilon}{S^\epsilon} \frac{\Gamma(2 + \epsilon) - (ST)^\epsilon \, e^{-St} \left[1 + \dfrac{\epsilon}{ST} + \dfrac{\epsilon(\epsilon - 1)}{(ST)^2} \cdots \right]}{1 - e^{-St}} \tag{23}$$

This means that the maximum value of intrinsic viscosity is given by relation

$$[\eta] = Hp^\epsilon \frac{P^\epsilon M_0^\epsilon}{S^\epsilon} \Gamma(2 + \epsilon) \tag{24}$$

Since we have assumed that $AP \ll S$, then these relations can in no case be used for living polymers when $S = 0$.

The eqs. (1) are not integrable by quadratures in the case $Q = 0$. From the final discussion of the results obtained in our previous paper,[1] there follows that in a very good approximation the polymerization process may

be divided into two parts.   First $S \neq 0$ and $Q = 0$, and later $S = 0, Q = 0$. In the region of connection of the two parts, for accuracy of the approximation we must take into account the case $Q \neq 0$.   An indication of the error we make by putting $Q = 0$ may be obtained by considering the first of the successive approximations.   From eqs. (A-5) and (A-9) there results:

$$d\rho_\nu/d\omega = \Sigma \, \mathcal{G}_k[(k + 1)^\nu - k^\nu] \tag{25}$$

If we note $\kappa = \int_0^t Q dl = \kappa_t$

$$\kappa_{\tau t} = \int_\tau^t Q dl = \kappa_t - \kappa_\tau$$

then according to eq (1):

$$\mathcal{K}_k = \int_{\tau=0}^{\tau=t} \mathcal{G}_k(\tau) e^{-\kappa_{\tau t}} d\sigma_\tau$$

$$\mathcal{G}_k^{(1)} = \int_{\tau=0}^{\tau=t} \mathcal{K}_k \, d\kappa_- + \mathcal{G}_k \tag{25'}$$

and, to a first approximation $\mathcal{G}_k$ is given by eq. (6).   Finally:

$$\frac{d\rho_\nu^{(1)}}{d\omega} = \frac{d\rho_\nu}{d\omega} + \int_{\tau=0}^{\tau=t} (1 - e^{-\kappa_{\tau t}}) \frac{d\rho_\nu}{d\omega} d\sigma_\tau \tag{25''}$$

$\rho_\nu^{(1)}$ being the first approximation with respect to ρ_ν, the zero-order approximation when $Q \neq 0$.

III. RESULTS AND DISCUSSION

The active polymer with r mers π_r^* can react with a monomer molecule at the rate P, changing into π_{r+1}^*, or it can be deactivated by a monomolecular process which takes place at the rate constant S.

The value of A can be obtained only from the polymerization kinetic equations.   At the desired accuracy it cannot be determined in any other way.   All the equations are valid for degrees of polymerization $\bar{r} > 10$, and practically in the field of application of equations (4) and (4').

The deactivation of oligomers of degrees of polymerization $\bar{r} < 10$ has been considered as negligible.   This is true as long as we do not work at very high monomer dilutions.

Relation (14'') permits computation of the polydispersity (Table I) by using only the monomer consumption in time and the rate constants P and S.

Though experimental studies concerning the variation of intrinsic viscosity with conversion, have been made our equations could not be applied to the existing data in the literature correlating determinations for such computations have not been made.

The variation of intrinsic viscosity with conversion in polymerization of styrene at $25°C$ initiated by allyl sodium in pentane[12] is the best suited for our results.

TABLE I
Discussion of Main Polymerization Reaction Cases

Polymerization character	Relation to be applied	Time t from beginning of reaction[a]	Relation for monomer consumption
Initiation slow or rapid	$[\eta] = Hp^\epsilon P^\epsilon M_0^\epsilon t^\epsilon$	Short	Any
Rapid initiation living polymers $(S = 0)$	$[\eta] = \dfrac{Hp^\epsilon \Omega^\epsilon M_0^\epsilon}{A^\epsilon}$	Any	$\ln(M_0/M) = APt$
Rapid initiation low conversions $(PA \ll S)$. Irreversible monomolecular deactivation	Eq. (22)	Not very long	$\ln(M_0/M) = (AP/S)(1 - e^{-St})$
"	Eq. (23)	Very long	"
"	Eq. (24)	"	"
Slow initiation, living polymers	General relation eq. (14)[b]	Any	Any
Slow initiation with irreversible deactivation	General eq. (14)[b]	Any	Any

[a] The times for which the relations can be easier applied for computations.

[b] In the case of eqs. (14) and (14′) the poorer approximation (10) or the better approximation (11) can be used.

The disadvantage of this experiment is that the constants for computation of molecular weights from intrinsic viscosity are not known.

In the following we aim to analyze the applicability of the relations deduced in this paper to the different questions developed in several theoretical works.

Burdon and Pepper's[13] scheme of the mechanism studied by Nanda[3] is as follows:

Initiation:

$$M + I \xrightarrow{\text{fast}} \pi_1{}^*$$

Growth:

$$\pi_r{}^* + M \xrightarrow{P} \pi_{r+1}{}^*$$
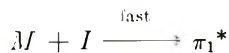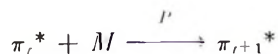
Spontaneous transfer:

$$\pi_r{}^* \xrightarrow{S_1'} \pi_r + I$$

Monomer transfer:

$$\pi_r{}^* + M \xrightarrow{S_2'} \pi_r + \pi_1{}^*$$
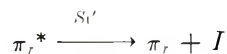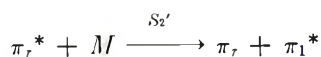
Monomolecular termination:

$$\pi_r{}^* \xrightarrow{\ S_0\ } \pi_r$$
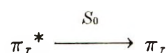
Then, in our equation

$$S = S_0 + S_1' + S_2' M \tag{26}$$

must be substituted.

As one can observe the monomer consumption follows the law:

$$\ln (M_0/M) = (AP/S_0) (1 - e^{-S_0 t}) \tag{27}$$

According to eq. (14′) we obtain directly the value for $\nu > 0$.

For $\nu = 0$ or for $\nu \simeq 0$, eq. (14′) is no longer applicable for the computation of the arithmetical or weight average of polymerization. For this case we use the equation

$$d\rho_0/dt = \mathcal{G}(S_1' + S_2' M)$$

$$\mathcal{G} = \sum_{r=1}^{\infty} \mathcal{G}_r = Ae^{-\sigma t} \tag{28}$$

Chiang and Hermans[6] studied the more special case in which $S_1' = 0$. Guiot[14] also assumes an instantaneous initiation

$$\pi_r{}^* + M \xrightarrow{\ P\ } \pi_{r+1}{}^*$$

$$\pi_r{}^* + M \xrightarrow{\ S_1\ } \pi_r$$
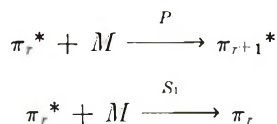
In relation (14′) we shall use $S = S_1 M$.

The bimolecular deactivation by impurities, studied first by Orofino and Wenger[15] and then by Coleman[2] and Nanda,[16] leads us to the substitution $S = S_3 Z$, where Z represents the respective impurity concentration.

The values S_0, S_1, S_2, S_0', S_1', S_2' are assumed to be dependent only on the temperature.

APPENDIX

The system of eqs. (1) admits also the more general type of particular solutions:

$$\mathcal{G}_r = X \frac{\omega^{r-k}}{(r-k)!} e^{-(\omega+\sigma)}$$

$$\mathcal{K}_r = X \int_{\tau=0}^{\tau=t} \frac{\omega_\tau^{r-k}}{(r-k)!} e^{-(\omega_\tau+\sigma_\tau)} d\sigma_\tau$$

$$r \geq k \tag{A-1}$$

r is an integer and positive.   Using the integration by parts, we obtain

$$G_r + \mathcal{K}_r = X\,\delta_{rk} + X\int_{\tau=0}^{\tau=t} e^{-\sigma_\tau}\,d\left[\frac{\omega^{r-k}}{(r-k)!}\,e^{-\omega}\right]$$

$$\delta_{rk} = \begin{cases} 0 & \text{if } r \neq k \\ 1 & \text{if } r = k \end{cases} \qquad (A\text{-}2)$$

The magnitudes

$$\rho_{\nu k} = \sum_{r \geqslant k} r^\nu (G_r + \mathcal{K}_r) = Xk^\nu \sum_{r \geqslant k} \delta_{rk} + X\int_{\tau=0}^{\tau=t} e^{-\sigma_\tau}\,d_\tau\,[R_{\nu k}(\omega_\tau)] \quad (A\text{-}3)$$

where

$$R_{\nu k} = \sum_{[r \geqslant k]} r^\nu \frac{\omega^{r-k}}{(r-k)!}\,e^{-\omega} \qquad (A\text{-}4)$$

may be calculated.   For k integer and positive

$$\sum_{r \geqslant k} \delta_{rk} = 1$$

$$R_{0k}(\omega) = 1$$

$$R_{\nu k} = k^\nu + [(k+1)^\nu - k^\nu]\,\omega + [(k+2)^\nu - 2(k+1)^\nu + k^\nu]$$

$$(\omega^2/2) + \ldots \qquad (A\text{-}5)$$

and then the total quantity of polymer is constant

$$\rho_{0k} = \sum_{r \geqslant k} (G_r + \mathcal{K}_r) = X = A \qquad (A\text{-}6)$$

For $t = 0$;

$$G_k = A$$

$$G_r = \mathcal{K}_r = \mathcal{K}_k = 0 \qquad r > k \qquad (A\text{-}7)$$

When the polymerization process can be approximated by several regions—the case studied by us begins practically at $t = a$ when we have the quantities A_r and B_r of active and inactive respectively, polymers, with r mers—then, by the hypothesis that the initiation had practically stopped at $t = a$:

$$G_r = \sum_{k=1}^{k=r} A_k\,\frac{\omega_{at}^{r-k}}{(r-k)!}\,e^{-[\omega_{at}+\sigma_{at}]}$$

$$\mathcal{K}_r = \sum_{k=1}^{k=r} A_k\int_{\tau=a}^{\tau=t} \frac{\omega_{a\tau}^{r-k}}{(r-k)!}\,e^{-[\omega_{a\tau}+\sigma_{a\tau}]}\,d\sigma_\tau + B_r \qquad (A\text{-}8)$$

and

$$\rho_\nu = \sum_{r=1}^{\infty} r^\nu(G_r + \mathcal{K}_r) = \sum_{k=1}^{\infty} (A_k + B_k)k^\nu + \sum_{k=1}^{\infty} A_k\int_{\tau=0}^{\tau=t} e^{-\sigma_{a\tau}}d_\tau\,[R_{\nu k}(\omega_{a\tau})]$$

$$(A\text{-}9)$$

The possibility of using the fractional or negative values of k to treat a more complex initiation like a instantaneous one is not excluded.

The calculus of $\rho_{\nu k}$ according to eqs. (A-3) and (A-4) is in general difficult, except for the case when $S = 0$ or (which amounts to the same thing) when we study the beginning of the polymerization process when $\Sigma \mathfrak{IC}_r \simeq 0$; hence eq. (A-3) becomes:

$$\rho_{\nu k} = A R_{k\nu}(\omega) \qquad (A\text{-}10)$$

The properties of the function $R_{\nu k}(\omega)$ are:

$$R_{\nu+1,k}(\omega) = \left(k + \omega + \omega \frac{\partial}{\partial \omega} \right) R_{\nu,k}(\omega) \qquad (A\text{-}11)$$

$$R_{\nu,k+1}(\omega) = \left(1 + \frac{\partial}{\partial \omega} \right) R_{\nu k}(\omega) = \frac{1}{\omega} [R_{\nu+1,k}(\omega) - k R_{\nu,k}(\omega)] \quad (A\text{-}12)$$

$$R_\nu(\omega) = e^{-\omega} + \omega \sum_{l \geq 0} \binom{\nu}{l} R_{\nu-l-1}(\omega) =$$

$$(\nu + \omega) R_{\nu-1}(\omega) + \sum_{l \geq 1} \left[\binom{\nu-1}{l+1} + \omega \binom{\nu-1}{l} \right] (- 1)^l R_{\nu-l-1}(\omega) \quad (A\text{-}13)$$

The relation (A-12) permits the transposition of the results for any k if we know $R_{\nu 1}{}^{(\omega)} = R_\nu(\omega)$.

For not very great values of ω we may calculate $R_\nu(\omega)$ according to eq. (A-4) or to:

$$R_\nu(\omega) = 1 + (2^\nu - 1)\omega + (3^\nu - 2 \times 2^\nu + 1)(\omega^2/2!) +$$

$$(4^\nu - 3 \times 3^\nu + 3 \times 2^\nu - 1)(\omega^3/3!) + ... \qquad (A\text{-}14)$$

but for $\omega \gg 1$ the asymptotic approximation $R_\nu^\infty(\omega)$ of $R_\nu(\omega)$ demonstrated in the final portion of this paper is very useful.

$$R_\nu^\infty(\omega) = \sum_{\nu+1 > l \geq 0} a_{l\nu} \, \omega^{\nu-l}$$

$$a_{0\nu} = 1$$
$$a_{1\nu} = \nu(\nu + 1)/2$$
$$a_{2\nu} = (\nu - 1)(\nu + 1)(3\nu + 2)/24 \qquad (A\text{-}15)$$
$$a_{3\nu} = (\nu + 1)\nu(\nu - 1)^2(\nu - 2)/48$$

TABLE II

Deviation of the Function R_ν Towards R_ν^∞ for $\nu = 1.5$

ω	$R_\nu(\omega)$	$R_\nu^\infty(\omega)$	$R_\nu - R_\nu^\infty$	$\dfrac{R_\nu - R_\nu^\infty}{R_\nu} \times 100$
0.1	1.1856	1.143	0.042	3.5
0.5	1.9788	2.963	0.015	0.8
1.0	3.0825	3.070	1.012	0.4
2.0	5.6195	5.618	0.001	0.03
3.0	8.5574	8.556	0.001	0.01

For $\nu = 1,2,3...$, i.e., for ν an integer and positive,

$$R_\nu^\infty (\omega) = R_\nu (\omega) \tag{A-16}$$

We have calculated $R_\nu(\omega)$ and $R_\nu^\infty(\omega)$ for $\nu = 1.5$ (Table II).

If the initiation is not instantaneous the superposition of some solutions of (A-1) type will permit us to calculate ρ_ν:

$$\rho_\nu = \int_{\tau=0}^{\tau=t} d\rho_0(\tau) \left[1 + \int_{\theta=\tau}^{\theta=t} e^{-\sigma_{\tau\theta}} R'_\nu (\omega_{\tau\theta}) d\omega_\theta \right]$$

$$= \rho_0(t) + \int_{\theta=0}^{\theta=t} d\omega_\theta \int_{\tau=0}^{\tau=\theta} e^{-\sigma_{\tau\theta}} R'_\nu(\omega_{\tau\theta}) \, d\rho_0(\tau)$$

$$\tag{A-17}$$

$$= \rho_0(t) + R_\nu'(0) \int_{\theta=0}^{\theta=t} d\omega_\theta \int_{\tau=0}^{\tau=\theta} e^{-\sigma_{\tau\theta}} d\rho_0(\tau)$$

$$+ \int_{\theta=0}^{\theta=t} d\omega_\theta \int_{\tau=0}^{\tau=\theta} R_\nu''(\omega_{\tau\theta}) e^{-\sigma_{\tau\theta}} d\omega_\tau \int_{u=0}^{u=\tau} e^{-\sigma_{u\tau}} d\rho_0(u)$$

for $\nu = 1$:

$$\rho_1 = M_0 - M = \rho_0(t) + \int_{\theta=0}^{\theta=t} d\omega_\theta \int_{\tau=0}^{\tau=\theta} e^{-\sigma_{\tau\theta}} d\rho_0(\tau)$$

$$- dM - d\rho_0 = d\omega_t \int_{\tau=0}^{\tau=t} e^{-\tau_{\tau t}} d\rho_0(\tau) \tag{A-18}$$

then

$$\rho_\nu = \rho_0(t) + R_\nu'(0) (M_0 - M - \rho_0)$$

$$- \int_{\theta=0}^{\theta=t} d\omega_\theta \int_{\tau=0}^{\tau=\theta} R_\nu''(\omega_{\tau\theta}) e^{-\sigma_{\tau\theta}} d_\tau(M + \rho_0) \tag{A-19}$$

Similarly, from relations (6) and (A-2) we deduce:

$$\mathcal{G}_r + \mathcal{K}_r = \int_{\tau=0}^{\tau=t} d\rho_0(\tau) \int_{\theta=\tau}^{\theta=t} e^{-\sigma_{\tau\theta}} d\theta \left[\frac{\omega_{\tau\theta}^{r-1}}{(r-1)!} e^{-\omega_{\tau\theta}} \right]$$

$$= \int_{\theta=0}^{\theta=t} d\omega_\theta \int_{\tau=0}^{\tau=\theta} d\rho_0(\tau) \frac{d}{d\omega_{\tau\theta}} \left[\frac{\omega_{\tau\theta}^{r-1}}{(r-1)!} e^{-\omega_{\tau\theta}} \right] e^{-\sigma_{\tau\theta}}$$

$$= \int_{\theta=0}^{\theta=t} d\omega_\theta \left\{ \frac{d}{d\omega_{\tau\theta}} \left[\frac{\omega_{\tau\theta}^{r-1}}{(r-1)!} e^{-\omega_{\tau\theta}} \right] \int_{u=0}^{u=\tau} d\rho_0(u) e^{-\sigma_{u\tau}} e^{-\sigma_{\tau\theta}} \Big|_{\tau=0}^{\tau=\theta} \right\}$$

$$+ \int_{\theta=0}^{\theta=t} d\omega_\theta \int_{\tau=0}^{\tau=\theta} d\omega_\tau \frac{d^2}{d\omega_{\tau\theta}^2} \left[\frac{\omega_{\tau\theta}^{r-1}}{(r-1)!} e^{-\omega_{\tau\theta}} \right] \int_{u=0}^{u=\tau} d\rho_0(u) e^{-\sigma_{u\tau}} e^{-\sigma_{\tau\theta}}$$

then

$$\mathcal{G}_r + \mathcal{K}_r = - \int_{\theta=0}^{\theta=t} d\omega_\theta \int_{\tau=0}^{\tau=\theta} e^{-\sigma_{\tau\theta}} \frac{d^2}{d\omega_{\tau\theta}^2} \left[\frac{\omega_{\tau\theta}^{r-1}}{(r-1)!} e^{-\omega_{\tau\theta}} \right] d_\tau(M + \rho_0)$$

$$r > 2$$

The concentration $\rho_0(t)$ is negligible with respect to the monomer concentration or with the value of ρ_ν, and therefore this last expression permits $\mathcal{G}_r + \mathcal{K}_r$ to be calculated by using only known quantities.

By changing the order of integration and integrating by parts eq. (A-19) becomes:

$$\rho_\nu = \rho_0 - \int_{\tau=0}^{\tau=t} d_\tau(M + \rho_0)R_\nu' (\omega_{\tau t}) e^{-\sigma_\tau t}$$

$$- \int_{\tau=0}^{\tau=t} d_\tau(M + \rho_0) \int_{\theta=\tau}^{\theta=t} R_\nu'(\omega_{\tau\theta})e^{-\sigma_{\tau\theta}}d\sigma_\theta \quad \text{(A-20)}$$

For living polymers $S = 0$ and, setting $\rho_0(t) = 0$, there results:

$$\rho_\nu \simeq - \int_{\tau=0}^{\tau=t} R_\nu'(\omega_{\tau t})dM(\tau) \quad \text{(A-21)}$$

If the initiation is instantaneous and $S > 0$ then eq. (A-3) becomes

$$\rho_\nu = - \int_{\tau=0}^{\tau=t} R_\nu'(\omega_\tau) d_\tau M \quad \text{(A-22)}$$

an expression analogous to (A-21).

For instantaneous initiation and S constant

$$M = M_0 \exp\{- (PA/S) (1 - e^{-St})\} \quad \text{(A-23)}$$

and then:

$$\omega_t = \int_0^t PM dt = \frac{PM_0}{S} e^{-PA/S}\left[E_i\left(\frac{PA}{S}\right) - E_i\left(\frac{PA}{S} e^{-St}\right)\right] \quad \text{(A-24)}$$

$$E_i(x) = 0.517... + \ln x + \frac{x}{1!1} + \frac{x^2}{2!2} + ... \quad \text{(A-25)}$$

and for x very large $E_i(x)$ has the asymptotic approximation:[17]

$$E_i(x) \simeq (e^x/x) [1 + (1/x) +...] \quad \text{(A-26)}$$

In the discussion of the limit cases we have used the incomplete γ function[17] [15]:

$$\gamma(\nu,x) = \int_0^x e^{-u} u^{\nu-1} du \quad \text{(A-27)}$$

For x relatively small:[17]

$$\gamma(\nu,x) = x^\nu \left(\frac{1}{\nu} - \frac{x}{(\nu + 1)1!} + \frac{x^2}{(\nu + 2)2!} +...\right) \quad \text{(A-28)}$$

and for x large:

$$\gamma(\nu,x) = \Gamma(\nu) - x^{\nu-1} e^{-x}\left[1 + \frac{\nu - 1}{x} + \frac{(\nu - 1)(\nu - 2)}{x^2} + ...\right]$$

$$\text{(A-29)}$$

The asymptotic behavior of $R_\nu(\omega)$ stated in eq. (A-15) is obtained by examining the Laplace transform of $f(1 + \tau, \nu)$ in the neighborhood of the value $\tau = 0$:[18]

$$f(1 + \tau,\nu) = \sum_{r \geqslant 1} \frac{r^\nu}{(1 + \tau)^r} = \sum_{r \geqslant 1} \varphi(r)$$

$$\varphi(r) = \frac{r^\nu}{(1 + \tau)^r} = \frac{u^\nu e^{-u}}{l_n^{\nu+1}(1 + \tau)}$$

$$u = r\, l_n(1 + \tau) \quad \text{(A-30)}$$

$$\int_{-1/2}^{1/2} \varphi(r + h)\,dh = \frac{r^\nu}{(1 + \tau)^r} \sum_{l \geqslant 0} \left(\frac{l}{\rho}\right) \frac{(-1)^l}{r^l} \xi_l(\tau)$$

$$\xi_l(\tau) = \sum_{2n \geqslant l} \frac{l_n^{2n-\epsilon}(1 + \tau)}{(2n - l)!\,(2n + 1)\,2^{2n}} \quad \text{(A-31)}$$

where n is an integer.   The functions $\xi_l(\tau)$ are holomorphic in the vicinity of the origin and

$$\xi_l(0) = \begin{cases} \dfrac{1}{(l + 1)2^l} & \text{for even } l \\[2mm] 0 & \text{for odd } l \end{cases} \quad \text{(A-32)}$$

$$\int_{1/2}^{\infty} \varphi(x)\,dx = \frac{\Gamma(\nu + 1)}{l_n^{\nu+1}(1 + \tau)} + S_0(\tau) = \sum_{r \geqslant 1} \int_{-1/2}^{1/2} \varphi(r + h)\,dh$$

$$= \sum_{l \geqslant 0} (-1)^l \binom{\nu}{l} f(1 + \tau,\nu - l)$$

then

$$f(1 + \tau,\nu) = \frac{1}{\xi_0(\tau)} \int_{1/2}^{\infty} \varphi(x)\,dx - \sum_{l \geqslant 1} (-1)^l \binom{\nu}{l} \frac{\xi_l(\tau)}{\xi_0(\tau)} f(1 + \tau,\nu - l)$$

$$\text{(A-33)}$$

It is noticed that $f(1, \nu - l) = \xi(l - \nu)$, the Riemann function: $S_0(\tau)$ of eq. (A-32) remains finite for $\tau \to 0$, $\tau > 0$.
If $-1 < \nu < 0$, then

$$f(1 + \tau,\nu) = \frac{a_{0\nu}\,\Gamma(\nu + 1)}{\tau^{\nu+1}} + S_1(\tau) \quad \text{(A-33)}$$

where $S_1(\tau)$ generally remains finite for $\tau \to 0$.   It may be seen that $a_{0\nu} = 1$. Using the recurrence relation (A-33) we find, successively, the behavior of $f(1 + \tau,\nu)$, for $0 < \tau < 1$, $1 < \nu < 2$ and then, in general:

$$f(1 + \tau,\nu) = \sum_{\nu+1 > l \geqslant 0} \frac{a_{l\nu}}{\tau^{\nu+1-l}}\; \Gamma(\nu + 1 - l) + S_{[\nu+2]}(\tau) \quad \text{(A-34)}$$

$[\nu + 2]$ being the entire part of $\nu + 2$. $\mathcal{S}_{[\nu+2]}(\tau)$ is also finite for $\tau \to 0$ and $a_{0\nu} = 1$.

For effective computation of the $a_{l\nu}$ coefficients it is preferable to use the expression given by eqs. (A-15) and (A-11), which lead us to the recurrency equation:

$$(\nu - l + 1)\, a_{l\nu} = a_{l+1,\nu+1} - a_{l+1,\nu} \tag{A-35}$$

References

1. Th. Deleanu and M. Dimonie, Part I to be published.
2. B. D. Coleman, F. Gornick, and G. Weiss, *J. Chem. Phys.*, **39**, 3233 (1963).
3. V. S. Nanda and R. K. Jain, *J. Chem. Phys.*, **48**, 1858 (1968).
4. C. H. Bamford and A. D. Jenkins, *Trans. Fafaday Soc.*, **56**, 907 (1960).
5. C. H. Bamford and H. Tompa, *Trans. Faraday Soc.*, **50**, 1097 (1954).
8. L. J. Gold, *Chem. Phys.*, **28**, 91 (1958).
9. V. S. Nanda and K. Jaim, *J. Polym. Sci. A-2*, **2**, 4583 (1964).
6. R. Chiang and J. J. Hermans, *J. Polym. Sci. A-1*, **4**, 2843 (1966).
7. J. J. Hermans, *J. Polym. Sci. C-12*, **4**, 345 (1966).
10. L. Reich and A. Schindler, *Polymerization by organometalic compounds*, John Wiley & Sons, Interscience Publ.
11. F. Reif, *Fundamentals of Statistical and thermal analysis*, McGraw Hill Book Co., New York, 1965 p. 612.
12. R. R. Cleland, R. L. Letsinger, and E. E. Magat, *J. Polym. Sci.* **39**, 249 (1959).
13. K. E. Burdon and D. C. Pepper, *Proc. Roy. Soc. 263 A*, 58 (1961).
14. A. Guiot *J. Polym. Sci. B*, **6**, 123 (1968).
15. T. A. Orofino and F. Wenger, *J. Chem. Phys.*, **35**, 532 (1961).
16. V. S. Nanda and R. K. Jain, *J. Polym. Sci. A-1*, **5**, 2269 (1967).
17. M. Abramovitz and J. Stegun, *Handbook of Mathematical Functions with formulas, graphs and mathematical tables*, Washington National Bureau of Standards (1965), (N.B.S. Applied Mathematics).
18. G. Doetsch, *Handbuch der Laplace Transformations*, Vol. 2, Birkhauser Verlag Basel, 1955.

Thermal Stability of Structurally Related Polymers Containing Carborane and Phthalocyanine Groups

A. D. DELMAN*, J. J. KELLY†, and B. B. SIMMS, *U.S. Naval Applied Science Laboratory, Brooklyn, New York 11251*

Synopsis

These studies were undertaken to determine the thermal behavior of structurally related polymers having a carborane nucleus in the recurring unit. Three of these products also contained phthalocyanine rings in their molecules. Results of thermal analysis studies show generally that the relative heat stability of the polymers conforms closely with indications given by similar investigations of structurally related intermediate and model compounds. A polymer with dimethylsiloxane units exhibited more resistance to thermal decomposition than similar products having urethane groups in their molecules. The urethane polymers derived from tolylene diisocyanate were found to be somewhat less heat-stable than analogous materials synthesized from methylenebis-(p-phenyl isocyanate). The relative order of thermal resistance of these materials follows that of more conventional polyurethane elastomers.

INTRODUCTION

A series of previous investigations showed that the heat stability of polymers can be predicted from the thermal behavior of model compounds.[1-4] In this connection, a recent study of structurally related intermediate and model compounds indicated that polymers containing phthalocyanine rings would probably exhibit greater resistance to thermal oxidation than similar products possessing carborane nuclei bonded to alkyl groups.[5] It might be expected, however, that polymers comprised essentially of such ring configurations in their skeletal chains would be too rigid for general use. Since it was known that some degree of increased flexibility could be achieved by incorporating spacers between ring structures, such polymers were prepared with methylsiloxane or urethane groups in the backbone. Although the model compound studies suggested that the introduction of these groups would tend to lower the heat stability of these macromolecules it was anticipated that they would be more heat stable than conventional methylsiloxane and urethane polymers because of the high thermal resistance of the phthalocyanine and carborane units. Improved thermal resistance was also expected because previous studies showed that the carborane nucleus inhibits the thermal oxidation of

* The Wool Bureau, Inc., Woodbury, N. Y. 11797.
† Allied Chemical Corp., Morristown, N. J. 07960.

111

methyl groups connected to silicon atoms by sterically hindering the access of oxygen to the molecules.[6] While no conclusive evidence has been gathered, it seemed reasonable to assume that the carborane unit might protect urethane linkages in a similar manner.   It was also suspected that the phthalocyanine ring would sterically hinder the oxidative decomposition of methylsiloxane and urethane groups because of its bulky character. From a comparison of the pyrolytic stability of commercially available polymers, it was expected that the product containing methylsiloxane units would be more resistant in this respect than analogous materials possessing urethane linkages.   This paper presents the results of thermal analysis studies of the polymers.

EXPERIMENTAL

Materials

Table I shows the repeating structures of the polymers that were examined after being dried for several hours in an oven at 105°C. The products were developed and synthesized,[6,7] by the Aerospace Group of General Precision, Inc., Little Falls, New Jersey. The phthalocyanine

TABLE I
List Of Polymers

Designation	Polymer
I	
II	
III	
IV	
V	

and *o*-carborane groups are denoted, respectively, by the symbols Pc and

$$-C-C-$$
$$\diagdown O \diagup$$
$$B_{10}H_{10}$$
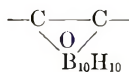
Thermal Stability Measurements

Thermogravimetric (TGA), isothermogravimetric (IGA), and differential thermal (DTA) analysis techniques were employed as described previously[8] to obtain information concerning the heat stability of the polymers.

Infrared Spectrophotometry

Infrared absorption spectra in the range 2.5–15.0 μ were obtained from Nujol mulls and KBr pellets with a Perkin-Elmer model 137 double-beam spectrophotometer equipped with sodium chloride optics.

RESULTS AND DISCUSSION

Figure 1 presents the TGA thermograms made from the polymers with urethane structures in their recurring units.   It is evident from these data
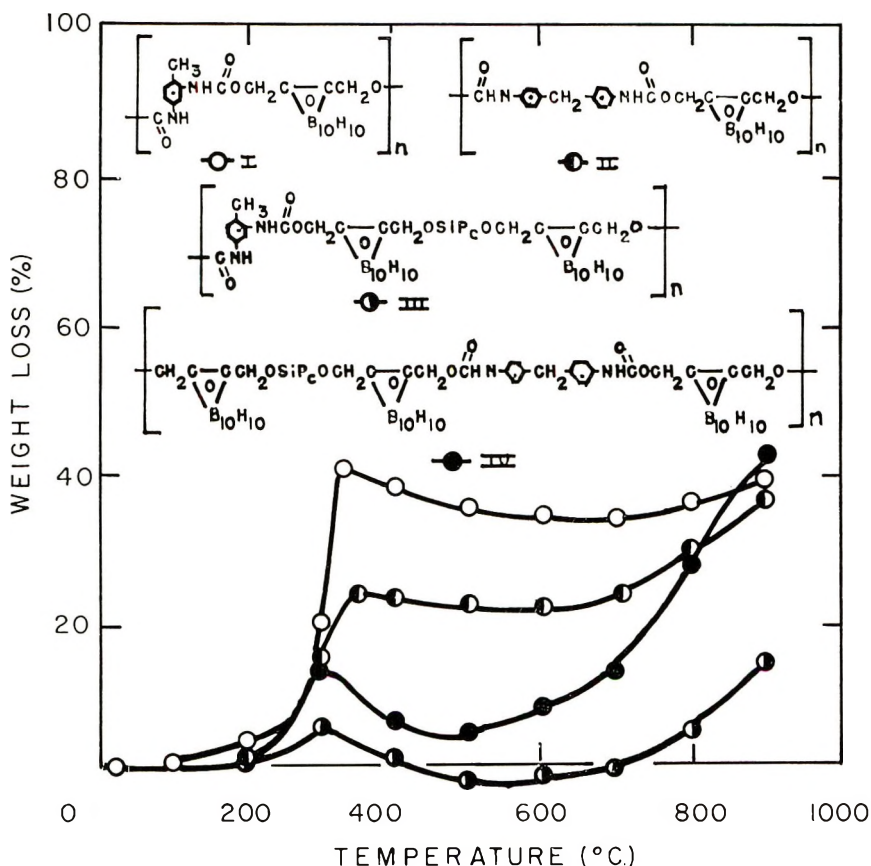
Fig. 1. TGA thermograms of urethane group-containing polymers.

that all of the products undergo a series of reactions that produce volatiles up to 350°C, weight gains in the region of 300–600°C, and additional losses between about 500 and 900°C when heated in air at 3°C/min. The general behavior of the polymers is similar to that of model compound bis[2 - (o - tolylcarbamoyloxymethyl) - carboranyl - 1 - oxymethyl]-[phthalocyanino] silicon.[5]

From the studies of polyurethanes derived from tolylene diisocyanate (TDI) by Ingham and Rapp[9,10] and investigations of similar products prepared from methylenebis(p-phenyl isocyanate) (MDI) by Slade and Jenkins,[11] it seems reasonable to attribute the initial weight loss exhibited by polymers I–IV to the dissociation of urethane groups. It is interesting to note from the temperatures at which volatilization began that polymer III is somewhat more heat-stable than I and product IV is slightly more resistant than II. Thus it appears that the polymers made from MDI are more heat stable than the materials prepared from TDI. This corresponds with the relative order of thermal resistance shown by conventional polyurethanes derived from TDI and MDI[11] and of the decomposition of the isocyanates alone.

The weight increase of the polymers at the temperature range of 300–660°C are reasonably associated with oxidation reactions. A comparison of the thermograms of the polymers with the same urethane group showed that the products having a higher ratio of bisoxymethylcarborane units per urethane structure underwent larger weight increases. This suggests that the weight gain exhibited by the polymers involved the oxidation of oxymethylcarborane groups. Since Grafstein and co-workers[12] demonstrated the stability of the o-carborane polyhedron towards oxidation, it is believed that the weight gains are due to the reaction of methylene units with oxygen. This is in agreement with results obtained previously for another polymer containing an alkyl group connected to a o-carborane polyhedron.[8]

The volatilization of residual products of thermal oxidation probably explains the weight losses observed at 500–900°C. From the thermal behavior of structurally similar intermediate and model compounds[5] it is believed that the volatilizable products remaining at this temperature range consisted largely of residual material containing carborane and phthalocyanine groups.

Figure 2 presents the TGA thermogram of polymer V. Except for the dimethylsiloxane units which replace the urethane groups, the repeating structure of the product is identical to that for polymer III. As in the case of the latter material, polymer V initially underwent a weight loss that was followed by an increase, and then a second decrease of weight. The thermal behavior of the polymer parallels that exhibited by the structurally related model compound bis(2-trimethylsiloxy-methylcarboranyl-1-oxy-methyl) [phthalocyanino] silicon.[5]

An initial weight loss of 22% was observed when polymer V was heated up to 338°C. Although the weight decrease exceeds the loss corresponding
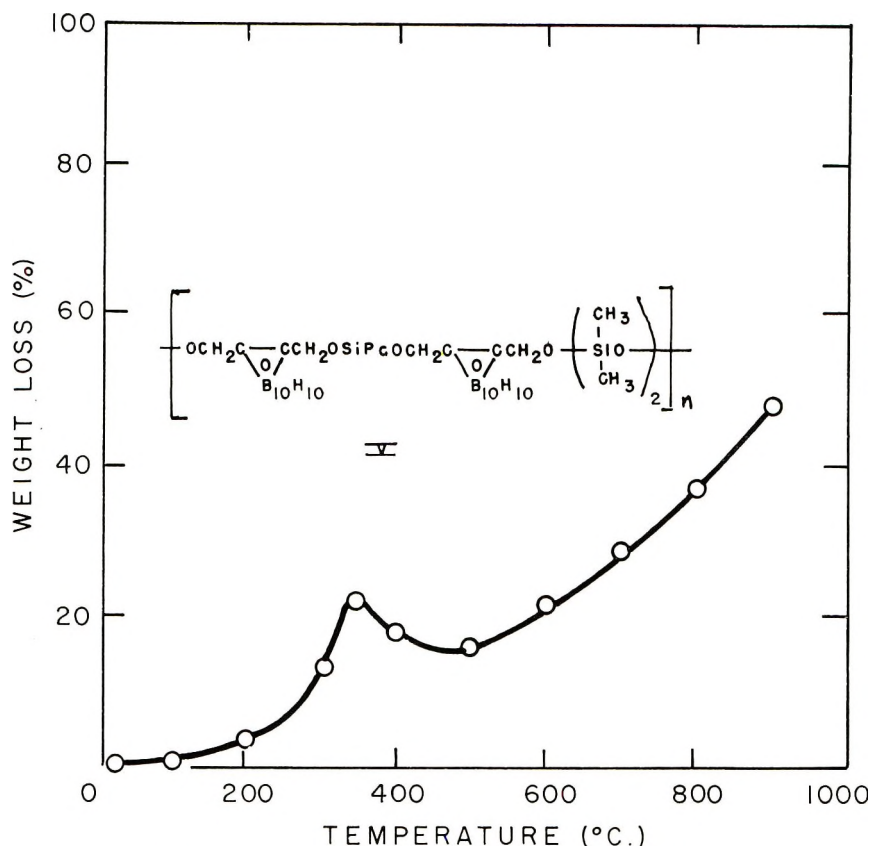
Fig. 2. TGA thermograms of dimethylsiloxane group-containing polymers.

to the complete rupture of the dimethysiloxane units, it is suspected from the studies of the heat stability of other carborane group-containing polymers having siloxane structures[13] that the volatile products were largely the result of Si-O bond cleavage.   Some weight loss may have also been due to the condensation of polymer chain ends.

Over the temperature range 338–460°C, polymer V underwent weight increases similar to products I to IV.   As in the case of the latter materials, the weight gains were probably produced by the oxidation of methylene groups.   From previous studies of polymers with repeating structures containing a carborane nucleus and dimethylsiloxane groups,[13] it also is possible that some of the weight gain may have been due to the oxidation of methyl units attached to residual silicon atoms.

At temperatures above 460°C, polymer V underwent additional weight losses.   This decomposition step is believed to be due to reactions involving the carborane and phthalocyanine groups in a manner similar to that expected for the polymers with urethane structures in their polymer chains. It is interesting to note that in the pyrolysis of metal phthalocyanines at about 450°C, free radicals have been trapped that were identified with the
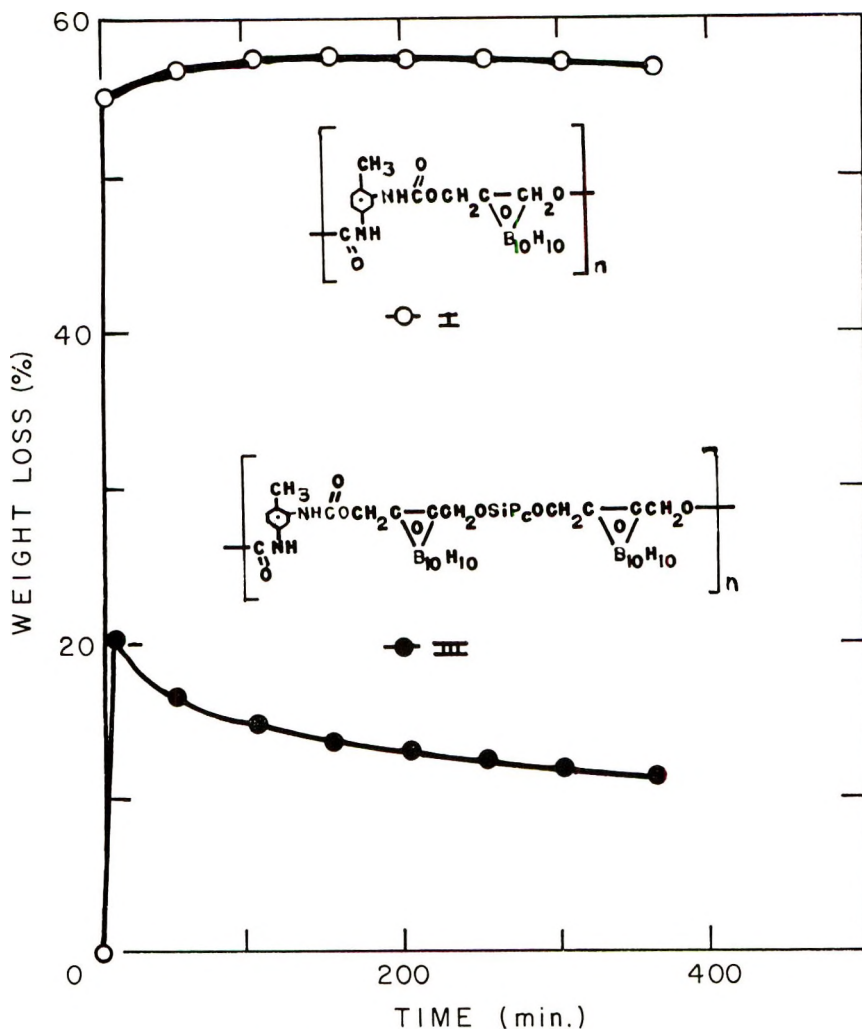
Fig. 3. IGA thermograms of polymers I and III.

rupture of permanently disordered ring structures.[14]   In addition, Graf-
stein and co-workers[15] reported that disubstituted o-carboranes have a
tendency to form volatile 1,2-exocyclic derivatives when they are heated.

The weight losses observed when the polymers with urethane groups were
heated in air for about 6 hr at 300°C are plotted in Figures 3 and 4.   A
comparison of these data shows that the products having a larger number
of carborane units per urethane group show smaller weight decreases.   In
addition, the results indicate that the polymers made from MDI are some-
what more heat stable than corresponding products derived from TDI.
This conforms with the relative order of thermal resistance of these materi-
als observed from the TGA experiments.

A number of significant changes were noted when infrared spectra from
the IGA residues were compared to those made from the original polymers.
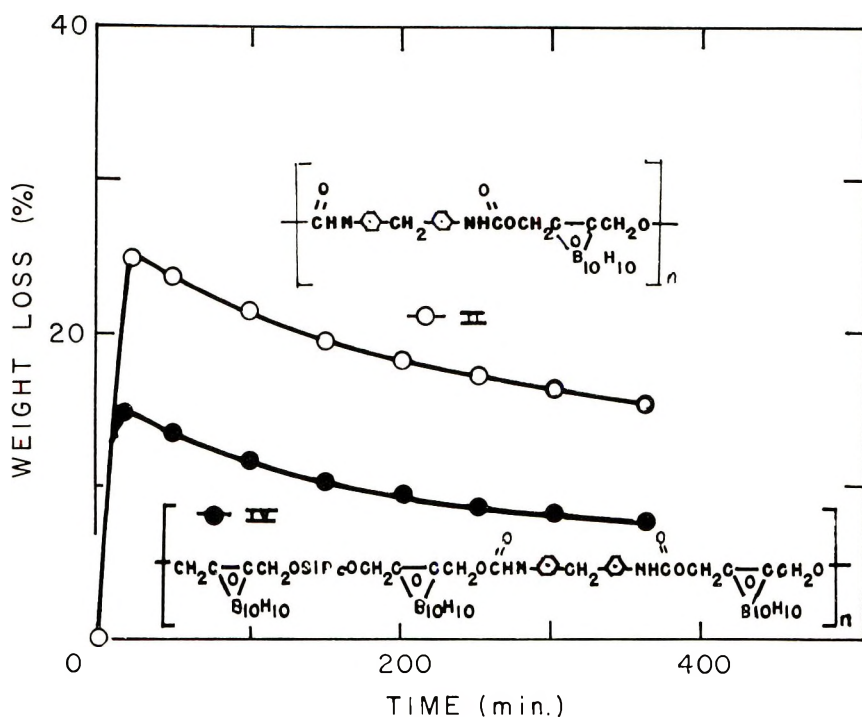
Fig. 4. IGA thermograms of polymers II and IV.

All of the spectra contained vibration modes that were due to the presence of the carborane polyhedron in the IGA residue. In addition, the spectra from the residues of polymers III and IV possessed an absorption band at 11.0 μ that is characteristic of the PcSi configuration. The absorption frequencies associated with aromatic groups of the urethane linkages and methylene units bonded to carborane nuclei in the original polymers were absent in the spectra of the IGA residues. Instead, new absorption bands appeared at 3.15 and 6.15 μ that are attributed to the formation of hydroxyl and carbonyl groups, respectively. It is interesting to note that absorption bands at 3.15 and 6.15 μ replaced the methylene vibration modes in the spectrum of 1,2-bis(hydroxymethyl)-carborane when it was heated in air for about 1 hr at 300°C.[5]

Thus, these infrared data seem to confirm that the carborane polyhedron and phthalocyanine ring are more resistant to thermal oxidation than the urethane groups derived from MDI and TDI and the methylene units adjacent to carborane nuclei in the polymer chains. From the studies by Hall[16] and Conley,[17] it is conceivable that the thermal decomposition of polymers I to IV may have been initiated as a result of the oxidation of methylene groups. In this connection, Saunders and Backus[18] reported that oxidation is an important factor in the thermal degradation of conventional polyurethanes.

Figure 5 shows the weight changes that were measured when polymer V was heated in air for about 6 hr at 300°C. During the first 3 hr, the
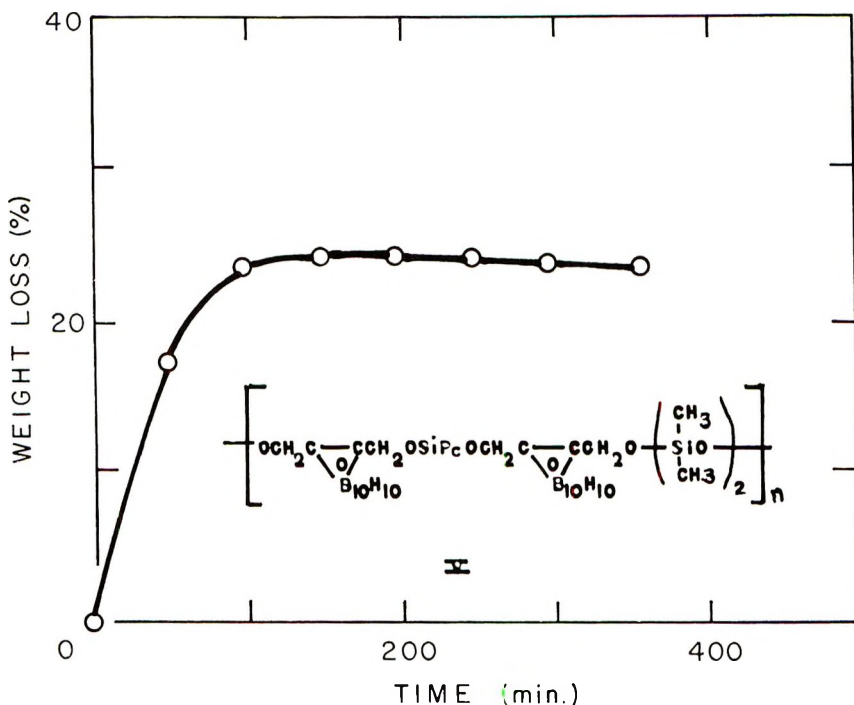
Fig. 5. IGA thermogram of polymer V.

product underwent a loss of 23.8%. A similar weight decrease was observed when the polymer was heated under TGA conditions to 338°C. A comparison of the IGA thermograms shows that the rate of initial weight loss of polymer V is lower than that of products I to IV. It might be inferred from these results that this product is somewhat more heat stable than the polymers that contain urethane groups. This is in agreement with the prediction made from similar studies of model compounds upon which the molecular structure of these polymers are based.

During the remaining 3 hr at 300°C, the polymer gained weight slowly. As indicated before, this period of weight increase is attributed to the oxidation of methylene groups connected to carborane nuclei, and possibly to reactions of residual methyl groups bonded to silicon atoms.

The infrared spectrum of the IGA residue from polymer V appeared similar to the spectra made after the isothermal treatment of products III and IV. The presence of absorption bands associated with the carborane polyhedron and the phthalocyanine structure again gave evidence of the good heat stability of these groups. The absence of vibration modes characteristics of dimethylsiloxane units confirmed that these groups were ruptured during the heating process. In addition, the appearance of new absorption frequencies attributed to hydroxyl and carbonyl configurations established that the polymer underwent thermal oxidation reactions when heated in air at 300°C. Thus, it might be implied from the close resem-

blance of the infrared spectra of the IGA residues from polymers III, IV, and V that these materials decomposed by similar processes, that is, through the thermal cleavage of urethane or dimethylsiloxane units and the oxidation of methylene groups bonded to carborane nuclei.
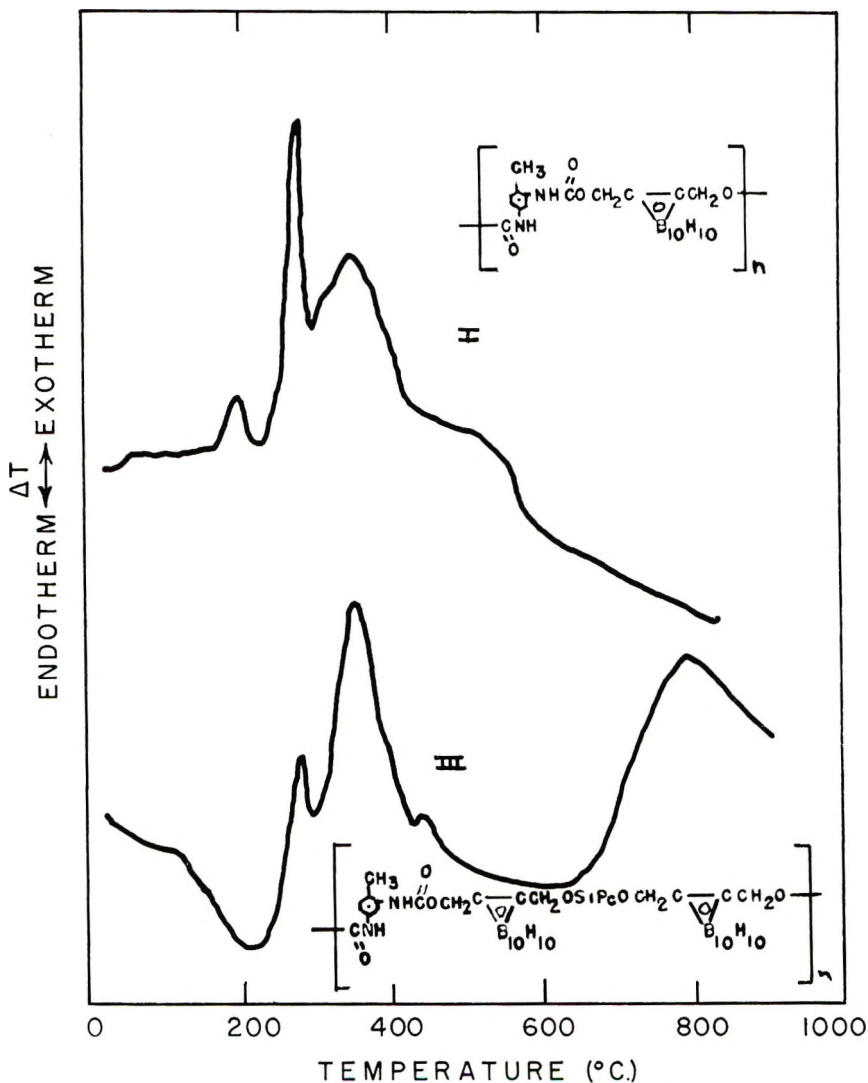
Fig. 6. DTA thermograms of polymers I and III.

Figures 6–8 present the DTA thermograms of the polymers. In general, the peaks of the thermograms show good correlation with points on corresponding TGA curves that indicate the occurrence of maximum or minimum rates of weight change. The exothermic transitions occurring below 200°C are reasonably associated with the reactions of polymer chain end groups.
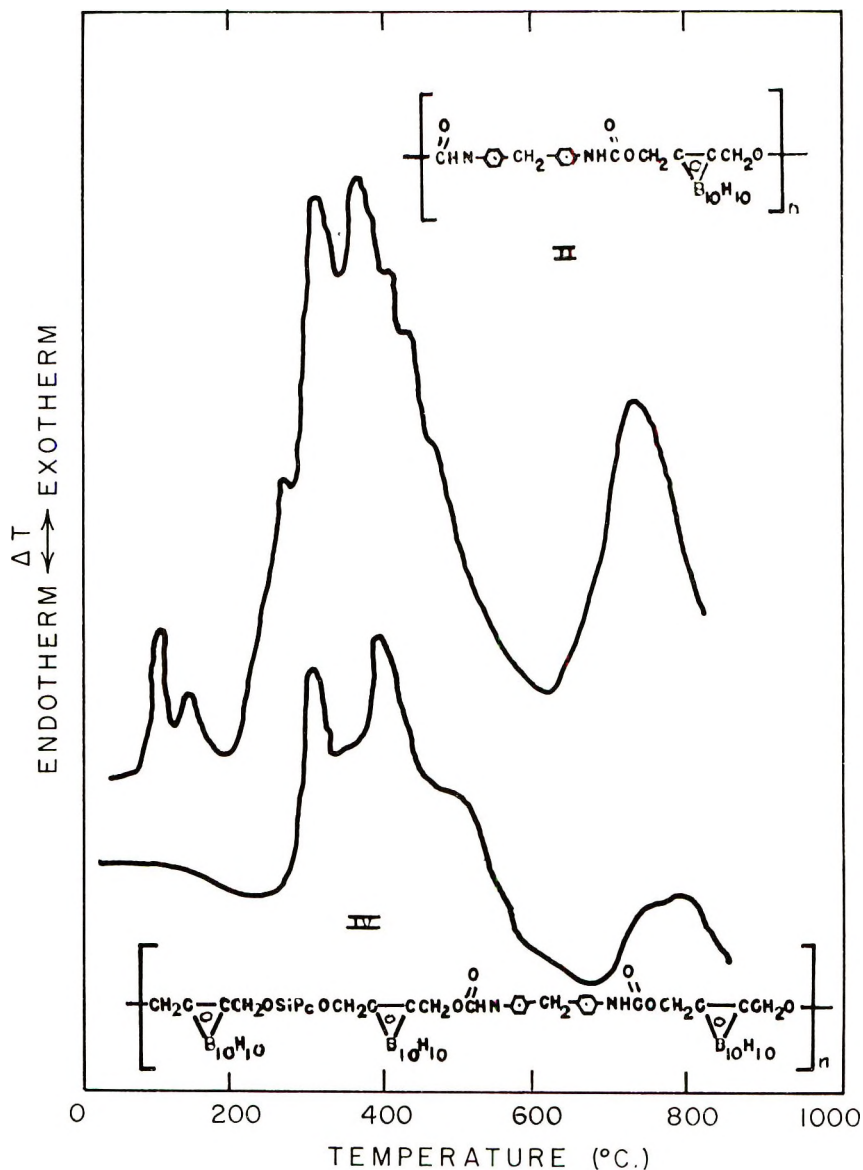
Fig. 7. DTA thermograms of polymers II and IV.

The exotherms appearing at higher temperatures were probably the result of drastic thermal oxidation of the polymer chains.

All of the polymers with urethane groups in their molecules underwent exothermic changes that have peaks at about 280–305°C and 355–385°C. These transitions were probably caused by the thermal rupture of urethane groups and the oxidation of methylene units adjacent to carborane nuclei. The peaks of the exotherms from polymers I and III appeared at lower
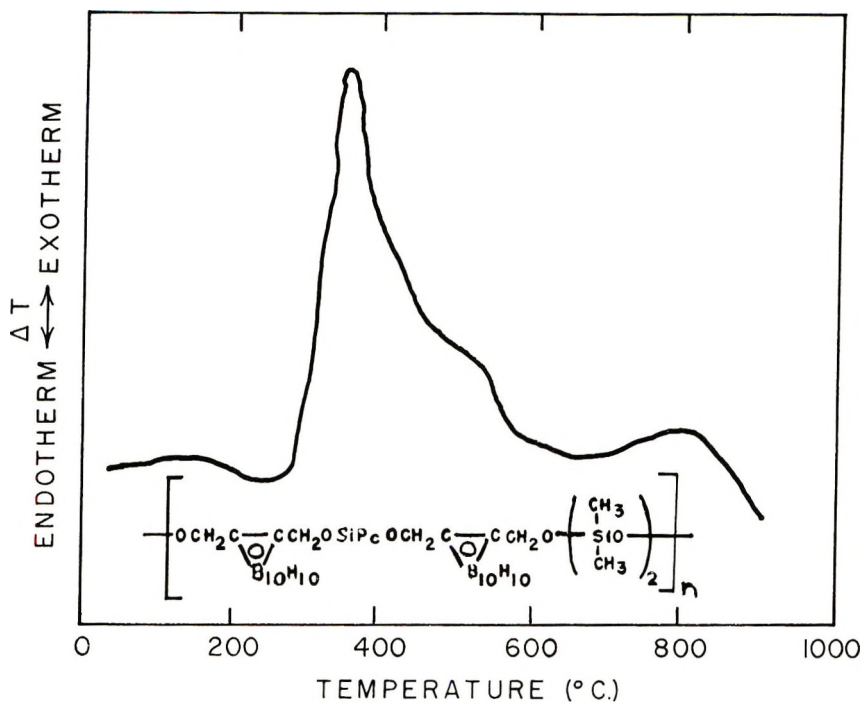
Fig. 8. DTA thermogram of polymer V.

temperatures than those given by products II and IV. It might be inferred from this that the polymers derived from MDI are more heat stable than those synthesized from TDI. This was also indicated by the results from the IGA experiments.

The shoulders appearing on the exotherms at approximately 440–470°C in the DTA thermograms given by polymers III and IV are attributed to the rearrangement of the phthalocyanine rings.[14] Similar shoulders were observed at about this temperature range on exotherms obtained from structurally related intermediate and model compounds.[5]

The exotherms with relatively broad peaks at about 725–805°C on the thermograms produced from polymers II, III and IV are reasonably associated with the thermal decomposition of residual carborane nuclei and probably disordered phthalocyanine rings. It is interesting to note that DTA thermograms obtained from other polymers containing molecules with carborane rings displayed exothermic transitions in this temperature region.[13] In addition, Joyner and Kenney[19] reported that a phthalocyaninosiloxane polymer derived from the thermal dehydration of $PcSi(OH)_2$ was thermally stable at 520°C for 2.5 hours, but decomposed when heated for 15 minutes at 625°C.

The thermogram from polymer V displays a strong exotherm that has a peak at 355°C and a shoulder at about 510°C. Previous studies of the structurally related model compound bis(2-trimethylsiloxymethylcar-

boranyl-1-oxymethyl)-[phthalocyanino] silicon indicated that the exo-
thermic peak resulted from the thermal oxidation of methylene groups, and
the shoulder was apparently caused by the disruption of the phthalocyanine
ring.[5]

A comparison of these data with the thermograms presented in Figures
6 and 7 showed that this peak of the DTA curve from polymer V appeared
at a higher temperature than those of the initial strong exotherms exhibited
by polymers I to IV. Again, as in the case of the data from the IGA experi-
ments, the results suggest that the polymer with dimethylsiloxane units in
its molecules is more heat-stable than those containing urethane groups.

In summary, the results show that the heat stability of the polymers
parallel the thermal resistance of intermediate and model compounds hav-
ing related molecular configurations, and are generally consistent with
predications made from other structural considerations. As postulated,
all of the products seemed to decompose initially because of the thermal
rupture of urethane or dimethylsiloxane units and through the oxidation
of methylene groups to leave residual materials containing the more heat
resistant carborane and phthalocyanine structures. The latter unit was
more stable than the former at temperatures above 350°C. The polymers
with methylsiloxane units were somewhat more resistant to pyrolytic
decomposition than those containing urethane groups. The heat stability
of the products with urethane structures corresponded generally with the
relative order of thermal resistance of the isocyanates employed in their
preparation. Although the susceptibility of the polymers to thermal de-
composition appears to be similar to that of more conventional dimethyl-
polysiloxanes and polyurethanes, the former exhibited much less weight
losses at temperatures below 600°C. This is attributed to the stabilizing
influence of the carborane nuclei on the oxidative decomposition of ad-
jacent methylene groups. The phthalocyanine rings probably had less
of an inhibiting influence because they were separated from the methylene
groups by oxygen atoms. The rupture of methylsiloxane and urethane
groups from the polymers at relatively low temperatures was probably
due to the lack of proximity of the carborane nuclei and phthalocyanine
rings to these structures. Previous studies also indicated that the protec-
tive effects of the carborane polyhedron decreases as the distance between
this group and other structures that are sensitive to thermal oxidation in-
creases.[6,13]

References

1. A. D. Delman, A. A. Stein, and B. B. Simms, *J. Macromol. Sci. (Chem.)*, **A1**, 147 (1967).

2. H. Nagy Kovacs, A. D. Delman, and B. B. Simms, *J. Polym. Sci. A-1*, **4**, 1081 (1966).

3. H. Nagy Kovacs, A. D. Delman, and B. B. Simms, paper presented at the Pacific Conference on Chemistry and Spectroscopy, Anaheim, Calif., Oct. 1967; published in *J. Polym. Sci. A-1*, **6**, 2103 (1968).

4. A. D. Delman, H. Nagy Kovacs, and B. B. Simms, paper presented at the American Chemical Society Midwest Regional Meeting, Columbia, Mo., Nov. 1967; published in *J. Polym. Sci. A-1*, **6**, 2117(1968).

5. A. D. Delman, J. J. Kelly, A. A. Stein, and B. B. Simms, paper presented at the 2nd International Conference on Thermal Analysis, Worcester, Mass., Aug. 1968, published in Thermal Analysis, Vol. 1, Academic Press, New York, 1969, p. 539.

6. General Precision, Inc., Thermally Stable Polymers for Electrical and Electronic Applications, 2nd Quarterly Progress Report, U.S. Navy Bureau of Ships Contract Nobs 94125, Little Falls, N. J., 15 May 1966.

7. General Precision, Inc., Thermally Stable Polymers for Electrical and Electronic Applications, 3rd Quarterly Progress Report, U.S. Navy Bureau of Ships Contract Nobs 94125, Little Falls, N. J., 15 Aug. 1966.

8. A. D. Delman, J. J. Kelly, A. A. Stein, and B. B. Simms, *J. Polymer Sci. A-1*, **5**, 2119 (1967).

9. J. D. Ingham and N. S. Rapp, *J. Polym. Sci. A*, **2**, 689 (1964).

10. J. D. Ingham and N. S. Rapp, *J. Polym. Sci. A*, **2**, 4941 (1964).

11. P. E. Slade, Jr., and L. T. Jenkins, in *Thermal Analysis of High Polymers (J. Polym. Sci. C*, **6**), B. Ke, Ed., Interscience, New York, 1964, p. 27.

12. D. Grafstein, J. Bobinski, J. Dvorak, J. E. Paustian, H. F. Smith, S. Karlan, C. Vogel, and M. M. Fein, *Inorg. Chem.*, **2**, 1125 (1963).

13. A. D. Delman, A. A. Stein, J. J. Kelly, and B. B. Simms, *J. Appl. Polym. Sci.*, **11**, 1979 (1967).

14. P. George, D. J. E. Ingram, and J. E. Bennett, *J. Amer. Chem. Soc.*, **79**, 1870 (1957).

15. D. Grafstein, J. Bobinski, J. Dvorak, H. Smith, N. Schwartz, M. S. Cohen, and M. M. Fein, *Inorg. Chem.*, **2**, 1120 (1963).

16. R. Q. Hall, *Chem. Ind.* (London) **1952**, 693.

17. R. T. Conley, *J. Appl. Polym. Sci.*, **9**, 1111 (1965).

18. J. H. Saunders and J. K. Backus, *Rubber Chem. Technol.*, **39**, 461 (1966).

19. R. D. Joyner and M. E. Kenney, *Inorg. Chem.*, **1**, 717 (1962).

Polymerization of Vinyl Monomers by Alkali Metal–Thiobenzophenone Complexes

YUJI MINOURA and SADAO TSUBOI, *Research Institute for Atomic Energy, Osaka City University, Sumiyoshi-ku, Osaka, Japan*

Synopsis

The polymerization of vinyl monomers by use of alkali metal (Li, Na, K)–thiobenzophenone complexes was studied. Monoalkali metal complexes of thiobenzophenone (thioketyls) induced the polymerization of vinyl monomers such as acrylonitrile (AN) and methyl methacrylate (MMA), and dialkali metal complexes of thiobenzophenone (dianion) induced the polymerization of styrene (St), butadiene (Bd), and isoprene (Ip) as well as AN and MMA. The polymerization of MMA with the dianion was initiated by both the mercaptide and the carbanion of the dianion, but that of styrene was initiated by the carbanion alone. In the case of polymerization of MMA by the thioketyl, the initial rate of polymerization depended on the catalyst concentration and the square of the monomer concentration. Similar results were obtained in the case of the dianion. The polymer yield increased with increasng polarity of sovents. In the copolymerization of AN with MMA, the copolymer obtained consisted almost of AN units. From these results, it was concluded that the polymerization proceeded by anionic mechanisms.

INTRODUCTION

It is known that nonenolizable thioketones react with alkali metals to give colored products which are unstable in air. These products are thought possibly to be metal thioketyls.[1−4]

Studies on the reactions of substituted thiobenzophenone with alkali metals and on the ESR spectra obtained from these products, have been reported.[5]

The polymerization of vinyl monomers with benzophenone metal ketyls has been reported by Inoue et al.[6] and Zilkha et al.,[7] but the polymerization of vinyl monomers by use of thiobenzophenone–alkali metal complexes has not been studied.

We carried out the reactions of thiobenzophenone with equimolar amounts of alkali metals (Li, Na, and K) and obtained deep red complexes which were known as thioketyls (I).

These thioketyls were found to induce the polymerization of vinyl monomers such as acrylonitrile (AN) and methyl methacrylate (MMA). The reactions of thiobenzophenone with more than twice the equimolar amount

of alkali metals showed the formation of dark red dialkali metal adducts (II).

$$I \qquad\qquad II$$
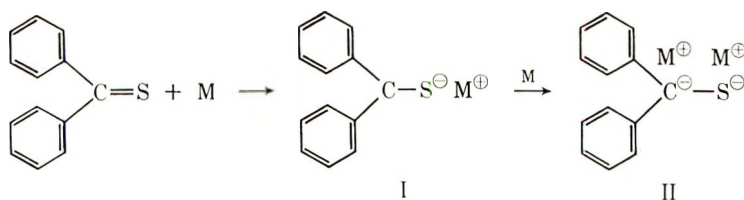
where M may be Li, Na, or K. These dimetallo adducts (II) had a greater reactivity than the thioketyls (I) and induced the polymerization of AN, MMA, styrene (St), isoprene (Ip), and butadiene (Bd).

The polymers with low degrees of polymerization were prepared with these high concentration complexes and the relationships between the degree of polymerization and the sulfur content in the polymers were investigated in order to clarify the difference between the reactivities of thioketyls and dimetallo adducts.

In the cases of the polymerizations of MMA with thioketyls, the polymerizations are thought to be initiated by the mercaptide anions and not by the radicals of thioketyls. The polymerization of MMA with disodium thiobenzophenone, however, is initiated by both the mercaptide ion and the carbanion.

Inoue and co-workers[6] considered an electron-transfer type initiation from alkali metals to St for the polymerization of St with dialkali metal benzophenone. In the case of polymerization of St with the dimetallo adducts (II), however, the polymerization was not initiated by the electron transfer type reaction, but by the carbanion of the dimetallo adducts (II).

EXPERIMENTAL

Thiobenzophenone

Thiobenzophenone was prepared by the following procedure.[3] A 125-ml portion of 95% ethanol containing 25 g (0.14 mole) of benzophenone was placed in a flask, cooled in an ice–salt freezing mixture. Hydrogen sulfide and hydrogen chloride were passed simultaneously into the solution for 3 hr with stirring. After 3 hr, the flow of hydrogen chloride was stopped and hydrogen sulfide alone was passed through for an additional 20 hr with continued ice cooling. The solid thiobenzophenone was filtered off from the ice-cold solution, immediately dried under high vacuum, and recrystallized twice from petroleum ether (bp 60–80°C). The long, needlelike crystals (mp 53–54°C) obtained were kept in a closed flask under an atmosphere of argon and stored in a cold and dark place; yield 18–21 g (66–77%).

Reagents

Acrylonitrile was purified by successive washings with 5% sulphuric acid, 5% sodium carbonate, and water. After being dried ($CaCl_2$), it was frac-

tionally distilled under nitrogen in the presence of calcium hydride. Methyl methacrylate was steam-distilled, washed with 5% caustic soda, and then with water. After being dried (anhydrous sodium sulfate), it was fractionally distilled under nitrogen in the presence of calcium hydride. Styrene was washed with 5% caustic soda and with water. After being dried ($CaCl_2$), it was fractionally distilled under nitrogen in the presence of calcium hydride. Isoprene was dried over calcium hydride and before use was fractionally distilled under nitrogen in the presence of calcium hydride. Butadiene was dried over calcium hydride and was trapped in a test tube with Dry Ice–methanol.

n-Hexane and diethyl ether were dried over sodium and distilled. Tetrahydrofuran and dioxane were purified by distillation in the presence of benzophenone sodium ketyl. Thioketone was purified by recrystallization when necessary.

Metal Thioketyl and Dimetal Complex

Monosodium Thiobenzophenone. A mixture of sodium (0.107 g, 0.009 mole) and thiobenzophenone (2.0 g, 0.01 mole) was stirred in 100 ml of anhydrous THF under nitrogen at room temperature for 24 hr. The color of the solution turned from blue to deep red within 1–2 hr, and the anion radical complex was formed.

When the solution was filtered after 6 hr, no residual sodium was found. The thioketyl solution was placed in a closed flask filled with argon gas and stored in a cool, dark place; material was removed for use with an injection syringe under an atmosphere of nitrogen or argon.

Disodium Thiobenzophene. A mixture of sodium (0.92 g, 0.04 mole) and thiobenzophenone (2.0 g, 0.01 mole) was stirred in 100 ml of anhydrous THF under nitrogen at room temperature for 24 hr. The color of the solution turned from blue to the dark red within 1–2 hr, and the dianion complex was formed. When this solution was filtered, unreacted sodium (0.46 g, 0.02 mole) remained. Storage and handling procedures were the same as those for monosodium thiobenzophenone.

Polymerization

The monomers and solvents were placed in a stoppered test tube. Any gases in the solution were removed by thorough outgassing and nitrogen was introduced in the test tube. The initiator was added with an injection syringe. The polymerization was carried out under high vacuum, and stopped by the addition to the reaction mixture of a mixture of hydrochloric acid and methanol. The polymers formed were filtered off, washed with methanol and water, and dried under reduced pressure at room temperature. The rate of polymerization was determined by measuring the weight of the polymer formed.

The average degree of polymerization of poly(methyl methacrylate) was calculated from the intrinsic viscosity measured in benzene at 30°C, with an Ubbelohde viscometer from the equation,[9] $\bar{P}_n = 2200[\eta]^{1.13}$. PAN

of low degree of polymerization was purified twice by precipitation from its solution in dimethylformamide with methanol, and in the case of PMMA, in benzene.

The molecular weights of polystyrene and poly(methyl methacrylate) of low degree of polymerization were measured using a Knauer vapor pressure osmometer in 1,2-dichloroethane at 45°C. The sulfur content was determined qualitatively by the sodium nitroprusside method and quantitatively by the method of Schöniger.[10] Infrared spectra of polymer films formed on a sodium chloride plate were measured with a Perkin-Elmer Model 337 spectrophotometer.

RESULTS AND DISCUSSION

Polymerization of Vinyl Monomers by Thiobenzophenone–Alkali Metal Complexes

We carried out the polymerization of vinyl monomers in THF at 0°C for a certain time using monolithium, -sodium, and -potassium thiobenzophenone complexes. Acrylonitrile (AN) and methyl methacrylate (MMA)

TABLE I
Polymerization of AN and MMA by Mono-Li, -Na,
and K Thiobenzophenone[a]

Ketyl	Monomer	[M], mole/l.	[I] $\times 10^2$, mole/l.	Polymer, g	Yield, %
Li	AN	3.0	0.865	0.004	2.48
			1.73	0.009	5.6
			3.49	0.980	61.1
			5.20	1.181	73.1
Li	MMA	1.88	0.865	—	—
			1.73	0.132	7.0
			3.49	1.551	82.5
			5.20	1.940	100
Na	AN	3.0	0.865	0.124	7.7
			1.73	0.280	17.4
			3.49	0.563	35.0
			5.20	1.039	64.5
Na	MMA	1.88	0.865	0.002	0.1
	MMA	1.88	1.73	0.177	9.4
			3.49	1.117	59.0
			5.20	1.138	60.5
K	AN	3.0	0.865	0.467	29.0
			1.73	0.921	57.2
			3.49	1.125	69.9
			5.20	1.565	97.2
K	MMA	1.88	0.865	—	—
			1.73	1.476	78.5
			3.49	1.827	97.1
			5.20	1.804	96.1

[a] Solvent, THF; polymerization temperature, 0°C; polymerization time, 75 min.

TABLE II

Polymerization of Vinyl Monomers by Di-Li, -Na, and K Thiobenzophenone[a]

| Dianion | Monomer | | [M], mole/l. | [I] × 10², mole/l. | Yield, % |
	Type	Vol, ml			
Li	AN	2	3.0	1.73	49.1
				3.49	56.0
	MMA	2	1.88	1.73	17.3
		2		3.49	73.6
	St	2	1.74	3.49	90.0
	Ip[b]	2	2.1	5.2	34.2
Na	AN	2	3.0	1.73	39.0
				3.49	56.6
	MMA	2	1.88	1.73	47.4
				3.49	68.5
	St	2	1.74	3.49	100
	Ip	2	2.1	5.2	34.2
	BD[c]	3	3.6	5.2	60.0
K	AN	2	3.0	1.73	56.8
				3.49	61.8
	MMA	2	1.88	1.73	100
				3.49	100

[a] Solvent, THF; at 0°C, polymerized for 75 min.

[b] THF, at 0°C, polymerized for 10 hr.

[c] THF, at −21°C, polymerized for 10 hr.

rapidly polymerized but styrene (St) and isoprene (Ip) did not polymerize. As shown in Table I, polymer yield increased in the order, Li < Na < K.

The polymerization of AN, MMA, St, Ip, and butadiene (BD) was carried out also with the use of the disodium, dilithium, and dipotassium thiobenzophenones, and the results are shown in Table II.

St and Ip did not polymerize with the thioketyls. In the case of the polymerization with the dialkali metal complex, AN and MMA polymerized readily, and St, Ip and BD polymerized with good yields. Therefore, it was thought that the dialkali metal complex of the thioketone had a greater activity towards vinyl monomers than the thioketyl (monoalkali metal complex). A similar trend was observed in the case of benzophenone complexes.[6]

Structures of Polyisoprene and Polybutadiene

The structures of polyisoprene and polybutadiene obtained from the polymerization by dialkali metal–thiobenzophenone complexes were determined from the infrared spectra.

In the case of polyisoprene, the percentages of all four structures (cis- and trans-1,4-, 1,2-, and 3,4-addition) were obtained from the extinction coefficients at 836, 889, 906, 1128, and 1151 cm⁻¹; the results are shown in Table III. The structures of polyisoprene consisted of 1,2- and 3,4-addition, and for any alkali metal the 3,4-addition was predominant.

TABLE III
Structures of Polyisoprene[a]

Alkali metal	1,2-Addition, %	3,4-addition, %	cis-1,4-addition, %	trans-1,4-addition, %
Li	25	75	0	0
Na	19	81	0	0
K	32	68	0	0

[a] Catalyst, dialkali metal thiobenzophenone, (0.043 mole/l.), [M] = 3.2 mole/l., solvent, THF; polymerization temperature, 0°C.; polymerization time, 18 hr.; conversion, 80–100%.

TABLE IV
Structure of Polybutadiene[a]

Alkali metal	cis-1,4-addition, %	trans-1,4-addition, %	1,2-addition, %
Li	39.3	3.9	56.8
Na	38.6	9.4	52.0
K	25.6	30.4	44.0

[a] Catalyst, dialkali metal thiobenzophenone (0.043 mole/l.); solvent, THF; polymerization temperature, −21°C; [M] = 3.6 mole/l.; polymerization time, 18 hr; conversion, 80–100%.

The results were the same as those for the structure of polyisoprene obtained from the polymerization in THF by alkyllithium.

In the case of polybutadiene, the percentages of all three structures (cis-1,4, trans-1,4-, and 1,2-) were determined from the extinction coefficients at 967, 911, and 680 cm^{-1} by using the method of Binder. The results are shown in Table IV. In this case, the 1,2-addition was predominant.

Dependence of the Initial Rate of Polymerization (R_p) on Monomer Concentration and Catalyst Concentration

The polymerization of MMA with monosodium thiobenzophenone was carried out in THF at 0°C. First, the dependence of the initial rate of polymerization R_p on catalyst concentration was studied over a concentration range of 0.013–0.043 mole/l. The time–conversion curve is shown in Figure 1. The initial rate of polymerization was obtained from the initial slope of the curve, and the relationship between the initial rate of polymerization and the catalyst concentration [C] is shown in Figure 2. It is found from this figure that the initial rate of polymerization was proportional to the catalyst concentration [C].

The dependence of the initial rate of polymerization on monomer concentration was studied in the concentration range of 0.94–2.35 mole/l. The initial rate of polymerization obtained from the time–conversion curve was plotted against the square of the monomer concentration is shown in Figure 3. It was found from this figure that the initial rate of polymeriza-
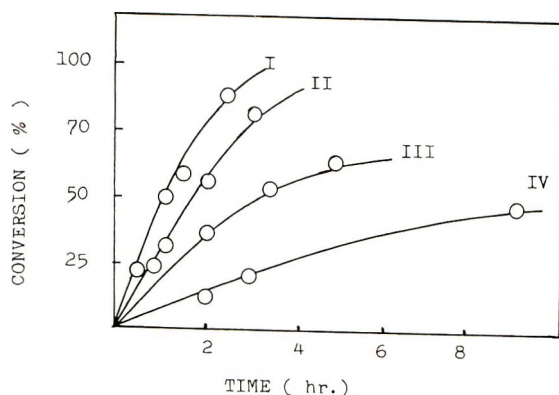
Fig. 1. Time-conversion curve for polymerization of MMA: (I) $[C]$ = 0.043 mole/l.; (II) $[C]$ = 0.023 mole/l.; (III) $[C]$ = 0.017 mole/l.; (IV) $[C]$ = 0.013 mole/l. Monomer, MMA (1.88 mole/l.); catalyst, monosodium thiobenzophenone; solvent, THF; polymerization temperature, 0°C.
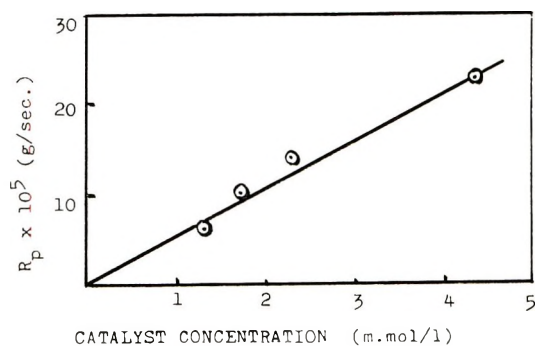
Fig. 2. Relationship between R_p and catalyst concentration. Monomer, MMA (1.88 mole/l.); catalyst, monosodium thiobenzophenone; solvent, THF; polymerization temperature, 0°C.
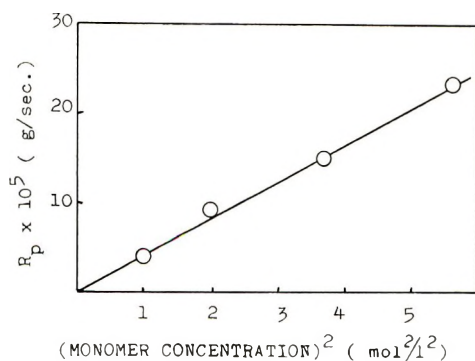
Fig. 3. Relationship between R_p and the square of the monomer concentration. Monomer, MMA; solvent, THF; polymerization temperature, 0°C; catalyst, monosodium thiobenzophenone.

tion was proportional to the square of monomer concentration. Therefore, $R_p = K_p[M]^2[C]$ was obtained for $[C] = 0.013-0.043$ mole/l. and $[M] = 0.94-2.35$ mole/l. The relationships shown above can be explained by the reactions (1)–(3).

Initiation:
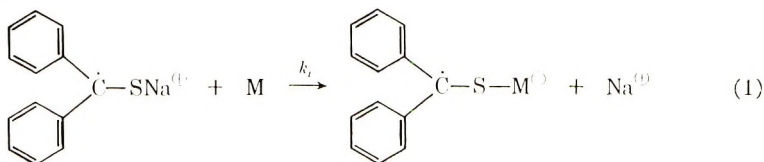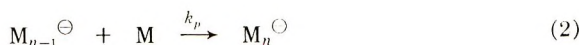
$$\text{(1)}$$

Propagation

$$M_{n-1}{}^{\ominus} + M \xrightarrow{k_p} M_n{}^{\ominus} \tag{2}$$

Termination:

$$\text{(3)}$$
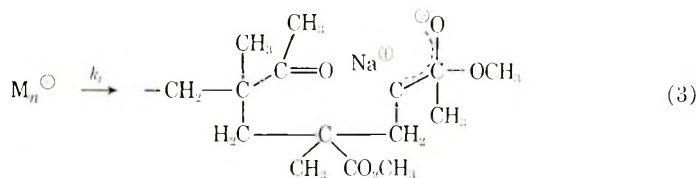
The polymerization of MMA with disodium–thiobenzophenone was carried out; the initial rate of polymerization depended on the catalyst concentration and the square of monomer concentration.

Relationship between the Degree of Polymerization and the Concentration of Catalyst and Monomer

The degree of polymerization of PMMA obtained in the previous section was determined from the intrinsic viscosity, and the results for thioketyl are shown in Figures 4 and 5. The degree of polymerization increased
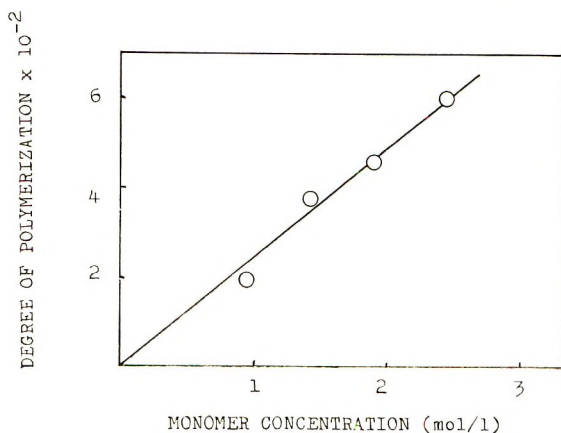
Fig. 4. Relationship between the degree of polymerization and the monomer concentration. $[C] = 0.013$ mole/l.

with increasing monomer concentration and decreased with increasing catalyst concentration. These results show that the polymerization is anionic. The same results were obtained in the case of the dianion also.
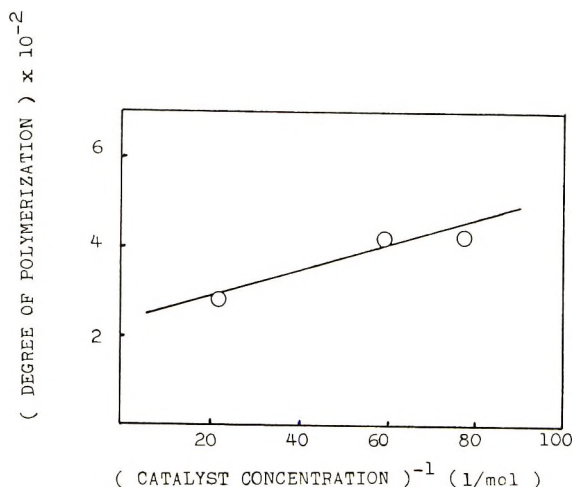
Fig. 5. Relationship between the degree of polymerization and the catalyst concentration. [M] = 1.88 mole/l.

In the case of thioketyl catalyst, when [C] = 0.013 mole/l. and [M] = 1.88 mole/l., the degrees of polymerization of PMMA calculated from the values of $[\eta]$ were found to be 3.4×10^2, 4.48×10^2 and 4.58×10^2, for the polymers obtained at 22.4, 47.7, and 78.2%, conversion, respectively.

Initiation Mechanism

Polymers of low degrees of polymerization were prepared by use of high concentrations monosodium thiobenzophenone. The polymers obtained were purified and qualitative and quantitative analyses for sulfur in the polymer and measurements of infrared spectra and molecular weight determinations were carried out. The results shown in Table V indicate that each polymer chain contains one sulfur atom. Therefore the polymerization is seen to have been initiated by one thioketyl molecule and proceeded by an anionic process.

Infrared spectra of all polymers showed an absorption band due to the hydroxyl groups at 3400 cm^{-1}. The copolymerization of AN with MMA at 0°C with the thioketyl catalyst gave a polymer which was found to consist of 92.6% AN from nitrogen analysis. Therefore the polymerization is thought to be initiated by the mercaptide ions of the thioketyl catalyst and not by the radicals of the thioketyl catalyst.

During the polymerization, the radicals of thioketyls are believed to be stabilized due to the resonance with the phenyl group, and at the termination stage they are thought to react with oxygen or water to form a hy-

TABLE V
Syntheses and Analyses of Polymers with Low Degrees of Polymerization[a]

| Monomer | [M], mole/l. | [C], mole/l. | Analysis | | | Molecular weight | Sulfur atoms/molecule of polymer |
			Sulfur	Hydroxyl group	Phenyl group		
AN	0.75	0.242	+	+	+	—	—
MMA	0.94	0.257	+	+	+	780	1.09
MMA	0.014	0.083	+	+	+	1700	1.06

[a] Catalyst, monosodium thiobenzophenone; polymerization temperature, 0°C; polymerization time, 30 min.

TABLE VI
Syntheses and Analyses of Polymers with Low Degrees of Polymerization[a]

| Monomer | [M], mole/l. | [C], mole/l. | Polymerization time, min | Sulfur | Molecular weight | | Sulfur/molecule of polymer | |
					Before oxidation	After oxidation	Before oxidation	After oxidation
MMA	1.88	0.143	60	+	1100	1110	0.95	0.92
St	1.45	0.238	5	+	514	1160	0.71	1.48

[a] Catalyst, disodium thiobenzophenone; polymerization temperature, 0°C; conversion, MMA (84%), St (91%).

droxyl group by way of the hydroperoxide. Consequently, the polymerization with thioketyl catalysts is considered to proceed as shown in eq. (4).
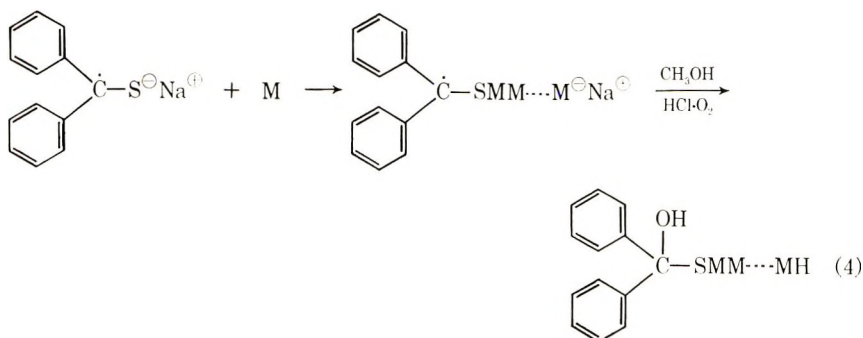
where M now denotes monomer (either MMA or AN). Polystyrene and poly(methyl methacrylate) of low degrees of polymerization were prepared by disodium thiobenzophenone catalysts of high concentration. The polymers were dissolved in benzene contained some iodine, and oxidized by passing air through the solution under continuous gentle heating for 5 hr. The solutions were then poured into a large quantity of methanol, and the polymers formed were separated and purified in the same way as described in the experimental section. The molecular weights of the polymers were determined and are shown in Table VI.

After oxidation the molecular weight of PMMA was approximately same as that of PMMA before the oxidation, but in the case of PSt, the molecular weight doubled after oxidation. In the polymerization of MMA by dialkali metal complex catalysts, MMA which can be initiated even by the mercaptide ion in a thioketyl catalyst, is initiated by both mercaptide ion and carbanion of the catalyst, as shown in eq. (5).
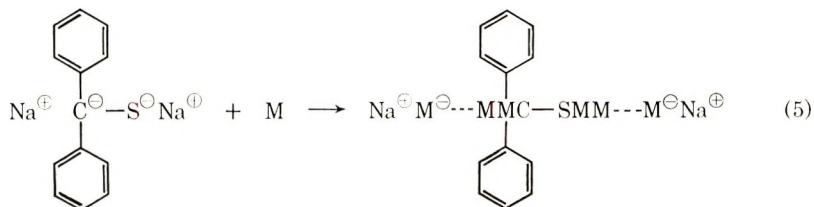
where M denotes methyl methacrylate. But in the case of styrene, which does not polymerize with a thioketyl catalyst, polymerization is initiated by only the carbanion of the dianion. Moreover, the weakly basic mercaptide ion does not attack the monomers and becomes mercaptan, which is readily oxidized at the termination. Therefore in the oxidation two polymers containing the mercaptan group may, couple as shown in eq. (6). Hence the molecular weight of polystyrene is doubled.
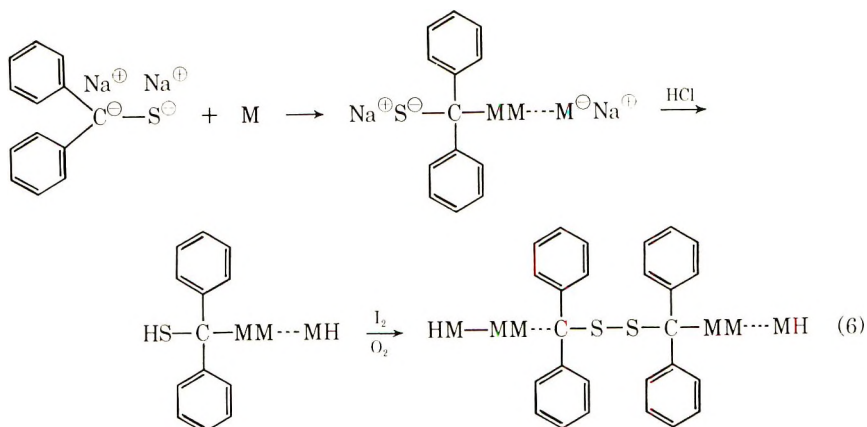
where M denotes styrene.

Solvent Effect

The polymerization of MMA with monosodium–thiobenzophenone was carried out in several solvents (THF, diethyl ether, dioxane and n-hexane).
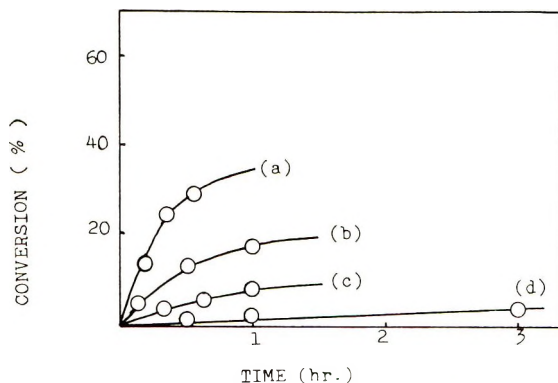
Fig. 6. Time-conversion curve for polymerization of MMS in various solvents: (a) THF; (b) diethyl ether; (c) dioxane; (d) n-hexane. Polymerization temperature, 10°C; monomer, MMA (1.88 mole/l.); catalyst, monosodium thiobenzophenone, THF solution (1 ml, [C] = 0.0216 mole/l.).
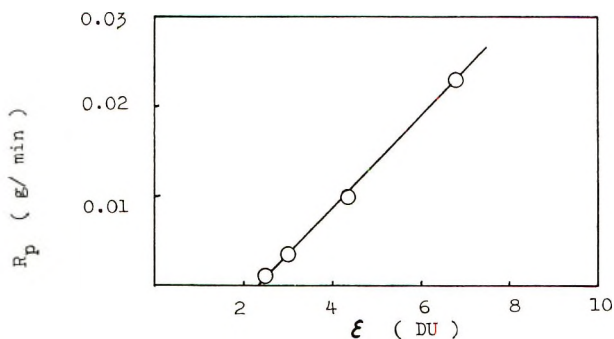
Fig. 7. Relationship between dielectric constant and the initial rate of polymerization.

Polymer yields were plotted against polymerization times and are shown in Figure 6.   On plotting the initial rate of polymerization obtained from the initial gradient of the curve against the dielectric constant, a linear relationship was obtained, as shown in Figure 7.   MMA did not polymerize in DMF and DMSO, and the color of the solution changed from the deep red of thioketyl to the violet.   Especially in DMF, some unidentified un-activated species seemed to have been formed, because a violet precipitate appeared.

Comparison of the Catalytic Activities of Monosodium Thiobenzophenone and Monosodium Benzophenone

The catalytic activities of monosodium thiobenzophenone and mono-sodium benzophenone was compared.   Polymerizations of MMA with these two catalysts were carried out in THF at 0°C, and time–conversion curves are shown in Figure 8.

It was found that monosodium benzophenone was a more reactive catalyst than monosodium thiobenzophenone.
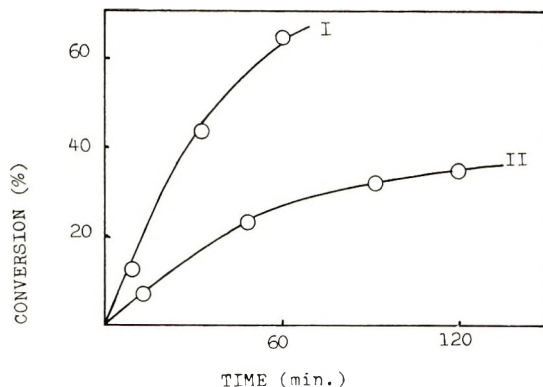
Fig. 8. Comparison of the catalytic activity of monosodium thiobenzophenone with that of monosodium benzophenone: (I) monosodium benzophenone (0.0173 mole/l.); (II) monosodium thiobenzophenone (0.0173 mole/l.).   Monomer, MMA (1.88 mole/l.); solvent, THF; polymerization temperature, 0°C.

Inhibition Effect of Thiobenzophenone

It is known that the thiocarbonyl group of thiobenzophenone readily forms a biradical.   It was previously confirmed that radicals existed in thiobenzophenones.[12]   Thereupon, the effect of thiobenzophenone on the radical polymerization was studied.   As shown in Figure 9, when a small amount of thiobenzophenone was added to the radical polymerization sys-tem of MMA initiated by azobisisobutyronitrile (AIBN), a considerable induction period was observed.   Therefore, thiobenzophenone is thought to act as an inhibitor in the radical polymerization system,
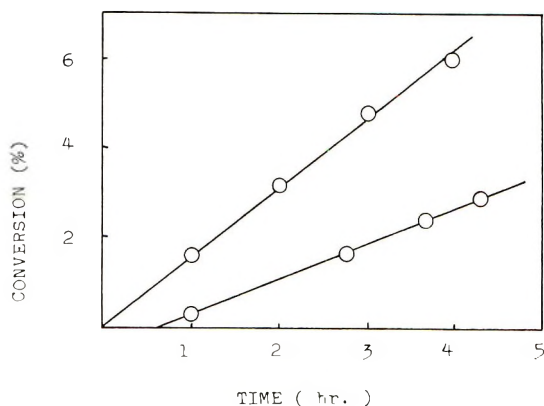
Fig. 9. Inhibition effect of thiobenzophenone on radical polymerization: [MMA] = 4.67 mole/l.; [AIBN] = 1.00×10^{-3} mole/l.; [thiobenzophenone] = 1.00×10^{-3} mole/l.; polymerization temperature, 50°C; solvent, benzene.

This inhibitory effect can be readily understood, as thiobenzophenone is known to react with AIBN [eq. (7)].[13]
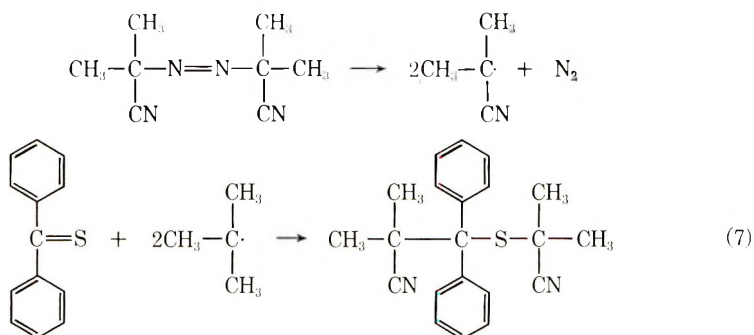
References

1. E. Campaigne, *Chem. Revs.*, **39**, 1 (1946).

2. A. Schönberg, *Ber.*, **58**, 1793 (1925).

3. E. Bergmann, M. Magat, and D. Wegenberg, *Ber.*, **63**, 2575 (1930).

4. E. Muller and W. Wiesemann, *Ann.*, **537**, 86 (1939).

5. E. G. Janzen and C. M. DuBose, Jr., *J. Phys. Chem.*, **70**, 3372 (1966).

6. S. Inoue, T. Tsuruta, and J. Furukawa, *Makromol. Chem.*, **36**, 77 (1959–1960); *ibid.*, **42**, 12 (1960).

7. A. Zilkha, P. Neta, and M. Frankel, *J. Chem. Soc.*, **1960**, 3357.

8. B. F. Gafton and E. A. Braude, in *Organic Syntheses*, Coll. Vol. 4, Wiley, New York, 1963, p. 927.

9. A. V. Tobolsky and B. Baysal, *J. Polym. Sci.*, **9**, 171 (1952).

10. W. Schöniger, *Mikrochim. Acta*, **1956**, 869.

11. J. L. Binder, *Anal. Chem.*, **26**, 1877 (1954).

12. Y. Minoura and S. Tsuboi, *Kogyo Kagaku Zasshi*, **70**, 1955 (1967).

13. G. Tsuchihashi and M. Fukuyama, private communication.

Characterization of Styrene–Acrylonitrile Copolymer by Pyrolysis Gas Chromatography

R. VUKOVIĆ and V. GNJATOVIC,

Research Institute, INA, Zagreb, Yugoslavia

Synopsis

Samples of styrene–acrylonitrile (SAN) copolymer of different compositions, molecular weights, block copolymers, and a blend of styrene and acrylonitrile homopolymers were prepared and characterized by the method of pyrolysis gas chromatography. On decomposition of SAN copolymer samples at 645°C, eleven components were identified, the most important of them being styrene, acrylonitrile, and propionitrile. By examination of the pyrolyzate composition during pyrolysis of the SAN copolymer of different compositions, it was established that the propionitrile yield was definitely decreased when the acrylonitrile concentration in copolymer was about 60 mole-%. Further, from the propionitrile yield, we could distinguish random SAN copolymer from the styrene–acrylonitrile homopolymer blend, and on the basis of propionitrile yield some information on the molecular structure of the copolymer could be obtained. The styrene yield depends linearly on the copolymer composition. This permits determination of copolymer composition on the basis of the styrene yield. Furthermore, the effects of decomposition temperature and of molecular weight on the yields of styrene and acrylonitrile were examined.

INTRODUCTION

There is a relatively small number of publications on the study of styrene–acrylonitrile(SAN) copolymer by the method of pyrolysis gas chromatography.[1–6] According to Voight,[1] it was possible to identify SAN copolymer by this method. Lebel[2] reported that this method could successfully be used to distinguish a homopolymer blend from the random SAN copolymer. Shibasaki and Kambe[3–5] determined that on the basis of styrene and acrylonitrile yields it was possible to get data on the structural composition of the copolymer. These authors succeeded in identifying, in addition to styrene and acrylonitrile, benzene, α-methylstyrene, and ethylbenzene by this method. The latter two components were found in trace amounts only.

We used the method of gas chromatography to separate acetonitrile and propionitrile from acrylonitrile and ethylbenzene, and α-methylstyrene from styrene; we identified eleven components which helped us to make a detailed study of the effect of the copolymer composition on the yields of the individual components of the pyrolysate. In addition, the effect of the

decomposition temperature and the molecular weight on the yields of styrene and acrylonitrile monomers was examined.

EXPERIMENTAL

Monomers and Initiators

Acrylonitrile (AN), Carlo Erba, purity 99%, was treated with concentrated NaOH and then washed repeatedly with distilled water. After that it was dried and distilled over calcium hydride. Styrene (St) was polymer grade (produced by Organsko Kemijska Industrija, Zagreb), with no traces of polymers, purity 99.96% and containing 12 ppm of p-tert-butyl catechol.

Lauroyl peroxide (Noury Van der Lande) and 2,2'-azobis-2-methyl-propionitrile (Eastman Organic Chemicals) were used without further purification.

Polymers and Polymer Blends

Samples of SAN copolymers of different composition were prepared by bulk polymerization at $70 \pm 1°C$ in the presence of lauroyl peroxide. After a conversion of 3–6% was reached, the polymer was precipitated with ethanol and then purified by precipitation with ethanol from an acetone solution. This procedure was repeated three times, after which the polymer was dried under vacuum to a constant weight. The composition of the prepared samples is shown in Table I.

TABLE I
Composition of SAN Copolymer Samples

Sample no.	AN in copolymer, mole-%[a]
1	12.5
2	28.8
3	38.5
4	47.5
5	58.0
6	62.0
7	77.0

[a] Calculated from nitrogen content (Kjeldahl).

Okirol N-3 (trade name of polystyrene produced by Organsko Kemijska Industrija) was purified by repeated precipitation of with methanol from a benzene solution. After three precipitations the polymer was dried under vacuum to constant weight.

Polyacrylonitrile was prepared by slurry polymerization as described by Wilkinson.[7]

The styrene– and acrylonitrile block copolymer was prepared according to the method of Frankel and et al.[8] with n-butyllithium as initiator.

Samples of azeotropic SAN copolymer of different molecular weights were prepared by suspension polymerization at 70 ± 1°C in the presence of 2,2'-azobis-2-methylpropionitrile of different concentrations. Table II shows the characteristics of these samples.

TABLE II

Molecular Weights of SAN Copolymer of Azeotropic Composition

Sample no.	$[\eta]$, dl/g	$M_v{}^a$
1	0.504	142000
2	1.020	370000
3	1.178	466700
4	1.418	623700

^{a} Calculated according to the data of Shimura et al.:[9] $[\eta] = 36 \times 10^{-5} M_v{}^{0.62}$.

Intrinsic viscosities were measured in a Cannon-Fenske capillary viscometer, No. 100, in methyl ethyl ketone at 30 ± 0.01°C.

Pyrolysis Apparatus, Gas Chromatograph, and Experimental Conditions

The pyrolysis apparatus used in this study has been described elsewhere.[10] The analysis of the decomposition products was carried out with the Model 800 Perkin-Elmer chromatograph, which was connected to the pyrolyzer by a short precut glass column. The analysis was carried out under the following conditions: column, Chromosorb P 30–60 mesh, 7 × 0.6 cm; analytical column, 20% poly(propylene glycol) UC oil LB-550-X on Chromosorb P 30–60 mesh, 200 × 0.6 cm, temperature 25–200°C; carrier gas, N$_2$; sample used, 1–5 mg.

RESULTS AND DISCUSSION

Determination of the Pyrolyzate Composition

On decomposition of SAN copolymers at a temperature of 645°C (Fig. 1) the following components were identified by calibration against pure substances: acetonitrile, acrylonitrile, propionitrile, benzene, allylcyanide, toluene, ethylbenzene, styrene, α-methylstyrene, diethylbenzene, and ethylvinylbenzene.

Quantitative analysis of the decomposition products was performed by measuring the peak area and using a calibration curve obtained for pure components. The quantitative yeilds of the individual components per milligram of sample is shown in Figure 2.

Figure 2 shows that, in addition to styrene and acrylonitrile the identified components obtained in the largest amounts are propionitrile, toluene, benzene and α-methylstyrene. The yield of acetonitrile from copolymers containing 31–63 wt-% of acrylonitrile amounts to 2–4 wt-%. When the AN content is below 31 wt-%, acetonitrile is found in concentration below
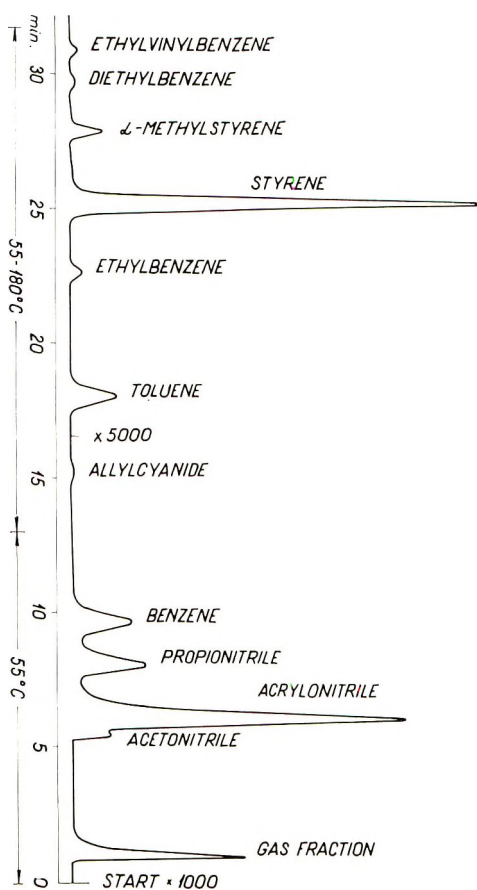
Fig. 1. Typical chromatogram of the products of azeotropic SAN copolymer. Pyrolysis temperature 645°C; column, 20% poly(propylene glycol) UC oil LB-550-X on Chromosorb P 30-60 mesh, 200 × 0.6 cm; carrier gas N_2, 38 ml/min.

1 wt-%. Figure 2 shows that the yield of component derived from styrene sequences in the copolymer decreases linearly with decreasing styrene concentration in the copolymer and that the yield of components derived from acrylonitrile sequences varies according to a curves having a maximum at an acrylonitrile content in the copolymer of about 50 wt-%.

It is also evident from Figure 2 that the total amount of identified products is less than 50 wt-%, while other products representing gaseous and heavy components are not identified.

The fact that propionitrile is completely separated from acrylonitrile and benzene was utilized for construction of Figure 3, which shows the difference in yields of propionitrile of the random copolymer at different acrylonitrile contents, compared with the yields of propionitrile obtained by decomposition of the mixture of styrene and acrylonitrile homopolymers. Figure 3 shows a pronounced difference in propionitrile yield be-

tween the random copolymer and the mixture of homopolymers at all the compositions and the important effect of copolymer composition on the propionitrile yield when the copolymer contains 60 mole-% or more of AN. It is apparent that at a higher acrylonitrile content the relative propio-
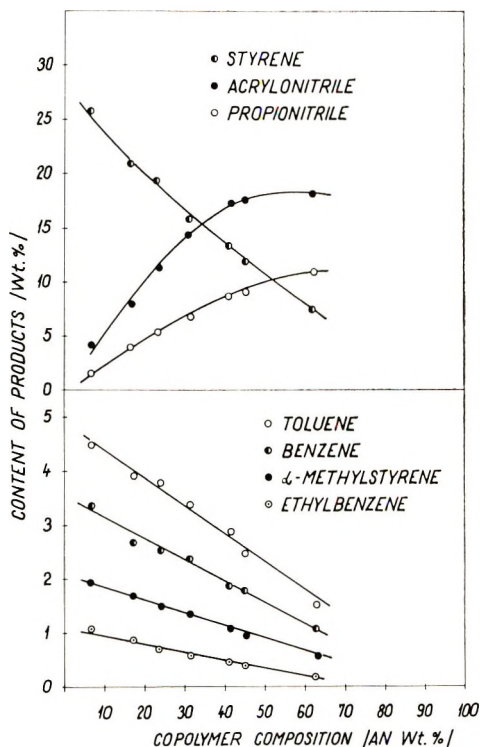
Fig. 2. Content of various components of the pyrolyzate of random SAN copolymer of different compositions calculated on the sample weight. Pyrolysis temperature 645°C, in N_2 stream.
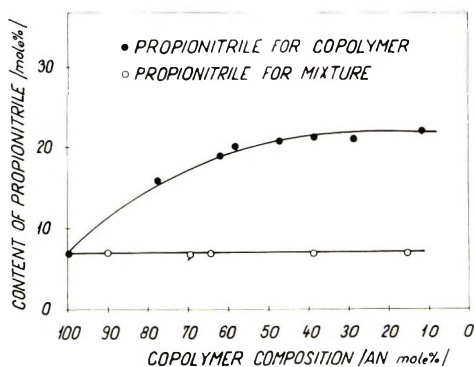
Fig. 3. Propionitrile yields on decomposition of SAN copolymer of different compositions and of the homopolymer mixture versus the acrylonitrile content in the sample. Pyrolysis temperature 645°C, in N_2 stream.
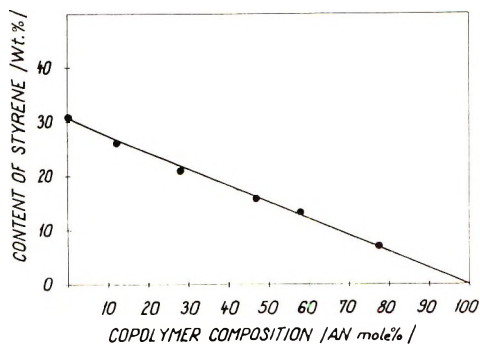
Fig. 4. Calibration curve for the determination of the copolymer composition. Styrene content of the pyrolyzate during the decomposition of random SAN copolymers of different compositions, calculated on the total sample weight. Pyrolysis temperature 645°C, in N_2 stream.
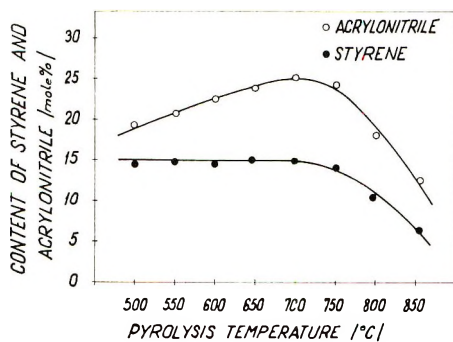
Fig. 5. Effect of decomposition temperature on the yields of styrene and acrylonitrile in the decomposition of azeotropic SAN copolymer in a stream of N_2. Yields were calculated on the total sample weight.
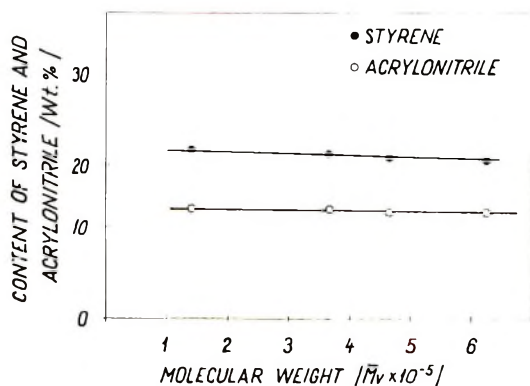
Fig. 6. Effect of the molecular weight of azeotropic SAN copolymer on the styrene and acrylonitrile yields. Calculations based on the total sample weight. Pyrolysis temperature 645°C, in N_2 stream.

nitrile yield is smaller as a consequence of the random SAN copolymer structure.

For different polystyrene and polyacrylonitrile mixtures, the propionitrile, styrene, and acrylonitrile yields remain constant at all homopolymer ratios. The block copolymer shows the same relative yield of propionitrile, acrylonitrile, and styrene as the corresponding mixtures and it is impossible to distinguish it from the homopolymer blend. The styrene yield expressed in weight per cent depends linearly on the copolymer composition expressed in mole per cent AN, so that the copolymer composition can easily be determined (Fig. 4).

Styrene and acrylonitrile yields of the decomposition of SAN copolymers of different compositions obtained in this study are different from the yield percentages reported by Shibasaki and Kambe.[3]

We suppose that this difference may be atrributable to a difference in the apparatus used[3,6] and of a difference in the separation of the components identified in the pyrolyzate (Fig. 1). Figure 1 shows that the acetonitrile and propionitrile peaks appear before and behind the acrylonitrile peak. Figure 2 shows that the concentration of these may have a significant effect on the differences in results. The same applies to the styrene content of the copolymer, because the α-methylstyrene and ethylbenzene peaks are completely separated from this of styrene.

Effect of Decomposition Temperature

The effect of the decomposition temperature in the range 500–860°C on the yields of styrene and acrylonitrile was studied. Figure 5 shows that the acrylonitrile yield continues to increase up to 700°C. Above this temperature the decomposition of acrylonitrile units begins, resulting in an increase of the content of more volatile components and decrease of the acrylonitrile content. The same figure shows that the increase of the temperature from 500 to 700°C has no influence on the styrene yield.

At above 700°C the styrene yield also decreases as a consequence of decomposition of the styrene units.

Effect of Molecular Weight

In order to examine the effect of molecular weight on the styrene and acrylonitrile yields, samples of azeotropic SAN copolymers of different molecular weights were pyrolyzed at 645°C.

Figure 6 shows the yields of styrene and acrylonitrile monomers depending on the change of the molecular weight.

It is apparent that the styrene yield is decreased by an insignificant amount and the acrylonitrile yield remains constant with increasing molecular weights.

References

1. J. Voight, *Kunststoffe*, **51**, 18 (1961).
2. P. Lebel *Rubber Plastics Age*, **46**, 677 (1965).
3. J. Shibasaki and H. Kambe, *Kobunshi Kagaku*, **21**, 71 (1964).
4. J. Shibasaki, *Kobunshi Kagaku*, **21**, 125 (1964).
5. J. Shibasaki, *J. Polym. Sci.*, *A-1*, **5**, 21 (1967).
6. F. A. Lehman and G. M. Brauer, *Anal. Chem.*, **33**, 873 (1961).
7. W. K. Wilkinson in *Macromolecular Syntheses*, Vol. II, J. R. Elliott, Ed., Wiley, New York, 1966, p. 78.
8. M. Frankel, A. Otolenghi, M. Alabeck, and A. Zilkha, *J. Chem. Soc*, **1959**, 5858.
9. J. Shimura, J. Mita, and H. Kambe, *J. Polym. Sci. B*, **2**, 403 (1964).
10. D. Deur-Šiftar, T. Bistrički, and T. Tandi, *J. Chromatog.*, **24**, 404 (1966).

Electron Spin Resonance Study on Homogeneous Catalysts Derived from *n*-Butyl Titanate and Triethylaluminum

HIDEFUMI HIRAI, KATSUMA HIRAKI, ISAMU
NOGUCHI, and SHOJI MAKISHIMA, *Department of
Industrial Chemistry, Faculty of Engineering, University of
Tokyo, Bunkyo-ku, Tokyo, Japan*

Synopsis

ESR spectra of homogeneous catalyst systems derived from *n*-butyl titanate and triethylaluminum at Al/Ti molar ratios of 1.0–10 were observed in toluene solution at several temperatures from −78°C to +25°C. In the whole range of Al/Ti molar ratios, a single signal with a *g* value of 1.951 was observed at −78°C and was associated with the first reaction intermediate. With increasing temperature, the intensity of the signal decreased gradually, while two series of signals appeared, depending on the Al/Ti molar ratio. At an Al/Ti molar ratio of 1.7, seven kinds of signals with *g* values of 1.960, 1.946, 1.950, 1.959, 1.980, 1.977, and 1.978, respectively, were observed. On the other hand, four kinds of signals with *g* values of 1.934, 1.966, 1.952, and 1.979, respectively, were found at Al/Ti molar ratios larger than 3. The structures of the species corresponding to the signals were discussed on the basis of the ESR spectra, the order of their growth and their hyperfine structures being considered. Two series of ESR signal were correlated to two kinds of active species for polymerization of styrene and butadiene, respectively.

INTRODUCTION

Alkyl titanate–triethylaluminum systems are known to be homogeneous Ziegler catalysts for polymerization of ethylene,[1] styrene,[2,3] and conjugated dienes.[4–8] Shilov et al.[9] found an ESR signal with a *g* value of 1.957 and a hyperfine structure of 11 components at a molar ratio of triethylaluminum to *n*-butyl titanate (Al/Ti ratio) of two and ascribed it to the structure I, in which the titanium atom was regarded as a trivalent state.[9,10] Takeda

I
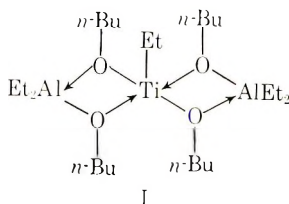
and his co-workers[2,3] reported a maximum catalyst activity at an Al/Ti

147

ratio of 1.4 in the polymerization of styrene and proposed both Ti(O-n-Bu)$_2$Et and structure I as the active species on the basis of the results of infrared and ESR spectra. This catalyst system has a maximum activity for polymerization of butadiene at an Al/Ti ratio of 5.8 but no activity at Al/Ti ratios less than 2.[11]

The reaction of n-butyl titanate with triethylaluminum seems rather complicated in relation to the catalytic activity of the system. In the present study, the reaction was examined by means of ESR spectrometry to determine the products over a wide range of Al/Ti ratios and at various temperatures.

EXPERIMENTAL

Materials

Toluene (Tokyo Kasei Co.) was refluxed over molten sodium metal and distilled under a slight positive nitrogen pressure. n-Butyl titanate (commercial grade) was purified by distillation at reduced pressure. Triethylaluminum was a commercial grade, Ethyl Corporation, without further purification. n-Butyl titanate and triethylaluminum were stored as the toluene solutions under nitrogen; the solutions were transferred with a syringe under a stream of nitrogen.

Procedure

The catalyst system was prepared in a 25-ml glass ampoule connected to both an ESR sample tube and a side-arm tube capped with a silicone rubber stopper. A 10-ml portion of toluene solution containing 0.1–1.0 mmole of n-butyl titanate was injected through the silicone rubber stopper with a syringe into the ampoule, which had previously been connected to a vacuum line for degassing. The solution in the ampoule was degassed three times and cooled to −78°C. A predetermined amount of triethylaluminum solution was added to this solution. About 0.7 ml of the mixture was transferred rapidly into the ESR sample tube cooled with Dry Ice–ethanol. Finally the ESR sample tube was sealed off.

ESR spectra were run in X-band with 100-kcps modulation on a Japan Electron Optics Laboratory Model JES-3BS spectrometer, equipped with a variable-temperature attachment and an integrator for intensity measurements. The first ESR measurements were made at −78°C and continued carefully at various temperatures from −78°C to +25°C, in order to detect all kinds of titanium(III) compounds present in the catalyst systems.

RESULTS AND DISCUSSION

ESR Spectra at Low Temperature

The catalyst system maintained at a temperature below −70°C yielded a single signal with a g value of 1.951 and a maximum slope width of 18
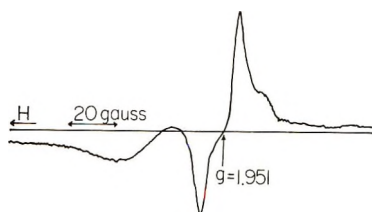
Fig. 1. ESR spectrum of n-butyl titanate–triethylaluminum catalyst system at −78°C. Conditions: Al/Ti ratio, 6.0; initial n-butyl titanate concentration, 0.015 mole/l.; modulation width, 1 gauss.
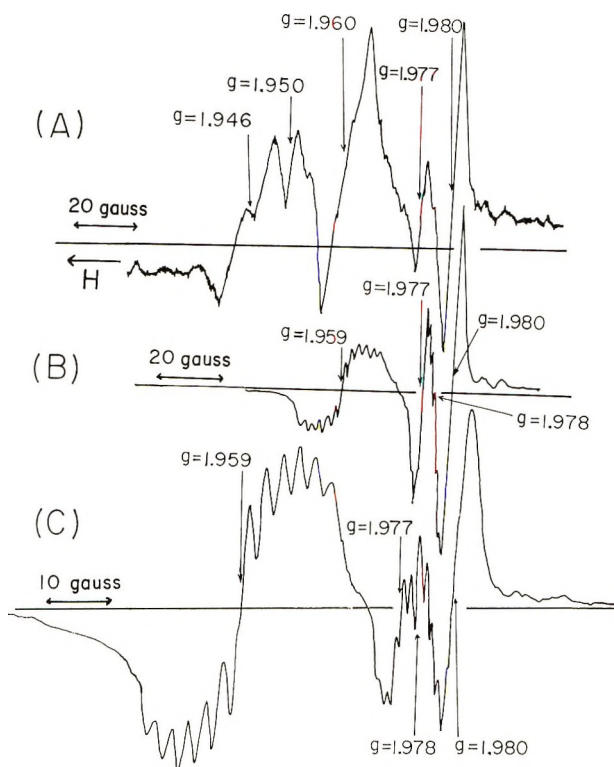
Fig. 2. ESR spectra of n-butyl titanate–triethylaluminum catalyst system at Al/Ti ratio of 1.7: (A) −37°C, 44 min. after the temperature began to rise from −78°C; (B) +14°C, after the sample was allowed to stand for 19 hr at room temperature (14–25°C); (C) +27.8°C, after the sample was allowed to stand for 6 days at room temperature. Conditions: intial n-butyl titanate concentration, 0.075 mole/l.; modulation width, 0.25 gauss.

gauss, regardless of Al/Ti ratio (see Fig. 1). The intensity of this signal decreased gradually with a slow elevation of temperature and became negligible in the range −30°C to +20°C, while new kinds of signals were observed simultaneously (see Fig. 2). Consequently, the former signal corresponds to a first reaction intermediate in the catalyst system.

Most of titanium(III) compounds have g values in the range of 1.86–2.01, with the exception of $MTi(SO_4)_2 \cdot 12H_2O$ (where M is rubidium or cesium).[12] In general, a titanium(II) or a vanadium(III) ion, with two $3d$ electrons, has too short a spin-lattice relaxation time in an octahedral or a near-octahedral environment to be detected by ESR spectroscopy at temperatures above $-78°C$.[13-15] An exceptional case is phenylbis(cyclopentadienyl)vanadium(III), which shows an ESR signal with a g value of 2.13 and a maximum slope width of about 1000 gauss at $27°C$.[16] The g value and the shape of this signal are quite different from those observed in the present study. In addition, the fact that a titanium(II) complex such as dichlorobis(acetonitrile)titanium(II) has a magnetic susceptibility deviating considerably from 2.82 indicates the strong interaction between the titanium atoms in the complex.[17] Bis(cyclopentadienyl)titanium dimer was diamagnetic and showed no ESR signal.[18] The titanium in the structure I, which was detected by ESR spectroscopy, was also regarded as a trivalent state.[9,10] Indeed, a titanium(III) species was isolated as the reaction product between triethylaluminum and a titanium(IV) compound, such as di-n-butoxybis(acetylacetonato)titanium(IV),[19] tetrachloro-titanium(IV),[20,21] or dichlorobis(cyclopentadienyl)titanium(IV).[22] It is very probable from the facts given above that all the ESR signals, observed in the present study can be assigned to the titanium(III) species.

The reaction between equimolar quantities of triethylaluminum and n-butyl titanate is expected to produce $AlEt_2(O\text{-}n\text{-}Bu)$, a compound which has a tendency for coordination or dimerization. If $AlEt_2(O\text{-}n\text{-}Bu)$ was coordinated with the titanium(III) species, the ESR signal would show a hyperfine structure on interaction of the unpaired spin with the ^{27}Al nucleus (spin $= 5/2$). The signal actually observed, however, had no hyperfine structure.

The process involved and the structure for the species ascribed to this signal can be reasonably explained as follows. The reaction between equimolar quantities of triethylaluminum and n-butyl titanate may yield a complex, $(n\text{-}BuO)_3TiEt \cdot (n\text{-}BuO)AlEt_2$, resulting in an instantaneous reduction to a complex $(n\text{-}BuO)_3Ti \cdot (n\text{-}BuO)AlEt_2$ at $-78°C$. The $(n\text{-}BuO)AlEt_2$ component of this complex prevents[23] the $Ti(O\text{-}n\text{-}Bu)_3$ from precipitating by coordination with titanium(III). The $(n\text{-}BuO)_3Ti \cdot (n\text{-}BuO)AlEt_2$ complex forms a dimer by means of bonding of vacant coordination sites of the titanium(III) with bridges of $Ti(III)\text{-}O(n\text{-}Bu)\text{-}Ti(III)$. A spin–spin exchange interaction between the two paramagnetic titanium(III) atoms with the same co-ordination circumstance[24] through this bridging bonds may cancel the hyperfine splitting due to the ^{27}Al nucleus. This kind of bridging bond $Ti\text{-}O(n\text{-}alkyl)\text{-}Ti$ exists in such compounds as trimeric n-alkyl titanate[25] or polymeric $Ti(O\text{-}n\text{-}Bu)_3$.[2,3,23] The titanium(III) in the dimer has a coordination number of five, probably due to the steric effect of n-butoxy groups, similar to structure I. No ethyl group is combined with the titanium(III), since the signal could be observed at a temperature

below 20°C and the species is the first precursor of I, which contains one ethyl group.

Thus, the process (1) and the structure II for the species were proposed.

$$[Ti(O\text{-}n\text{-}Bu)_4]_3 + (AlEt_3)_2 \rightarrow (n\text{-}BuO)Ti \cdot (n\text{-}BuO)AlEt_2$$

(1)

II
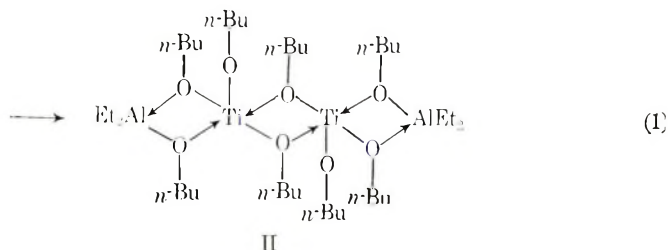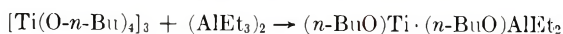
ESR Spectra at Triethylaluminum to n-Butyl Titanate Molar Ratios Less than 2

Typical ESR spectra at an Al/Ti ratio of 1.7 are shown in Figure 2. Several kinds of signals appeared with increasing temperature from $-78°C$ to $+25°C$, while the signal with the g value of 1.951 decreased gradually. Figure 3 plots the relative intensity of these signals versus reaction time. In this paper the new signals will be referred to as the first, the second, . . ., and the seventh signal, in the order in which they appear.

Three kinds of comparatively weak signals appeared at $-38°C$; the first signal with a g value of 1.960 and a maximum slope width of 13.5
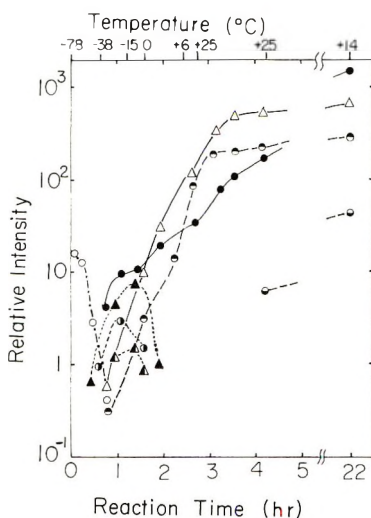
Fig. 3. Plots of relative intensities of ESR signals in n-butyl titanate–triethylaluminum catalyst system at Al/Ti molar ratio of 1.7: (O) first intermediate (g value = 1.951); (▲) first signal (g value = 1.960); (◑) second signal (g value = 1.946); (▲) third signal (g value 1.950); (◖) fourth signal (g value = 1.959); (●) fifth signal (g value = 1.980); (△) sixth signal (g value = 1.977); (◕) seventh signal (g value = 1.978).

gauss; the second one with a g value of 1.946, a hyperfine structure of two components, and a coupling constant of 8.3 gauss; the third one with a g value of 1.950 and a maximum slope width of 3 gauss (see Fig. 2). As shown in Figure 3, the intensity of these signals becomes negligible at $6°C$.

Three other kinds of new signals began to become apparent at $-30°C$ and were quite prominent at $25°C$ (see Fig. 3); these were the fourth signal with a g value of 1.959, a hyperfine structure of 11 components and a coupling constant of 2.3 gauss; the fifth signal with a g value of 1.980 and a maximum slope width of 3.5 gauss; the sixth one with a g value of 1.977 and a maximum slope width of 2.7 gauss. The seventh signal, with a g value of 1.978, a hyperfine structure of 11 components, and a coupling constant of 1.0 gauss formed overlapping with the sixth one, after the catalyst system had been allowed to stand at $25°C$ for 2 hr.

The second and the third signals were expected to correspond to unstable intermediates, the structures of which could not yet be determined. The fourth signal can be assigned to the same one ascribed by Shilov et al.[9] to structure I. They reported that the intensity of the signal corresponded to about 10% of the amount of the initial titanate. The first, fifth, and sixth signals are plausibly associated with the same signals observed by Takeda and his co-workers.[2,3] Each of the species corresponding to these three signals is considered to have a structure analogous to II on the basis of the lack of hyperfine structure and to contain one or several moles of triethylaluminum in place of the $AlEt_2(O-n-Bu)$ component of II. It is conceivable that the species associated with the seventh signal has a structure analogous to I, because of the similarity of the hyperfine structure. In addition, the species probably contains one mole of triethylaluminum coordinated instead of the component $AlEt_2(O-n-Bu)$ of I, since the seventh signal appeared only at a later stage of the reaction than the fourth signal did. The most probable structure, on the basis of these results, for this species is the structure III. The facts that the fourth, fifth, sixth, and

III
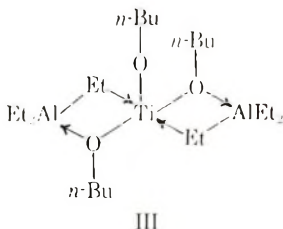
seventh signals appeared simultaneously can best be explained by the existence of equilibria among the species corresponding to these signals, triethylaluminum and $AlEt_2(O-n-Bu)$.

ESR Spectra at Triethylaluminum to n-Butyl Titanate Molar Ratios Greater than 3

Figure 4 shows spectra at Al/Ti ratios of 6 and 10. The signal with a g value of 1.951, observed at a temperature below $20°C$, disappeared
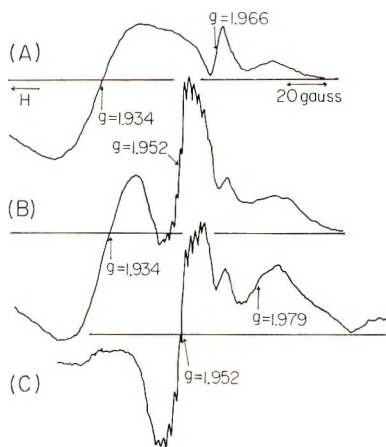
Fig. 4. ESR spectra of n-butyl titanate–triethylaluminum catalyst system at Al/Ti molar ratios of 6 and 10:   (A) Al/Ti = 6, 1.5 hr after the temperature began to rise from $-78°C$; (B) Al/Ti = 6, 24 hr after the temperature had arrived at $+25°C$; (C) Al/Ti = 10, 2.0 hr after the temperature began to rise from $-78°C$.   Conditions: temperature, 25°C; initial n-butyl titanate concentration, 0.015 mole/l.; modulation width, 1 gauss.

gradually, while four new signals appeared.   These four signals will be referred to as the eighth, ninth, tenth, and eleventh signals, respectively, according to the order of their appearance.

In the earlier stage of the reaction at an Al/Ti ratio of 6, the first two signals appeared simultaneously; the eighth signal with a g value of 1.966 and a maximum slope width of 10 gauss; the ninth, with a g value of 1.934 and a maximum slope width of 40 gauss.   At later stages at this Al/Ti ratio, a tenth signal, with a g value of 1.952, a hyperfine structure of 11 components, and a coupling constant of 2.6 gauss, was noted.   At an Al/Ti ratio of 10, the eleventh signal with a g value of 1.979 and a maximum slope width of 29 gauss appeared besides the eighth and tenth ones.

The eighth signal was weak and had no hyperfine structure.   The species responsible for this signal possibly has a structure similar to II and contains more of coordinated triethylaluminum than II or III does, since the component $AlEt_2(O\text{-}n\text{-}Bu)$ can be replaced by an excess of triethylaluminum. The species responsible for the tenth signal possibly has a structure analogous to III, owing to the similarity of the hyperfine structure.   The species probably contains more of triethylaluminum in place of the component $AlEt_2(O\text{-}n\text{-}Bu)$ than III does, because the tenth signal appeared only at larger Al/Ti ratio than the seventh signal.   It is plausible that the species corresponding to the tenth signal may have the structure IV.
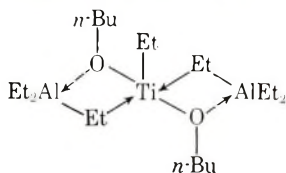
IV

Neither the ninth or the eleventh signal had hyperfine structure but both had a larger maximum slope width than any of the signals without hyperfine structure described above (the first, third, fifth, sixth, and the eighth signals). The species corresponding to the ninth and the eleventh signals may contain more triethylaluminum than III does. These considerations suggest that these species have a new kind of bridging bond, for example, Ti(III)–CH$_2$(CH$_3$)–Ti(III), or Ti(III)–O(n-Bu)–Ti(II).

An absorption intensity of the signal observed at an Al/Ti ratio of six in the presence of butadiene corresponded to 0.5% or less of the amount of initial titanate.[26,27] This value was also approximately equal to that of the signals produced in the catalyst system without the monomer. Accordingly, the formation of the titanium(III) species was a minor part of the reaction products at this Al/Ti ratio, while the main products could not be detected by ESR measurements in these conditions.

Summary of ESR Spectra and Catalytic Activity for Polymerization

The g value of the ESR signals observed with the reaction of n-butyl titanate with triethylaluminum are summarized in Table I; the number of components in the hyperfine structures is also given. Table I shows that the catalyst systems yield many kinds of titanium(III) compounds, depending on the Al/Ti ratio, the reaction time, and the temperature. The

TABLE I
Summary of ESR Spectra

Al/Ti ratio	At −78°C			At room temperature				
						g value[a]		
0.5[b]					1.960			
1.0				1.959(11)	1.960			
1.4[b]				1.962(11)		1.976[c]		1.980[c]
1.5				1.959(11)		1.977	1.978(11)	1.980
1.7[d]	1.951			1.959(11)		1.977	1.978(11)	1.980
2.0[e]				1.957(11)				
2.0[f]				1.959(11)				1.979
2.6[b]				1.962(11)		1.976[c]		1.980[c]
3.4	1.951	1.934	1.952(11)		1.966			
6.0	1.951	1.934	1.952(11)		1.966			
7.2	1.951	1.934	1.952(11)		1.966		1.979	
10.0	1.951		1.952(11)		1.966		1.979	

[a] Number of components of the hyperfine structure given in parentheses.

[b] Data of Takeda and his co-workers.[2,3]

[c] These signals have been assigned to a doublet with a g value of 1.978 by Takeda and his co-workers.[2,3]

[d] Transient signals with g values of 1.946, 1.950, and 1.960 were found at temperatures from −38°C to +6°C.

[e] Data of Shilov et al.[9]

[f] Data of Angelescu et al.[10]

arresting feature about this table is that two series of titanium(III) compounds exist at Al/Ti ratio smaller and larger, respectively, than 2.9.

The catalytic activity for polymerization of styrene was at its maximum at Al/Ti = 1.4 and negligible at Al/Ti > 3.[2,3] On the other hand, the activity for polymerization of butadiene was at its maximum at Al/Ti = 5.8 and negligible at Al/Ti < 2.[11] These facts are distinct evidence that the active species for polymerization of styrene is quite different from that for polymerization of butadiene. The active species for polymerization of styrene was assigned to titanium(III) species containing one alkyl group and two or more alkoxy ones.[2,3]

Dawes and Winkler[11] reported that the catalyst system showed a gradual decrease in the initial rate of the polymerization of butadiene upon standing. This fact indicates the active species for butadiene to be a titanium(III) or a titanium(II) compound, which is expected to be reduced to the lower valence state on aging. The concentration of the active species for butadiene was reported to be lower by a factor roughly 10^{-3} relative to that of the initial titanate.[11] This fact seems to be associated with the very small amount of titanium(III) species, detected by ESR measurements at Al/Ti = 6. In addition, the active species for polymerization of 1,3-pentadiene with this kind of catalyst should contain at least one alkoxy group, because an optically active poly-1,3-pentadiene was synthesized with (−)menthyl titanate-triethylaluminum catalyst.[8] The inference that the active species possibly holds at least one alkyl group is supported by the analogy to the fact that the radioactivity was found in the poly-1,2-butadiene obtained with tris-(acetylacetonato)vanadium(III)–^{14}C-labeled triethylaluminum catalyst and that this polymer had a similar microstructure to that obtained with the alkyl titanate–triethylaluminum catalyst.[28]

The active species for butadiene with the latter catalyst is proposed, on the above facts and of the structures of titanium(III) species observed at Al/Ti > 3, to be a titanium(III) species which can be converted with liberation of coordinated components into a species containing two alkyl groups and an alkoxy group. This is also supported by a study[26,27] carried out to examine the growing ends in the polymerization of conjugated dienes in the presence of the monomers.

References

1. C. E. H. Bawn and R. Cymcox, *J. Polym. Sci.*, **34**, 139 (1959).

2. M. Takeda, K. Iimura, Y. Nozawa, N. Koide, and M. Hisatome, *J. Polym. Sci.*, C, **23**, 741 (1968).

3. M. Takeda, K. Iimura, Y. Nozawa, M. Hisatome, and M. Watanabe, paper presented at the 13th Symposium on Polymers, The Society of Polymer Science, Japan, Tokyo, 1964; *Preprints*, p.121.

4. G. Wilke, *Angew. Chem.*, **68**, 306 (1956).

5. G. Natta, *J. Polym. Sci.*, **48**, 219 (1960).

6. G. Natta, L. Porri, A. Carbonaro, and G. Stoppa, *Makromol. Chem.*, **77**, 114 (1964).

7. G. Natta, L. Porri, and A. Carbonaro, *Makromol. Chem.*, **77**, 126 (1964).

8. G. Natta, L. Porri, and S. Valenti, *Makromol. Chem.*, **67**, 225 (1963).

9. T. S. Djabiev, R. D. Sabirova, and A. E. Shilov, *Kinetika i Kataliz*, **5**, 441 (1964).

10. E. Angelescu, C. Nicolau, and Z. Simon, *J. Amer. Chem. Soc.*, **88**, 3910 (1966).

11. D. H. Dawes and C. A. Winkler, *J. Polym. Sci. A*, **2**, 3029 (1964).

12. Landolt-Börnstein, *Neue Serie Gruppe II*, Vol. 2, Springer Verlag, Berlin, 1966 p. **4-1**.

13. J. Lambe and C. Kikuchi, *Phys. Rev.*, **118**, 71 (1960).

14. A. Abragam and M. H. L. Pryce, *Proc. Roy. Soc.* (London), **A205**, 135 (1961).

15. R. J. Kokes, in *Experimental Methods in Catalysis Research*, R. D. Anderson, Ed., Academic Press, New York, 1968, Chap. 11.

16. J. C. W. Chien and C. R. Boss, *J. Amer. Chem. Soc.*, **83**, 3767 (1961).

17. G. W. A. Fowles, T. E. Lester, and R. A. Walton, *J. Chem. Soc.*, *A*, **1968**, 1081.

18. G. W. Watt, L. J. Baye, and F. O. Drummond, Jr., *J. Amer. Chem. Soc.*, **88**, 1138 (1966).

19. A. Yamamoto, S. Ikeda, and M. Murai, paper presented at a Symposium on Organometallic Compounds, Chemical Society of Japan, Tokyo, 1965; *Preprints*, p. 60 (1965).

20. M. D. Groenwege, *Z. Physik. Chem.* (Frankfurt), **18**, 147 (1958).

21. G. Natta, P. Corradini, and G. Allegra, *J. Polym. Sci.*, **51**, 399 (1961).

22. G. Natta, P. Pino, G. Mazzanti, and U. Giannini, *J. Amer. Chem. Soc.*, **79**, 2975 (1957).

23. A. N. Nesmeyanov, O. V. Nogina, and R. Kh. Freidlina, *Izvest. Akad. Nauk. SSSR., Otdel. Khim. Nauk.*, **1956**, 373; *Chem. Abstr.*, **50**, 15413 (1956).

24. G. K. Pake, *Paramagnetic Resonance*, Benjamin, New York, 1962, Chap. 4.

25. C. N. Caughlan, H. S. Smith, W. Katz, W. Hodgson, and R. W. Crowe, *J. Amer. Chem. Soc.*, **73**, 5652 (1951).

26. H. Hirai, K. Hiraki, I. Noguchi, T. Inoue, and S. Makishima, to be published.

27. K. Hiraki, T. Inoue, H. Hirai, and S. Makishima, paper presented at The 17th Annual Meeting on Polymers, Society of Polymer Science, Japan, Tokyo, 1968; Preprint I-210.

28. G. Natta, L. Porri, G. Zanini, and L. Fiore, *Chim. Ind.* (Milan) **41**, 526 (1959).

Equilibrium Concentration of Trioxane in Cationic Polymerization

T. MIKI, T. HIGASHIMURA, and S. OKAMURA,
Department of Polymer Chemistry, Kyoto University, Kyoto, Japan

Synopsis

In the cationic polymerization of trioxane and tetraoxane near room temperature, the equilibrium trioxane concentration is not negligible during polymerization. In this work, tetraoxane was polymerized with $BF_3 \cdot O(C_2H_5)_2$ in various solvents and the equilibrium concentration of trioxane produced during the polymerization of tetraoxane and equilibrated with the growing polyoxymethylene chain was determined. The equilibrium trioxane concentrations were 0.05, 0.13, and 0.19 mole/l. in benzene, ethylene dichloride, and nitrobenzene at 30°C, respectively, and 0.20 mole/l. in ethylene dichloride at 50°C. The values in ethylene dichloride showed that the approximate values of ΔH_p and ΔS_p^0 were -4.2 kcal/mole and -9.7 cal/mole-deg., respectively.

INTRODUCTION

Thermodynamic studies of addition polymerization have been extensively carried out, and heat of polymerization, entropy of polymerization, and equilibrium monomer concentration have been determined experimentally or calculated theoretically for many monomers.[1] It is very important and of considerable interest to known these thermodynamic values for other monomers for which thermodynamic studies have not been made. However, a precise determination of equilibrium monomer concentration from monomer–polymer equilibrium during polymerization demands strict conditions. To establish a reasonably mobile equilibrium between monomer and polymer, it is necessary (*1*) that a certain concentration of active centers is continually present in the polymerization system and (*2*) that in such a system only long-chain polymer is present at equilibrium and there is no danger of side reaction; in addition (*3*) it is desirable that the polymerization proceeds homogeneously.

Extensive studies of polymerization of trioxane and tetraoxane suggest strongly that the equilibrium trioxane concentration near room temperature is not negligible.[2,3] However, it seemed impossible to determine equilibrium trioxane concentration by the same method as used for the determination of equilibrium concentration of dioxolane[4] and tetrahydrofuran.[5] The polymerization of trioxane seems to fulfill the first condition mentioned above because it proceeds like a "living" system,[6] but not the second and the third conditions: the formation of the polymer is ac-

companied by the formation of tetraoxane as a side reaction;[2] also, the polymerization of trioxane proceeds heterogeneously in all solvents studied to date.

For the determination of equilibrium trioxane concentration, it is necessary to find a system in which the formation of a large amount of solvent-insoluble polyoxymethylene is suppressed, but the degree of polymerization of solvent-soluble polyoxymethylene is large enough to permit the equilibrium between polymer and monomer to be discussed; concentrations of compounds other than trioxane and the polymer should be as low as possible.

As an approximation to such a system, the polymerization of tetraoxane at the "critical" concentration[3] was selected, mainly because it proceeds homogeneously. In the polymerization of tetraoxane at high concentrations by $BF_3 \cdot O(C_2H_5)_2$, both trioxane and solvent-insoluble polymer are formed. With decreasing initial concentration of tetraoxane approaching the critical concentration, only trioxane (and no solvent-insoluble polymer) is produced, and tetraoxane is almost completely consumed. However, the formation of trioxane in the polymerization of tetraoxane at less then the critical concentration suggests the existence of solvent-soluble polymer of unknown chain length. Thus the polymerization of tetraoxane at the critical concentration is considered to be a good system for determination of equilibrium concentration of trioxane.

In this work, the equilibrium trioxane concentration will be determined approximately by making use of the tetraoxane polymerization at low concentrations, and the related thermodynamic quantitites will be obtained.

EXPERIMENTAL

Purification of materials and the procedures of the tetraoxane polymerization were the same as described in a previous paper.[3] Determinations of the amount of tetraoxane consumed and of trioxane produced were carried out by gas chromatography with the use of an internal standard as also described in the previous paper.[3] The amount of methanol-insoluble polymer was determined gravimetrically.

RESULTS AND DISCUSSION

Trioxane was previously detected during the polymerization of tetraoxane catalyzed by $BF_3 \cdot O(C_2H_5)_2$ in ethylene dichloride at 30°C.[3] These results needed to be clarified and confirmed. Tetraoxane was polymerized at various polymerization temperatures. The results of the polymerization of tetraoxane catalyzed by $BF_3 \cdot O(C_2H_5)_2$ in ethylene dichloride at 50°C are shown in Figure 1.

In this case, the rates of tetraoxane (TeX) consumption and of trioxane (ToX) formation were larger than those at 30°C. The amounts of tri-
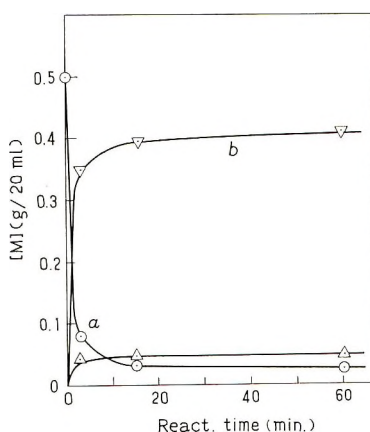
Fig. 1. Change in the concentration of each component with reaction time in the polymerization of tetraoxane catalyzed by $BF_3 \cdot O(C_2H_5)_2$ in ethylene dichloride at 50°C.: (○) consumption of tetraoxane; (▽) formation of trioxane; (△) formation of methanol-insoluble polymer. $[TeX]_0 = 0.208$ mole/l.; $[BF_3 \cdot O(C_2H_5)_2]_0 = 10$ mmole/l.

oxane and the polymer formed at various initial concentrations at a reaction time of 60 min are summarized in Table I and illustrated in Figure 2. $[ToX]_{60}$ (shown in the fourth column of Table I) denotes the concentration of trioxane at reaction time of 60 min and was calculated on the assumption that the total volume of the system at 60 min is equal to the initial volume. Moreover, in every run investigated, the reaction proceeded down to a residual tetraoxane concentration of less than 8 mmole/l. As is clear from Table I and Figure 2, with decreasing initial concentration of tetraoxane, the polymer yield decreased and the yield of trioxane increased.
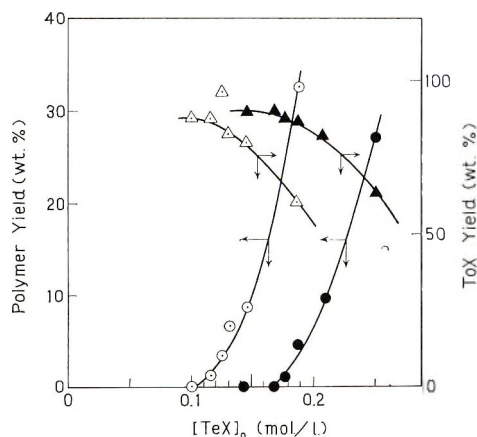
Fig. 2. Relationship between the initial tetraoxane concentration and the yield (○, ●) of the methanol-insoluble polymer on (△, ▲) trioxane at 60 min reaction time in the polymerization of tetraoxane catalyzed by $BF_3 \cdot O(C_2H_5)_2$ in ethylene dichloride: (●, ▲) at 50°C; (○, △) at 30°C.

TABLE I

Conversion of Tetraoxane (TeX) to Methanol-Insoluble Polymer (P) and to
Trioxane (ToX) in the Polymerization of Tetraoxane in Ethylene Dichloride[a]

Polymer-ization temperature, °C	$[TeX]_0$, mole/l.	Conversion to P, wt-%	Conversion to ToX, wt-%	$[ToX]_{60}$, mole/l.
50	0.250	27.2	63.3	0.211
	0.208	9.7	82.0	0.228
	0.187	4.6	86.7	0.217
	0.177	1.0	87.3	0.206
	0.167	0	90.0	0.200
30	0.187	32.7	61.2	0.153
	0.146[b]	8.6	80.0	0.156
	0.130	6.6	82.7	0.142
	0.125[b]	3.3	96.5[c]	—
	0.116	1.3	87.5	0.136
	0.100[b]	0	87.5	0.117

[a] Reaction time, 60 min.; $[BF_3 \cdot O(C_2H_5)_2]_0 = 10$ mmole/l.

[b] Data of Miki et al.[3]

[c] Large value maybe due to experimental error (should be about 85%).

However, the actual concentration of trioxane in the system was almost constant. This concentration of trioxane measured might thus represent the equilibrium concentration of trioxane on the basis of the following considerations: trioxane is formed by depolymerization from the growing chain end which is formed by the catalyst with tetraoxane at the initial stages of polymerization; the equilibrium between trioxane and polymer is established because trioxane also reacts with the growing chain end. Also, the concentration of trioxane measured is larger at the higher polymerization temperature. Thus, the equilibrium concentration of trioxane is determined as the amount of trioxane produced in the homogeneous polymerization of tetraoxane at a critical concentration on the assumption that the degree of polymerization of the solvent-soluble growing chain is sufficiently great. Experimentally, the equilibrium concentration of trioxane was determined by extrapolation of trioxane concentrations at various initial concentrations of tetraoxane to zero polymer yield in order to avoid the heterogeneity of the reaction system, as the concentration of trioxane measured tended to increase very slightly with the polymer yield.

The equilibrium concentration of trioxane graphically determined from data shown in Table I and in the previous paper[3] is summarized in Table II. The equilibrium trioxane concentration was dependent on the nature of solvent used; it increased with increasing polarity of solvent. This suggests that the depolymerization takes place to a greater extent in a polar solvent than in a nonpolar solvent. The kinetic treatment in the trioxane polymerization at low-concentrations in a polar solvent requires care because the equilibrium trioxane concentration near room temperature in a polar solvent cannot be negligible.

TABLE II

Equilibrium Trioxane Concentration [M]$_e$ in Solution Polymerization[a]

Temperature, °C	Solvent	[M]$_e$, mole/l.
30	Benzene	0.05
30	Ethylene dichloride	0.13
30	Nitrobenzene	0.19
50	Ethylene dichloride	0.20

[a] Catalyst: $BF_3 \cdot O(C_2H_5)_2$.

In addition, on the basis of the values obtained, approximate thermodynamic quantities are obtained. The heat and entropy of polymerizations of trioxane in ethylene dichloride with $BF_3 \cdot O(C_2H_5)_2$ as catalyst, ΔH_p and ΔS_p^0, respectively, were calculated by using the values of the equilibrium concentrations of trioxane (0.13 mole/l. at 30°C and 0.20 mole/l. at 50°C) according to eq. (1) formulated by Dainton:[1]

$$T_c = \Delta H_p / (\Delta S_p^0 + R \ln[M]_e) \tag{1}$$

where T_c is critical temperature and [M]$_e$ is equilibrium monomer concentration at T_c.

These are:

$$\Delta H_p = -4.2 \text{ kcal/mole}$$

$$\Delta S_p^0 = -9.7 \text{ cal/mole deg}$$

These values are for a phase transition from monomer dissolved in ethylene dichloride to polymer dissolved in ethylene dichloride with $BF_3 \cdot O(C_2H_5)_2$ as catalyst. These values are considered to be reasonable with respect to order of magnitude in view of literature values of dioxolane[4] ($\Delta H_p = -5.5$ kcal/mole, $\Delta S_p^0 = -15.0$ cal/mole-deg) and tetrahydrofuran[5] ($\Delta H_p -5.5$ kcal/mole, $\Delta S_p^0 = -20.8$ cal/mole deg), both for a phase transition from liquid monomer to polymer dissolved in monomer.

On the other hand, Leese and Baumber reported[7] that the trioxane polymerization reaction is athermal until insoluble polymer is formed. So our data concerning the heat of trioxane polymerization (ΔH_p) does not coincide with Leese's results. This discrepancy might be due to the fact that Leese and Baumber measured the heat of polymerization directly in the polymerization of trioxane. As was reported[8] previously, a large amount of tetraoxane was produced by depolymerization until insoluble polymer formed in the polymerization of trioxane. The athermal reaction until insoluble polymer formed might be due to the simultaneous occurrence of polymerization with respect to trioxane and depolymerization with respect to tetraoxane. If the formation of tetraoxane by depolymerization until insoluble polymer is formed were suppressed, the reaction might be exothermic.

References

1. F. S. Dainton and K. J. Ivin, *Quart. Rev.*, **12**, 61 (1958).

2. T. Miki, T. Higashimura, and S. Okamura, *J. Polym. Sci. A-1*, **5**, 95 (1967).

3. T. Miki, T. Higashimura, and S. Okamura, *J. Polym. Sci. A-1*, **5**, 2997 (1967).

4. L. I. Kuzub, M. A. Markevich, A. A. Berlin, and N. S. Enikolopyan, *Vysokomol. Soedin.*, **10**, 2007 (1968).

5. B. A. Rozenberg, O. M. Chekhuta, E. B. Ludwig, A. R. Gantmakher, and S. S. Medvedev, *Vysokomol. Soedin.*, **6**, 2030 (1964).

6. T. Higashimura, T. Miki, and S. Okamura, *Bull. Chem. Soc. Japan*, **39**, 25 (1966).

7. L. Leese and M. W. Baumber, *Polymer*, **6**, 269 (1965).

8. T. Miki, T. Higashimura, and S. Okamura, *J. Polym. Sci. A-1*, **5**, 2977 (1967).

Interfacial Syntheses of Polyphosphonate and Polyphosphate Esters. II. Dependence of Yield and Molecular Weight on Solvent Volumes and Concentrations of Comers in Basic Polymerization of Hydroquinone and Phenylphosphonic Dichloride

F. MILLICH and C. E. CARRAHER, Jr.,* *Chemistry Department, Polymer Section, University of Missouri-Kansas City, Kansas City, Missouri 64110*

Synopsis

The interfacial polymerizations of hydroquinone with phenylphosphonic dichloride, in the presence of barium hydroxide or sodium hydroxide, were studied and contrasted. Polymer yields and molecular weights were shown to vary with concentration of the comer reactants, with the comer ratio, and with the relative amounts of carbon tetrachloride and aqueous phases, but not with concentration of barium ion. The latter supports the impression that the reaction zone is situated in the aqueous phase. The method of Millich and Carraher, employing pH control, yields products of high molecular weights and some results which are distinct from those achieved with the use of sodium hydroxide.

INTRODUCTION

Stirred interfacial polymerization systems may be subject to many variables. Morgan[1] lists the following parameters affecting polymer yield and molecular weight in such systems: sequence of mixing reactants, temperature, nature of reactants, comer ratio, number of insoluble particles present, pH, size and shape of the reaction vessel, efficiency of mixing, nature of solvents, ratio of volumes of immiscible phases, reactant concentrations, and amounts and types of acid acceptor, ionizable salts, and impurities and terminators (such as monofunctional reactants).

Of these variables, the concentration of one of the comer pair of reactants cannot be varied without also affecting either the comer ratio, the concentration of the other reactant, or the solvent ratio. Also, the addition of a simple electrolyte to the aqueous phase can affect the solubility partition coefficients of any reactant which has a finite solubility in both of the immiscible phases.

---

* Present address: Department of Chemistry, University of South Dakota, Vermillion, South Dakota 57069.

In the first paper of this series,[2] a method and the experimental procedure of rapid polycondensation of hydroquinone (HQ) and phenylphosphonic dichloride (PPD) were described in which the basicity of the aqueous medium could be maintained effectively constant in the range in which HQ and its monoesters undergo acid dissociation. Evidence was presented which indicates that HQ and phenolic polymer end groups react as anions in the polymerization.

This system is sensitive to many of the above mentioned parameters. During the very rapid polymerization in strongly basic media, the polycondensation reaction is in serious competition with concurrent, rapid and thorough alkaline hydrolyses of the poly(phosphonate ester), the phenylphosphonic dichloride, and the chlorophosphonyl end groups of oligomeric intermediates. These several reactions may be expected to have individual dependencies on the reaction parameters, differing in kind and degree, which holds the promise that one or more sets of reaction conditions can be found whereby one or another of the competing reactions may be favored.

The base-promoted reactions are so rapid, and the reaction parameters so plentiful that detailed kinetic study of the separate reactions is extremely laborious. Instead, polymer yield and product intrinsic viscosity may be used as indices of conditions which favor the polycondensation reaction, and the dependence of these indices on the reaction parameters can be informative. In this paper, results are given showing the dependence of polymer yields and viscosities on reactant concentrations of HQ and PPD, examined for the method of Millich and Carraher.[2,3] Contrasting results of polymerizations employing completely soluble strong base are also presented and discussed.

RESULTS AND DISCUSSION

All of the procedures are described in the previous paper.[2]

The yield and polymer solution viscometry data appear in Table I for varying organic phase volume as the aqueous phase volume is held constant, in the system in which the reagent base is Ba(OH)$_2$. A maximum in yield occurs at a 5:1 H$_2$O:CCl$_4$ volume ratio. Morgan[1a] reports that maxima in polymer yield and molecular weight are normally observed in stirred interfacial systems as the volume of the solvent phase is varied, but that the determining reasons are not easily identified conclusively. The product molecular weight, indicated by the limiting viscosity number (LVN) in dimethyl sulfoxide, is essentially constant except at the smallest value of the solvent ratio. Table II shows the results of varying the organic phase volume in the system in which the strong reagent base (NaOH) is completely water-soluble. In order to provide sufficient alkaline capacity to neutralize all of the acid liberated during the very rapid reaction, all of the base must be present at the beginning of the reaction. The maximum yield occurs at a different value of the solvent ratio than in the Ba(OH)$_2$ system, and the values of LVN are lower. Further, no polymer is formed when PPD is used without solvent in the 5N NaOH system.

TABLE I

Total Yield and Unfractionated Polymer Solution Viscometry Data
of the Barium Hydroxide-Promoted Polycondensation of Hydroquinone
(HQ) and Phenylphosphonic Dichloride (PPD) as a Function of
the Organic Phase Volume[a]

Volume CCl₄, ml[d]	Solvent volume ratio H₂O:CCl₄	Acid chloride in organic phase, vol-%	Total yield, %	LVN, ml/g[b]
0	1:0	100	29	27
1	100:1	75	37	29
2	50:1	60	52	30
5	20:1	38	59	29
10	10:1	23	65	32
20	5:1	13	82	29
25	4:1	11	74	30
50	2:1	6	69	29
100	1:1	3	66	28
200	1:2	2	56	30
300	1:3	1	36	22

[a] Volume of H₂O, 100 ml; amount of Ba(OH)₂, 0.040 mole; PPD:HQ molar ratio 0.021:0.021.

[b] LVN (limiting viscosity number) obtained by extrapolation to infinite dilution of data on polymer solutions in dimethyl sulfoxide at 25°C in the concentration range of 1–10 g/100 ml.

TABLE II

Total Yield and Unfractionated Polymer Solution Viscometry Data in
the Sodium Hydroxide-Promoted Polycondensation of Hydroquinone
(HQ) and Phenylphosphonic Dichloride (PPD) as a Function of
Organic Phase Volume[a]

Volume CCl₄, ml	Volume ratio H₂O:CCl₄	Total yield, %	LVN, ml/g[b]
0	1:0	0	—
25	1:1	85	15
50	1:2	85	22
75	1:3	46	6
100	1:4	20	2

[a] Volume of aqueous NaOH (5N), 25 ml; PPD:HQ molar ratio 0.021:0.021.

[b] LVN (limiting viscosity number) obtained by extrapolation to infinite dilution of data on polymer solutions in dimethyl sulfoxide at 25°C in the concentration range of 1–10 g/100 ml.

Table III shows the polymer yield and LVN data for the Ba(OH)₂ system in which the aqueous phase volume was varied and other parameters were kept the same. Initial and final pH values were greater than 12. Barium hydroxide octahydrate is soluble to the extent of 8 g/100 ml (i.e., 0.25M) at 20°C in water, so that all experiments but one (i.e. that employing 200 ml of water and 0.040 mole Ba(OH)₂ in Table III) were conducted in the solutions initially saturated with Ba(OH)₂. Minor differences at the

different $Ba(OH)_2$ levels can be attributed to the larger number of solid particles of $Ba(OH)_2$ present at the higher level. Maximum yield occurs at $2:1$ $H_2O:CCl_4$ volume ratio. The LVN is found to vary with the amount of water present, showing a maximum at $1:1$ $H_2O:CCl_4$ volume ratio. Thus, as the aqueous phase is varied, the optimization of yield and molecular weight tends to be parallel, although it is not exactly coordinated. Although conditions which are favorable to polycondensation do benefit the achievement of both good yields and high molecular weights, some alkaline degradation of long polymer chains can take place without materially reducing polymer yield. The same parameter was investigated in

TABLE III

Total Yield and Unfractionated Polymer Solution Viscometry Data
of the Barium Hydroxide-Promoted Polycondensation of Hydroquinone
(HQ) and Phenylphosphonic Dichloride (PPD) as a Function of Aqueous Phase
Volume and Amount of Barium Hydroxide[a]

Amount $Ba(OH)_2$, mole	Volume H_2O, ml	Solvent volume ratio $H_2O:CCl_4$	Total yield, %	LVN, ml/g[b]
0.051	0	0	0	—
0.051	50	1	69	40
0.051	100	2	72	30
0.051	150	3	64	28
0.051	200	4	49	27
0.040	0	0	0	—
0.040	10	1:5	58	32
0.040	50	1	64	37
0.040	100	2	69	29
0.040	150	3	63	20
0.040	200	4	46	20

[a] Volume of CCl_4, 50 ml; PPD:HQ molar ratio, 0.021:0.021.

[b] LVN (limiting viscosity number) obtained by extrapolation to infinite dilution of data on polymer solutions in dimethyl sulfoxide at $25°C$ in the concentration range of $1–10$ g/100 ml.

a 0.5 N NaOH system, shown in Table IV. Again, the LVN values are lower than those generally obtained with $Ba(OH)_2$. Inspection of Table II and those experiments in the second half of Table IV in which sufficient NaOH was used to maintain an alkaline medium indicates that yields are diminished by reactant dilution in either the organic or the aqueous phase.

Table V shows polymer yield and LVN for the $Ba(OH)_2$ system in which the molar ratio of the comers was varied. The uncommon result found is that as the comer ratio varies from unity, an increase occurs in both LVN and yield (based on the comer which is used in limiting amount). In the system with $5N$ NaOH, shown in Table VI, the opposite effect is observed for both properties. Again, the molecular weights obtained with $Ba(OH)_2$ are superior.

TABLE IV

Total Yield and Unfractionated Polymer Solution Viscometry Data
in the Sodium Hydroxide-Promoted Polycondensation of Hydroquinone
(HQ) and Phenylphosphonic Dichloride (PPD) as a Function of
Aqueous Phase Volume and the Amount of Base[a]

Volume ratio of $H_2O:CCl_4$	Volume 0.5 N aqueous NaOH, ml	Molar equivalents of base	pH of the final solution (calculated)	Total yield, %	LVN, ml/g[b]
0:1	(2 g solid NaOH)	0.0500	—	0	—
1:1	25	0.0125	1.0	2	1
2:1	50	0.0250	1.0	18	2
3:1	75	0.0375	1.2	47	3
4:1	100	0.0500	12.9	51	12
6:1	150	0.0750	14.0	58	24
8:1	200	0.1000	14.0	27	9

[a] Volume of CCl_4, 25 ml; PPD:HQ molar ratio, 0.021:0.021.

[b] LVN (limiting viscosity number) obtained by extrapolation to infinite dilution of data on polymer solutions in dimethyl sulfoxide at 25°C in the concentration range of 1–10 g/100 ml.

TABLE V

Total Yield and Unfractionated Polymer Solution Viscometry
Data of the Barium Hydroxide-Promoted Polycondensation of Hydroquinone
(HQ) and Phenylphosphonic Dichloride (PPD) as a Function of
the PPD:HQ Molar Ratio[a]

PPD:HQ molar ratio	Total yield, %	LVN, ml/g[b]
0.048:0.021	95	47
0.026:0.021	89	41
0.021:0.021	64	38
0.021:0.026	79	38
0.021:0.048	86	44

[a] Volume of water, 50 ml; volume of CCl_4, 50 ml; amount of $Ba(OH)_2$, 0.040 mole;

[b] LVN (limiting viscosity number) obtained by extrapolation to infinite dilution of data on polymer solutions in dimethyl sulfoxide at 25°C in the concentration range 1–10 g/100 ml.

Table VII shows the results of experiments with the $Ba(OH)_2$ system in which the comer ratio and the solvent ratio were each fixed at unity, but the concentration of the reactants was varied. Polymer yield is found to be fairly constant, but the polymer molecular weight increases with reactant dilution—results which are in contrast with that observed with the NaOH system (see above).

Table VIII shows that variation of the barium ion concentration, over the range investigated, has negligible effect on polymer yield and LVN. Relatively high concentrations of barium ion are present (i.e., calculated range = 0.038–0.91 mole/l., assuming the solubility product does not

vary appreciably in the present range of ionic strength). Morgan[1b] suggests that the addition of neutral salts may have either beneficial or detrimental effects in interfacial polymerization.

TABLE VI
Total Yield and Unfractionated Polymer Solution Viscometry Data
in the Sodium Hydroxide-Promoted Polycondensation of Hydroquinone (HQ)
and Phenylphosphonic Dichloride (PPD) as a Function of PPD/HQ Molar Ratio[a]

PPD:MQ molar ratio	Total yield, %	LVN, ml/g[b]
0.042:0.021	65	3
0.028:0.021	68	10
0.021:0.021	85	15
0.021:0.028	25	3
0.021:0.042	20	2

[a] Volume of aqueous NaOH, (5N), 25 ml; volume of CCl₄, 25 ml.

[b] LVN (limiting viscosity number) obtained by extrapolation to infinite dilution of data on polymer solutions in dimethyl sulfoxide at 25°C. in the concentration range of 1–10 g/100 ml.

TABLE VII
Total Yield and Unfractionated Polymer Solution Viscometry Data
of the Barium Hydroxide-Promoted Polycondensation of Hydroquinone (HQ)
and Diphenylphosphonic Dichloride (PPD) as a Function of the Amount of Comer[a]

Amount of each comer present, mole	Total yield, %	LVN, ml/g[b]
0.0350	57	29
0.0280	56	33
0.0210	64	38
0.0140	57	41

[a] Volume of water, 50 ml; volume of CCl₄, 50 ml; amount of $Ba(OH)_2$, 0.040 mole; PPD:HQ molar ratio, 1.

[b] LVN (limiting viscosity number) obtained by extrapolation to infinite dilution of data on polymer solutions in dimethyl sulfoxide at 25°C in the concentration range of 1–10 g/100 ml.

TABLE VIII
Total Yield and Unfractionated Polymer Solution Viscometry Data
of the Barium Hydroxide-Promoted Polycondensation of Hydroquinone (HQ) and
Phenylphosphonic Dichloride (PPD) as a Function of the Amount of BaCl₂ Added[a]

BaCl₂ added, mole	Total yield, %	LVN, ml/g[b]
0.000	63	20
0.050	62	20
0.100	64	19

[a] Volume of water, 150 ml; volume of CCl₄, 50 ml; amount of $Ba(OH)_2$, 0.040 mole; PPD:HQ molar ratio, 0.021:0.021.

[b] LVN (limiting viscosity number) obtained by extrapolation to infinite dilution of data on polymer solutions in dimethyl sulfoxide at 25°C. in the concentration range of 1–10 g/100 ml.

In the interfacial polycondensation of PPD and 1,6-hexamethylenediamine, using the $Ba(OH)_2$ system, the present authors found[4] that the addition of $BaCl_2$ to the aqueous phase markedly improved the yield of the polyphosphonamide. If it is assumed that the effect of increased electrolyte concentration acts to drive the diamine from solution in the aqueous phase (salting out) into the reaction zone, which is situated in the organic phase near the interface, then the conclusion might be drawn from the results above that condensation of phenoxide anions takes place in a reaction zone situated in the aqueous phase near the interface.

SUMMARY

The method employed, in which the pH of the medium is maintained effectively constant in a desired range during the entire course of basic polymerization, has been shown to achieve polymers of high molecular weight.* It may be expected that the molecular weight distribution may also be narrower than that obtained with the sodium hydroxide media commonly reported in patent literature. The method of Millich and Carraher[3] also provides wider latitude in varying solvent ratios—for instance, avoiding the limitation obvious in Table IV.

The polycondensation of HQ with PPD was investigated for conditions which varied about the reference point of equimolar amounts of the reactants and equal volumes of the organic and aqueous phases, in the general reactant concentration range of 0.2 molar. Polymer yields and molecular weights have been found to vary, more widely in the NaOH than in the $Ba(OH)_2$ system. It is difficult at this time to integrate that data around the reference point into a simple, intelligible representation of a low number of coordinates, but it may be seen from the data presented that the $Ba(OH)_2$ system has advantages over, and characteristics distinct from the NaOH system. Two specific examples of this are seen in the effect of varying the comer ratio, and the success of the $Ba(OH)_2$ system when CCl_4 is not used. Other parameters affecting polymer yield and molecular weight will be reported in a subsequent paper.

References

1. P. W. Morgan, *Condensation Polymers: By Interfacial and Solution Methods,* Wiley, New York, 1965, (a) pp. 67–76; (b) pp. 91–95.

2. F. Millich and C. E. Carraher, Jr., *J. Polym. Sci. A-1,* in press.

3. F. Millich and C. E. Carraher, Jr., U. S. Patent pending, Appl. No. 697,033 (January 11, 1968).

4. C. E. Carraher, Jr., D. Winthers and F. Millich, *J. Polym. Sci. A-1,* in press.

* The correlation of molecular weights with solution properties, will be presented in a subsequent article in this series.

Benzimidazole Polymers from Aldehydes and Tetraamines

JERRY HIGGINS and C. S. MARVEL, *Department of Chemistry,
University of Arizona, Tucson, Arizona 85721*

Synopsis

A new method for the preparation of benzimidazole polymers is described. The solution polymerization of aromatic tetraamines with isophthalaldehyde bis bisulfite adduct in *N,N*-dimethylformamide (DMF), *N,N*-dimethylacetamide (DMAc), *N*-methyl-2-pyrrolidone (MP), and dimethyl sulfoxide (DMSO) produced polybenzimidazoles with viscosities (η_{inh}) in the range of 0.3–0.5 measured in formic acid solution. Also a model compound study with benzaldehyde, benzaldehyde diethyl acetal, and benzaldehyde bisulfite adduct with *o*-phenylenediamine was carried out. The results showed that the reaction of benzaldehyde bisulfite adduct with *o*-phenylenediamine in DMAc as the solvent gave quantitative yields of 2-phenylbenzimidazole. Excellent yields of 2-phenylbenzthiazole, 2-phenylbenzoxazole, and 2-pyridylbenzimidazole were also obtained with the benzaldehyde bisulfite adduct and picoline-2-carboxaldehyde bisulfite adduct with *o*-aminothiophenol, *o*-aminophenol, and *o*-phenylenediamine. The reaction conditions for the preparation of the polymers and the model compounds are very mild and the reaction times range from 15 min to 1 hr for the model compounds and 3–5 hr for the polymers. Longer reaction times did not increase the viscosities of the polymers to any extent.

MODEL COMPOUND STUDY

In 1961 Vogel and Marvel[1] were successful in preparing high molecular-weight polybenzimidazoles by the melt condensation of phenyl esters with aromatic tetraamines. More recently, Gray and co-workers[2] were successful in preparing poly-2,2'-(1,4-phenylene)-5,5'-bibenzimidazole from 3, 3',-4,4'-tetraaminodiphenyl and 1,4-diacetylbenzene using a reaction initially described by Elderfield and Meyer[3] for preparaing simple benzimidazoles. A model compound study of this reaction using acetophenone and *o*-phenylenediamine showed that methane was evolved in the final stage of the reaction.

Another method which appeared to be promising for the preparation of polybenzimidazoles is the condensation of aldehydes with amines. The reaction of benzaldehyde with *o*-phenylenediamine has been reported several times in the literature,[4,5] but side reactions, such as the formation of disubstituted benzimidazoles (aldehydines), have prevented this reaction from being useful as a means of producing polymers.

In order to determine if aromatic aldehydes and their derivatives would be useful in the formation of heterocyclic polymers, a systematic study of the condensation of benzaldehyde (I), benzaldehyde diethyl acetal (II), benzaldehyde bisulfite adduct (III), and picoline-2-carboxaldehyde bi-sulfite adduct (IV) was carried out in DMF and DMAc with *o*-phenylene-diamine (V), *o*-aminothiophenol (VI), and *o*-aminophenol (VII). The products obtained in this study were 2-phenylbenzimidazole (VIII), 2-phenylbenzthiazole (IX), 2-phenylbenzoxazole (IX), and 2-pyridyl-benzimidazole (XI). The results of this study are outlined in Table I.

TABLE I
Model Compounds

Reactants	Solvent	Time heated in nitrogen, hr	Time heated in air, hr	Product obtained	Yield, %
I, V	DMF	2	20	VIII	25–31
I, V	10% HOAc–DMF	2	18	VIII	26
II, V	DMF	2	18	VIII	26
II, V	DMF[a]	2	18	VIII	27
III, V	DMF	2	18	VIII	92–95
III, V	DMAc	20	0	VIII	98–99
III, V	DMAc	15 min	0	VIII	98–99
III, VI	DMAc	30 min	0	IX	93
III, VII	DMAc	30 min	8[b]	X	84
IV, V	DMAc	40 min	0	XI	91

[a] Trichloroacetic acid (0.1 g.) added as catalyst.

[b] Refluxed with an equivalent amount of sulfur.

The results in Table I show that the benzaldehyde bisulfite adduct condensed with *o*-phenylenediamine is the best method for preparing heterocyclics under these reaction conditions. The yield of 2-phenyl-benzimidazole is essentially quantitative. By washing the product only once with water, it melted over a 3°C temperature range (294–297°C). Similar product isolation techniques with benzaldehyde and benzaldehyde diethyl acetal gave a thick oil, and diethyl ether was used as the washing solvent. The aliphatic aldehydes when reacted as the bisulfite adducts would not eliminate hydrogen under these reaction conditions. Also sulfur was required to extract hydrogen in the case of 2-phenylbenzoxazole under these reaction conditions.

It is not exactly clear why the bisulfite adducts proceed to such good yields while the aldehydes and acetal give such poor yields. It is known,[4,5] however, that when aldehydes are reacted with diamines the major by-products (in many cases the major product) are the aldehydines. These disubstituted benzimidazoles were predicted to arise from the diimines

formed in the initial stages of the reaction. The diimines undergo rearrangement under the reaction conditions to produce the aldehydes. From this knowledge it may be that the bisulfite adducts are less reactive thus giving more time for ring closure and preventing the formation of the diimines. The reaction of benzaldehyde bisulfite adduct with *o*-phenylenediamine appears to begin around 60–70°C. This can be predicted by a sharp color change to bright yellow and the precipitation of sodium bisulfite.

POLYMERIZATIONS

Three polymerizations were chosen for these studies. They consisted of the condensation of isophthalaldehyde bis(bisulfite adduct) with 3,3',4,4'-tetraaminodiphenyl (XII),[1] 3,3',4,4'-tetraaminodiphenyl ether (XIII),[5] and 1,2,4,5-tetraaminobenzene (XIV).[1] The results of these studies are outlined in Table II. The yields were essentially quantitative.
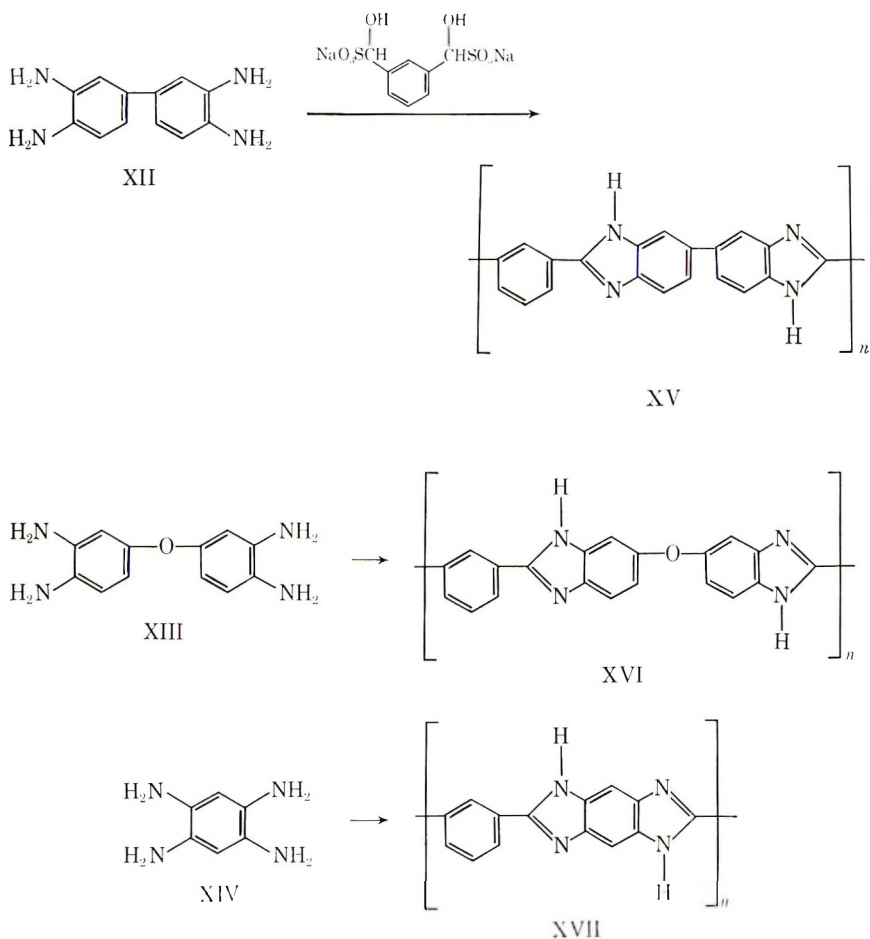
The polymerizations were carried out by refluxing the reactions in the selected solvents for a short time in a nitrogen atmosphere and then continuing the reactions open to the air for the remaining reaction time or by refluxing in a nitrogen atmosphere for the entire reaction time.

All polymers were soluble in formic acid, however, as the viscosity values approached 0.5 the polymers were only slightly soluble in DMF, DMAc, and DMSO.

The bis(bisulfite adduct) was easily prepared from isophthalaldehyde in a 15% water solution of methanol.

TABLE II
Polymerizations

Reaction number	Tetra-amine[a]	Solvent	Time heated in nitrogen, hr	Time heated in air, hr	Viscosity η_{inh}[b]	λ_{max}, mμ (H$_2$SO$_4$)
1	XII	DMF	2	18	0.34	337
						253
2	XII	MP[c]	3	18	0.29	338
						253
3	XII	MP[c]	5	16	0.33	337
						253
4	XII	DMAc	3	18	0.45	335
						252
5	XIII	DMAc	2	16	0.38	326
						245
6	XIII	DMSO	5	14	0.55	323
						245
7	XII	DMSO	5	14	0.51	335
					0.24[d]	252
8	XII	DMAc	20	0	0.42	338
						253
9	XIII	DMAc	20	0	0.38	327
						245
10	XIV	DMAc	40	0	0.45	346
						241
11	XII	DMAc	40	0	0.52	338
						252
12	XII	DMAc	3	0	0.31	337
						253
13	XII[e]	DMAc	5	0	0.47	336
						252
14	XII[f]	DMAc	5	0	0.38	337
						252

[a] Equal molar quantities of monomers were used except where indicated.

[b] Measured in formic acid except where indicated (0.025–0.500 g/100 ml).

[c] N-Methyl-2-pyrrolidone.

[d] Measured in DMSO.

[e] A 3% weight excess of isophthalaldehyde bis(bisulfite adduct) was used.

[f] A 3% weight excess of 3,3′,4,4′-tetraaminodiphenyl was used.

EXPERIMENTAL

Model Compounds

2-Phenylbenzimidazole from Benzaldehyde and o-Phenylenediamine

Nonacid-Catalyzed Reaction. Benzaldehyde (10.60 g, 0.10 mole) and *o*-phenylenediamine (10.80 g, 0.10 mole) were added to 100 ml of DMF and refluxed in a nitrogen atmosphere for 2 hr. The reaction vessel was then opened to the air and the solution refluxed for 20 hr. After the refluxing period all but about 15–20 ml of the DMF was distilled at 50–60 mm pressure. Diethyl ether (50 ml) was added and the mixture stirred for 30 min. The 2-phenylbenzimidazole was filtered and dried at 100°C *in vacuo* overnight to give 6 g (31%) of cream-colored product melting at 280–292°C. Concentration of the ether solution yielded 1–3 g of additional product.

Acid-Catalyzed Reaction. The same procedure as above was carried out in a 10% acetic acid–DMF solution. A 5–6 g yield of 2-phenylbenzimidazole was obtained (26–31%). The crude product melted at 279–290°C. Recrystallization (C_2H_5OH–H_2O) gave a pure product which melted at 295–297°C; lit.[1] mp, 300°C.

2-Phenylbenzimidazole from Benzaldehyde Diethyl Acetal and
o-Phenyl-enediamine

Non-Acid-Catalyzed Reaction. Benzaldehyde diethyl acetal (18.00 g, 0.10 mole) and *o*-phenylenediamine (10.80 g, 0-10 mole) were added to 100 ml DMF and refluxed in a nitrogen atmosphere for 2 hr. The reaction vessel was then opened to the air and refluxed for an additional 18 hr. All but about 15–20 ml of the DMF was removed by distillation at 50–60 mm pressure. Ethyl ether (50 ml) was added and the mixture stirred for 30 min. After filtering and drying, 5 g (26%) of 2-phenylbenzimidazole was obtained. The product melted at 296–298°C.

Acid-Catalyzed Reaction. The same reaction as above was carried out in DMF containing 0.10 g of trichloroacetic acid. About 6 g (31%) of 2-phenylbenzimidazole was obtained. The product melted at 294–297°C.

2-Phenylbenzimidazole from Benzaldehyde Bisulfite Adduct and
o-Phenylenediamine

Benzaldehyde bisulfite adduct (22.42 g, 0.107 mole) and *o*-phenylenediamine (11.56 g, 0.107 mole) were added to 100 ml of DMF and the reaction mixture was heated at reflux for 15–20 min in a nitrogen atmosphere. The DMF was removed by distilling at reduced pressure, and 50 ml of water was added and the mixture stirred for 30 min. The 2-phenylbenzimidazole was filtered, washed twice with 20-ml portions of water, and dried to give an almost white product (19 g, 98%) melting at 294–297°C.

2-Phenylbenzthiazole from Benzaldehyde Bisulfite Adduct and o-Aminothiophenol

Benzaldehyde bisulfite adduct (4.48 g, 0.021 mole) and o-aminothiophenol (2.62 g, 0.021 mole) were added to 50 ml DMAc and the reaction mixture refluxed for 30–45 min in a nitrogen atmosphere. The DMAc was removed by distilling at reduced pressure, and 30 ml of water was added. The reaction mixture was stirred for 30 min, filtered, and washed with two 20-ml portions of water, and dried to give about 4 g (91–94%) of 2-phenyl-benzthiazole melting at 111–113°C; lit.[7] mp, 111°C.

2-Phenylbenzoxazole from Benzaldehyde Bisulfite Adduct and o-Aminophenol

Benzaldehyde bisulfite adduct (4.48 g, 0.021 mole) and o-aminophenol (2.29 g, 0.021 mole) were added to 50 ml DMAc and refluxed for 30 min in a nitrogen atmosphere. The reaction flask was then opened to the air 0.9 g of sulfur was added. The reaction was refluxed for 8 hr and the DMAc was then removed by distilling at reduced pressure. About 30 ml of water was added and the reaction mixture stirred until the product crystallized. The crude 2-phenylbenzoxazole was dissolved in 100 ml of ether; the ether solution was filtered and the ether removed at water aspirator pressure to yield about 3 g (80–84%) crude product. The crude product was sublimed to give a white crystalline product melting at 104–105°C; lit.[8] mp, 103°C.

2-Pyridylbenzimidazole from Picoline-2-carboxaldehyde and o-Phenylenediamine

Picoline-2-carboxaldehyde bisulfite adduct (4.62 g, 0.021 mole) and o-phenylenediamine (2.27 g, 0.021 mole) were added to 50 ml DMAc and the reaction mixture refluxed for 40–50 min in a nitrogen atmosphere. The DMAc was removed by distilling at reduced pressure, and 30 ml of water was added to the reaction mixture and stirred for 30 min. The product was filtered and dried to yield about 3.8 g (90–92%) of 2-pyridylbenzimidazole. Recrystallization (C_2H_5OH–H_2O) gave a product melting at 220–222°C; lit.[9] mp, 226°C.

Isophthalaldehyde Bis(bisulfite Adduct)

Isophthalaldehyde (5.0 g, 0.037 mole) and sodium bisulfite (8.80 g, 0.085 mole) were added to a stirred solution of 500 ml of methanol containing 75 ml of water. The reaction mixture was stirred overnight at room temperature. The product was filtered and the filter cake pressed free of most of the solvent. After washing with 50–60 ml of warm methanol the white product was filtered and dried in vacuo for 8 hr at 100°C. After drying, there was obtained 10.5 g of white product, mp >300°C. Analysis by the silver sulfite method gave approximately 3% excess of sodium bisulfite in the product.

Polymerizations

The following procedure is typical of all the polymerization reactions. The ultraviolet and infrared spectra of the polymers were identical to those reported previously.[1]

Preparation of Poly-2,2'-(1,3-phenylene)-5,5'-bibenzimidazole

3,3',4,4'-Tetraaminodiphenyl (0.6310 g, 0.00294 mole) and isophthalaldehyde bis(bisulfite adduct) (1.0388 g, 0.00304 mole 3% excess) were added to 100 ml DMAc and refluxed for 5 hr in a nitrogen atmosphere After a short time some polymer began to precipitate. After the reaction time about two-thirds of the DMAc was removed by distilling at 40–50 mm pressure and the remaining solution poured into 100 ml of distilled water. The cream-colored polymer precipitated and was removed by suction filtration. The polymer cake was washed thoroughly twice with 25-ml portions of water and dried *in vacuo* at 160°C for 10 hr. A quantitative yield of poly-2,2'-(1,3-phenylene)-5,5'-bibenzimidazole was obtained. The inherent viscosity, measured in formic acid, was 0.47.

Also equimolar quantities of isophthalaldehyde *bis*(bisulfite adduct) with 3,3',4,4'-tetraaminodiphenyl ether (XIII) and 1,2,4,5-tetraaminobenzene (XIV) gave quantitative yields of polymers with viscosities similar to those reported for 3,3',4,4'-tetraaminodiphenyl (XII) (see Table II).

References

1. H. Vogel and C. S. Marvel, *J. Polym. Sci.*, **50**, 511 (1961).
2. D. N. Gray, L. L. Rauch, and E. L. Strauss, paper presented to the Division of Polymer Chemistry, American Chemical Society Meeting, Chicago, September 1967; *Polymer Preprints*, **8** (2), 1138 (1967).
3. R. C. Elderfield and U. B. Meyer, *J. Amer. Chem. Soc.*, **76**, 1883 (1954).
4. A. Ladenburg, *Ber.*, **11**, 1648 (1978).
5. J. B. Wright, *Chem. Revs.*, **48**, 397 (1951).
6. R. T. Foster and C. S. Marvel, *J. Polym. Sci. A*, **3**, 417 (1965).
7. A. W. Hofman, *Ber.*, **13**, 1236 (1880).
8. H. L. Wheeler, *Am. Chem. J.*, **17**, 400 (1895).
9. Farbenfabriken Bayer A.-G., German Pat. 949,059 (Sept. 13, 1956).

Kinetics of High-Intensity Electron-Beam Copolymerization of a Divinyl Urethane and 2-Hydroxyethyl Methacrylate

S. S. LABANA, *Scientific Research Staff, Ford Motor Company, Dearborn, Michigan 48121*

Synopsis

The kinetics of the electron-beam-induced copolymerization of di(2'-methacryloxy-ethyl)-4-methyl-*m*-phenylenediurethane (DVU) with 2-hydroxyethyl methacrylate (HEMA) were studied. Monomer mixtures containing 1.96–82.8% DVU have been described at dose rates of 1.7–17 Mrad/sec with the use of 270-kV electrons. Based on rates of conversion, gel formation, and intensity-rate data, a kinetic scheme is proposed in accord with a model which undergoes unimolecular termination and for which the copolymerization and gel formation take place in a crosslinked network swollen with monomers. The rate of gel formation is: $\ln[(1 + g)/(1 - M_2 g)] = A(1 + M_2)t$, where g is the gel fraction, M_2 is the mole fraction of DVU in the monomer charge, and A is $k_p k_i / k_t$. Up to 55% conversion, the rate of disappearance of unsaturation for concentrated DVU solutions ($M_2 > 0.03$) is: $\ln[M_0/M(1 - M_2 g)] = A(1 + M_2)t$, where M is the total unsaturation. For dilute solutions of DVU, the rate expression for pregel copolymerization simplifies to: $\ln(M_0/M) = A(1 + M_2)t$. These results show that at a certain optimum concentration of monovinyl monomer—70% in the present system—both rapid reaction rates and complete copolymerization occur. Because of the inability of gel bonds to undergo polymerization, a limiting conversion is reached for copolymerizing mixtures containing insufficient monovinyl monomer.

INTRODUCTION

Copolymerization kinetics of monovinyl monomers with divinyl or polyvinyl monomers to form insoluble networks using electron-beam radiation have received little attention so far: Burlant and Hinsch describe the kinetics of high-intensity, low-energy electron-beam-induced copolymerization of styrene with unsaturated polyesters, and explain their results on the basis of activated radicals formed in discrete volume elements,[1] although more conventional homogeneous free-radical kinetics apply when low-intensity γ-rays are used.[2]

This paper describes the kinetics of network copolymerization of di(2'-methacryloxyethyl)-4-methyl-*m*-phenylenediurethane (I) (DVU) with 2-hydroxyethyl methacrylate (HEMA), by use of 270-kV electrons.

179

$$\begin{array}{c}
\text{CH}_3 \\
| \\
\text{NHCOOCH}_2\text{CH}_2\text{OOC}-\text{C}=\text{CH}_2 \\
\end{array}$$

$$\text{NHCOOCH}_2\text{CH}_2\text{OOC}-\text{C}=\text{CH}_2$$

$$\begin{array}{c}
\text{CH}_3 \qquad\qquad\qquad | \\
\text{CH}_3
\end{array}$$
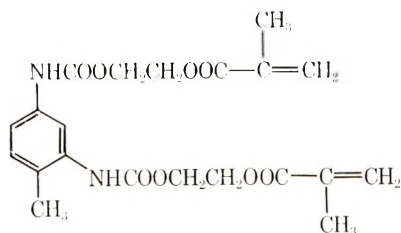
I

EXPERIMENTAL

Materials

2-Hydroxyethyl Methacrylate. An aqueous solution of 2-hydroxyethyl methacrylate (HEMA 96% from Rohm and Haas) was repeatedly extracted with pentane to remove dimethacrylate esters. The monomer was then dissolved in dichloromethane and washed with 5% aqueous sodium carbonate to remove methacrylic acid. The dichloromethane solution was washed with 10% sodium chloride solution and dried over anhydrous magnesium sulfate. After removing the solvent, the monomer was distilled *in vacuo* through a 10 × 1 in. column packed with glass helices, bp 58°C/3 mm, n_D^{25} 1.4505.

Di(2'-methacryloxyethyl)-4-methyl-*m*-phenylenediurethane (I). The diurethane I was prepared by slowly adding 4-methyl-*m*-phenylene diisocyanate (from Matheson, Coleman and Bell, mp 20–22°C), (0.23 mole) to a 60% solution of 2-hydroxyethyl methacrylate (0.5 mole) in 2-butanone containing 0.1% triethylenediamine. The temperature was maintained at 40°C by controlling the rate of addition of the diisocyanate. When the infrared analysis showed complete reaction (no absorption at 2270 cm^{-1}), the solution was chilled to obtain the white crystalline product. Recrystallization from 2-butanone gave pure divinylurethane, mp 95°C.[3]

Polymerization

Monomer mixtures containing less than 0.3 mole fraction (59 wt-%) of divinylurethane were deoxygenated by blowing nitrogen through them for 20 min. Monomer mixtures containing more than 0.3 mole fraction of divinylurethane were too viscous for gas bubbling and were degassed under high vacuum by the freeze thaw technique and stored under nitrogen. In a nitrogen atmosphere a thin film of deoxygenated monomer mixture was cast on a sodium chloride plate, covered with an 0.025 mm thick Teflon film and clamped in an infrared cell mount.

The polymerization was carried out at 30°C by exposing the sample, in a nitrogen atmosphere, to a 270 kV electron beam at intensities ranging from 1.7 to 17 Mrad/sec. The dose absorbed was measured by using the blue cellophane method.[4] The rate of polymerization was followed by noting the rate of disappearance of the "olefinic" 1639, 944, and 813 cm^{-1}

peaks by use of a Perkin-Elmer model 237B infrared spectrophotometer. A Teflon film was used in the reference beam. The three peaks gave the same data for the disappearance of unsaturation up to 50% conversion. The disappearance of the 943 cm^{-1} peak above 50% conversion was complicated by the appearance of a peak of 962 cm^{-1}. The data from the 943 cm^{-1} peak above 50% conversion, therefore, were not used. During the polymerization, a new absorption peak appeared at 746 cm^{-1} and is assigned to the formation of a polymer of DP greater than 4.[5] The appearance of the 746 cm^{-1} peak followed the disappearance of unsaturation up to 90% conversion and then remained constant. Conversions were calculated from the peak heights by using the baseline technique[6] and were reproducible to $\pm 3\%$.

Gel Fractions

For gel fraction determination, a known amount (about 0.5 g) of the copolymer prepared under a nitrogen atmosphere as a film on aluminum foil was placed in a double thimble made of monel wire cloth, 100 mesh inside and 200 mesh outside. The soluble fraction was first extracted for 72 hr with acetone containing 1% ethyl mercaptan as inhibitor, and then with acetone containing 15% water. The extraction with aqueous acetone was carried out to ensure the removal of any poly(2-hydroxyethyl methacrylate) which is not soluble in dry acetone. The thimble with its contents was dried to constant weight under vacuum at 65°C. The fraction of the copolymer retained in the thimble was taken as the gel fraction. Gel fractions were reproducible to $\pm 7\%$.

Reactivity Ratios

Monomer mixtures of known compositions were polymerized to about 5% conversions in 0.05 mm films on steel panels. The copolymer was
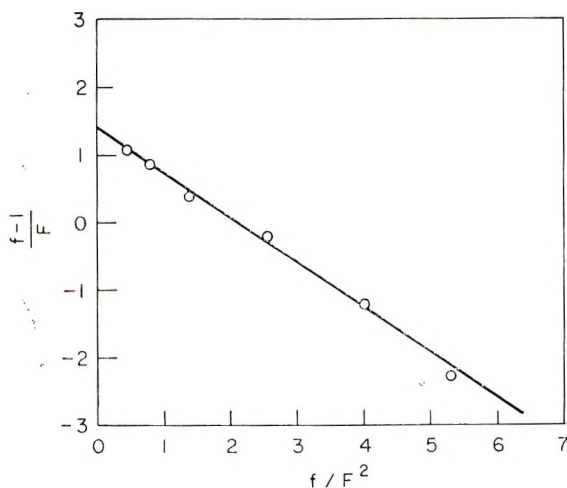
Fig. 1. Fineman-Ross plot for DVU–HEMA copolymerization.

isolated by successive washes with acetone and aqueous acetone to remove monomer and homopolymer, respectively. The amount of divinyl ure-thane in the copolymer was calculated from nitrogen analyses. The divinyl fractions in the copolymer were reproducible to within 3 percent. The Fineman-Ross plot[7] (Fig. 1), obtained by using twice the molar con-centration of DVU in the monomers as suggested by Wiley and Sale,[8] gave reactivity ratios of $r_1 = 1.4 \pm 0.1$ and $r_2 = 0.8 \pm 0.1$ (r_2 refers to DVU).

RESULTS AND DISCUSSION

Six compositions of divinyl urethane and 2-hydroxyethyl methacrylate containing 1.96–82.8 wt-% of divinylurethane were copolymerized by a 270 kV electron beam at a dose rate of 3.3 Mrad/sec. The results are given in Table I and plotted in Figure 2. The mole fraction of DVU in the monomer charge is represented by M_2.

The conversion curves obtained from monomer charge containing low ($M_2 < 0.07$) DVU are quite different from those obtained from monomer charge containing high ($M_2 > 0.07$) DVU. At very low DVU concentra-tions ($M_2 < 0.05$), the polymerization is almost proportional to the dose absorbed up to 20% conversion. Polymerization rates then decrease between 20 and 25% conversion before undergoing a rapid increase. Be-
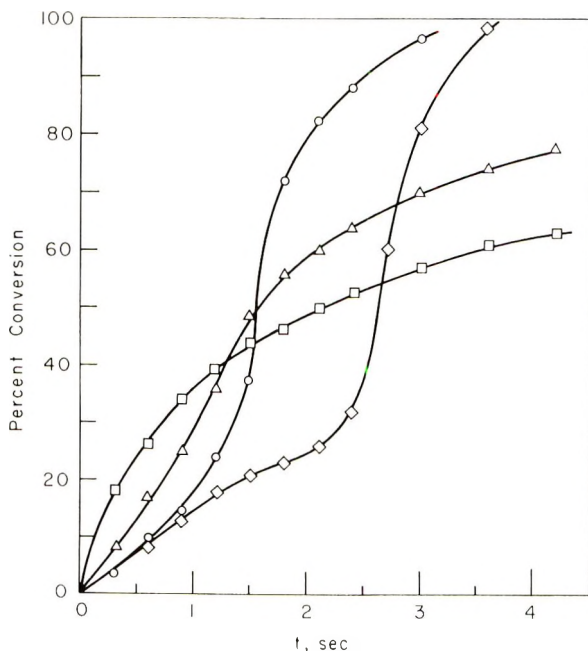
Fig. 2. Percent conversion as a function of time for DVU and HEMA mixtures at various DVU mole fractions: ($\diamond$) $M_2 = 0.005$; (O) $M_2 = 0.07$; ($\triangle$) $M_2 = 0.30$; ($\square$) $M_2 = 0.59$. Dose rate 3.3 Mrad/sec.
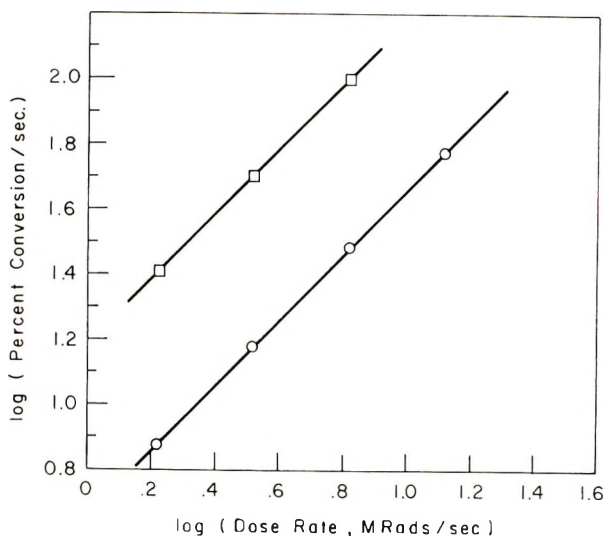
Fig. 3. A log–log plot of rate of polymerization vs. radiation intensity at various DVU mole fractions: (O) $M_2 = 0.005$; (□) $M_2 = 0.59$.   Dose rates 1.7–17 Mrad/sec.

Fig. 4. ESR spectrum of irradiate monomer mixture containing 59% DVU.

tween 25 and 80% conversions, the rates are maximum. At DVU concentrations of over 0.15 mole fraction, the conversion curves show no inflection points. For monomer mixtures containing more than 0.09 mole fraction of DVU, disappearance of unsaturation is not complete because, in the absence of mobile monomer, the double bonds attached to the gel cannot undergo polymerization. The initial rates are enhanced as DVU concentration is increased above 0.09 molar. Thus, these results show that there exists an optimum concentration of monovinyl compound—70%—at which both rapid rates and complete copolymerization occurs.

Continued irradiation of monomer mixture containing 20% DVU (M_2 = 0.07) up to a dose of 25 Mrad in nitrogen atmosphere shows neither

a change in the crosslink density of the gel as measured by swelling in acetone nor produces unsaturation in the polymer. Therefore, homolytic chain cleavage by radiation during the polymerization is negligible.

Figure 3 shows a log-log plot of rates vs intensities for monomer mix-

TABLE I
Conversion of Unsaturation of DVU and HEMA Mixtures
at Dose Rate of 3.3 Mrad/sec

DVU in monomers		Time, sec.	Conversion, %
Mole fraction M_2	Wt-%		
0.0059	1.96	0.3	4
		0.6	7
		0.9	14
		1.2	18
		1.5	20
		1.8	23
		2.1	26
		2.4	29
		2.7	31
		3.0	41
		3.3	70
		3.6	80
		3.9	90
		4.2	100
0.010	3.26	0.3	3
		0.6	8
		0.9	13
		1.2	18
		1.5	21
		1.8	23
		2.1	26
		2.4	32
		2.7	60
		3.0	81
		3.6	98
0.047	14.2	0.3	5
		0.6	8
		0.9	15
		1.2	20
		1.5	28
		2.1	66
		2.4	90
		3.0	100
0.070	20.0	0.3	4
		0.9	18
		1.2	25
		1.5	37
		1.8	72
		2.1	82
		2.4	88
		3.0	97

TABLE I (continued)

DVU in monomers			
Mole fraction M_2	Wt-%	Time, sec.	Conversion, %
0.30	59.0	0.3	8
		0.6	14
		0.9	25
		1.2	36
		1.5	48
		1.8	56
		2.1	60
		2.4	64
		3.0	70
		3.6	74
		4.2	77
0.59	82.8	0.3	18
		0.6	26
		0.9	34
		1.2	39
		1.5	44
		1.8	47
		2.1	50
		2.4	53
		3.0	57
		3.6	61
		4.2	65

tures containing 0.006 and 0.6 mole fractions of DVU at dose rates ranging from 1.7 to 17 Mrad/sec. Slopes of the straight lines for two DVU concentrations give intensity exponent of 0.97 ± 0.06, establishing that the rates of copolymerization are directly proportional to the intensity of the electron beam.

The dependence of the rate of polymerization on intensity may arise in two ways: from polymerization in independent tracks, which overlap at high intensities[1,9] or from first-order termination of polymer radicals. In the present study, no decrease is observed in the intensity dependence of the rate of polymerization up to a dose rate of 17 Mrad/sec; this observation is taken as an indication that unimolecular termination of polymer radicals occurs; under these conditions, the spatial distribution of radicals does not affect the kinetics.

Unimolecular termination may result either by chain transfer to a stable, nonpropagating radical or by inactivation of polymer radicals by their burial in the gel phase. The ESR spectrum (Fig. 4) of the irradiated mixture containing 59 wt-% DVU shows the presence of only the methacrylate radical (II),[10]

$$-CH_2-\underset{\underset{COO-}{|}}{\overset{\overset{CH_3}{|}}{C}}\cdot$$

II
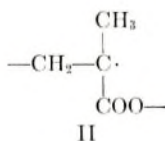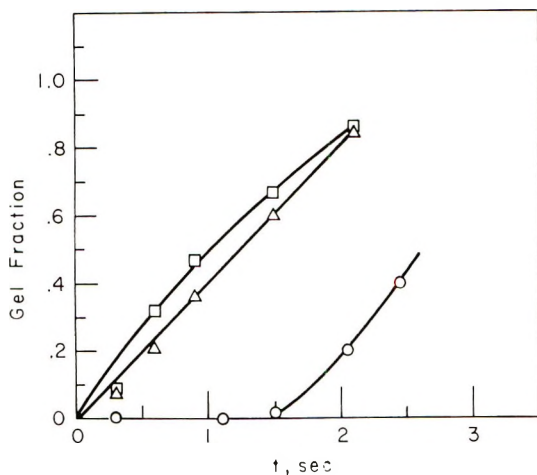
Fig. 5. Gel fractions as a function of time for copolymerization of DVU and HEMA at various DVU mole fractions: (O) $M_2 = 0.07$; (△) $M_2 = 0.30$, (□) $M_2 = 0.59$. Dose rate 3.3 $Mrad/sec$.

hence the chain transfer to stable radicals is excluded. It is suggested that in concentrated solution of DVU—M_2 greater than 0.3—the unimolecular termination of growing chains arises, at least in part but perhaps not exclusively, from the "buried" polymer radicals which exist in the gel phase.

TABLE II
Gel Fractions From Copolymerization of DVU and HEMA
By Electron Beam at 3.3 Mrad/sec

DVU in monomers			
Mole fraction M_2	Wt-%	Time, sec	Gel fraction, g
0.07	20	0.3	0
		1.2	0
		1.5	0.02
		2.1	0.20
		2.4	0.40
0.30	59	0.3	0.10
		0.6	0.21
		0.9	0.37
		1.5	0.60
		2.1	0.85
0.59	83	0.3	0.10
		0.6	0.32
		0.9	0.47
		1.5	0.67
		2.1	0.87

When DVU and HEMA copolymerize, the start of the gel formation depends on the amount of DVU in the monomer charge. For monomer mixtures containing 59 or 83% divinlyurethane (M_2 = 0.30 or 0.59), the gel formation begins at less than 5% conversion. For monomer mixtures containing 20% divinylurethane (M_2 = 0.07), the gel formation starts at 40% conversion. Gel fractions are given in Table II and plotted in Figure 5.

Because of the insolubility of the copolymer in common solvents, the molecular weights of the copolymer could not be determined, nor could the gel be hydrolyzed either by sulfuric acid or potassium hydroxide. The kinetic chain length can, however, be estimated by using Flory's equation[11] relating gel point α_g to the fraction of double bonds, ρ, in the divinyl monomer and the degree of polymerization DP of the copolymer:

$$(DP - 1) = 1/\alpha_g \rho \tag{1}$$

For the data for monomer charge containing 4.7 mole-% DVU (ρ = 0.092, α_g = 0.48), the kinetic chain length is calculated to be 22. It is to be noted that the deviations observed from the gel point theory always lead to a low estimate of the kinetic chain length.[12-14]

KINETIC SCHEME

Solutions Containing Above 0.3 Mole Fraction DVU

Based on the rates of disappearance of unsaturation, gel fractions, and intensity dependence of rates, a kinetic scheme similar to that proposed for the homopolymerization of DVU[3] is presented, which incorporates the following assumptions: at and beyond the gel point, the system comprises gel highly swollen with the mixture of the monomers; the gel contains pendant double bonds to which growing sol radicals are added; the radicals attached to the gel add to the double bonds in the sol phase and the gel fraction increases; because of the immobility of gel radicals and gel double bonds, reaction between gel radicals and gel double bonds is precluded; the same initiation, propagation, and termination rate constants apply to both monomer units in the sol and gel phases; and termination is unimolecular. This scheme is given in eqs. (2)–(8).

Initiation:

$$(1 - g) \rightarrow \dot{S}$$

$$\text{Rate} = k_i(1 - g) \tag{2}$$

$$\cdot g \rightarrow \dot{G}$$

$$\text{Rate} = k_i g \tag{3}$$

Propagation

$$\dot{S} + S \rightarrow S$$

$$\text{Rate} = 2k_p[\dot{S}][S] \tag{4}$$

$$\dot{S} + G \rightarrow \dot{G}$$

$$\text{Rate} = k_p[\dot{S}][G] \tag{5}$$

$$\dot{G} + S \rightarrow \dot{G}$$

$$\text{Rate} = k_p[\dot{G}][S] \tag{6}$$

Termination:

$$\dot{S} \rightarrow S$$

$$\text{Rate} = k_t[\dot{S}] \tag{7}$$

$$\dot{G} \rightarrow G$$

$$\text{Rate} = k_t[\dot{G}] \tag{8}$$
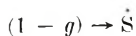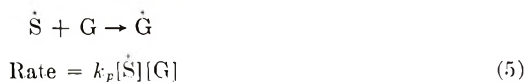
In these equations, g is the gel fraction; $(1 - g)$ is the sol fraction; $\dot{S}$ is a sol radical; $\dot{G}$ is a gel radical; S and G are double bonds in the sol and gel phases, respectively; k_i and k_p, and k_t are initiation, propagation, and termination rate constants, respectively.

Assuming steady-state conditions for reactive free radicals in the sol and gel phases, the concentrations of $\dot{S}$ and $\dot{G}$ are given by eqs. (9) and (10), respectively.

$$[\dot{S}] = \frac{k_i(1 - g)}{k_p[G] + k_t} \tag{9}$$

$$[\dot{G}] = \frac{k_i[k_p[G]/k_t + g]}{k_p[G] + k_t} \tag{10}$$

The kinetic chain length n is given by eq. (11).

$$n = R_p/R_t = \frac{k_p([S] + [G])[\dot{S}]}{k_t([\dot{S}] + [\dot{G}])} + \frac{k_p[S]([\dot{S}] + [\dot{G}])}{k_t([\dot{S}] + [\dot{G}])} \tag{11}$$

If $[\dot{S}]$ is small compared to $([\dot{S}] + [\dot{G}])$, eq. (11) is approximated by

$$n = k_p[S]/k_t \tag{12}$$

Considering that one double bond is incorporated in the gel phase for each DVU copolymerized, the unsaturation in gel and sol phase for copolymerizing mixture containing M_2 mole fraction of DVU is given by:

$$[G] = M_2gM \tag{13}$$

$$[S] = (1 - M_2g)M \tag{14}$$

which lead to

$$[S] = (1/M_2)[G](1 - M_2g)/g \tag{15}$$

For an average kinetic chain length of the copolymerizing system, taken at a point where $[S] \cong (1/M_2)[G]$, both M_2 and g being about 0.5, we get:

$$k_p[G]/k_t = nM_2 \tag{16}$$

Subsequently we shall be concerned only whether nM_2 is much larger than 1, therefore a small error in the approximate value of $k_p[G]/k_t$ has no effect on the final kinetic equations. Substituting for $k_p[G]/k_t$ from eq. (16) into eqs. (8) and (10), we obtain

$$[\dot{S}] = k_i(1 - g)/(1 + nM_2)k_t \tag{17}$$

$$[\dot{G}] = k_i(nM_2 + g)/(1 + nM_2)k_t \tag{18}$$

For a kinetic chain length of about 22, nM_2 is large so that we can approximate

$$1 + nM_2 = nM_2$$

$$g + nM_2 = nM_2 \tag{19}$$

Equations (17) and (18) then simplify to

$$[\dot{S}] = k_i(1 - g)/nM_2k_t \tag{18}$$

$$[\dot{G}] = k_i/k_t \tag{19}$$

Unsaturation in the sol and gel phases can be described by

$$[G] = M_2gM \tag{20}$$

$$[S] = (1 - M_2g)M \tag{21}$$

where M is the total unsaturation.

Differentiating eq. (20), we get

$$\frac{dg}{dt} = \frac{1}{M_2M} \frac{d[G]}{dt} - \frac{[G]}{M_2M^2} \frac{dM}{dt} \tag{22}$$

From the kinetic scheme, we can write

$$\frac{d[G]}{dt} = k_p[\dot{S}][G]M_2 + k_p[\dot{G}][S]M_2 \tag{23}$$

which on substitution for $[\dot{S}]$, $[\dot{G}]$, $[S]$, and $[G]$, and simplification yields,

$$d[G]/dt = AM_2(1 - M_2g)M \tag{24}$$

where $A = k_pk_i/k_t$.

From the kinetic scheme, the rate of the disappearance of unsaturation is

$$-dM/dt = 2k_p[\dot{S}][S] + k_p[\dot{S}][G] + k_p[\dot{G}][S] \tag{25}$$

Equation (25) on substitution for $[\dot{S}]$, $[\dot{G}]$, $[S]$, and $[G]$, and simplification, leads to

$$-dM/dt = A(1 - M_2g)M \tag{26}$$

On combining eqs. (22), (24), and (26), we obtain

$$dg/dt = A(1 - M_2g)(1 + g) \tag{27}$$

which, for the limits $t = 0$, $g = 0$, integrates to

$$\ln \frac{(1 + g)}{(1 - M_2g)} = (1 + M_2)At \tag{28}$$
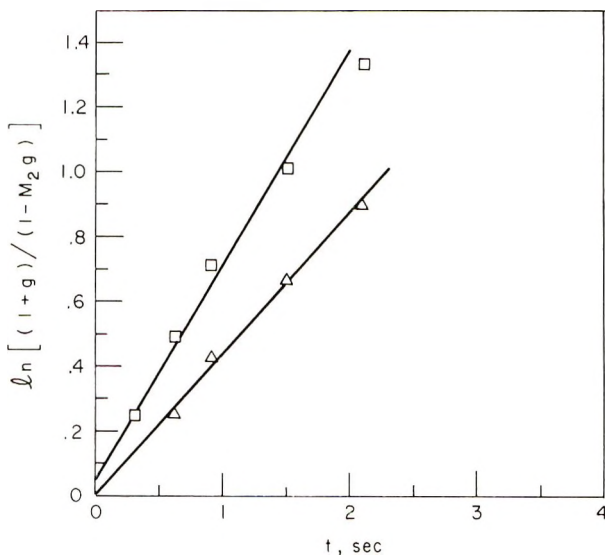
Fig. 6. A plot of $\ln[(1 + g)/(1 - M_2g)]$ vs. time according to eq. (28) at various DVU mole fractions: ($\triangle$) $M_2 = 0.30$, ($\square$) $M_2 = 0.59$.
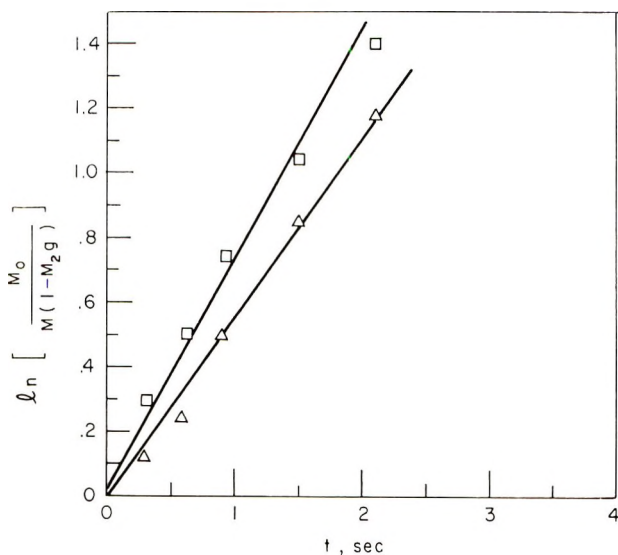
Fig. 7. A plot of $\ln[M_0/M(1 - M_2g)]$ vs. time according to eq. (31) at various DVU mole fractions: ($\triangle$) $M_2 = 0.30$; ($\square$) $M_2 = 0.59$.

As predicted by eq. (28), a plot of $\ln[(1 + g)/(1 - M_2 g)]$ versus times gives a straight line (Fig. 6) indicating the reasonableness of the scheme to describe gel formation up to a gel fraction of 0.7.

Disappearance of unsaturation can be described as follows. Equation (28) can be rearranged:

$$(1 - M_2 g) = (1 + M_2)/(1 + M_2 e^{Bt}) \tag{29}$$

where

$$B = (1 + M_2) k_p k_i / k_t \tag{30}$$

On integration, for the limits $M = M_0$ at $t = 0$,

$$\ln[M_0/M(1 - M_2 g)] = A(1 + M_2)t \tag{31}$$

A linear plot of $\ln[M_0/M(1 - M_2 g)]$ versus time, predicted by eq. (31), is shown in Figure 7, indicating that the proposed kinetic scheme satisfactorily describes the disappearance of unsaturation up to 50% conversion.

Dilute Solutions of DVU

For very dilute DVU solutions, the initial copolymerization takes place without gel formation. The kinetic scheme in this region simplifies; consequently eqs. (9) and (10) become

$$[\dot{S}] = k_i/k_t \tag{32}$$

$$[\dot{G}] = 0 \tag{33}$$

The rate of copolymerization is then given by

$$-dM/dt = 2k_i k_p M/k_t \tag{34}$$
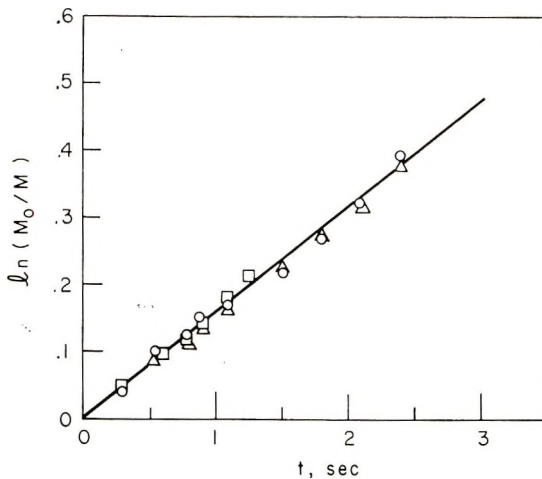
Fig. 8. A plot of $\ln[M_0/M)]$ vs. time according to eq. (35) at various DVU mole fractions, (O) $M_2 = 0.01$; (△) $M_2 = 0.05$, (□) $M_2 = 0.07$.

which on integrating for the limit at $t = 0$, $M = M_0$ leads to

$$\ln(M_0/M) = 2At \qquad (35)$$

For solutions containing less than 20 wt-% DVU ($M_2 \lesssim 0.07$), a plot of $\ln(M_0/M)$ versus time gives a straight line up to 30% conversion (Fig. 8) as predicted by Eq. (35). The above model, therefore, simplifies correctly to non-gel-forming kinetics at very low DVU concentrations.

Kinetic Parameters

The values of A, i.e., $k_p k_i/k_t$ calculated for different monomer concentrations by various equations are given in Table III.

TABLE III
Values of $k_p k_i/k_t$ For Copolymerization of DVU With HEMA

DVU in monomer charge		$k_p k_i/k_t$, sec^{-1}	Equation from which calculated
Mole fraction M_2	Wt-%		
0.59	83	0.42	(28)
		0.42	(31)
0.30	59	0.35	(28)
		0.37	(31)
0.07	20	0.08	(35)
0.05	14	0.08	(35)
0.01	3.3	0.08	(35)
0.006	2	0.08	(35)

These values of $k_p k_i/k_t$ compare favorably with the value of 0.14 sec^{-1} for pure divinylurethane.

The kinetic chain length for very dilute DVU solutions is given by

$$n = 2k_p[\mathrm{S}]/k_t \qquad (36)$$

On substituting the value of 22 for n and 4.8 mole/l. for [S] in eq. (36), the value of k_p/k_t obtained is 2.3. The value of k_i then is calculated to be 3.5×10^{-2} mole/l.-sec. The free-radical yield G_R (the number of initiating radicals formed per 100 eV of energy absorbed), calculated from this value of k_i, is 8, a number reasonable for methacrylate monomers.

References

1. W. Burlant and J. Hinsch, *J. Polym. Sci. A*, **3**, 3587 (1965).

2. W. Burlant and J. Hinsch, *J. Polym. Sci. A*, **2**, 2135 (1964).

3. S. S. Labana, *J. Polym. Sci. A-1*, **6**, 3283 (1968).

4. E. J. Henley and D. Richman, *Anal. Chem.*, **28**, 1580 (1956).

5. R. Zbinden, *Infrared Spectroscopy of High Polymers*, Academic Press, New York, N. Y., 1964, p. 87.

6. R. T. Conley, *Infrared Spectroscopy*, Allyn and Bacon, Boston, Mass., 1966 p. 210.

7. M. Fineman and S. D. Ross, *J. Polym. Sci.*, **5**, 259 (1950).

8. R. H. Wiley and E. E. Sale, *J. Polym. Sci.*, **42**, 491 (1960).

9. A. Chapiro, *Radiation Res.*, **6**, 11 (1957).

10. F. Szocs and K. Ulbert, *J. Polym. Sci. B*, **5**, 671 (1967).

11. P. J. Flory, *Principles of Polymer Chemistry*, Cornell Univ. Press, Ithaca, N. Y., 1953, pp. 138, 143, 391.

12. C. Walling, *J. Amer. Chem. Soc.*, **67**, 441 (1945).

13. W. Simpson, T. Holt, and R. J. Zetie, *J. Polym. Sci.*, **10**, 489 (1953).

14. C. H. Bamford, R. W. Dyson and G. C. Eastmond, in *Macromolecular Chemistry*, *Prague 1965 (J. Polym. Sci. C*, **16**), O. Wichterle and B. Sedláček, Eds., Interscience, New York, 1967, p. 2425.

Polymerization of Coordinated Monomers. III. Copolymerization of Acrylonitrile–Zinc Chloride, Methacrylonitrile–Zinc Chloride or Methyl Methacrylate–Zinc Chloride Complex with Styrene

TADASHI IKEGAMI and HIDEFUMI HIRAI,

*Department of Industrial Chemistry, Faculty of Engineering,
University of Tokyo, Hongo, Bunkyo-ku, Tokyo, Japan*

Synopsis

The 1:1 or 2:1 complex of acrylonitrile, methacrylonitrile, or methyl methacrylate with ZnCl₂ was copolymerized with styrene at the temperature of 0–30°C without any initiator. The structure of the copolymer from methyl methacrylate complex and styrene was examined by NMR spectroscopy. The complexes of acrylonitrile or methacrylonitrile with ZnCl₂ gave a copolymer containing about 50 mole-% styrene units. The complexes of methyl methacrylate yielded an alternating copolymer when the feed molar ratio of methyl methacrylate to styrene was small, but with increasing feed molar ratio the resulting copolymer consisted of about 2 moles of methyl methacrylate per mole of styrene. The formation of a charge-transfer complex of styrene with a monomer coordinated to zinc atom was inferred from the ultraviolet spectra. The regulation of the copolymerization was considered to be effected by the charge-transfer complex. The copolymer resulting from the 2:1 methyl methacrylate–zinc chloride complex had no specific tacticity, whereas the copolymer from the 1:1 complex was richer in coisotacticity than in cosyndiotacticity. The change of the composition of the copolymer and its specific tacticity in the polymerization of the methyl methacrylate complex is related to the structure of the complex.

INTRODUCTION

When polar vinyl monomers such as acrylonitrile (AN), acrylic esters, and vinylpyridines form complexes with Lewis acids, their reactivities and copolymerizabilities change, as reported by several authors.[1–3] Recently Arita et al.[4] showed that the copolymerization of AN with styrene (St) was initiated by the addition of zinc chloride to give rise to a copolymer with alternate properties. They concluded that the complex formation with ZnCl₂ changed the values of Q and e of AN and that the alternate properties were ascribed to the large difference of Q and especially e values between complexed AN and St. Hirooka and co-workers[5] also reported that the complexes of acrylic monomers (nitrile and esters) with alkyl aluminum halides copolymerized with olefins to give alternating copoly-

195

mers at a temperature as low as $-78°C$ without initiator. This mode of polymerization was designated as coordination copolymerization.

During the study of polymerization of complexed monomers such as those mentioned above,[6-8] the authors found that the complexes of AN, methacrylonitrile (MAN), and methyl methacrylate (MMA) with ZnCl₂ dissolved in aromatic solvents, e.g., benzene and toluene, anomalously and the ultraviolet spectra of the aromatic solvents changed in the shape of the band at 250 mμ.[9] It is assumed that this phenomenon is due to the donor–acceptor interaction between the complexes and the aromatic molecules.

A charge-transfer complex is expected to form when the stronger donor, e.g., St, is used as the aromatic compound and an alternating copolymerization of St with the complexed monomers appears to occur, as in the case of St–maleic anhydride.

In this study, the complexes of AN, MAN, and MMA with ZnCl₂ polymerized with St at 0–30°C without any initiator. The structures of the resulting polymer chain were determined by NMR spectroscopy in the case of the MMA complex–St system. The polymerization processes were investigated by ultraviolet spectroscopy. The alternating copolymerization was discussed in terms of the formation of an intermediate charge-transfer complex.

EXPERIMENTAL

Materials

MAN was prepared by dehydrating acetonecyanhydrine with phosphorus pentoxide. Other monomers and solvents were purified by the usual methods. Zinc chloride was purified by sublimation.

Preparation of Complexes

The complexes were prepared according to the procedures reported in the previous paper.[8] The complexes for polymerization were prepared by dissolving ZnCl₂ in the mixture of monomer and solvent at a predetermined molar ratio of monomer to ZnCl₂.

Method for Polymerization

In the cases of MAN and AN complexes, solutions of the complexes in benzene were used for polymerization. The MMA complex, which was liquid at polymerization temperature, was used without solvent. The typical procedure was as follows. The complex and styrene were mixed in an ampoule in an atmosphere of nitrogen below 0°C and then degassed and sealed off *in vacuo*. The polymerization began immediately after the temperature of the reaction mixture was raised to the polymerization temperature. After completion of the polymerization, the contents of the ampoule were poured into a solvent (*N,N*-dimethyl-formamide for AN, acetone for MAN and chloroform for MMA) and then precipitated by the

addition of methanol containing hydrochloric acid. This treatment was repeated several times to remove zinc chloride from the copolymer. The purified copolymer was dried at 60°C *in vacuo*. The composition of the copolymer was determined by elemental analysis for the AN–St and MAN–St copolymers or by NMR spectroscopy for MMA–St copolymer.

Structure and Tacticity of Copolymer

NMR spectra were measured for MMA–St copolymer at 70°C to investigate its tacticity and structure. Peak area of signals for methoxy protons were determined and analyzed according to the method of Yamashita and co-workers.[10]

Spectral Measurement

NMR spectra were obtained with a Japan Electron Optics Laboratory Model C-60 spectrometer at 60 Mc.

Ultraviolet spectra of the polymerization system were recorded on a Hitachi Model EPI-S2 spectrometer.

Infrared spectra of the complexes were obtained by using a Japan Spectroscopic Model 102 and 103 spectrometer.

RESULT AND DISCUSSION

Properties of Complexes

AN and MAN complexes are colorless crystals at room temperature, but MMA complexes are liquid above −20°C. In both the 2:1 and 1:1 complexes the monomers coordinate to the zinc atom by lone-pair electrons on either the nitrogen atom of the nitrile group or the oxygen atom of carbonyl group, that is, by σ-type coordination (Table I). The chemical shifts of the protons, especially the vinyl protons of the monomers move towards lower field upon complex formation, as shown in Table II. The AN and MAN complexes are stable in benzene or toluene, since no absorption bands due to free monomer appear in their infrared spectra.

TABLE I
Changes in the Infrared Frequency of Monomer on Complex Formation[a]

Complex	Composition[b]	$\Delta\nu(C{\equiv}N)$, cm^{-1}	$\Delta\nu(C{=}O)$, cm^{-1}	$\Delta\nu(C{=}C)$, cm^{-1}
$ZnCl_2(AN)$	1.05	+50		—
$ZnCl_2(AN)_2$	2.02	+50		—
$ZnCl_2(MAN)_2$	1.99	+40		−5
$ZnCl_2(MMA)$	1.02		−20, −60	−3
$ZnCl_2(MMA)_2$	1.97		−20	−3

[a] AN, $\nu(C{\equiv}N)$ at 2225 cm^{-1}, $\nu(C{=}C)$ at 1620 cm^{-1}; MAN, $\nu(C{\equiv}N)$ at 2230 cm^{-1}, $\nu(C{=}C)$ at 1623 cm^{-1}; MMA, $\nu(C{=}O)$ at 1723 cm^{-1}, $\nu(C{=}C)$ at 1635 cm^{-1}.
[b] Molar ratio of monomer to $ZnCl_2$.

TABLE II

Changes in Proton Chemical Shift of Monomer on Complex Formation[a]

Complex	$\Delta\tau(\alpha\text{-}CH_3$ or $\alpha\text{-}H)$, ppm	$\Delta\tau(OCH_3)$, ppm	$\Delta\tau(H_c)$[b] ppm	$\Delta\tau(H_t)$[b] ppm
$ZnCl_2(AN)$	−0.42		−0.64	−0.60
$ZnCl_2(AN)_2$	−0.38		−0.43	−0.42
$ZnCl_2(MAN)_2$	−0.10		−0.33	−0.38
$ZnCl_2(MMA)$	−0.13	−0.25	−0.32	−0.26
$ZnCl_2(MMA)_2$	−0.08	−0.19	−0.34	−0.21

[a] Chemical shift (τ) is referred to tetramethylsilane $(\tau = 10.00$ ppm) at 60 Mcps. For pure monomer; AN, $\tau(\alpha\text{-}H)$ at 4.10 ppm, $\tau(H_c)$ at 3.90 ppm and $\tau(H_t)$ at 3.97 ppm; MAN, $\tau(\alpha\text{-}CH_3)$ at 8.00 ppm, $\tau(H_c)$ at 4.18 ppm, and $\tau(H_t)$ at 4.29 ppm; MMA $\tau(\alpha\text{-}CH_3)$ at 8.13 ppm, $\tau(OCH_3)$ at 6.30 ppm, $\tau(H_c)$ at 4.45 ppm and $\tau(H_t)$ at 3.96 ppm.

[b] H_c and H_t, vinyl protons cis and trans to the nitrile or the ester group, respectively.

The dissolution behavior of these complexes in aromatic hydrocarbons is very anomalous. When the 2:1 complex was added to benzene at a molar ratio of benzene to monomer (B/M) less than unity, it did not dissolve completely. When B/M was near unity, only one liquid phase formed. Two liquid layers appeared as B/M became larger than unity. It was found by chemical analysis that the upper solution consisted of monomer and benzene, and that the lower layer consisted of monomer, zinc chloride, and benzene, B/M in this layer being approximately unity.

Copolymerization

All complexes began to copolymerize with St as soon as the temperature of the polymerization mixture was raised to the polymerization temperature. The results are summarized in Tables III–V.

AN–ZnCl₂ Complex. The polymerization proceeded smoothly; especially the 1:1 complex polymerized rapidly. Figure 1 shows the composition diagram for the copolymers of the 1:1 or the 2:1 complex and St. The copolymers thus obtained were found to contain St and AN units in a molar ratio of 1:1 over a wide range of the feed monomer compositions. The conversion in a given time had a maximum at a feed monomer composition of 1:1 molar ratio.

MAN–ZnCl₂ Complex. The rate of polymerization was not so high as that for AN–ZnCl₂ complexes. The resulting copolymer contained St and MAN in a molar ratio of about 1:1 at lower feed monomer molar ratios of the complex to St, while the content of MAN in the copolymer increased at higher feed monomer molar ratios (Fig. 2). When hydrogen cyanide, which was produced during the preparation of MAN monomer, was not completely removed by the treatment with silver oxide, the composition diagram for this copolymerization system was similar to that for the MMA–ZnCl₂ complex described below (Fig. 3). This is reasonably ascribed to a cationic polymerization of St by hydrogen cyanide.

MMA–ZnCl₂ Complex. Cationic homopolymerization of St was found to occur in addition to the radical polymerization. The polymerization proceeded very rapidly at 30°C but slowly at 0°C. The cationic polymerization of St could be initiated by the 2:1 methyl acetate–ZnCl₂ com-

TABLE III

Copolymerization of the AN–ZnCl₂ Complexes with Styrene[a]

AN coordinated to ZnCl₂ in monomer[m_1], mole-%	Time, min	Conversion, %	N, %[b]	AN unit in copolymer, mole-%
1:1 AN–ZnCl₂ complex				
10	5	2.3	9.32	51.7
20	5	9.5	9.59	52.6
30	5	13.2	9.68	53.2
50	5	18.7	9.47	52.3
70	5	16.2	9.34	51.7
80	5	21.8	9.82	53.8
90	5	6.3	9.47	52.3
2:1 AN–ZnCl₄ complex				
10	20	3.5	9.69	53.2
20	30	10.0	9.23	51.3
30	30	10.7	8.87	49.9
50	20	24.4	9.24	51.4
70	30	7.1	9.09	51.1
80	30	5.0	8.63	48.7
90	30	3.1	9.45	52.2

[a] Reaction temperature, 30°C; a 50 mole-% solution of the complex in benzene was used.
[b] By elemental analysis; 8.91% for the 1:1 copolymer.

TABLE IV

Copolymerization of the 2:1 MAN–ZnCl₂ Complex with Styrene[a]

MAN coordinated to ZnCl₂ in monomer [m_1], mole-%	Time, min	Conversion, %	N, %[b]	MAN unit in copolymer, mole-%
10	100	2.3	7.95	48.9
20	100	1.6	7.85	48.5
50	100	1.3	6.77	42.9
80	100	2.5	8.70	52.6
90	320	8.4	10.06	59.0

[a] Reaction temperature, 30°C; a 50 mole-% solution of the complex in benzene was used.
[b] By elemental analysis; 8.18% for the 1:1 copolymer.

TABLE V
Copolymerization of the MMA–ZnCl₂ Complexes with Styrene[a]

MMA coordinated to ZnCl₂ in monomer[m₁], mole-%	Time, min	Con-version, %	MMA unit in Copolymer mole %	Tacticity[b]		
				x, %	y, %	z, %
1:1 MMA–ZnCl₂ complex						
10	5	2.8	51.5	26	27	47
30	5	3.4	63.8	20	34	47
50	5	7.9	58.0	27	32	41
70	5	2.4	73.0	41	33	26
90	5	1.6	72.6	52	27	21
2:1 MMA–ZnCl₂ complex						
10	40	7.3	51.5	26	48	26
20	40	2.2	49.0	28	44	28
50	40	1.6	56.5	26	40	34
70	40	2.7	62.0	30	41	29
80	40	2.5	67.0	40	40	20
90	40	1.4	71.0	50	33	17

[a] Reaction temperature, 30°C.

[b] Tacticity was determined by NMR spectroscopy according to the method of Itoh and Yamashita.[10]

plex, but the rate of polymerization by this complex was lower than that by the MMA complex; that is, MMA is a more effective cocatalyst for the cationic homopolymerization of St with zinc chloride as a catalyst. The composition diagram for this system seems to be anomalous, as shown in Figure 3. Treatment of the resulting copolymer with cyclohexane to re-move polystyrene gave the composition diagram of Figure 4. At the lower monomer molar ratios of the complex to St, the molar ratio of MMA to St in the copolymer is 1:1; with increasing molar ratio of the complex to St, the molar ratio of MMA to St in the copolymer approaches 2:1.
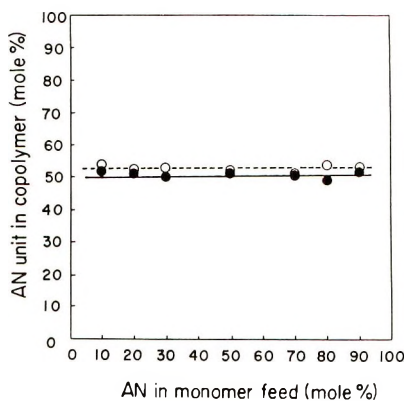
Fig. 1. Composition diagram for the copolymerization of AN-ZnCl₂ complexes with styrene: (○) ZnCl₂(AN)–St; (●) ZnCl₂(AN)₂–ST.
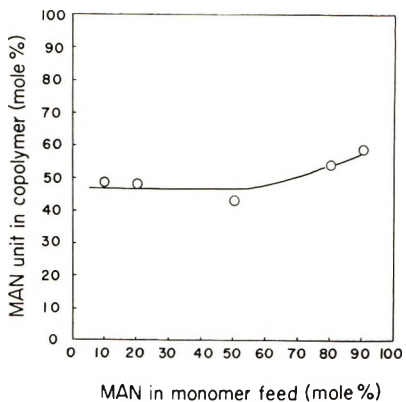
Fig. 2. Composition diagram for the copolymerization of the 2:1 MAN–ZnCl₂ complex with styrene.
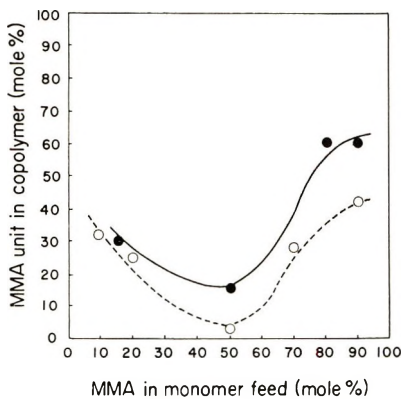
Fig. 3. Composition diagram for the copolymerization of the 1:1 MMA–ZnCl₂ complex with styrene: (●) at 0°C; (○) at 30°C.
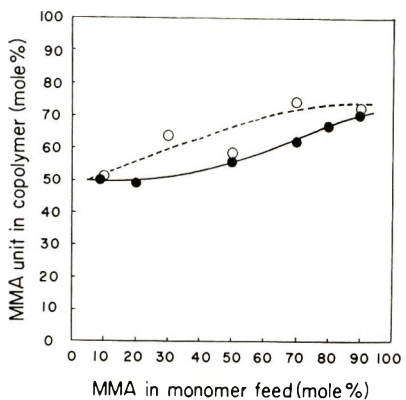
Fig. 4. Composition diagram for the copolymerization of the MMA–ZnCl₂ complex with styrene after treatment with cyclohexane: (○) ZnCl₂(MMA)–St; (●) ZnCl₂(MMA)₂–St.

NMR Spectra of Copolymer

The NMR spectra of the copolymer obtained from the MMA–ZnCl₂ complex–St system are shown in Figure 5. The copolymers containing equal amounts of each of the monomer units exhibit the three split peaks of α-methyl group. Among the three peaks of the methoxy proton, the two peaks at the higher field are intense. The presence of these characteristic peaks indicates that the copolymer has an alternating structure of MMA and St.[11] The splitting characteristic of the α-methyl proton is also observed in copolymers containing a higher amount of MMA unit than St unit. The relative intensities of the three peaks of methoxy protons are summarized in Table V. The relative ratio of coisotacticity x: heterotacticity y: cosyndiotacticity z was calculated to be $1:2:1$ in the copolymer with an MMA/St molar ratio of about unity which was obtained from the 2:1 complex. This value means that the stereoregulation of the copolymer is completely random. On the other hand, the 1:1 complex yielded a copolymer with a higher content of coisotacticity. In the polymerization of the 1:1 complex–St system, a certain structural factor of the complex would contribute to the stereospecificity.
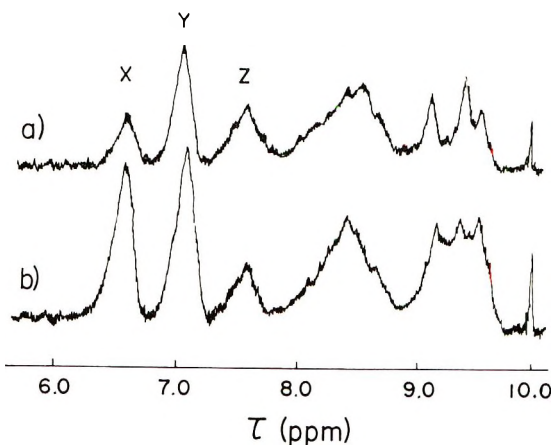
Fig. 5. NMR spectra of copolymers derived from the 2:1 MMA–ZnCl₂ complex with styrene: (a) 52 mole-% MMA units; (b) 67 mole-% MMA units.

Ultraviolet Spectra of Polymerization System

Spectral measurements on the polymerization system are possible when the system is diluted with benzene, since the rate of polymerization is reduced by dilution. Figure 6 shows the ultraviolet spectrum of the lower layer of the polymerization solution of the ZnCl₂(AN)₂–St system. The molar ratio of AN to St in the lower layer approaches 1:1 with increasing St/AN shown in the figure, because of the anomalous dissolution of the complex as described before. In this spectrum a shoulder appeared, superposed upon the absorption band of St which shifted to higher wavelength.
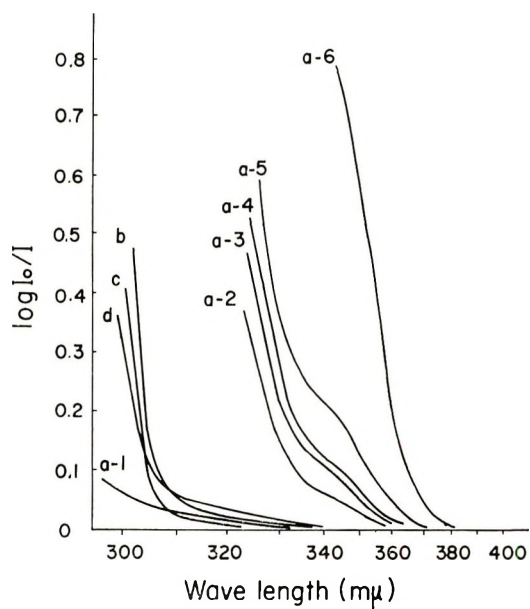
Fig. 6. Ultraviolet spectra of $ZnCl_2(AN)_2$–St system: (a-1) St/AN = 0; (a-2) St/AN = 0.25, (a-3) St/AN = 0.67; (a-4) St/AN = 1.0; (a-5) St/An = 2.3, (a-6) St/AN = 9.0, (b) St; (c) pure AN–St (1:1); (d) $ZnCl_2(PN)_2$–St (1:1).
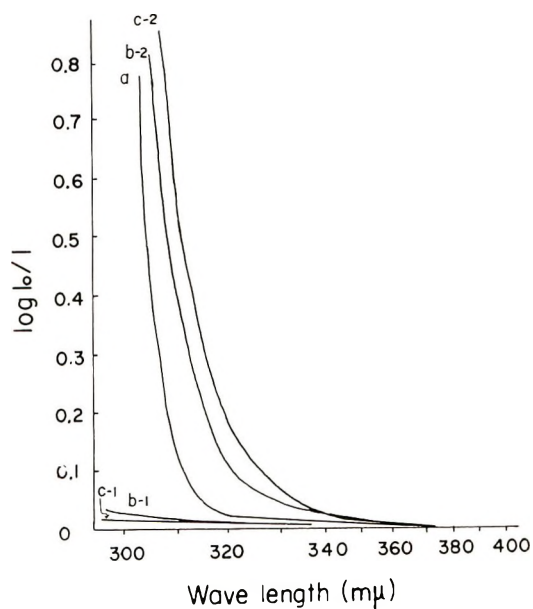
Fig. 7. Ultraviolet spectra of (a) St, (b-1) $ZnCl_2(MAN)_2$, (b-2) $ZnCl_2(MAN)_2$–St (1:1); (c-1) $ZnCl_2(MMA)_2$; (c-2) $ZnCl_2(MMA)_2$–St (1:1).

The shift of the absorption band of St was also observed in the polymerization system of St–MAN or MMA complex (Fig. 7).   The new absorption band and the shift of the absorption band of St are believed to be due to either the interaction of St with $ZnCl_2$ or with AN coordinated to $ZnCl_2$.
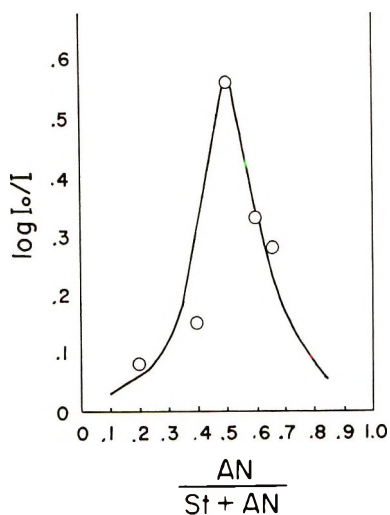
Fig. 8. Continuous variation curve of the band at 345 mμ of the $ZnCl_2(AN)_2$–St system diluted with benzene solution of $ZnCl_2(PN)_2$ complex.
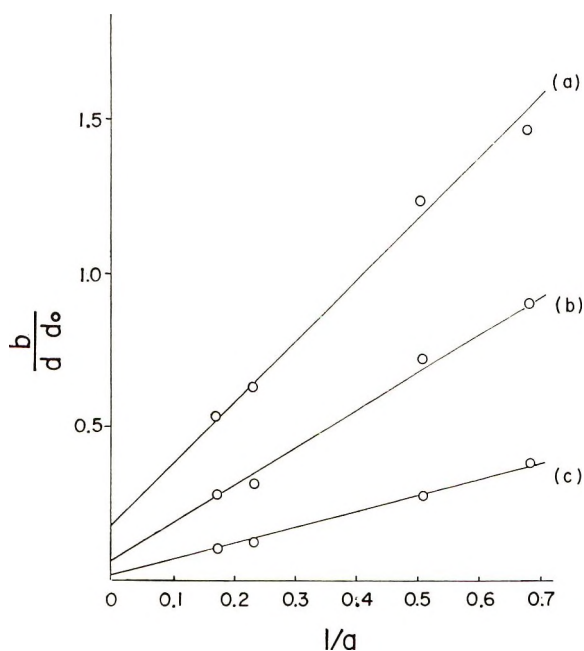
Fig. 9. Ketelaar plot for the $ZnCl_2(AN)_2$–St system: (a) 310 mμ, (b) 320 mμ and (c) 330 mμ.

The complex solution itself has no absorption band in the range of 300–400 mμ. Neither a new absorption band nor a shifted band of St appears in the spectrum of the St–propionitrile (PN)–ZnCl$_2$ complex system. The free AN–St system shows no indication of the formation of a charge-transfer complex as in the case of AN–isobutyl vinyl ether system.[12] From these observation it can be concluded that the new absorption band is attributable to a charge-transfer complex of St with AN coordinated to ZnCl$_2$. This is a new type of charge-transfer complex.

A continuous variation measurement of this new band showed a maximum at an equimolar AN/St ratio as shown in Figure 8, that is, the charge-transfer complex is of the 1:1 type. The equilibrium constant of the charge-transfer complex of eq. (1) was estimated by the method of Ketelaar et al.[13]

$$\tfrac{1}{2}ZnCl_2(AN)_2 + St \overset{K}{\rightleftharpoons} C\text{-}T \text{ complex} \tag{1}$$

For this system eq. (2) is valid,

$$\frac{b}{d - d_0} = \frac{1}{aK(k_c - k_b)} + \frac{1}{k_c - k_b} \tag{2}$$

where a and b are the concentrations of AN and St, respectively, d and d_0 are the absorption of this system and that of the solution without AN, and k_c and k_b are the molar absorption coefficients of the C-T complex and of St, respectively. Values of $b/(d - d_0)$ were plotted against $1/a$ as shown in Figure 9. The values of K obtained by this method are summarized in

TABLE VI
Estimation of the Equilibrium Constant K of the Charge-Transfer Complex[a]

Wavelength, mμ	$1/K(k_c - k_b)$	$1/(k_c - k_b)$	$K \times 10^2$
310	0.50	0.02	4.0
320	1.21	0.07	5.6
330	1.99	0.18	9.1
		Avg.	6.2

[a] The concentration of the 2:1 AN–ZnCl$_2$ complex varied from 1.47 to 5.87 mole/l. and that of St was 8.76 $\times$ 10^{-2} mole/l. The solution of the 2:1 propionitrile–ZnCl$_2$ complex in benzene (molar ratio of benzene to the complex = 2.0) was used for the dilution of the AN complex and St.

Table VI. No appreciable changes in the infrared and NMR spectra of these polymerization systems were observed because of the low concentration of the charge-transfer complex.

When the MMA complex was mixed with 1,1-diphenylethylene, the mixture was colored green to yellow. The ultraviolet spectrum showed an absorption band at 420 mμ, which suggests the presence of the cation of 1,1-diphenylethylene.[14]

Charge-Transfer Complex

Charge transfer complexes such as maleic anhydride–St[15] and tetra-cyanoethylene–Benzene[16] are known. AN, MAN, and MMA monomers have electron-withdrawing substituents such as CN and C=O, so that they are electron acceptors. They, however, are not so strongly electron acceptor in nature as maleic anhydride or tetracyanoethylene, and consequently they themselves can not form charge-transfer complexes with St.

The complexes of these monomers with $ZnCl_2$ are formed through the coordination of lone-pair electrons to the zinc atom. From the fact that the vinyl protons of these complexes are shifted to lower fields in their NMR spectra, the electron acceptability of the double bond is expected to increase; that is, the coordination of the monomer to the metal atom has an effect similar to substitution of the monomer by polar conjugative groups such as those in tetracyanoethylene or maleic anhydride. It is plausible that this effect enabled these monomers to form charge-transfer complexes with St.

The charge-transfer bands of the MAN–$ZnCl_2$ or MMA–$ZnCl_2$ complex–St system appear to be hidden in the shifted absorption band of St. The equilibrium constant of $K = 0.06$ indicates that 15% of monomer pair is in the form of a charge-transfer complex at a feed monomer ratio of 1:1 under the polymerization condition (concentration of monomer = 2.97 mole/l.). The concentration of the charge transfer complex would be higher in the actual polymerization system, since the spectral measurement was carried out in a solution diluted with benzene, which is considered to be a weak donor.

Mechanism for Polymerization

Although the initiation is uncertain, the propagation step of polymerization may proceed by a free-radical mechanism as suggested by Arita et al.[4] The polymerization would be initiated by a biradical form from the charge-transfer complex of the vinyl monomer–$ZnCl_2$ complex–St or the abstraction of a hydrogen atom by the charge-transfer complex as reported by Matsuda and Abe[17] for the copolymerization of maleic anhydride with St.

The alternating copolymerization may be explained on the basis of one of the following: (1) the difference of Q and e values between two monomers;[18] (2) electron transfer between the propagating radical and the monomer;[19] (3) the formation of a charge-transfer complex.[20] The first two explanations are applicable mainly to ordinary copolymerization. If the Q–e scheme is applied to this charge-transfer system, the values of Q and e of vinyl monomer coordinated to zinc chloride may be extraordinarily large. However, Arita et al.[4] calculated the Q and e values of the AN–$ZnCl_2$ complex in the polymerization of AN with St in the presence of zinc chloride and obtained the following values: $Q = 24$, $e = 2.53$. In this case the contribution of the charge-transfer complex is small, since

their experiments were carried out at a lower concentration of $ZnCl_2$ and at a higher temperature (60°C).

The polymerizations in the present study were effected not at a low concentration of $ZnCl_2$ but with the use of the vinyl monomer–$ZnCl_2$ complexes themselves, and at rather low temperatures (0–30°C). The observation of the charge-transfer complex is favorable for the mechanism of the charge-transfer complex polymerization. In the case of the AN–$ZnCl_2$ complex, the alternating structure of the copolymer is inferred from the retention of the 1:1 molar ratio of AN to St of the copolymer over a wide range of molar ratio of monomers in the feed. This alternating character is reasonably explained by the polymerization of the charge-transfer complex of the AN–$ZnCl_2$ complex–St. The estimated concentration of the charge-transfer complex is 15% of the monomer pair at the a monomer molar ratio of 1:1 in this polymerization. In consideration of this low concentration of the charge transfer complex, its reactivity will be quite high. The composition diagram for the MMA–$ZnCl_2$ complex–St system is different from
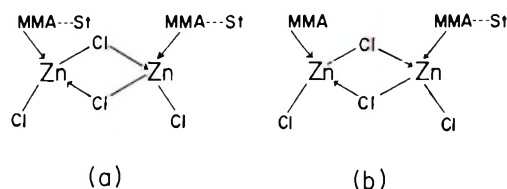
Fig. 10. Structure of the C-T complex for MMA–$ZnCl_2$ complex–St system; (a) 1:1 type; (b) 2:1 type.

that for the AN complex system. A dimer structure was proposed for the 1:1 MMA–$ZnCl_2$ complex on the basis of the stoichiometry, the nature of the complex, and both its infrared and NMR spectra.[7] At a lower MMA:St molar ratio, the 1:1 type of the charge-transfer complex would be predominant, while at the higher molar ratios the 2:2 type of complex would increase in amount. The structures of the charge-transfer complexes proposed are shown in Figure 10. The similarity in behavior of the 2:1 and 1:1 complexes would be due to the formation of the 1:1 dimer type complex by dissociation of the 2:1 complex.

Many reports of copolymerization by a mechanism involving a charge-transfer complex polymerization have been published.[21] The formation constant of such charge-transfer complex, however, is usually very low.[22] Provided that the propagation step proceeds through the charge-transfer complex alone, the reactivity of the charge-transfer complex should be quite high, since the concentration of the charge transfer-complex is low. It seems necessary to assume that a molecular complex in which the components interact weakly would participate in the copolymerization.

References

1. M. Imoto, T. Otsu, and Y. Harada, *Makromol. Chem.*, **65**, 180 (1963).

2. M. Imoto, T. Otsu, and M. Nakabayashi, *Makromol. Chem.*, **65**, 194 (1963).

3. S. Tazuke and S. Okamura, *J. Polym. Sci. A-1*, **5**, 1083 (1967).

4. K. Arita, S. Yabumoto, K. Ishii, M. Kawamori, and H. Yano, paper presented at 16th Discussion Meeting on Macromolecules, Society of Polymer Science of Japan, Fukuoka, 1967; *Preprints*, IIB 04.

5. M. Hirooka, H. Yabuuchi, S. Morita, S. Kawasumi, and K. Nakaguchi, *J. Polym. Sci. B*, **5**, 47 (1967).

6. H. Hirai, S. Okuzawa, T. Ikegami, and S. Makishima, *J. Fac. Eng. Univ. Tokyo*, **b29**, 115 (1967).

7. S. Okuzawa, H. Hirai, and S. Makishima, *J. Polym. Sci. A-1*, **7**, 1039 (1969).

8. H. Hirai, T. Ikegami, and S. Makishima, *J. Polym. Sci. A-1*, **7**, 2059 (1969).

9. T. Ikegami and H. Hirai, *Chem. Comm.*, **1969**, 159.

10. K. Itoh and Y. Yamashita, *J. Polym. Sci. B*, **3**, 625 (1965).

11. M. Hirooka, H. Yabuuchi, J. Iseki, and Y. Nakai, *J. Polym. Sci. A-1*, **6**, 1381 (1968).

12. S. Tazuke, T. Yamane, and S. Okamura, paper presented at 17th Discussion Meeting on Macromolecules, Society of Polymer Science of Japan, Matsuyama, 1968; *Preprints*, 22 A 04.

13. J. A. A. Ketelaar, C. Vande Stolpe, A. Goudsmit, and W. A. Dzcubas, *Rec. Trav. Chim.*, **71**, 1104 (1952).

14. V. Gold and F. L. Tye, *J. Chem. Soc.*, **1952**, 2172.

15. W. G. Barb, *Trans. Faraday Soc.*, **49**, 143 (1953).

16. R. S. Merrifield and W. D. Phillips, *J. Amer. Chem. Soc.*, **80**, 2778 (1958).

17. M. Matsuda and K. Abe, *J. Polym. Sci. A-1*, **6**, 1441 (1968).

18. C. C. Price, *J. Polym. Sci.*, **1**, 83 (1946).

19. C. Walling and F. R. Mayo, *J. Polym. Sci.*, **3**, 895 (1948).

20. P. D. Bartlett and K. Nozaki, *J. Amer. Chem. Soc.*, **68**, 1495 (1946).

21. S. Iwatsuki and Y. Yamashita, *Kagaku*, **22**, 44 (1967).

22. S. Iwatsuki and Y. Yamashita, *Makromol. Chem.*, **89**, 205 (1965).

Radiolysis of Poly(vinyl Chloride)

R. SALOVEY and J. P. LUONGO, *Bell Telephone Laboratories, Incorporated, Murray Hill, New Jersey 07974*

Synopsis

Allyl free-radical intermediates are detected by ultraviolet absorption at 255 mμ in poly(vinyl chloride) irradiated at $-196°$C and stored at $25°$C. In vacuum at $25°$C, allyl radicals are converted into polyenyl free radicals and polyenes. From the nature of allyl radical decay in vacuum, radical chain transfer between polyenyl radicals and poly(vinyl chloride) is inferred. Allyl and polyenyl free radicals are scavenged by oxygen on post-irradiation storage in air.

INTRODUCTION

The exposure of poly(vinyl chloride) to ionizing radiation at $25°$C yields long sequences of conjugated double bonds or polyenes.[1] Electron spin resonance studies are consistent with a radical chain dehydrochlorination reaction.[2,3] Post-irradiation color formation occurs in vacuum at $25°$C at constant radical concentration.[4] The presence of free-radical scavengers suppresses the formation of polyenyl radicals and color. Irradiation and electron spin resonance measurements at $-196°$C reveal short-lived (at $25°$C) primary free radical intermediates.[3] Further information concerning these reactive species may be derived from the absorption spectrum at $25°$C of poly(vinyl chloride) films irradiated in vacuum at $-196°$C. Absorption studies on thin films of poly(vinyl chloride) irradiated to low doses at $-196°$C with 1 MeV electrons are described. The resultant kinetic information may be germane to the mechanism of poly(vinyl chloride) radiolysis.

EXPERIMENTAL

Experimental procedures are similar to those previously described.[4] Poly(vinyl chloride) powder (Opalon-660, Monsanto Chemical Co.) was molded in vacuum ($127°$C, 5700 psi) to yield colorless, transparent films, 4 mils thick. Films were placed in quartz tubes (6 mm ID, pure fused quartz, thin wall transparent, Vitreosil, Thermal American Fused Quartz Co.). Tubes were evacuated for 6 hr at 10^{-5} mm and irradiated in liquid nitrogen ($-196°$C) with 1 MeV electrons from a van de Graaff generator. The total dose was 1.8 Mrad and the dose rate, 3.5 Mrad/min.[5] Samples were irradiated in a rounded portion of the tube and moved to an unirradia-

209

ted flattened section for absorption studies. Following irradiation, samples were stored in a dewar of liquid nitrogen for about 20 min. Visible and ultraviolet absorption (700–200 mμ) were recorded in vacuum at 25°C, following post-irradiation storage at this temperature, with a Cary 14 spectrophotometer. Band intensities were measured by using a standard baseline technique.

The effect of oxygen was examined by opening the tube and admitting air at an early stage of post-irradiation storage. In addition a film of poly-(vinyl chloride) irradiated at −196°C in vacuum and stored for more than 1 month at 25°C in vacuum was opened to air and its absorption spectrum recorded at repeated intervals.

RESULTS

The ultraviolet-visible spectrum at 25°C of poly(vinyl chloride) films irradiated at −196°C and warmed to 25°C is characterized by a prominent band at 255 mμ (Fig. 1, lower trace). The absorption at 255 mμ increases
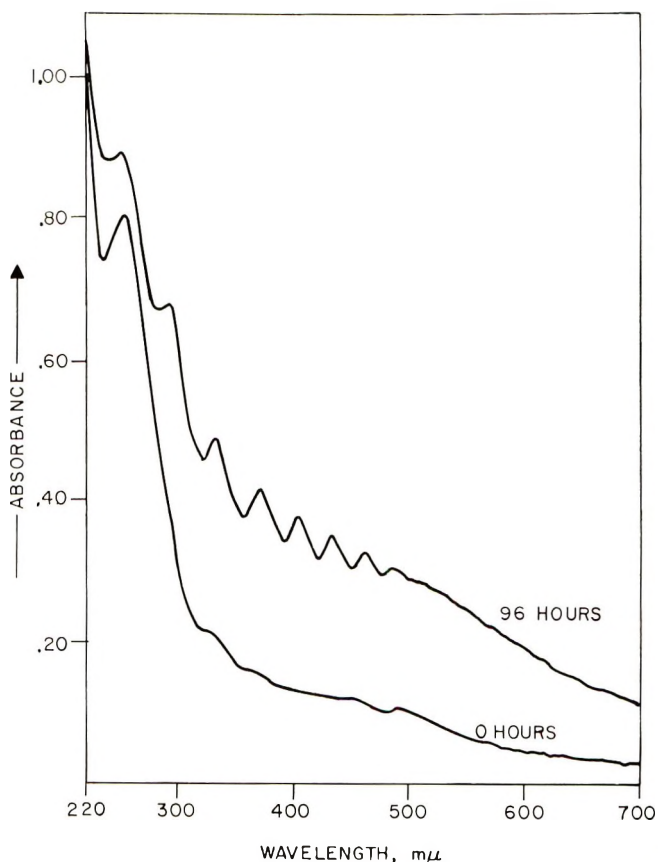
Fig. 1. Absorption spectra of poly(vinyl chloride) at 25°C, irradiated at −196°C and stored at 25°C in vacuum.
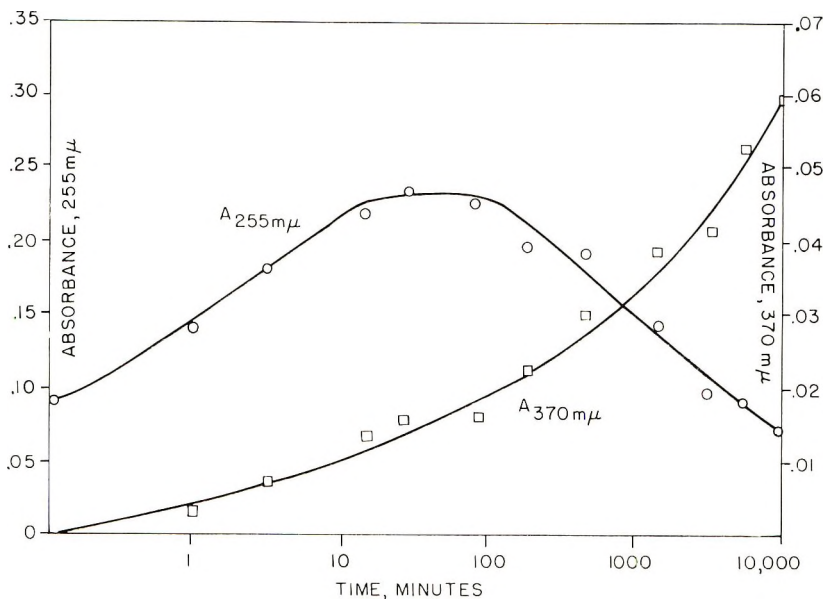
Fig. 2. Optical density at 255 and 370 mμ at 25°C of poly(vinyl chloride) irradiated at −196°C and stored at 25°C in vacuum.

on aging in vacuum at 25°C, attains a relatively constant value, and then decreases (Fig. 2). A series of regular absorption peaks characteristic of long-chain polyenes[1] appears several hours after irradiation and increases in vacuum at 25°C (Fig. 1, top trace).[4] The formation and decay of the band at 255 mμ and the formation of the absorption peak at 370 mμ in vacuum at 25°C are plotted in Figure 2. After aging for 96 hr in vacuum, the polyene absorption bands are quite prominent (Fig. 1) and increase on subsequent storage in vacuum for 30 days. However, 24 hr after opening this tube, the polyene absorption bands, particularly the band at 290 mμ, decreased markedly.

An identical sample of poly(vinyl chloride) was irradiated at −196°C and its ultraviolet-visible spectrum recorded at intervals over a period of 10 min in vacuum at 25°C. The tube was then opened, admitting air to the sample, and the spectrum recorded at intervals. Three of the spectra recorded in air are shown in Figure 3. Absorption curves are displaced vertically for clarity. The formation and decay of absorption maxima at 255 and 370 mμ are recorded in Figure 4. The band at 255 mμ decreases more rapidly in air than under vacuum. The polyene structure appears, persists for several hours and decays.

DISCUSSION

Following the irradiation of poly(vinyl chloride) at −196°C and during post-irradiation storage in vacuum at 25°C, an increasing concentration of long sequences of conjugated double-bond structures (polyenes) is formed.
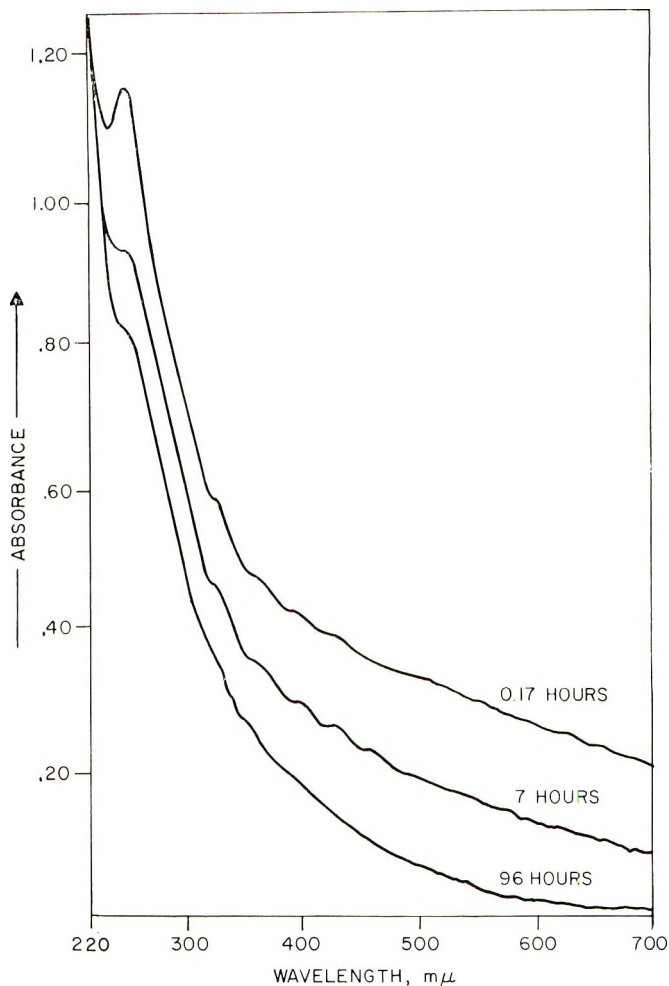
Fig. 3. Absorption spectra of poly(vinyl chloride) at 25°C, irradiated at −196°C, stored at 25°C in *vacuo* for 10 min and then in air.

A series of absorption bands which increase in intensity with time result from the polyene structure. Polyenes are products of dehydrochlorination initiated by primary free radicals resulting from radiolytic carbon–chlorine bond scission. Most of the primary free radicals produced by irradiation at −196°C decay within several minutes at 25°C in vacuum[3] to yield polyenyl free radicals. From electron spin resonance studies it is suggested, by analogy to irradiated polyene acids[6] that the conjugated double bond sequence exceeds 5 under these conditions. The increase in the intensity of the absorption band at 255 mμ coincides with a decrease in the primary free radical concentration[3] and it is inferred that the absorption band at 255 mμ corresponds to a short chain polyenyl free radical intermediate. An ultraviolet absorption band at 258 mμ has been assigned to the allyl
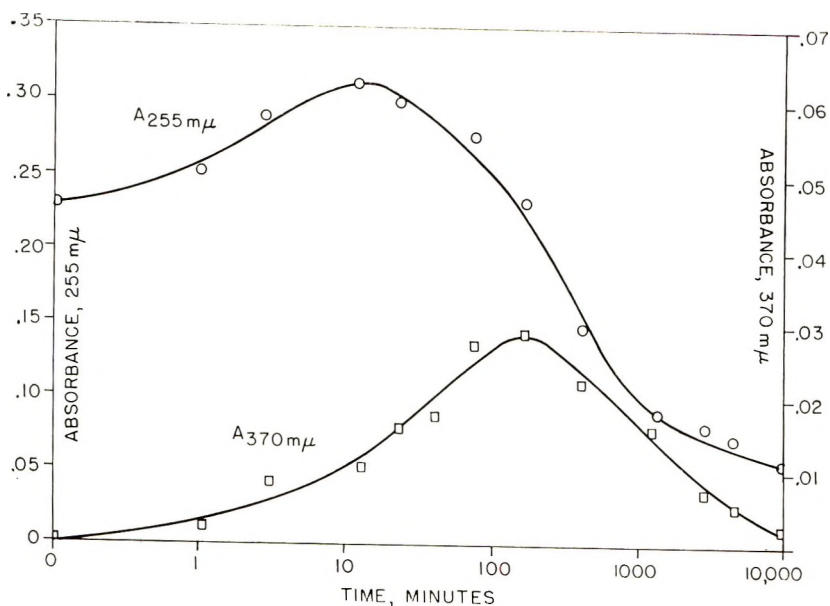
Fig. 4. Optical density at 255 and 370 mμ at 25°C of poly(vinyl chloride) irradiated at −196°C and stored at 25°C in vacuum for 10 min and then in air.

free radical.[7] Substituted allyl free radicals in irradiated poly(vinyl chloride) can result from the evolution of hydrogen chloride by primary radicals and by radical products of chain transfer reactions between poly-enyl radicals and poly(vinyl chloride). Continual formation and decay of the allyl radical intermediate lead to a temporary steady-state concentration. Since a relatively small concentration of allyl radical intermediates exists in the presence of a large concentration of polyenyl free radicals, the electron spin resonance spectrum is characteristic of the latter.

The formation of polyenyl free radicals of increasing sequence length and of decreasing reactivity ultimately decreases the concentration of inter-mediate allyl radicals. The decay in polyene concentration in the sample stored for 30 days *in vacuo* followed by exposure to air exhibits a rate similar to polyenyl free radical decay in electron spin resonance studies.[4] Diffusion of oxygen into the film and reaction with long chain polyenyl free radicals account for these effects. The possibility of oxidation of long chain poly-enes cannot be excluded, however. The reactivity of polyenyl free radicals decreases with increasing chain length and reaction with oxygen should be most rapid for shorter polyenyl radicals. The band at 290 mμ which decays rapidly in air may be due to a short-chain polyenyl free radical[3] and accordingly reacts most readily in the aged specimen following exposure to oxygen.

The dehydrochlorination of allyl free radicals to form longer chain radicals and/or polyenes may be suppressed by oxygen scavenging at an early stage of post-irradiation storage. The apparent difference in initial allyl radical

concentration in Figures 2 and 4 is likely due to the extreme sensitivity to storage time at 25°C in vacuum. Slight variations in the time allowed for the sample to warm up from −196°C account for this variability. The admission of air soon after irradiation leads to a decrease in the band at 255 mμ and reduced formation of longer-chain polyenyl structures. Polyenyl free radicals react slowly with oxygen and will also decay in air. It is possible that the series of absorption bands observed in the visible portion of the spectrum (Fig. 3) is due entirely to relatively short polyenyl free radicals. Reaction of these free radicals with oxygen accounts for the loss of the bands in the visible spectrum on exposure to air. Thus, oxygen scavenging soon after irradiation results in complete and rapid suppression of visible absorption since the absorbing species are short polyenyl free radicals. Reaction with oxygen following prolonged post-irradiation storage *in vacuo* results in partial suppression of visible absorption, as long-chain polyenyl radicals and polyenes are probably present.

CONCLUSIONS

Allyl free-radical intermediates are detected at 25°C in ultraviolet absorption spectra of poly(vinyl chloride) irradiated at −196°C. The concentration of allyl radicals increases to a temporary steady-state value and then decreases on post-irradiation storage *in vacuo* at 25°C. Allyl radicals result from dehydrochlorination of primary radical products of ionizing irradiation during early stages of post-irradiation aging. Allyl radicals also result from chain transfer between polyenyl free radicals and parent polymer to yield polyenes. Since the reactivity of polyenyl free radicals probably decreases with increasing chain length, transfer reactions become less likely, and the allyl radical concentration decays. The concentration of polyenes and polyenyl free radicals increases on storage *in vacuo* at 25°C. The concentration of allyl and polyenyl free radicals decays by reaction with oxygen during post-irradiation storage in air.

References

1. G. J. Atchison, *J. Appl. Polym. Sci.*, **7**, 1471 (1963).
2. A. A. Miller, *J. Phys. Chem.*, **63**, 1755 (1959).
3. E. J. Lawton and J. S. Balwit, *J. Phys. Chem.*, **65**, 815 (1961).
4. R. Salovey, J. P. Luongo, and W. A. Yager, *Macromolecules*, **2**, 198 (1969).
5. W. E. Falconer and R. Salovey, *J. Chem. Phys.*, **44**, 3151 (1966).
6. M. W. Hanna, A. D. McLachlan, H. H. Dearman, and H. M. McConnell, *J. Chem. Phys.*, **37**, 361 (1962).
7. D. M. Bodily and M. Dole, *J. Chem. Phys.*, **44**, 2821 (1966).
8. D. M. Bodily and M. Dole, *J. Chem. Phys.*, **45**, 1428 (1966).

Reactions of Polyolefins with Strong Lewis Acids

WAYNE L. CARRICK, *Research and Development Department, Union Carbide Corporation Chemicals and Plastics, Bound Brook, New Jersey, 00805*

Synopsis

Treatment of a cyclohexane solution of low density polyethylene and polystyrene with anhydrous aluminum chloride causes chemical reaction between the two polymers which results in the formation of a graft copolymer. The initial copolymer-forming reaction is very rapid, and prolonged contact of the polymers with aluminum chloride causes subsequent degradation in molecular weight. Treatment of separate solutions of polyethylene, isotactic polypropylene, and ethylene–propylene copolymers with aluminum chloride was studied as a function of time. The intrinsic viscosities of the polymers dropped from initial values of 2.4–6.5 to 0.55–0.85 in 5 min, followed by a slower decline over the next 2 hr. In the case of polypropylene, the low molecular weight fragments largely retained the isotactic structure, which demonstrates that stereochemical isomerization is not a major reaction.

INTRODUCTION

It is well known that aluminum chloride and other strong acids attack organic compounds.[1] This is the basis of the large family of Friedel-Crafts reactions,[2] wherein aromatic compounds are substituted by reaction with alkyl halides, olefins, etc. Aluminum chloride also reacts with saturated aliphatic compounds to cause isomerization,[3,4] cracking,[5] addition to olefins,[6] and a variety of other reactions. Although reactions of this type are very numerous in the chemistry of small molecules, except for carbonium ion polymerizations,[7,8] they have not been extensively applied to polymers.[2,9–13] The present investigation was intended to determine the reactivity of aluminum halides with polyethylene, ethylene–propylene copolymers, and other polyolefins.

EXPERIMENTAL

Polymer Degradation with Aluminum Chloride

A 3-liter round-bottomed flask was fitted with a stirrer, reflux condenser, and nitrogen inlet tube. The flask was charged with 2 liters of o-dichlorobenzene and 100 g of high-density polyethylene, melt index = 0.03, η = 2.93, and heated to 140°C with stirring to effect solution of the polymer. The temperature was then adjusted to 130°C with a nitrogen blanket maintained over the solution. A solution of 5.0 g of anhydrous aluminum

215

TABLE I
Aluminum Chloride Treatment of High-Density Polyethylene

Reaction time, min	Intrinsic viscosity $[\eta]$, dl/g	Methyl, wt-%
0	2.93	0.25
1	0.66	2.66
5	0.56	2.94
10	0.53	3.09
15	0.34	3.13
25	0.35	3.10
35	0.29	3.05
45	0.26	3.15
55	0.28	2.90
65	0.26	3.15
75	0.25	3.32
135	0.23	3.80
Linear polyethylene wax	0.17	1.3

chloride in 50 ml o-dichlorobenzene was added.   At periodic intervals, 100–200 ml aliquots of the solution were removed and quenched in methanol to precipitate the polymer which was recovered and dried.

Similar degradation experiments were carried out with the use of an amorphous ethylene–propylene copolymer, 60% propylene, $\eta = 2.35$, and an isotactic polypropylene, $\eta = 6.47$. The results are summarized in Table I and Figure 1.   The low molecular weight fractions from the polypropylene treatment were still stereoregular (isotactic) as shown by the
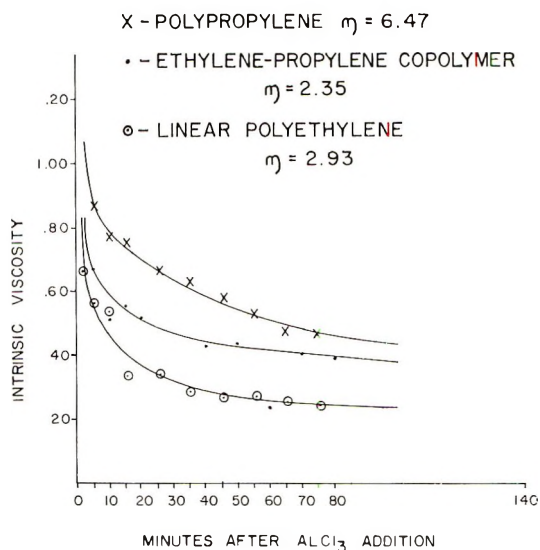
Fig. 1. Degradation of polyolefins by aluminum chloride: ($\times$) polypropylene, $\eta = 6.47$; ($\bullet$) ethylene–propylene copolymer, $\eta = 2.35$; ($\circ$) linear polyethylene, $\eta = 2.93$.

sharp infrared absorption at 10.02 μ (crystalline)[14] which was almost as intense as the 10.26 μ band (amorphous).

Preparation of Polyethylene–Polystyrene Graft Copolymer

A solution of 70 g DYNH polyethylene (2.0 melt index, 0.920 g/ml density) and 30 g Bakelite SGN-3000 polystyrene in 1 liter of boiling cyclohexane was prepared in one flask and a solution of 5.0 g anhydrous aluminum chloride in 1 liter of boiling cyclohexane was prepared in a second flask. The aluminum chloride solution was rapidly added to the polymer solution with vigorous stirring. Approximately 100-ml samples of the above solution were removed at various intervals over a reaction period of 100 min. Each sample was precipitated in 500 ml of methyl ethyl ketone
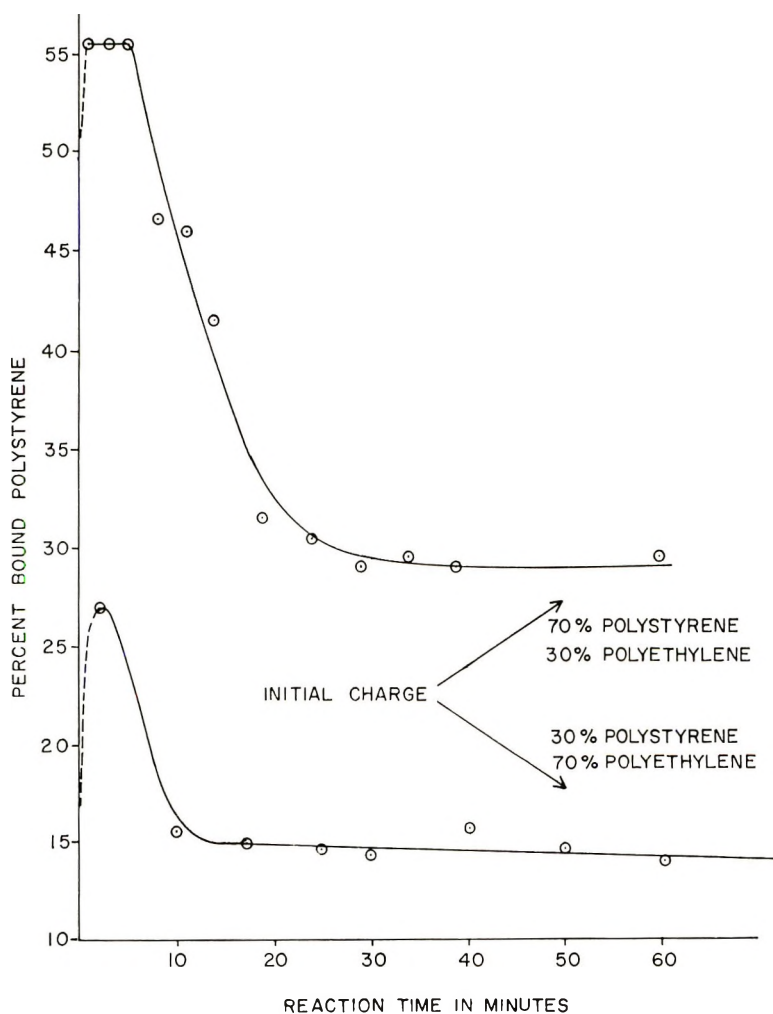
Fig. 2. Percent bound polystyrene in polyethylene–polystyrene block copolymers.

TABLE II
Physical Properties of a Polyethylene–Polystyrene Graft Polymer

Property	
Bound polystyrene, %	22
Yield strength, psi	729
Tensile strength, psi	2049
Modulus, psi	24,100
Elongation, %	22
Melt index, 190°C	No flow

(MEK), and the resulting solid was removed by filtration, redissolved in benzene, and again precipitated into MEK. Polystyrene homopolymer is completely soluble in MEK, so this procedure extracts out polystyrene and leaves behind a residue of polyethylene and polyethylene–polystyrene graft copolymer.

The concentration of polystyrene in samples containing 0–50% polystyrene was estimated by comparison of the ratio of infrared absorptions at 13.9 μ (polyethylene) and 14.4 μ (polystyrene) with a standard curve of the concentration ratio of polyethylene to polystyrene versus the 13.9 μ/14.4 μ ratio obtained with known mechanical mixtures of polyethylene and polystyrene. For samples containing 50–100% styrene a similar calibration curve utilizing the 13.9 μ (polyethylene) and 6.25 μ (polystyrene) absorptions was used. In all cases pressed films −1.5 mils thick were employed. Analytical data on the samples prepared above are summarized in Figure 2. Properties are shown in Table II.

When boron trifluoride etherate was used in place of aluminum chloride, no graft copolymers formed. Precipitation of the solution into MEK gave complete separation of the polyethylene and polystyrene.

In a control experiment a solution of 400 g of DYNH polyethylene, 25 g anhydrous aluminum chloride, and 3 liters of cyclohexane was heated at reflux (80°C) for 1.5 hr and precipitated into methanol. The recovered material could be pressed into a film, cold-drawn, and superficially resembled the starting material. However, treatment of polyethylene for 17 hr under these conditions or for shorter times at higher temperatures, converted it to a soft, waxy, solid.

Cationic Polymerization of Styrene
in the Presence of a Branched Polyethylene

A solution of 50 g DYGT polyethylene (branched, low molecular weight, polyethylene by the high-pressure process) in 100 g of styrene monomer was prepared, and the styrene was polymerized by the addition of a few drops of boron trifluoride etherate. Styrene homopolymer was removed from the gross product by solution in benzene and precipitation into methyl ethyl ketone. The polyethylene residue from this extraction showed a small infrared absorption at 14.35 μ which indicated the presence of about 2–3%

bound styrene (or polystyrene) derived either from addition to the tertiary hydrogens in the polyethylene or by alkylation of a styrene (or polystyrene) molecule.

Cationic Polymerization of Propylene in the Presence of C_2–C_3 Copolymer

A solution of 20 g of ethylene–propylene copolymer ($\sim$50%, C_3, prepared by $AlEt_3$–$TiCl_3$ catalyst) in 150 ml of cyclohexane was prepared at 70°C, then cooled to 30°C. Aluminum bromide (10 mmole) in 10 ml of cyclohexane was added, and propylene was bubbled through the solution at 1 g/min for 2 hr. The product was coagulated in methanol, washed in methanol, and dried; yield 40 g. This product was successively extracted with MEK to separate the carbonium ion-polymerized polypropylene oil.[15,16] The copolymer residue, 18 g, had an infrared spectrum identical with that of the starting material.

RESULTS

Prolonged treating of solutions of polyolefins with either aluminum chloride or aluminum bromide caused the viscosity of the solutions to decrease, indicating reduction in molecular weight. The data of Figure 1 show the decrease in intrinsic viscosity of the polymer as a function of time for linear polyethylene, ethylene–propylene rubber, and polypropylene, respectively. In all three cases there is a rapid drop in intrinsic viscosity from the initial values of 2.4–6.5 dl/g down to the 0.55–0.85 dl/g range in 5 min, followed by a somewhat slower decline in intrinsic viscosity over the next 2 hr.

The data of Table I show that there is an isomerization process, in addition to the degradation reaction. In the case of the high-density polyethylene the methyl content increases as the intrinsic viscosity of the polymer is decreased. In order to make a quantitative statement about the degree of isomerization it is necessary to know the number-average molecular weights of the polymer samples which cannot be rigorously obtained from the present data. However, in a qualitative sense the methyl contents of the samples are much too high to be due to endgroups alone, as shown by comparison with the last sample, which is a linear polyethylene of comparable intrinsic viscosity.

Somewhat surprisingly, it was also found that on treatment of mixed solutions of polyethylene and polystyrene in cyclohexane with aluminum chloride graft copolymer of polyethylene and polystyrene was formed. The grafting reaction is very rapid and occurs under somewhat milder conditions than the polymer degradation reaction. As shown by Figure 2 the maximum amount of polystyrene bound to polyethylene molecules is formed in the first 5 min of reaction with longer reaction times giving less graft polymer. Presumably, the initially formed copolymer undergoes subsequent degradation at the longer reaction times.

DISCUSSION

The Lewis acid-catalyzed addition of isobutane to isobutylene to form isooctane has been extensively studied and is thought to proceed by the following steps: reaction of aluminum chloride with some polar species to form an ionic complex,

$$AlCl_3 + HX \rightarrow (H)^{\oplus}(AlCl_3X)^{\ominus} \qquad (1)$$
$$\text{polar reagent}$$

formation of a carbonium ion from isobutylene,

$$CH_3-\underset{\underset{CH_2}{|}}{\overset{\overset{CH_3}{|}}{C}} + (H)^{\oplus}(AlCl_3X)^{\ominus} \rightarrow CH_3-\underset{\underset{CH_3}{|}}{\overset{\overset{CH_3}{|}}{C}}^{\oplus} + AlCl_3X^{\ominus} \qquad (2)$$

addition of the carbonium ion to olefin.

$$\underset{CH_3}{\overset{CH_3}{\diagdown}}C{=}CH_2 + \underset{CH_3}{\overset{CH_3}{\diagup}}{}^{\oplus}C-CH_3 \rightarrow CH_3-\overset{\oplus}{\underset{CH_3}{\overset{|}{C}}}-CH_2-\underset{CH_3}{\overset{CH_3}{\overset{|}{C}}}-CH_3 \qquad (3)$$

reaction of the new carbonium ion with isobutane

$$CH_3-\overset{\oplus}{\underset{CH_3}{\overset{|}{C}}}-CH_2-\underset{CH_3}{\overset{CH_3}{\overset{|}{C}}}-CH_3 + H-\underset{CH_3}{\overset{CH_3}{\overset{|}{C}}}-CH_3 \rightarrow CH_3-\underset{CH_3}{\overset{CH_3}{\overset{|}{C}}}-CH_2-\underset{CH_3}{\overset{CH_3}{\overset{|}{C}}}-CH_3 + {}^{\ominus}C-CH_3 \quad (4)$$

and repetition of the series makes a catalytic process.

$$R^{\oplus} + R-CH_2-CH_2-CH_2-CH_2{\sim} \rightleftharpoons$$

$$RH + R-CH_2-CH_2-\overset{\oplus}{CH}-CH_2- \qquad (5a)$$

$$R^{\oplus} + R'-CH_2-\underset{\underset{CH_3}{|}}{\overset{\overset{H}{|}}{C}}-CH_2-\underset{\underset{CH_3}{|}}{\overset{\overset{H}{|}}{C}}-CH_2{\sim} \rightleftharpoons$$

$$RH + R'-CH_2-\underset{\underset{CH_3}{|}}{\overset{\overset{H}{|}}{C}}-CH_2-\overset{\oplus}{\underset{\underset{CH_3}{}}{C}}-CH_2{\sim} \qquad (5b)$$

$$R^{\oplus} + R''-CH_2-\underset{\underset{\bigcirc}{|}}{\overset{\overset{H}{|}}{C}}-CH_2-\underset{\underset{\bigcirc}{|}}{\overset{\overset{H}{|}}{C}}-CH_2{\sim} \rightleftharpoons$$

$$RH + R''-CH_2-\underset{\underset{\bigcirc}{|}}{\overset{\overset{H}{|}}{C}}-CH_2-\overset{\oplus}{\underset{\underset{\bigcirc}{}}{C}}-CH_2{\sim} \qquad (5c)$$

In the present case, it is also likely that the initial carbonium ions are formed by reaction of the aluminum halide with fortuitous impurities (such as water, olefin, hydrogen chloride, alkyl halide, etc.), with the resulting ion then attacking the polymer backbone.

The resulting polymer ions can then undergo cleavage simply by rearrangement of electrons:

$$R—CH_2—CH_2—CH—CH_2—— \longrightarrow RCH_2^{\oplus} + CH_2=CHCH_2—— \tag{6}$$

Methyl branching can be introduced either by a direct isomerization [eq. (7)] or by repolymerization of olefinic fragments [eq. (8)].

$$R—CH_2—CH_2—\overset{\oplus}{C}H—CH_2—— \longrightarrow \overset{\oplus}{C}H_2—CH—CH_2——$$
$$\underset{CH_2—R}{|} \tag{7}$$

$$\overset{RH}{\swarrow}$$

$$CH_3—CH—CH_2—— + R^{\oplus}$$
$$\underset{CH_2—R}{|}$$

$$2\ CH_2=CH—CH_2—— \xrightarrow[HX]{AlCl_3} ——CH_2—\overset{\overset{CH_3}{|}}{CH}—CH_2—CH_2—CH_2—— \tag{8}$$

Graft copolymers of polyethylene and polystyrene could conceivably be formed when an olefinic (or carbonium ion) polyethylene fragment [such as from eq. (5a) or (6)] undergoes a Friedel-Crafts addition to one of the aromatic nuclei of polystyrene.

$$——CH_2—CH=CH_2 + ——\overset{\overset{H}{|}}{C}—CH_2—\overset{\overset{H}{|}}{C}—CH_3 \longrightarrow ——\overset{\overset{H}{|}}{C}—CH_2—\overset{\overset{H}{|}}{C}—CH_2 \tag{9}$$

Conducting the polymer degradation reactions in the presence of other types of aromatic ligands could conceivably be used to make a variety of graft polymer or telogen species.

It is particularly interesting to consider the fate of the polymer ions [eq. (5)] formed when the polymer is either a branched polyethylene, a copolymer, or isotactic polypropylene. In principle, those ions might react further with polymerizable monomers to form new polymers [eq. (10)]

$$ (10) $$

However, when boron trifluoride etherate was used to polymerize styrene in the presence of a branched polyethylene and the resulting product washed free of polystyrene homopolymer, the recovered product showed only traces (estimated at 2–3%) of aromatic absorption in the infrared spectrum. This indicates that negligible styrene incorporation occurred. Similarly, when propylene was polymerized in the presence of C_2–C_3 copolymer, the recovered copolymer showed no weight increase and no change in the

8.7 μ infrared absorption which is due to the $-\overset{\mid}{\underset{\mid}{C}}-$H structure.[17,18] When

isotactic polypropylene was degraded in molecular weight by aluminum chloride attack, the recovered low molecular weight product retained its isotacticity. This fact argues that the formation of the polymer ion [eq. (5)] is essentially irreversible, since equilibration would form atactic polypropylene. The combined lack of equilibration in this case and lack of subsequent reaction in the C_2–C_3 copolymer case probably means that once the ion is formed on the polymer backbone, chain cleavage occurs rapidly and probably irreversibly, even though the cleavage process necessarily involves conversion of secondary-to-primary or tertiary-to-secondary ions which is energetically difficult.

References

1. C. A. Thomas, *Anhydrous Aluminum Chloride in Organic Chemistry*, Reinhold, New York, 1948.

2. G. A. Olah, Ed., *Friedel-Crafts and Related Reactions*, Interscience, New York, 1964.

3. F. C. Conden, in *Catalysis*, Vol. VI, P. H. Emmet, Ed., Reinhold, New York, 1958, p. 43.

4. H. Pines and N. E. Hoffman, in *Friedel-Crafts and Related Reactions*, Vol. II, G. A. Olah, Ed., Interscience, New York, 1964, p. 1211.

5. H. H. Voge, in *Catalysis*, Vol. VI, P. H. Emmett, Ed., Reinhold, New York, 1958, p. 407.

6. R. M. Kennedy, in *Catalysis*, Vol. VI, P. H. Emmett, Ed., Reinhold, New York, 1958, p. 1.

7. D. C. Pepper, *Friedel-Crafts and Related Reactions*, Vol. II, Part 2, G. A. Olah, Ed., Interscience, New York, 1964, p. 1293.

8. A. M. Eastham, in *Encyclopedia of Polymer Science and Technology*, Vol. III, H. F. Mark and N. G. Gaylord, Eds., Interscience, New York, 1965, p. 35.

9. W. J. Burlant and A. S. Hoffman, *Block and Graft Polymers*, Reinhold, New York, 1960.

10. H. C. Haas, P. M. Kamath, and N. W. Schuler, *J. Polym. Sci.*, **24**, 85 (1957).

11. G. Kockelbergh and G. Smets, *J. Polym. Sci.*, **33**, 227 (1958).

12. P. H. Plesch, *Chem. Ind.* (London), **1958**, 954.

13. R. G. Newberg, C. K. Schramm, and H. W. Bowman, German Pat. 1,165,271; *Chem. Abstr.*, **61**, 4572b (1964).

14. J. P. Luongo, *J. Appl. Polym. Sci.*, **3**, 302 (1960).

15. C. Y. Liang and W. R. Watt, *J. Polym. Sci.*, **51**, 814 (1961).

16. V. L. Folt, J. J. Shipman, and S. Krimm, *J. Polym. Sci.*, **52**, S 20 (1963).

17. N. Sheppard and D. Simpson, *Quart. Revs.*, **7**, 19 (1953).

18. P. E. Wei, *Anal. Chem.*, **33**, 215 (1961).

Electrochemical Anionic Polymerization of 4-Vinylpyridine in Pyridine

S. N. BHADANI and G. PARRAVANO, *Department of Chemical and Metallurgical Engineering and Macromolecular Research Center University of Michigan, Ann Arbor, Michigan 48104*

Synopsis

The preparation of poly-4-vinylpyridine (poly-4VP) by electrochemical polymerization of 4-vinylpyridine (4VP) in pyridine containing sodium tetraphenylboron (NaBPh$_4$) is described. Information on the influence of monomer concentration, current density, polymerization rate, molecular weight, and electrochemical efficiency is presented. The polymerizations were performed under conditions of constant electrolysis current. Polymer formed in the cathodic compartment only, where a red-orange solution developed after about 15 min of electrolysis time. The optical absorption spectra of these colored solutions were studied. Cyclic voltammograms of 4VP in pyridine and NaBPh$_4$ are also reported, and the influence of the scan rate upon peak current is described. The results indicate that the polymerization was anionic and nonterminating. The characteristics of the electrochemical polymerization of 4VP in pyridine are compared with those of the same monomer in liquid NH$_3$. In the former case, the catholyte was homogeneous, and polymer growth occurred in the liquid phase, while in the latter growth took place in a heterogeneous environment. Kinetic consequences of these physical differences are pointed out. Suggestions for the mechanism of this electrochemical initiation are advanced.

INTRODUCTION

In a recent study of the electrochemical polymerization of 4-vinylpyridine (4VP) in liquid NH$_3$ containing NaCl or NaN$_3$, it was shown that a polymeric red-orange mass formed exclusively around the cell cathode (Pt). This system produced high electrochemical yields and polymers of high molecular weight ($\sim 10^5$). Chain transfer or termination with monomer or solvent did not occur readily. However, the originally homogeneous liquid phase soon became heterogeneous because of the insolubility of poly-4VP in liquid NH$_3$.

In the present communication we report investigations of the electrochemical anionic polymerization of 4VP in pyridine. Pyridine represents an attractive medium for electrochemical polymerizations since it dissolves a variety of monomers and polymers including poly-4VP, it provides a good electrical conducting medium by dissolving a large number of inorganic and organic salts, and, since it has pK_b = 8.8, it may be expected

225

to support many anionic as well as free radical polymerizations.   In this latter instance, it has already been tested in a polymerization system with chemical initiation.[2]   Pyridine as a solvent for electrochemical polymerization has not been fully tested, since only a short report on the electrochemical polymerization of styrene in pyridine has appeared.[3]   For these reasons it seemed interesting to study whether 4VP could be polymerized electrochemically in pyridine and, if polymerization resulted, to assess some of the characteristics of the polymerization and to verify whether this polymerization possessed features different from the known heterogeneous, electrochemical, living polymerization of this monomer in liquid NH_3.

The results of this study are reported in this communication together with information on monomer reduction potentials obtained by cyclic voltammetry under conditions similar to those employed for polymerization.

EXPERIMENTAL

Materials

Pyridine was dried over CaH_2 for several days at room temperature and then fractionally distilled in a wetted-wall column under N_2 atmosphere. The middle fraction was collected in a flask containing CaH_2.   The flask was attached to a vacuum system and the pyridine was flash distilled into a thoroughly dried and evacuated flask with CaH_2.   The final purified pyridine was kept stirred over CaH_2 on the vacuum manifold.   4VP was purified and stored as described previously.[4]   Sodium tetraphenyl-boron ($NaBPh_4$) from a commercial source was used without further purification.
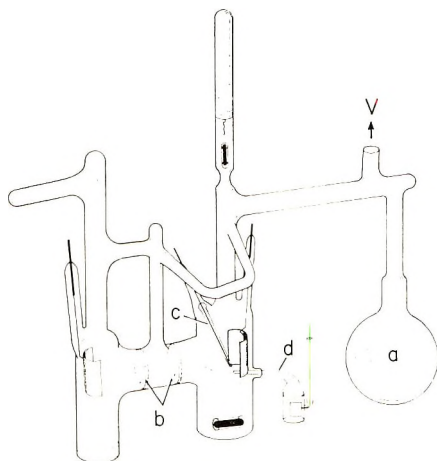

Fig. 1. Electrolytic cell used to study polymerization of 4VP in pyridine: (a) filling bulb; (b) fritted glass disks; (c) micro Pt electrode; (d) reference electrode; (v) vacuum line.

Equipment

The electrolytic cell used is shown in Figure 1. Two Pt electrodes (1 × 1 in.) were housed in the cell which was divided by two fritted glass discs (medium porosity) of 2 cm diameter. The cathode compartment of the electrolytic cell contained also a planar Pt microelectrode ($^1/_6$ in. diameter). An Ag/AgCl reference electrode with a Luggin capillary was also sealed to the cathode compartment. The preparation of the Ag/AgCl reference electrode has already been described.[5] This type of multielectrode electrolytic cell could be used for electrochemical polymerization and analytical work under high vacuum conditions. A Wenking 6IRH potentiostat, coupled with a Wavetek Model 111 voltage function generator and a Honeywell x-y recorder were employed.

Polymerization Procedure

A known amount of NaBPh$_4$ was introduced into the filling bulb (d in Fig. 1), and the electrolytic cell was attached to the vacuum line. The apparatus was evacuated and electrically baked at $\sim$10^{-6} torr and 60°C for 12–16 hr. The vacuum manifold and connected parts were flushed several times with purified N$_2$. The required amount of pyridine was flash distilled into the bulb and degassed thoroughly by repeated freezing and thawing cycles. The apparatus was sealed off from the vacuum line and the contents of the filling bulb were thoroughly mixed at room temperature, and transferred to the anode, cathode, and reference electrode compartments. The monomer was introduced into the cathode compartment by breaking the ampule attached to the cathode compartment. The total volume of the solution was 105 ml and that of the catholyte 65 ml. All electrolytic runs were carried out at room temperature. At the end of a run the electrolyzed monomer solution containing dissolved polymer was slowly added to well stirred tetrahydrofuran (THF) at 0°C. The polymer precipitated as white flock; it was filtered, washed with THF, and vacuum-dried overnight at 50°C. Polymer molecular weights were obtained as described previously.[1]

RESULTS

Cyclic Voltammetry

The cyclic voltammograms of 4VP were obtained in anhydrous pyridine solution containing 3 × 10^{-2} mole/l. NaBPh$_4$. The monomer exhibited a cathodic peak at −2.15 V (Fig. 2). At higher potential (> −2.4 V) a new peak appeared, probably from the reduction of pyridine or NaBPh$_4$. An anodic peak was found at −0.6 V. It was attributed to the oxidation of the reduction product formed at potential > −2.25 V, since it did not appear when the potential scan was limited to −2.25 V. The anodic peak at −0.6 V occurred also in the absence of 4VP.
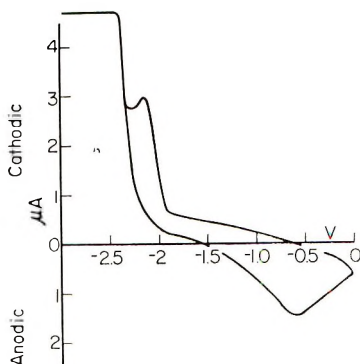
Fig. 2. Cyclic voltammogram of 4VP, 8.1 mole/l. in pyridine with 30 mmole/l. NaBPh₄ at 25°C. Planar Pt microelectrode.
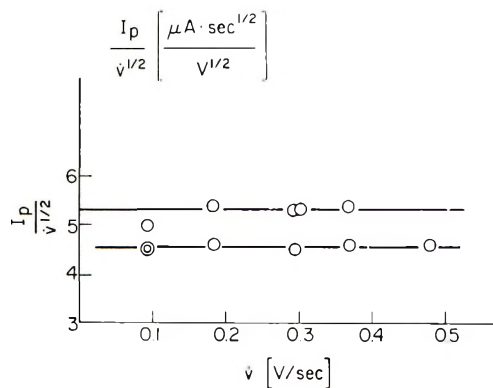

Fig. 3. Plot of $I_p/\dot{v}^{1/2}$ vs. $\dot{v}$ for the cathodic reduction of 4VP in pyridine containing 30 mmole/l. NaBPh₄: (top) 8.1 mmole/l. 4VP; (bottom) 15.1 mmole/l. 4VP.

The cathodic peak current increased with increasing scan rate. Plots of $I_p/\dot{v}^{1/2}$ vs $\dot{v}$, where I_p and $\dot{v}$ are the current peak and scan rate, respectively, showed horizontal straight lines (Fig. 3). A 40 mV shift in peak potential was noted for a 5-fold change in scan rate (from 0.1 to 0.5 V/sec). No linear dependence of cathodic peak current on monomer concentration was observed.

The resistance compensation was not employed because the ohmic drop in the electrolytic cell was negligible (<0.002 V). The solution of tetraphenylboron in pyridine provided a highly electrical conducting medium. Therefore, the exclusion of the resistance compensation did not affect our experimental results.

Polymerization and Polymer Characteristics

All polymerizations were carried out under conditions of constant current electrolysis. Because of practical difficulties, polymerization with constant current electrolysis was not performed.

TABLE I

Electrochemical Polymerization of 4VP in Pyridine with 20 mmole/l. NaBPh$_4$ at 25°C

| Run	Monomer addition, g		Current, mA	Time of electrolysis, min	Polymer yield, g	$[\eta]$, dl/g	MW $\times$ 10^{-4}, g/mole	Electrical efficiency, moles polymer/Faraday
	First	Second						
AI	2.97	—	2	31	2.71	1.46	30.5	0.23
AII	2.97	0.99	2	30	3.78	1.76	40.0	0.27
BI	0	2.97	2	30	0.82	0.86	14.1	0.16
BII	0	2.97	5	35	2.87	0.86	14.1	0.19
C	2.97	—	3	25	2.74	1.21	23.2	0.25
D	2.97	—	4	21	2.70	1.10	20.2	0.24
EI	2.97	—	5	22	2.86	1.06	19.2	0.22
EII	2.97	2.18	5	22	4.98	1.32	26.3	0.25
F	2.97	—	1	65	2.52	2.24	56.7	0.10
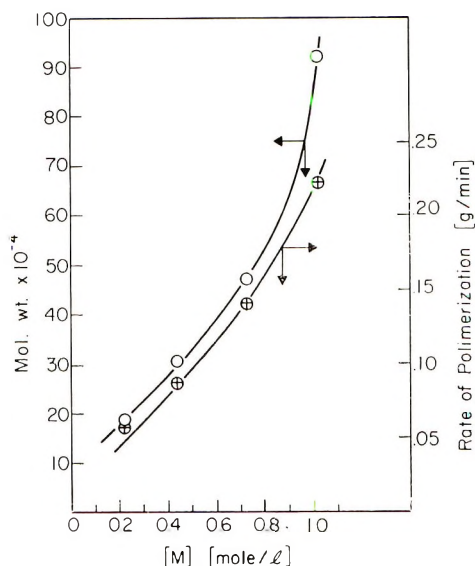
Fig. 4. Polymerization rate (⊕) and molecular weight (○) vs. monomer concentration for the electrochemical polymerization of 4VP in pyridine at 25°C, current density 2mA/cm².

An induction period of 15 min was observed for polymerization but not for the formation of an orange-red mass around the cathode. Upon passage of the electric current through the 4VP solutions an orange-red mass (characteristic color of living 4VP anions) appeared immediately around the cathode but disappeared quickly in the solution and no polymerization occurred for few minutes. Probably this resulted from living anions formed at the cathode and initially consumed by residual impurities present in the solution. After the impurities had been purged by reaction with the 4VP anions, polymerization started, and the catholyte became viscous and orange-red. The induction period was dependent upon the impressed current.

Upon introduction of air, moisture, or other foreign substances, the catholyte color disappeared. Furthermore the polymerization did not occur without passage of the electric current or if these impurities were originally present. It was found that the polymerized orange-yellow or orange-red solution obtained after cessation of the electrolysis retained the ability to continue the polymerization if additional monomer was supplied to it. In some experiments (AII, EII, Table I), a second ampule of the monomer was introduced into the catholyte compartment after complete polymerization of the original amount. After addition of the second aliquot no current was passed through the solution. The catholyte was stirred for 15 min and then polymerization was terminated with the addition of a few drops of methanol. The polymer yields were almost equal to the total amounts of monomer used, as shown by comparison with control experiments AI, EI (Table I). The molecular weights of the polymer in-

creased from 305000 to 400000 (experiments AI and AII) and from 192000 to 263000 (experiments EI and EII).

Integral rates of polymer formation increased, whereas polymer molecular weights decreased with increasing current densities. The observations on polymerization rate and polymer molecular weight are summarized in Table I.

Figure 4 shows the effect of monomer concentration on the integral rate of polymerization and molecular weights at a constant current of 2mA.

The polymers obtained were white and soluble in CH_3OH, CH_3Cl, and dimethylformamide, but insoluble in H_2O, $(CH_3)_2CO$, THF, and petroleum ether. C_6H_6 and $C_6H_5CH_3$ were found to swell the polymers. Polymers melted in the range of 160–190°C. No significant differences were found in the infrared spectra between poly-4VP produced electrochemically in pyridine, in liquid NH_3,[1] or chemically in toluene with BuLi.[4]

When an equimolar mixture of 4VP and styrene in pyridine was subjected to electrolysis at 2mA, no copolymer formed, but only poly-4VP, as indicated by the infrared spectra and solubility behavior of the resulting polymers.

Optical Absorption Spectrum

The absorption spectra of the orange-red solution, obtained by electrolysis of 0.43 mole/l. 4VP in pyridine at room temperature, are shown in Figure 5 (curves a and b). Curve b shows the spectrum measured 20 hr after the measurement of curve a. The initial 373 mμ peak decreased with time and a distinct peak at 570 mμ appeared.

When a solution of 0.3 mole/l. 2VP in pyridine was subjected to electrolysis at 1 mA for 60 min, the catholyte became viscous and yellow. The
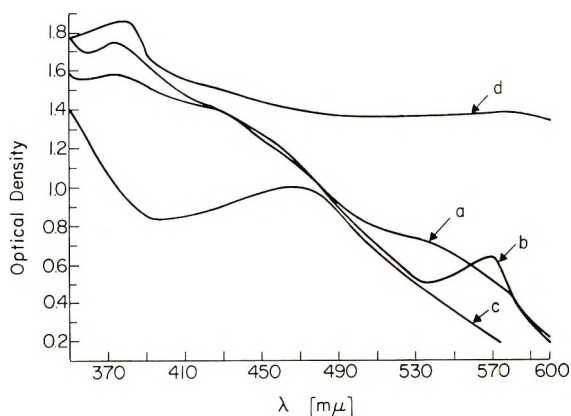

Fig. 5. Absorption spectra of 4VP and 2VP in pyridine containing 20 mmole/l. NaBPh$_4$ at 25°C: (a) 0.43 mole/l. 4VP electrolyzed for 30 min at a current of 2 mA; (b) spectrum measured 20 hr after the measurement of curve a; (c) 0.30 mole/l. 2VP electrolyzed at 1 mA for 60 min; (d) pyridine containing 20 mmole/l. NaPBh$_4$ electrolyzed in the absence of monomer at 3 mA for 28 min.

liquid showed an absorption maximum at 470 mμ (curve c in Fig. 5). The color and absorption spectrum of the yellow solution remained unchanged for a long period of time.

The electrolysis of NaBPh$_4$ in pyridine (3 mA for 28 min) resulted in the formation of deep yellow color at the catholyte. This color gradually changed to green and finally to blue. Curve d in Figure 5 represents the spectrum of the blue solution displaying a peak at 380 mμ.

To explore whether or not yellow and blue solutions of reduced pyridine would initiate polymerization of 4VP, experiments BI and BII (Table I) were performed. In run BI pyridine was electrolyzed until it became deep yellow and then 4VP was introduced. The catholyte rapidly became pink-red and subsequently turned again to faint yellow. In experiment BII pyridine was subjected to electrolysis until the catholyte became deep blue. On addition of 4VP, the blue solution again became deep pink-red and viscous. In both cases polymers with high molecular weight were obtained (Table I).

DISCUSSION

The results presented in the previous section clearly show that 4VP can be polymerized electrochemically in pyridine containing NaBPh$_4$. As a result of the passage of the electrical current, polymer formation occurred exclusively in the cathode compartment, and the catholyte became yellow or orange-red depending on current intensity while the anolyte remained colorless. In the cyclic voltammetry experiments the peak at -2.15 V (Fig. 2) is attributed to direct electron transfer from the Pt cathode to the vinyl bond of 4VP resulting in the formation of monomeric radical anions. This has been further corroborated by the linear dependence of $I_p/\vartheta^{1/2}$ with (Fig. 3), as is expected for an electrochemical mechanism.[6] Direct elec-
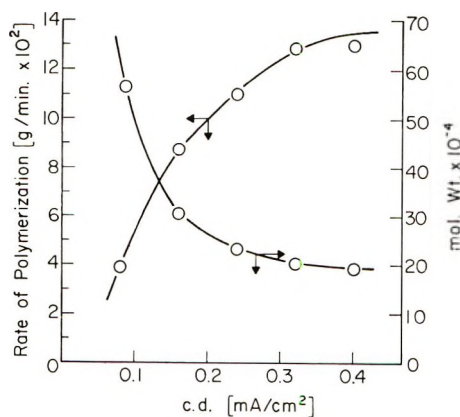

Fig. 6. Polymerization rate and molecular weight vs. current density for the electrochemical polymerization of 0.43 mole/l. 4VP in pyridine with 20 mmole/l. NaBPh$_4$ at 25°C.

tron transfer to vinyl monomers was previously reported.[1,7]   The absence of the anodic peak, when the scan was limited to −2.25 V, points out that anodic electron transfer from the radical anions is slow or irreversible or the radical anions react rapidly.

The integral rates of polymer formation increased and polymer molecular weights decreased with increasing current density (Fig. 6).   This is expected, since a high current density increases the concentration of initiating species which in turn enhances propagation rate and decreases polymer molecular weight.   Polymerization rates and molecular weights increased with monomer concentration (Fig. 4).   A fivefold increase in monomer concentration enhanced the molecular weight by about a similar amount.   In the 4VP–liquid NH₃ systems,[1] the integral rates of polymerization and the polymer molecular weights were found to be almost independent of monomer concentration.   The authors[1] had suggested that hindrance of monomer diffusion into polymer deposits, in which active centers were imbedded, caused the polymerization rate and molecular weight to be independent of the initial monomer concentration.   Unlike liquid NH₃, pyridine furnished a homogeneous reaction medium, hence polymer growth took place preponderantly in the liquid phase where monomer molecules were easily accessible to growing polymer chains.   Therefore in such systems, where chain transfer and termination processes are absent or at least negligible, the molecular weight of polymer is likely to increase with the increase of monomer concentration.   The two-stage monomer addition experiments (AI and AII, and EI and EII, Table I) indicate that the polymerization of 4VP in pyridine is nonterminating.

The electrolysis of an equimolar mixture of 4VP and styrene in pyridine resulted exclusively in the formation of poly-4VP.   This is to be expected in anionic polymerization, because 4VP, having relatively high electron affinity, is more reactive than styrene with growing polymeric anions.   It should be noted that the increase in molecular weight upon the addition of the second aliquot of monomer does not exactly correspond to that expected if all the monomer were employed to add to the existing chains.   Secondary reactions may have been responsible for this.

The electronic spectra of living polymer of 2VP and 4VP in THF exhibit an absorption maximum at 315 mμ.[8]   In pyridine nonterminated poly-4VP showed a peak at 373 mμ (Fig. 5a) and nonterminated poly-2VP at 450 mμ (Fig. 5c).   Since pyridine is a more polar solvent than THF (dielectric constants: pyridine-12.3, THF-7.6), carbanions derived from 2 VP and 4 VP may exist in pyridine as free anions or solvent separated ion pairs. Therefore the occurrence of red bathochromic shifts is likely.[9,10]   It was found that the initial 373 mμ peak decreased with time and a new peak at 570 mμ appeared (Fig. 5b).   This change may be attributed to side reactions of living polymers.[11]

In previous work[12−14] it was discovered that the reduction of anhydrous pyridine by alkali metals results in the formation of a yellow solution which gradually changes to green, then blue.

The electronic spectrum of the yellow solution was found to contain a broad band at 330 mμ and that of the blue solution two bands at 381 and 590 mμ. The yellow color was attributed to pyridyl radical anions and the blue color to 4,4'-bipyridyl radical anions.[14] The absorption spectra at 381 and 590 mμ are equivalent to those in the same region found in this study (Fig. 5d). The results from runs BI and BII demonstrate that the electrolyzed solutions of pyridine are capable of initiating the polymerization of 4VP resulting in the formation of high molecular weight polymers. Pyridyl and/or 4,4'-bipyridyl radical anions may be responsible for initiating polymerization.

Mechanism of Polymerization

In the present system three possible modes of initiation can be visualized, namely: (1) direct electron transfer from cathode to monomer:

$$M + e^- \rightleftharpoons M^-$$
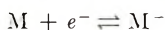
where M, e$^-$ represent monomer and electron, respectively: (2) electron transfer to monomer from Na metal deposited on the cathode:

$$Na^+ + e^- \rightleftharpoons Na$$
$$Na + M \rightleftharpoons M^-Na^+$$
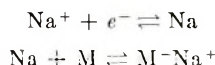
(3) initiation by pyridyl radical anions formed by reduction of pyridine:
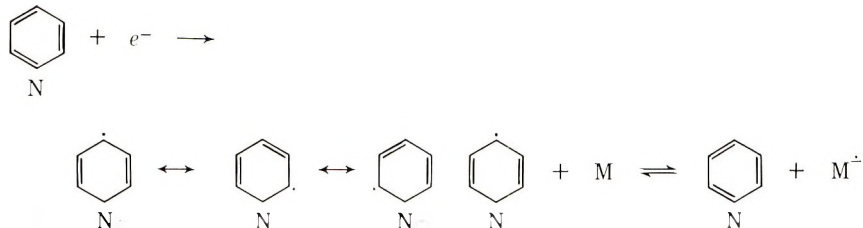
The results from cyclic voltammetry show that the reduction potential of the solvent (or NaBPh$_4$) is more negative than that of 4VP (Fig. 2). Therefore, scheme (1) would be preponderant for initiation, although other initiation processes cannot be ruled out because of close proximity of reduction potentials of monomer, solvent, and salt. Ideal anion–radical growth is characterized by an electrochemical efficiency of 1 while for ideal dianion growth it is 0.5. The electrochemical efficiency is given by the average number of polymer molecules produced per electron. The observed electrochemical efficiency is about 0.22 (Table I). This is attributed to residual impurities present in the polymerizing solution, and it is supported by the observation of an induction period during polymerization. It is probable that radical anions formed at the electrode dimerize, resulting in the formation of dianions which lead dianionic growth of polymerization. The sensitivity of the reaction to air, moisture, and protic substances, the high polymerization rate, and the nonterminating behavior suggest that anionic intermediates are responsible for the propagation process.

In the liquid NH_3–4VP system, the propagation step occurred near the electrode surface or within the polymer deposited on the cathode because the resulting polymers were insoluble in liquid NH_3 and adhered to the electrode. In contrast to this behavior, polymer formation in pyridine occurred at the electrode and in solution because of the solubility of the growing polymers.

CONCLUSIONS

The experimental findings of this work revealed the following.

(*1*) The passage of an electric current through 4VP solutions of pyridine in the presence of dissolved $NaBPh_4$ produces homogeneous, nonterminating polymerizations of the monomer at smooth Pt cathodes.

(*2*) Poly-4VP of high molecular weight ($\sim 10^5$) is formed in the catholyte.

(*3*) The reduction potential of the monomer at Pt cathode (-2.2 V) is more positive than that of pyridine and $NaBPh_4$ (> -2.48 V).

(*4*) The polymerization rate and polymer molecular weight increased with monomer concentration. The rate of polymerization decreases while the polymer molecular weight increases with current density.

(*5*) After having been subjected to electrolysis, pyridine initiates polymerization without further passage of electrical current and produces polymer in high yield and with high molecular weight.

References

1. D. G. Laurin and G. Parravano, in *Macromolecular Chemistry Brussels–Louvain 1967* (*J. Polym. Sci. C*, **22**), G. Smets, Ed., Interscience, New York, 1968, p. 103.

2. S. Tazuke and S. Okamura, *J. Polym. Sci. A-1*, **4**, 141 (1966).

3. J. Y. Yang, W. E. McEwen, and J. Kleinberg, *J. Amer. Chem. Soc.*, **79**, 5833 (1957).

4. P. P. Spiegelman and G. Parravano, *J. Polym. Sci. A*, **2**, 2245 (1964).

5. D. J. G. Ives and G. J. Janz, Eds., *Reference Electrodes Theory and Practice*, Academic Press, New York, 1961, p. 203.

6. R. S. Nicholson and I. Shain, *Anal. Chem.*, **36**, 706 (1964); *ibid.*, **37**, 178 (1965).

7. B. L. Funt and F. D. Williams, *J. Polym. Sci. A*, **2**, 865 (1964).

8. C. L. Lee, J. Smid, and M. Szwarc, *Trans. Faraday Soc.*, **59**, 1192 (1963).

9. R. Waack and M. A. Doran, *J. Phys. Chem.*, **67**, 148 (1963).

10. T. E. Hogen-Esch and J. Smid, *J. Amer. Chem. Soc.*, **88**, 307 (1966).

11. G. Spach, M. Levy, and M. Szwarc, *J. Chem. Soc.*, **1962**, 355.

12. A. Carrington and J. Santos-Veiga, *Mol. Phys.*, **5**, 21 (1962).

13. R. L. Ward, *J. Amer. Chem. Soc.*, **83**, 3623 (1961).

14. C. D. Schmulbach, C. C. Hinckbly, and D. Wasmund, *J. Amer. Chem. Soc.*, **90**, 6600 (1968).

Uses of Electron Paramagnetic Resonance in Studying Fracture

K. L. DEVRIES, D. K. ROYLANCE,* and M. L. WILLIAMS,
College of Engineering, University of Utah, Salt Lake City, Utah 84112

Synopsis

The uses of electron paramagnetic resonance (EPR) in studying aspects of polymer fracture are discussed. The sensitivity of EPR is such that all phases of fracture are not amenable to investigation by these means. This paper attempts to define those areas where the authors' experience would indicate that success might or might not be expected. A discussion of the difference between the tensile fracture of drawn polymer fibers, in which strong signals are obtained, and cast and molded materials is given.

INTRODUCTION

The original studies of Zhurkov and his associates[1,2] in the USSR and the later work by Williams et al.[3,4] and Campbell and Peterlin[5] have demonstrated the usefulness of electron paramagnetic resonance (EPR) in studying polymer fracture. At first, this method would seem to open unlimited avenues for research and provide a panacea for fracture studies. There are, however, a number of areas where the authors have attempted to use this technique but have not met with much success. Because a number of groups have expressed interest in conducting studies using these methods, it was thought it might be well to describe the techniques developed. In addition, the areas of fracture research in which the authors' experience would indicate that EPR will or will not be likely to reveal much in the way of quantitative information will be discussed. Since some of these studies (where negative results were obtained) have interesting implications, it was thought it might be well to report some of these findings as well as some limits on the usefulness of the method so as to reduce duplication and repetition of searches along blind paths.

BACKGROUND

EPR is a form of absorption spectroscopy in which electromagnetic radiation in the microwave region induces transitions between energy levels arising from Zeeman-type splittings in an assemblage of paramagnetic electrons. As such, it deals with systems of elementary particles which

---

* Present address: U. S. Army Materials and Mechanics Research Center, Watertown, Massachusetts.

have a net electronic moment (unpaired electron spins). Thorough descriptions of EPR, its uses, and applications are found in several recent reviews and books.[6-10] In polymer materials, fracture under mechanically applied stress involving molecular bond rupture should result in the creation of free radicals and their accompanying characteristic unpaired electrons; thus, it might logically be studied by this method. An EPR analysis, however, has two practical requirements: sufficient number of free radicals must be produced, and the half-life of the free radicals formed must be long enough to record. The Varian E-3 equipment used in these tests operates in the x-band region ($\sim$9.5 ghz) and has a sensitivity of about $5 \times 10^{10} \Delta H$ (ΔH, the line width in gauss) spins under ideal conditions.

If one views a polymer as being composed of long more or less parallel chains looped together in an orderly array, then a polymer having the density and molecular structure of nylon would have approximately 10^{14} chains passing through each square centimeter of area normal to the direction of the chains.[5] Assuming a covalent bond energy of approximately 80 kcal/mole and that a fracture surface can be approximated as a plane of such broken bonds, the theoretical fracture energy per unit area is roughly 250 ergs/cm². Experimental macroscopic crack growth and tearing studies indicate a value more than an order of magnitude higher than this. It would appear, therefore, that fracture is more complex than a simple cleavage of atomic bonds along the fracture surface. Alternately, one can use the tabulated bond strengths along with the number of broken bonds to compute the ideal tensile strength of a polymer. If it is assumed that a few angstroms of displacement is sufficient to separate or rupture a bond, one finds that a polymer should possess a tensile strength of the order of 10^6 psi (see the discussion by Peterlin[5]). This estimate is one or two orders of magnitude higher than experimental values. This latter discrepancy might be reasonably attributed to the inhomogeneity of the internal stress field due to such factors as local stress concentrations, interchain entanglements, folds, or alternating amorphous regions between regions of crystallinity. There are several possible explanations for the large surface energy discrepancy. (1) Bonds will be broken throughout the volume of the specimen, not solely on the single plane of major cleavage. Energy is required to rupture these bonds as well as those nearer the fracture surface. (2) Bond rupture or cracks might nucleate at a great many sites but not all of them progress to macroscopic size and subsequent fracture. (3) The true fracture surface might be much larger than the apparent area due to the roughness of the fracture surfaces. (4) Other dissipative functions such as plastic or viscoelastic mechanisms are operative in front of a progressing crack. (5) Secondary (van der Waal) bonds are broken and absorb energy during the untangling of the chains.

It is likely that all of these mechanisms are active to some extent and one might expect the gross behavior to be the summation of simultaneous effects of several phenomena such as chain slippage, viscous energy dissipations, and bond scission. These processes would be expected to vary with poly-

mer type, sample crystallinity, and testing conditions, e.g., strain rate, temperature, humidity, atmosphere. EPR spectroscopy, being able to detect and monitor bond breakage, should be a powerful tool for elucidating the relative importance of these various mechanisms and how they vary with testing or service conditions.

APPARATUS AND EXPERIMENTAL PROCEDURES

In addition to the Varian E-3 electron paramagnetic resonance spectrometer used in these studies, auxiliary equipment included a variable temperature control unit and a programmed loading fixture. The former maintained the sample at any fixed temperature between $-180°C$ and $+300°C$ and permitted control of the atmospheric environment. The loading frame and hydraulic servo system was designed to load the sample at constant stress, strain, strain rate, stress rate, or with relative ease, any reasonable preprogrammed loading.

For sensitivity reasons, the spectrum normally recorded on an EPR spectrometer is the first derivative of the absorption curve. Its second integral is proportional to the number of unpaired electrons in the cavity. In this study this integration was numerically accomplished on a Univac 1108 computer. A comparison of this double integral with that for the "pitch" standards provided by Varian Associates gave a quantitative measure of the free radicals (ruptured bonds) present. It was determined, however,
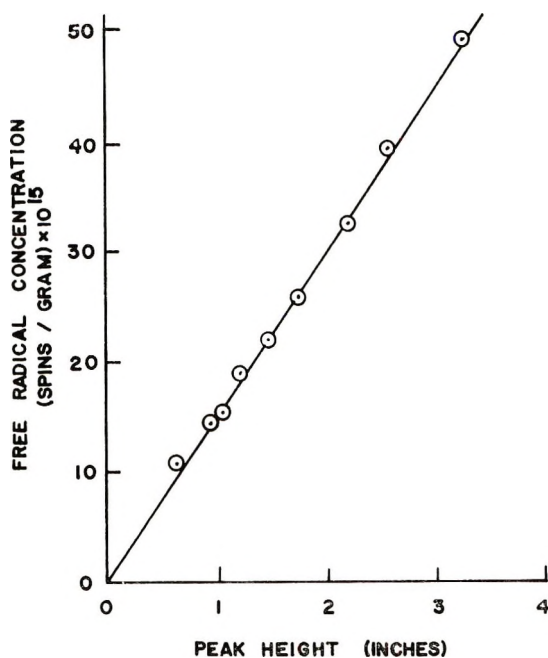

Fig. 1. A comparison of the free-radical concentration (obtained from twice integrating the spectra) with the height of the first peak.

that in some cases this process could be substantially simplified. It can be shown that for a Gaussian or Lorentz distribution, the peak height of the derivative of the function is proportional to the first integral. For polymers with simple spectra it often was possible, through comparison with the double integral, to show experimentally that the peak height of the spectra was proportional simply to the second integral. Figure 1 shows the number of unpaired electrons (spins) determined by numerical double integration versus peak height for nylon 6. Similar results were obtained for nylon 66 and polyethylene. These results greatly facilitate the experimental observations. The rate of bond rupture can as a result be monitored by tuning the spectrometer to the field strength and frequency of one of the spectra peaks and observing its growth as a function of time.

OUTLINE OF STUDIES

These versatile techniques have been found to be useful in a wide variety of studies of fracture and other types of mechanical degradation or failure. Since the authors began using this tool approximately two years ago, they have begun investigations into: fracture of polymer materials under tensile stress; post-fracture analysis of materials after combined loading; fracture remnants from explosive and impact damaged specimens; fracture surfaces originating from machining, grinding, and crushing operations; cumulative damage in polymers during cyclic and other programmed loadings; the role of environment, such as temperature, humidity, atmosphere (i.e., inert gases, oxygen, and ozone) upon free radical concentrations; the effects of various solvents upon stress crazing in plastics; and free-radical concentration in living tissue, such as collagen.

In addition to studying the results of mechanical degradation processes, certain effects of γ-radiation have also been explored. In this connection it may be observed that a comparatively large amount of work with EPR had been carried out on effects of radiation upon materials. Comparison with these studies permitted a correlation and standardization for our subsequent studies of mechanical degradation because of the similarity in the spectra.

This paper, however, is restricted primarily to discussion of some positive and negative results encountered in attempting to correlate quantitative measurement of free-radical concentration with mechanically induced microscopic flaw formation.

EXPERIMENTAL RESULTS

Tensile Fracture

The microwave cavity of the E-3 spectrometer is approximately 1.1 cm in diameter and 2.5 cm in length. The sample itself is usually restricted to less than 0.9 cm in diameter, which corresponds to a cross-sectional area of approximately 0.5 cm². Hence, based on the background discussion above,

Fig. 2. Typical spectrum obtained during tensile loading to fracture of nylon 6 fibers.

one might expect a plane passing perpendicular to the axis of such a cylindrical sample would cut approximately 10^{14} bonds resulting in twice that number of free radicals.[5] Because approximately 1 in. of the specimen length is in the microwave cavity, if bond rupture takes place at points removed from the primary fracture surface or if this surface is very irregular, the free radical concentration could be substantially increased. On the other hand, if untangling rather than fracturing of the chains takes place or if the crack can select a path requiring fewer chain scissions, the number could very possibly be reduced.

Studies were conducted on a variety of polymers in molded, cast, extruded, and drawn fiber forms. Except for the drawn fibers, only barely detectable signals, at best, have been obtained in any of these materials. In these latter highly crystalline and oriented materials, strong signals were

developed by tensile loadings (Figs. 2–5).   Such signals were first produced
at stresses greater than approximately 60% of the ultimate fracture stress.
Figures 2, 3, 4, and 5 show spectra for nylon 6 (drawn 4:1), nylon 66; poly-
ethylene fibers, and polyester fibers, respectively.   The nylon 6 was pro-
vided by Allied Chemical Company, the Nylon 66 by DuPont, and the
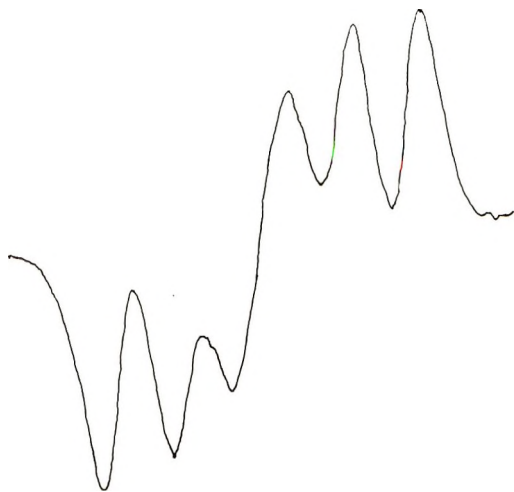

Fig. 3. Typical spectrum obtained during tensile loading to fracture of nylon 66 fibers.
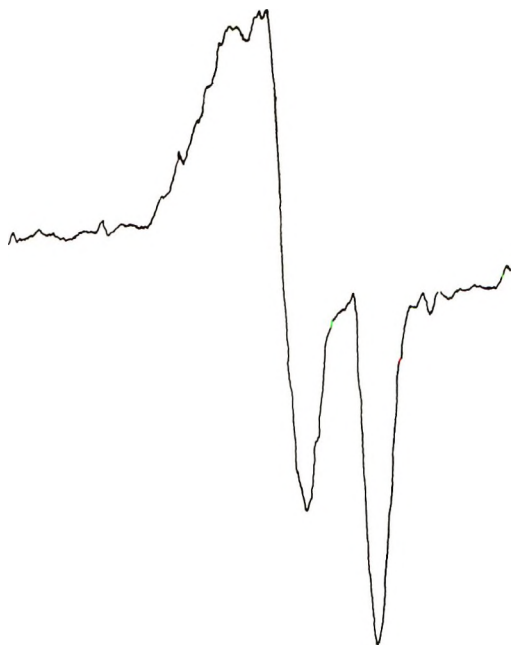

Fig. 4. Typical spectrum obtained during tensile loading to fracture of polyethylene
fibers.

Fig. 5. Typical spectrum obtained during tensile loading to fracture of polyester fibers
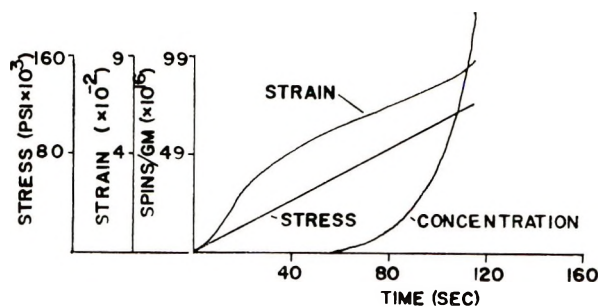

Fig. 6. Computer-reduced data from a constant load rate test of nylon 6 fibers.

polyethylene and polyester fibers by American Viscose Division, FMC Corporation. All were stated by their manufacturer to be of high purity. For example, x-ray fluorescence studies of the nylon 6 fibers indicated that the only inorganic ions present in substantial amounts were copper, 61 ppm; iodine, 0.2%; and all other metals less than 2 ppm. To date, nylon 6 has been studied most extensively. We shall discuss it briefly as being somewhat typical of the behavior of polymeric fibers.

With the current spectrometer sensivity, the EPR spectra develop at stresses significantly below the fracture stress. At fracture, the nylon 6 samples typically generated 10^{17} free radicals/cm^3 of material in the cavity. Figure 6 shows the increase in stress, strain, and free-radical concentration (obtained from computer reduction of the data) for a constant-stress rate test. The kinetics of the bond-rupture process has been interpreted by Zhurkov[1] in terms of a pseudo-empirical relation in which, at constant temperature,

$$\dot{c} = \beta e^{\gamma \sigma}$$

where $\dot{c}$ is the rate of free-radical production, σ is the applied (engineering) stress, and β and γ are constants characteristic of the material. As discussed elsewhere,[11] our studies have confirmed this equation only for a constant stress rate loading. For other loadings it leads to discrepancies if
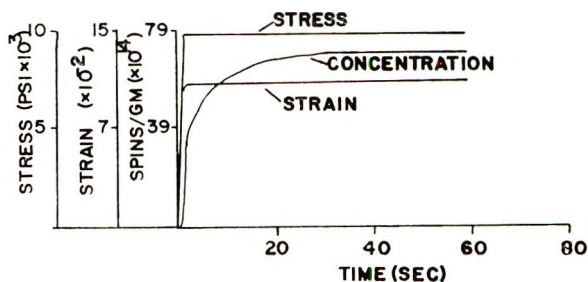
Fig. 7. Computer-reduced data for a creep test of nylon 6 fibers.
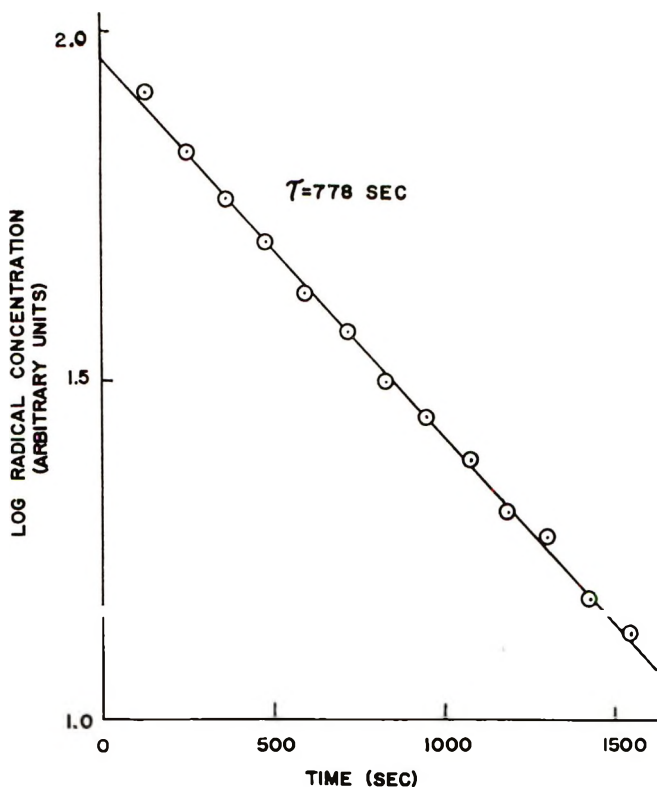
Fig. 8. Decay of EPR signal produced by tension in nylon 6 fibers vs. time.

σ is taken as the macroscopic stress and if c is measured from the time of loading. For example, the Zhurkov relation would predict for constant stress (a creep test) that the free-radical concentration increases linearly with time. Quite obviously, from the data for this loading in Figure 7, this is not the case for the fibers studied. For very high stresses, the rapid increase in concentration of Figure 7 decreased to a quasi-steady-state rate that might be approximated by a Zhurkov-type equation. There appears to be some reason for believing that the behavior can be explained in terms of rate processes and kinetic concepts in conjunction with macroscopic

Fig. 9. Very weak EPR spectrum from several pieces of PMMA after fracture.

stress relaxation or random distributions in the tie chains between crystallites. Such a model is being developed but is too involved to be presented here.

For comparative purposes, a variety of different experiments was conducted with molded and cast polymers in an attempt to obtain EPR signals during tensile fracture of PMMA, nylon, PVC, polyethylene, polystyrene, and polyurethane rubber. In all cases, any EPR signal was below the sensitivity threshold of our present equipment for the specimen volume examined.

It was next attempted to increase the fracture surface and hence, the number of newly created free radicals by fracturing the samples before
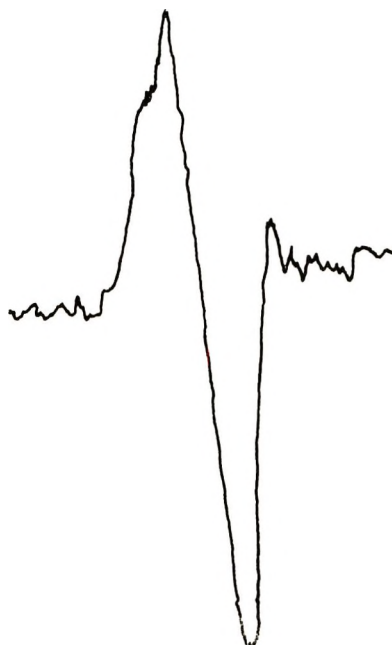
Fig. 10. EPR spectrum from roughly 10^{13} free radicals in the cavity resulting from γ-irradiation.
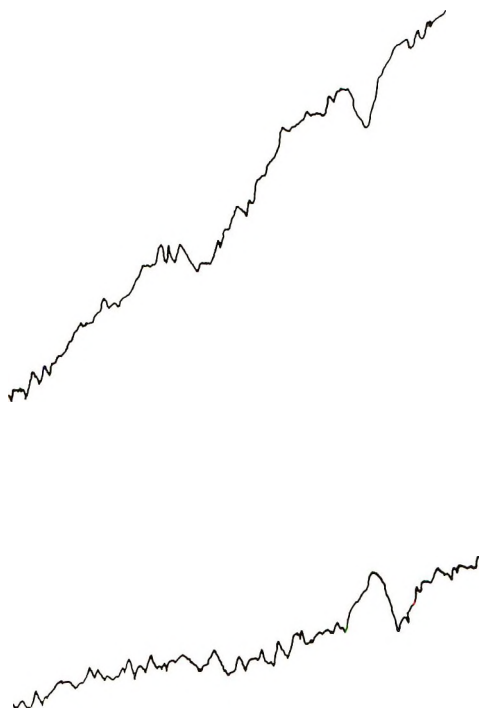
Fig. 11. EPR spectra of fracture pieces of nylon and polyethylene rods. Note gain for these spectra is increased by $3.2 \times$ that for Figures 9 and 10.

inserting them into the cavity, quickly cutting off the fractured ends, and quenching to liquid nitrogen temperature so as to "freeze in" any free radicals formed. At liquid nitrogen temperature, free radicals are very stable and can be kept for days with little if any loss due to recombination, etc. These tensile specimens were rods initially 3/16 in. in diameter. The elapsed time from initiation of tensile loading through fracture and quenching was never more than approximately 5 sec. In such a short time, our studies on free radicals formed by other means would indicate that very little of the initial EPR signal should decay. For example, the tests on nylon fibers indicate the decay constant in air at room temperature to be of the order of 800 sec as indicated in Figure 8. This work is further substantiated by γ-irradiation studies on similar materials. One complication here might be that if the newly formed free radicals lie almost entirely at the free surfaces, they might immediately react with oxygen or other agents in the surrounding air, thus substantially reducing this decay rate.

After quenching, the fracture "stubs" were placed in a quartz tube and maintained at temperatures below $-160°C$ while the spectra were taken. In this way considerably more fracture surface (up to eight or ten pieces) could be placed in the cavity at one time. Also by "freezing" the free radicals, the spectra could be recorded over much longer times with a longer recorder time constant, thereby substantially increasing the system sensitivity and

resolution. Only for PMMA was there then any detectable EPR signal. This result is shown in Figure 9 for six fracture pieces in the 2.5 cm length of quartz tubing. For comparison purposes, Figure 10 shows the spectra (gain and other EPR settings the same as in Figure 9) for approximately 10^{13} free radicals (total number in cavity) induced in nylon by γ-irradiation. Figure 11 shows typical spectra for two other materials treated similarly to that of the PMMA of Figure 9. In this case the gain was increased by a factor of 3; the slope in the curve is due to a background shift at this higher amplification. No obvious free radical signals were present. The same materials were fractured under torsional stresses and similarly treated and observed. The PMMA gave a signal similar to that of tension (still extremely low); all of the others gave negative results.

Impact Fracture

C. D. Lundergan of Sandia Corporation, Albuquerque, New Mexico, recovered some PMMA samples from an explosive impact test. These pieces, originally in a large flat plate, had a typical volume of 1–2 cm.³ They were recovered within about 1 min of impact and quickly quenched to liquid nitrogen temperature. Some of the pieces contained visual cracks. By using a $^1/_8$-in. diameter core drill, samples were obtained at liquid nitrogen temperature and at slow speeds to avoid heating. These cores were then studied in the EPR cavity at $-160°C$. Once again, little signal above the background noise was present, but those signals which were observed could possibly have arisen from bond scission during the coring operation. In these and other negative studies it might be possible, however, to enhance the signal by using a time averaging computer. Initial attempts along these lines have been encouraging.

Fracture Due to Machining

Grinding and machining operations also can produce large amounts of new fracture surfaces in comparatively small quantities of material, thus providing another means of generating EPR specimens. Every polymeric material tested, including such materials as collagen, tooth enamel, and dentin produce strong EPR signals after such treatment. (For example, Figure 12 shows a spectrum due to approximately 30 mg of ground nylon 6.) Studies are now under way in which these methods are used to investigate the number of bonds broken per unit area of new surface formed and depth of damage at surfaces as a function of fracturing mode and fracture conditions. Early results in this respect indicate that nylon 6 ground at liquid nitrogen temperature, where it behaves rather brittlely, develops between 10^{13} to 10^{14} broken bonds/cm² of new surface formed. These studies further indicate that the majority of these broken bonds lie within a few microns of the surface, and that the crack propagates through amorphous regions surrounding the more ordered regions in semicrystalline polymers such as nylon and polyethylene.[12]
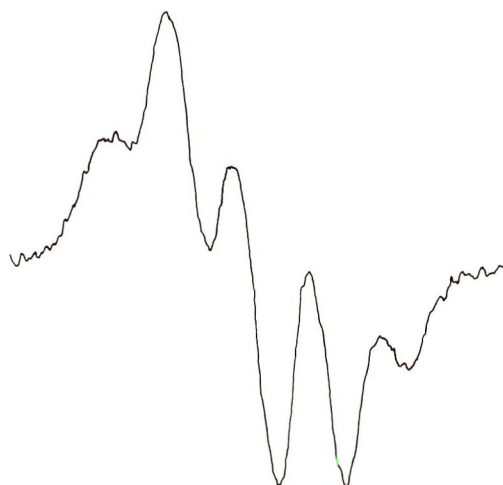
Fig. 12. EPR spectrum resulting from the grindings of 30 mg of nylon 6.

Fatigue Fracture

Some preliminary results have been obtained by using EPR techniques to study bond rupture under alternating tensile stress. Figure 13 shows the cumulative increase in free-radical concentration when an alternating stress of ± 35000 psi has been superimposed upon a mean stress of 70000 psi. It is found that in such cases the number of bonds that rupture before final failure is substantially lower than the value for fracture under a monotonically increasing stress. For the case shown in the figure it is reduced approximately by a factor of ten.[11] Efforts to explain the bond rupture in terms of a Zhurkov-type relation[1] with the constants determined from constant stress rate tests did give at least qualitative agreement with the experimental results.

DISCUSSION

The most unexpected result of these studies was the very large differences in the behavior of the drawn fibers and other forms of the same materials. While the tensile strength of nylon and polyethylene is increased roughly ten times by the drawing operation, the radical concentration at fracture increases from something less than $10^{11}-10^{13}/cm^3$ to approximately $10^{17}/cm.^3$ This increase of more than 10^5 in number of broken bonds might be explained in a number of different ways.

(1) The extent of bond breakage along a fracture surface might be smaller in the cast or molded material than in the fibers. This could be the case if fracture involved a large amount of unraveling of chains rather than their scission. Alternately, the cracks might be able to follow paths where fewer bonds need be broken to fracture the molded samples than in the highly oriented fibers.

Fig. 13. Stress, strain, and free-radical concentrations as functions of time during cyclic loading of nylon 6 fibers.

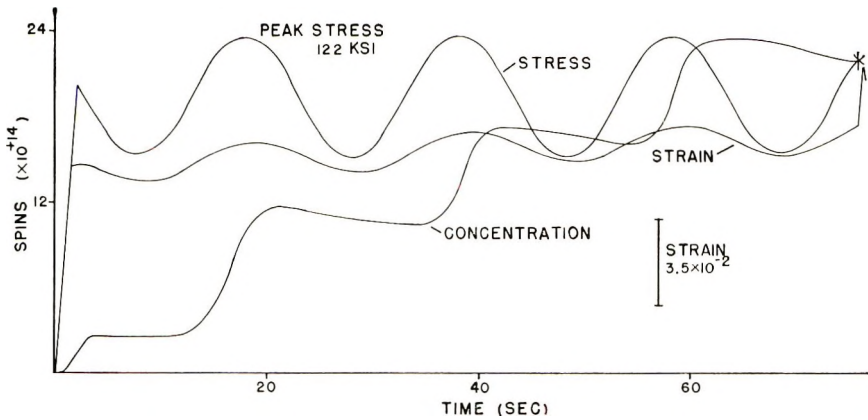(2) Chain rupture might be much more localized in the cast or molded material than in drawn fibers where it is distributed more uniformly throughout the loaded material. Our studies do seem to indicate that in the fibers the free radical distribution is distributed throughout the volume. If this is the case, it might logically follow that what is observed in the fibers is growth of a great many cracks from atomic size until one or more attain a critical (Griffith) size at which failure occurs. Since in most of these studies we are involved with bundles ($\sim$5000 one-mil filaments), it is possible that a great many such cracks might be present and growing at a time. The other materials, on the other hand, might fail at pre-existing flaws or have very few microcracks growing at any given time, in which case damage and bond rupture could be confined to a much smaller region of the sample. Even in this case, however, if significant amounts of bond rupture occur along the fracture surface, it should be possible to accumulate enough fracture surfaces to detect the breakage. To date, as previously noted, our attempts with tensile specimens have resulted in, at best, barely detectable signals. Also a few tests have been conducted on larger fibers; bundles of 20 monofilament fibers (each about 0.030 in. in diameter) of nylon and polyethylene exhibited behavior similar in all respects to the smaller fibers. As a result we are led to the conclusion that the size of the fibers is not the most significant factor.

(3) As a final alternative, it could be that a large number of bonds are broken but due to impurities or other causes, the free radicals so formed are so unstable and short-lived that the concentration never attains an easily detectable level. Peterlin[5,13] has reported the presence of an unidentified impurity in some nylon fibers studied in his laboratory which combined with the free radicals formed by fracture, forming a second free radical that is very stable, lasting several days at room temperature. It might be hypothesized that other types of impurities are present in most polymers that can react with the free radicals in such a way as to annihilate them. If such
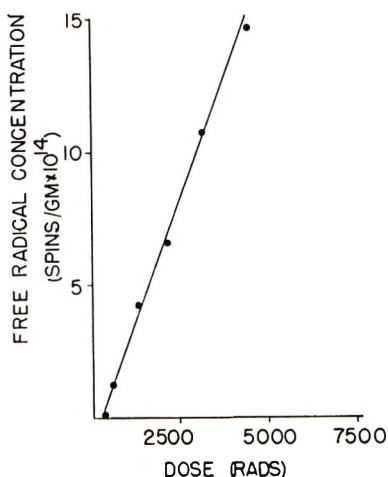
Fig. 14. Free radical concentration vs. γ-irradiation dose in nylon 66.
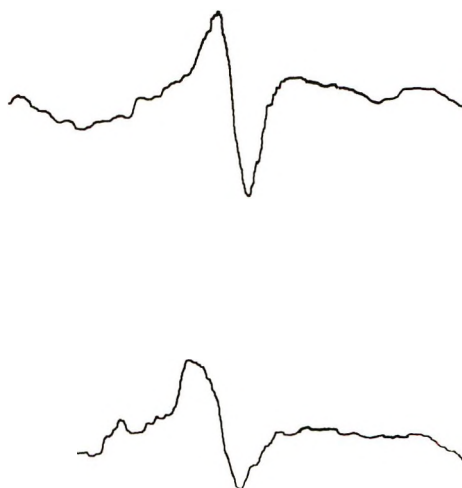
Fig. 15. Spectra in nylon 66 resulting from γ-irradiation at liquid nitrogen temperatures and then subsequently annealed at room temperature: (upper curve) annealed 1 min; (lower curve) annealed 6 min.

were the case, these impurities need to be present only in sufficient quantity as to annihilate the free radicals formed by tensile fracture but not in too large of concentrations since strong reasonably stable EPR signals are obtained from operations capable of producing large numbers of broken bonds, such as grinding and γ-irradiation. The decay constant of these signals depends on the temperature and atmosphere present but is of the order of minutes or more at room temperature in air. As a partial check of this impurity hypothesis, free radicals, were produced at varying levels of γ-irradiation at liquid nitrogen temperature. The irradiation dosage was varied from 50 to 100000 rad. The number of free radicals

produced for a given amount of irradiation is shown in Figure 14. Within experimental error, the number of free radicals is directly proportional to dosage. No significant difference in behavior was observed between the very low and higher dosage levels. Figure 15 compares the signal for 100-rad irradiation for a nylon 66 sample with a volume of 0.16 cm^3 immediately after irradiation at liquid nitrogen temperature with the same material annealed for 6 min at room temperature. Quite obviously no very rapid decay is apparent. In addition, it is difficult to see why such an impurity would be present in the other forms of all of the materials but not in any of the fibers of some of the same materials that were tested.

A somewhat related possibility is that the free radicals so formed are largely at or near the surface where they can react quickly and combine with agents in the air or testing atmosphere. Quite likely this does take place to some extent and the problem is not easily treated. Our results here are not as conclusive. However, tensile tests were conducted in various inert atmospheres, including helium and oxygen-free nitrogen. The free-radical concentration was still not increased sufficiently to be readily detectable. Another problem with this explanation is that in the fibers a strong EPR signal is present some time before macroscopic fracture is apparent, independent of the testing atmosphere. Once again, it would be difficult to explain why the free radicals are so reactive with the atmosphere in one case but not the other.

It is our opinion that the most likely answer is a combination of (1) and (2) above, i.e., damage is more local, cracks are able to follow paths requiring less bond rupture, and the unraveling of the polymer chains plays a more dominant role in the molded and cast materials than in the fibers. If this hypothesis is correct, it would appear that the materials scientist or engineer might have to use entirely different approaches for different forms of chemically identical materials when attempting to "design" better and stronger materials.

In closing, we might speculate that the ultimate properties of semicrystalline polymers are to a large extent dependent on the character of the regions between the crystallites or micelles. If such is the case, the strength and fracture properties of such a material should be strongly dependent on the number, orientation, and length distribution of the "tie chains" connecting the crystalline regions. It can be demonstrated that a rupture surface by following a path through these "glassy regions" results in the scission of an order of magnitude less bonds than one might expect were it to follow a straight plane normal to the tensile axis.[12] In related but different types of experiments, Peterlin et al. have shown that these regions are significantly changed by drawing and working operations.[13–15] One might then hypothesize that both the difference in tensile strength and the even more drastic difference in the build-up in free-radical concentration before fracture might be explained in terms of these changes. Three changes apparently take place: (1) the size of the crystallites and amorphous regions between them are altered; (2) the orientation and size of the crystallites and possibly

the number, orientation, and length of tie chains are altered; (3) the amount of material in the glassy regions is changed.

Based on these microscopic effects the following alteration in fracture properties might be expected. The fracture strength in drawn fibers would be higher because first, more bonds would need to be broken and second, because of orientation and size effects, it could be more difficult to nucleate a catastrophic (Griffith) flaw somewhat analogous to the effect of grain size on ultimate properties of metals. Third, the orientation and distribution of tie chain effective lengths might be more favorable so that at any given gross load, more of these would actively share the load on the submicroscopic scale. The total number of bonds broken would be higher because more bonds would need to be broken to complete separation. This effect alone could account for perhaps a two- or three-fold increase, but not the observed four to five orders of magnitude change. Also, the distribution of free radicals (broken bonds) would likely be more uniform throughout the sample volume because of arguments similar to the second and third reasons given above.

References

1. S. N. Zhurkov, *Intern. J. Fracture Mechanics*, **1**, 311 (1965).

2. S. N. Zhurkov, A. Y. Savostin, and E. E. Tomashevskii, *Dokl. Akad. Nauk SSSR*, **195**, 707 (1969).

3. M. L. Williams and K. L. DeVries, *Proceedings of the Fourth Army Materials Conference*, Syracuse Univ. Press, Syracuse, N. Y., 1968.

4. K. L. DeVries, D. K. Roylance, and M. L. Williams, paper presented at Sixth ICRPG Working Group on Mechanical Behavior Meeting, Pasadena, California, December 4-6, 1967.

5. D. Campbell and A. Peterlin, *J. Polym. Sci. B*, **6**, 481 (1968).

6. M. Bersohn and J. C. Baird, *Electron Paramagnetic Resonance*, Benjamin, New York, 1966.

7. G. E. Pake, *Paramagnetic Resonance*, Benjamin, New York, 1962.

8. W. C. Landgraf, *EPR'S Role in Free Radical Chemistry*, Varian Associates, Palo Alto, Calif., 1964.

9. H. M. Asseheim, *Introduction to Electron Spin Resonance*, Plenum Press, New York, 1967.

10. A. H. Maki, *Amer. Rev. Phys. Chem.*, **18**, 9 (1967).

11. K. L. DeVries and M. L. Williams, paper presented at Fifth International Congress of the Society of Rheology, Kyoto, Japan, October 5-19, 1968.

12. D. K. Backman and K. L. DeVries, *J. Polym. Sci.*, in press.

13. A. Peterlin, personal communication.

14. A. Peterlin and G. Meinel, *J. Polym. Sci. B*, **5**, 197 (1967).

15. A. Peterlin and R. Corneluissen, *J. Polym. Sci. A-2*, **6**, 1273 (1968).

Radiation Chemistry of Aqueous Poly(ethylene Oxide) Solutions. I

P. A. KING and J. A. WARD, *Sterling Forest Research Center, Union Carbide Corporation, Tuxedo, New York 10987*

Synopsis

The γ radiolysis of aqueous high molecular weight poly(ethylene oxide) solutions has been studied. The crosslinking and eventual gelation of these solutions appears to occur via an indirect effect. Solubility measurements on the gelled solutions showed that the ratio of crosslinking to degradation is about four. $G(H_2)$ increased from 1.3 in neutral solutions to 3.5 in 0.1N HCl solutions. In heavy water solutions, HD is the major gaseous product. Solvated electrons are not important precursors to hydrogen at neutral pH. Intramolecular crosslinking appears to be an important phenomenon in solutions of high molecular weight polymers.

INTRODUCTION

While most radiation chemical studies of polymers systems are concerned with direct effects of radiation on pure solid polymers, a number of workers have studied the radiolysis of polymer solutions. Aqueous polymer solutions are particularly attractive, since one can study the effects of radicals produced in water on the polymer without interference by reactions of polymer radicals with the solvent. Since the G values for the intermediates produced in water are now reasonably well established, the interpretation of results should be straightforward, at least in regard to the initial reactions of these intermediates with the polymer.

Poly(ethylene oxide) is commercially available in various molecular weight grades ranging from CARBOWAX with $\bar{M}_n \sim 6000$ or lower up to poly(ethylene oxide) with weight-average molecular weighs up to 4×10^6. The properties of dilute solutions range from extremely viscous ($\eta > 1 \times 10^6$ cP, in a 4% solution) down to practically waterlike viscosity. Several studies have been made on radiolysis of poly(ethylene oxide) solutions,[1–3] but except for the most recent work,[3] these authors have been concerned with the lower molecular weight grades. This work is almost solely concerned with high molecular weight samples.

In a study of the radiolysis of aqueous poly(ethylene oxide) solutions, Charlesby[1] has arrived at the conclusion that the crosslinking and eventual gelation of dilute ($\sim$0.5 to $\sim$20%) solutions arise from a "direct" effect,

253

i.e., energy absorbed directly by the polymer molecules is solely responsible for radical formation and crosslinking.

$$ROCH_2CH_2OR \xrightarrow{\sim\sim} ROCH_2\overset{.}{C}HOR + H \qquad (1)$$

$$H + ROCH_2CH_2OR \rightarrow H_2 + ROCH_2\overset{.}{C}HOR \qquad (2)$$

$$2\ ROCH_2\overset{.}{C}HOR \rightarrow crosslink \qquad (3)$$
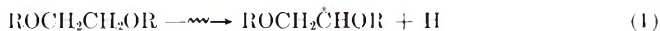
He states that "indirect" effects are not important, i.e., radicals formed by energy absorption in the water do not contribute to the crosslinking.

$$H_2O \rightarrow e^-_{s},\ H\cdot,\ \cdot OH,\ H_2O_2 \qquad (4)$$

$$\cdot OH + ROCH_2CH_2OR \rightarrow H_2O + ROCH_2\overset{.}{C}HOR \qquad (5)$$
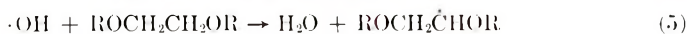
Since low molecular weight ethers are known[4] to be quite reactive toward both H and ·OH, it is logical to expect that polymer radicals will be formed by reactions with these intermediates.

The results presented here have led us to exactly the opposite conclusion; namely, that the "indirect" effect must be the major source of polymer radicals.

EXPERIMENTAL

Several grades of POLYOX, Union Carbide brand poly(ethylene oxide), were studied, ranging from WSR-35 having a weight-average molecular weight of $\sim$250 000 to WSR-701 (coagulant grade) having a weight-average molecular weight in excess of 3×10^6. Solutions were made by several methods; the one most generally used was to rapidly sift the POLYOX into highly agitated distilled water, followed by more gentle mixing for several hours. No extensive purification of the polymer samples was attempted.

The highly viscous solutions were extremely hard to degas satisfactorily. Several freeze–pump–thaw cycles still left measurable amounts of oxygen and also led to a large percentage of irradiation cells being broken. Samples were, therefore, degassed by pumping directly on the solution. This procedure results in small quantities of water being pumped away, but the change in concentration of the solution is negligible.

Irradiations were carried out in two separate ^{60}Co sources, one a nominally 4000-Ci source at a dose rate of 0.11 Mrad/hr and a 1000-Ci source at a dose rate of $\sim$0.05 Mrad/hr as determined by the standard Fricke dosimeter solution.

Molecular weight determinations were performed by using a static membrane osmometer[5] and a Ubbelohde viscometer at 30°C. Gaseous products were collected and were analyzed on an Atlas CH4 mass spectrometer.

RESULTS

The bulk viscosity of the POLYOX solutions decreased markedly at low doses. After this initial sudden drop, the viscosity remained reasonably constant until the onset of gelation produced a sharp increase. Typical results are shown in Figure 1.
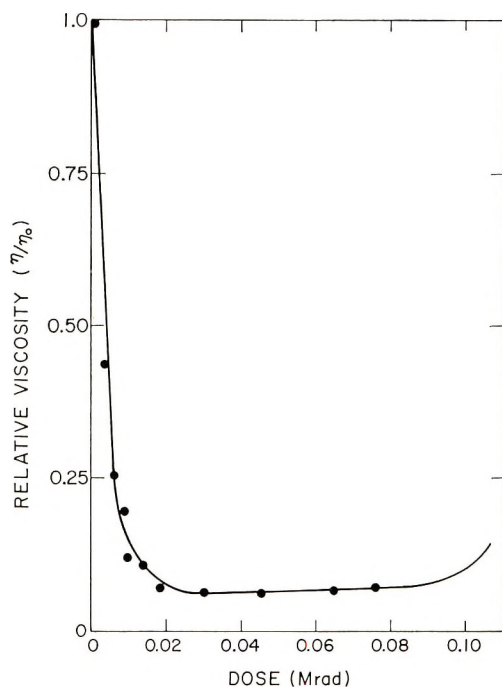
Fig. 1. Viscosity of irradiated 2% Polyox WRS-701 solution as a function of dose.
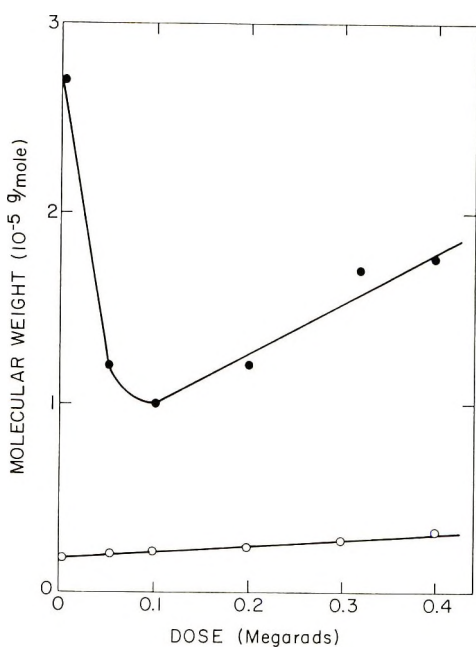
Fig. 2. Viscosity-average (●) and number-average (○) molecular weights as a function of dose for a 0.5% solution of WSR-35.

The intrinsic viscosity also decreases at low dose but began to increase again with increasing dose. This initial decrease in intrinsic viscosity apparently is not associated with degradation caused by the presence of residual oxygen since the number average molecular weight showed an approximately linear increase with dose. Figure 2 is a plot of the viscosity-average[6] and the number-average molecular weights versus dose for a 0.5% solution of WSR-35. The G value for crosslinking calculated from the number average molecular weight data is G(crosslink) = 0.27. A G value based only on the energy absorbed by the polymer is unreasonably large; $G > 50$.
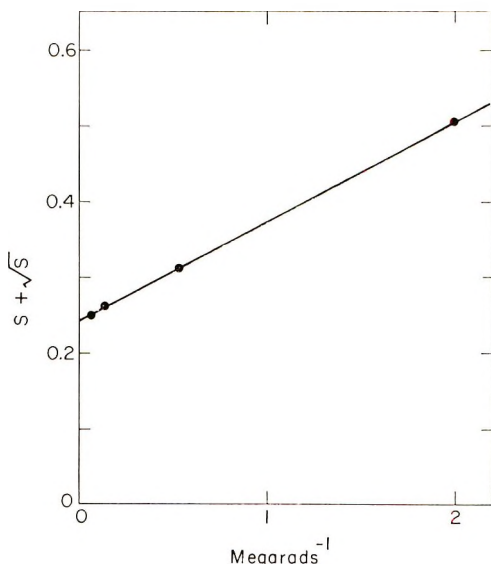
Fig. 3. Charlesby-Pinner plot for a 2% solution of WSR-701.

The initial decrease in viscosity is an indication that degradation is occurring simultaneously with crosslinking. A more quantitative estimate of the magnitude of the degradation can be gotten from solubility data. Figure 3 is the familiar Charlesby-Pinner plot[7a] of the sol plus the square root of sol ($s + \sqrt{s}$) versus the reciprocal dose for a 2% solution of WSR-701. Similar results were obtained for other concentrations and for other molecular weight grades of POLYOX. In all cases, the intercept was 0.25–0.30, indicating the ratio of crosslinking to degradation is about 4:1. It is not possible to extend these data to higher doses, since syneresis occurs which eventually produces two distinct layers; the top layer being mostly water with the highly crosslinked POLYOX in a layer beneath the water. At high doses the soluble fraction begins to increase. This is not surprising, since the gel no longer resembles the solution and the absorption of radiation by this "dry" gel should not be directly comparable to irradiation effects in solution.
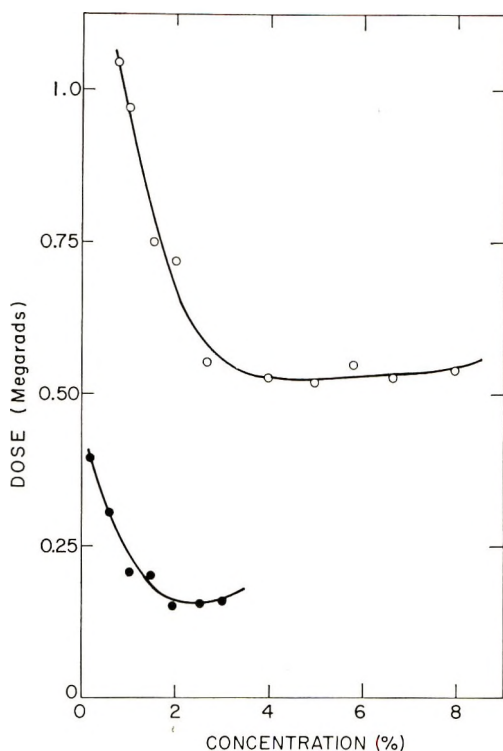
Fig. 4. Gelation dose vs. concentration for (O) WSR-35 and (●) WSR-701.

Figure 4 shows the variation of gelation dose as a function of concentration for two different molecular weight grades of POLYOX. The WSR-35 results are very similar to Charlesby's[1] data, except that the doses required to gel his samples were about a factor of two larger. The discrepancy here cannot be explained by inefficient degassing techniques on his part, since even nondegassed solutions gelled at doses lower than one Megarad.

Charlesby[1] stated that the gel dose measurements were not reproducible. Ethers are known for their instability,[8] and polyethers in particular degrade upon standing.[9] The differences between our results and Charlesby's as well as his poor reproducibility can, therefore, be explained on the basis of degradation of his samples prior to irradiation.

It was not possible to gel the solutions at either low pH (<3) or high pH (>12). Again, this was observed by Charlesby. This pH effect was observed for several different acids (HCl, H_2SO_4, H_3PO_4, and $HClO_4$) and therefore, the effect is not peculiar to the anion.

The "molecular" hydrogen yield from irradiated aqueous solutions is 0.45 while $G(H)$ and $G(e^-)$ are 0.5 and 2.8, respectively.[10] If all of these potential sources of hydrogen reacted with POLYOX to give H_2, $G(H_2)$ would be greater than three. Since, as shown in Table I, the hydrogen yield is ~1.3, not all of the intermediates yield hydrogen exclusively. At low pH,

TABLE I
Hydrogen Yields in Irradiated 2% POLYOX Solutions[a]

pH	$G(H_2)$
~1	3.5
3.0	2.4
5.0	1.3
7.0	1.3

[a] Dose $= 9 \times 10^{18}$ eV/g.

TABLE II
Hydrogen Yields From Irradiated 2% POLYOX–D_2O Solutions[a]

	$G(H_2)$	$G(D_2)$	$G(HD)$
Neutral	0.05	0.29	0.59
Acidic[b]	0.61	0.24	2.72

[a] Dose $= 9 \times 10^{18}$ eV/g.

[b] $0.1N$ HCl; solution acidified by adding concentrated HCl.

however, where the solvated electrons are quickly converted to hydrogen atoms,[11] $G(H_2)$ increases to 3.

A further demonstration of the reaction of hydrogen atoms with Polyox is the distribution of H_2, HD, and D_2 in irradiated heavy water solutions. Here the "molecular" yield of hydrogen will be exclusively D_2, while abstraction reactions by D atoms will lead to HD. Table II shows that most of the hydrogen arises from the abstraction reaction since the mixed isotope is the dominant product. In acidic solutions, where the electrons are converted to deuterium atoms, the gas yield increases.

DISCUSSION

The proof that crosslinking occurs via an indirect process is straightforward. Since both H and OH, which are produced in significant yields by the irradiation of water, are reactive toward ethers, polymer radicals must be the result of these reactions. The gas yields demonstrate conclusively that hydrogen atoms are reacting with the polymer. Further proof comes from the heavy water experiments where HD is the most important product. Since OH is considerably more reactive than H, it is logical to expect that POLYOX radicals should result from reaction (5) also. Since the polymer radicals are produced indirectly, the crosslinking must be an indirect process.

Charlesby's evidence for a direct effect is the relative constant gelation dose over a range of concentration (Fig. 4). If the assumption is true that there is one crosslink for every two weight-average molecules at the gel point,[12] an increase in concentration from, say, 1% to 2% requires a doubling in the number of crosslinks. A direct effect easily explains a constant gelation dose since a doubling in concentration doubles the amount of energy absorbed by the polymer, and presumably twice as many crosslinks

will result.   An indirect effect nominally requires that the gelation dose be directly proportional to concentration.   Figure 4 gives rather powerful evidence for a direct effect, and we must attempt to explain it.

We can explain this behavior while maintaining that gelation occurs via an indirect effect by invoking intramolecular crosslinking.   In both cases above, it is tacitly assumed that all of the polymer radicals lead to inter-molecular crosslinks, i.e. G(radicals) = 2.0 G(crosslink).   It is generally agreed that the increase in gel dose at very low concentrations (<0.5%) is due to effects of intramolecular crosslinking.[13,14]   At low concentrations, the probability for a radical site finding another radical site on the same mole-cule becomes greater than the probability for finding a radical site on a dif-ferent molecule.   The gel dose would correspondingly increase as the con-centration decreased.   But once the minimum in gel dose is reached, for some reason it is assumed that no more intramolecular crosslinking is oc-curring.   There is no reason to expect that this would be true.

If, instead of assuming that G(intra) = 0 at the minimum, we assume that G(intra) is further decreasing with concentration, then we can explain the gel dose behavior.   If direct effects can be neglected, we would expect that the total crosslinking yield would be constant, G(total) = G(inter) + G(intra) = constant.   Since G(intra) is decreasing, G(inter) must increase, and the total effect may be to keep the gelation dose constant.   While this explanation is not proven, it at least shows that the two sets of experiments are not incompatible.

This point of intramolecular crosslinking should not be underestimated.   It is common practice to assume that the radicals are produced homo-geneously throughout any irradiated system.   This is almost certainly in-correct.   Even in an isolated spur where only one event (one ionization or excitation) occurs, two radicals will be produced.   It is entirely likely that the two radicals may be on the same molecule, and intramolecular reactions are possible.

In the "average" spur where, say, six radicals are produced, the likelihood of intramolecular reactions becomes greater.   When it is realized that some 30% of the energy is deposited in "blobs" and short tracks[15] where the radical density is extremely high, then we must conclude that intramolecu-lar crosslinking will be important even in concentrated solutions.

Charlesby's estimate of the G value for crosslinking radicals was 4.46 based on energy absorbed by the polymer.   In this calculation of G (cross-linking) he used the original weight-average molecular weight (really the viscosity-average molecular weight) of the POLYOX sample.   No correction was made for the degradation which was occurring simultaneously.   The molecular weight which should be used in this calculation must take into account this degradation.[7b]   In effect, the sample is first degraded to some lower molecular weight and then crosslinked.   The correct molecular weight is this new, lower one which would result from the degradation be-fore crosslinking occurred.   The magnitude of this correction depends in large extent on the molecular weight distribution, and in particular on the

ratio of weight-average to number-average molecular weights $\bar{M}_w/\bar{M}_n$. The larger this ratio is, the larger the correction will be.

POLYOX samples, in contrast to the lower molecular weight Carbowaxes, are well known for their very broad molecular weight distributions[16] and have $\bar{M}_w/\bar{M}_n$ ratios as high as 40. The correction for Polyox samples will, therefore, be substantial. For example, suppose that $\bar{M}_w/\bar{M}_n = 14$ with $\bar{M}_W = 2.7 \times 10^5$ and $\bar{M}_n = 0.19 \times 10^5$ (Fig. 2). The initial (fictitious) degradation will reduce both of these numbers, but $\bar{M}_w$ will be decreased to a much larger extent than will $\bar{M}_n$. The result will be that $\bar{M}_w/\bar{M}_n$ will decrease and may even approach 2. For 0.25 degradations per initial weight-average molecule (see results) which is 0.018 degradations per number-average molecule, $\bar{M}_n$ will decrease only slightly to 0.187×10^5.

If $\bar{M}_w/\bar{M}_n$ decreases to 5 (Fig. 2),* then $\bar{M}_w = 0.935 \times 10^5$, and the calculated G(crosslinking radical) is 12.9. If larger values for M_w/M_n were assumed, this large G value would be even higher. While radical yields of this magnitude cannot be ruled out on thermochemical grounds, still we believe that the indirect effect offers a more satisfactory explanation.

In neutral solutions $G(\mathrm{H_2})$ is only ~1.3, but as the pH decreases, $G(\mathrm{H_2})$ increases to 3. The low $G(\mathrm{H_2})$ at neutral pH is comprised of "molecular" hydrogen, hydrogen atoms, and only a small contribution from solvated electrons. At low pH, all of the electrons react to give H atoms:

$$e^-{}_s + \mathrm{H^+}{}_s \rightarrow \mathrm{H} \cdot \tag{6}$$

which in turn react to give $\mathrm{H_2}$. However, at neutral pH, most of the electrons must be reacting with some other species in the solution before they can react with water to give hydrogen atoms.

A reaction with peroxide is likely,

$$e^-{}_s + \mathrm{H_2O_2} \rightarrow \cdot \mathrm{OH} + \mathrm{OH}^- \tag{7}$$

but this cannot account for all of the electrons, since $G(e^-{}_s) > G(\mathrm{H_2O_2})$. Pulse radiolysis of low molecular weight ($\bar{M}_w \simeq 15\ 000$) poly(ethylene oxide) solutions[17] gives some evidence that a reaction between electrons and polymer radicals is occurring.

$$e^-{}_s + \mathrm{ROCH_2\dot{C}HOR} \rightarrow \mathrm{Products} \tag{8}$$
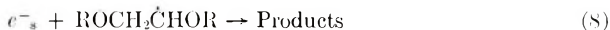
At short times after the pulse, the ultraviolet absorption attributed to the polymer radical decayed at approximately the same rate as did that of the solvated electrons. While the possibility was not mentioned, a reaction between the two species is likely.

The reactions leading to degradation and particularly the degradation at low pH are not clear-cut. A reaction between polymer radicals and peroxide is a distinct possibility:

$$\mathrm{ROCH_2\dot{C}HOR} + \mathrm{H_2O_2} \rightarrow \mathrm{ROCH_2CHO} + \mathrm{ROH} + \mathrm{OH} \tag{9}$$

---

* Actually these data include the effect of crosslinking on the viscosity average molecular weight. Since crosslinking will increase $\bar{M}_v$ and since what we really want is $\bar{M}_w$ after degradation occurs but before any crosslinking occurs, the $\bar{M}_w$ which we should use in the calculation should be even smaller.

A similar reaction has been proven in the photolysis of ethanol–H_2O_2 solution.[18]   In addition, the reaction between electrons and polymer radicals may lead to chain cleavage.

$$e^-_s + ROCH_2\dot{C}HOR \rightarrow RO^- + ROCH=CH_2 \qquad (10)$$

A unimolecular dissociation of the backbone radical

$$ROCH_2\dot{C}HOR \rightarrow ROCH=CH_2 + RO \rightarrow ROCHCHO + R \qquad (11)$$

has not been considered, because these reactions are expected to be quite slow.   Furthermore, the pulse work gave no evidence for a first-order decay of these radicals.

Since $G(H_2)$ increased at low pH, G(polymer radical) must also increase. We might then expect that the crosslinking yield would increase since there are more radicals present.   This is obviously not the case since degradation predominates at low pH.  Unirradiated POLYOX solutions are particularly unstable at low pH, but this degradation occurs over a period of days whereas irradiated solutions degrade immediately.   An acid-catalyzed decomposition of the polymer radical may be the answer, but there is no obvious reason to expect that the unimolecular reaction would subject to acid catalysis.

While it is tempting to explain the decreased efficiency of gelation at high pH by the lack of reaction between O^- and POLYOX,[19] e.g.

$$\cdot OH + OH^- \rightleftarrows O^- + H_2O \qquad (12)$$

$$O^- + ROCH_2CH_2OR \rightarrow \text{no reaction} \qquad (13)$$
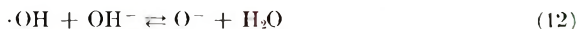
or the conversion of H atoms to electrons,[20] this explanation is not favored. Recent work[21] has shown that the rate constant for the reaction of O^- with alcohols is still quite large.

It is possible to explain this behavior in accordance with recent observations made in this laboratory on the effect of structure breaking salts on conformational changes in poly(ethylene oxide) solutions.[22]   At high salt concentrations, the neutron inelastic scattering spectrum shows that the polymer chain begins to behave more like a disordered molecule and loses its helical structure.   In other words, the polymer will become less extended (more spherical).   With the polymer contained in a more tightly packed spherical configuration, the chances for an intermolecular reaction will lessen since it is more likely that a radical site will be situated in the interior of the sphere.   The rate of intermolecular crosslinking will, therefore, decrease and the overall effect will be to form more intramolecular crosslinks.

The hydrogen yields in Tables I and II deserve more comment.   In acidic solution the G values for hydrogen in light and heavy water are the same (~3.5), while in neutral solutions the total amount of hydrogen produced in H_2O is significantly higher than the yield in D_2O solutions, (1.3 compared to 0.93).

While there is still some disagreement[23,24] as to the absolute magnitude of the yields of H and e^-_{aq}, it is generally agreed that the sum of H (or D),

e^-_{aq}, and molecular hydrogen is the same in H_2O and D_2O. In acidic Polyox solutions where all of these intermediates eventually go on to produce hydrogen, we would, therefore, expect that the total hydrogen yields would be the same in D_2O and H_2O. This is observed.

In neutral solutions, however, where it is apparent that solvated electrons are not contributing significantly to the hydrogen yield, we would expect a correlation between the G values for atomic and molecular hydrogen and the total yield of hydrogen. In H_2O, $G(H) + G_{H_2} \approx 1.0$ while in D_2O, $G(D) + G_{D_2} \simeq 0.85$.[23] A smaller G (total hydrogen) is expected in the heavy water solutions. This is observed.

References

1. A. Charlesby and P. M. Kopp, *Proc. Roy. Soc.* (London), **291A**, 129 (1966).

2. C. Decker, M. Vacherot, and J. Marchal, *C. R. Acad. Sci.* (Paris), **261**, 5104 (1965).

3. R. A. Van Brederode, F. Rodriguez, and G. G. Cocks, *J. Appl. Polym. Sci.*, **12**, 2097 (1968).

4. G. Scholes and R. L. Wilson, *Trans. Faraday Soc.*, **63**, 2983 (1967).

5. R. W. Callard, F. E. Bailey, Jr., and R. D. Lundberg, *J. Polym. Sci.*, **47**, 507 (1969).

6. F. E. Bailey, Jr., J. L. Kucera, and L. G. Imhof, *J. Polym. Sci.*, **32**, 517 (1958).

7. A. Charlesby, *Atomic Radiation and Polymers*, Pergamon Press, New York–London, 1960, (a) p.173; (b) p. 171.

8. C. Walling, *Free Radicals in Solution*, Wiley, New York–London, 1957, p. 412.

9. C. W. McGary, Jr., *J. Polym. Sci.*, **46**, 51 (1960).

10. A. O. Allen, *Radiation Res. (Suppl. 4)*, 54 (1964).

11. S. Gordon, E. J. Hart, M. S. Matheson, J. Rabani, and J. K. Thomas, *Discussions Faraday Soc.*, **36**, 193 (1963).

12. P. J. Flory, *Principles of Polymer Chemistry*, Cornell Univ. Press, Ithaca, N. Y., 1953, p. 358.

13. I. Sakurada and Y. Ikada, *Bull. Inst. Chem. Res., Kyoto Univ.*, **42**, 32 (1964).

14. A. Henglein and W. Schnabel, *Current Topics Radiation Res.*, **2**, 1 (1966).

15. A. Mozumder and J. L. Magee, *Radiation Res.*, **28**, 203 (1966).

16. C. Booth and C. Price, *Polymer*, **7**, 85 (1966).

17. A. Charlesby, P. J. Fydelor, P. M. Kopp, J. P. Keene, and A. J. Swallow., in *Pulse Radiolysis*, M. Ebert, J. P. Keene, A. J. Swallow, and J. H. Baxendale, Eds., Academic Press, New York–London, 1966, p. 193.

18. J. Barrett, A. L. Mansell, and R. J. M. Ratcliffe, *Chem. Commun.*, 48, **1968**.

19. E. J. Hart, *J. Amer. Chem. Soc.*, **75**, 6169 (1953).

20. S. Nehari and J. Rabani, *J. Phys. Chem.*, **69**, 1609 (1963).

21. G. Hughes and H. A. Makada, *Trans. Faraday Soc.*, **64**, 3276 (1968).

22. P. G. Assarsson, P. S. Leung, and G. J. Safford, *Polymer Preprints*, **10**, 1241 (1969).

23. Z. D. Draganić, O. I. Mićić, and M. T. Nenadović, *J. Phys. Chem.*, **72**, 511 (1968).

24. A. Appleby and H. A. Schwarz, *J. Phys. Chem.*, **73**, 1937 (1969).

Precipitation of Some Nonionic Polymers by Octylammonium Thiocyanate

SHUJI SAITO, *Momotani Juntenkan, Ltd., Minatoku, Osaka 552, Japan*

Synopsis

The effects of various alkylammonium thiocyanates (ethyl, butyl, hexyl, and octyl) on aqueous solutions of polyvinylpyrrolidone (PVP) and poly(vinyl alcohol–acetate) copolymer (PVA-Ac) were studied and compared with the effects caused by the respective chlorides. Whereas the PVP solution was hardly affected by the chlorides, it was precipitated by n-octylammonium thiocyanate (OASCN) at dilute concentrations and dissolved at higher concentrations. On taking the effects of ammonium chloride and thiocyanate on the solubility of PVA-Ac as references, with increasing of alkyl chain length, alkylammonium chlorides raised the polymer solubility steadily; on the contrary, the thiocyanates at dilute concentrations, except for ethylammonium thiocyanate, lowered it, and OASCN at dilute concentrations was a particularly strong salting-out agent. The amount of binding of OASCN to the polymers in the precipitated systems was measured. The precipitation was attributed to ion-pair binding of OASCN to the polymers, and the mechanism was discussed in terms of the interaction between the water structure-breaking SCN$^-$ and the water structure-making hydrophobic groups.

INTRODUCTION

A previous study of the salt effect on a nonionic polymer in aqueous solution[1] suggested considerable cation-anion interaction on the polymer chain for tetrapropylammonium iodide compared with the bromide. In such a combination of cation and anion both having a tendency to accumulate to the nonionic polymer, an irregular salt effect takes place. As an extreme case, when the cation has a long alkyl chain and therefore tends to associate well with the polymer, its salts exert quite an interesting effect, depending on the nature of the anions. For example, it was found that in sharp contrast to the chloride, in aqueous solution dodecylammonium thiocyanate changes remarkably the configuration of some nonionic polymers such as polyvinylpyrrolidone[2] and even solubilizes water-insoluble poly(vinyl acetate).[3] This was ascribed to the binding of the long-chain cations to the polymers with the aid of thiocyanate ions. Since in this binding the length of the alkyl chain of the cation plays a dominant role, it seemed desirable to investigate further the effect of alkylammonium thiocyanates with various alkyl chains on the solution properties of some polymers and to compare it with that of the analogous chlorides.

EXPERIMENTAL

Preparation of Alkylammonium Thiocyanates

Alkylammonium thiocyanates were prepared from the alkylammonium sulfates $(RNH_3)_2SO_4$ by a metathetical reaction with barium thiocyanate. Ethylammonium and n-butylammonium sulfates were made by neutralization of the respective amines [70% aqueous ethylamine solution, and Extra Pure grade n-butylamine (Tokyo Kasei Kogyo Co., Japan)] with sulfuric acid in aqueous solution. As ethylammonium sulfate is very hygroscopic, its aqueous solution was separated and washed repeatedly with acetone and dried over P_2O_5 under vacuum. The butylammonium sulfate was precipitated with acetone and recrystallized several times from methanol-acetone. n-Hexylammonium and n-octylammonium sulfates were converted from the respective chlorides by metathesis with silver sulfate in methanolic solution. After it was confirmed that no free chloride ions were detected, the filtrates were dried. The hexylammonium and octylammonium sulfates thus produced were repeatedly recrystallized from methanol–acetone.

Each alkylammonium sulfate was reacted with an equivalent amount of barium thiocyanate $Ba(SCN)_2 \cdot 2H_2O$ (Wako Pure Chemical Co., Japan) in water. After removal of $BaSO_4$, a small excess of either component in the filtrate was further adjusted by careful titrations of solution of the coreactant. By repeating this procedure, the sulfates could be changed into the thiocyanates of sufficient purity. It was estimated that any excess component was on the order of 10^{-4} in mole ratio. In the case of octylammonium thiocyanate (OASCN), however, since the $BaSO_4$ produced was dispersed very stably, the colloidal solution was flocculated with methanol before filtration. The filtrates were then condensed over a water bath at about 60°C (prolonged heating at 100°C. caused decomposition).

The concentrations of the stock solutions of these thiocyanates (about 0.5–1 M) were determined by gravimetric analysis of SCN^- as $CuSCN$ with cupric sulfate and sulfurous acid;[4] results were checked by drying the solutions over P_2O_5 *in vacuo*. The results agreed within 0.5%. All the alkylammonium thiocyanates were extremely hygroscopic.

Other Materials

n-Alkylammonium chlorides (ethyl, butyl, hexyl, and octyl) were the same as used before.[1]

Polyvinylpyrrolidone (PVP) was a commercial product (Luviskol K90, Badische Anilin & Soda Fabrik, Germany) and poly(vinyl alcohol–acetate) copolymer (PVA-Ac) with 30.0% acetate content and a degree of polymerization 2000 was supplied by the Nippon Synthetic Chemical Ind. Co., Japan. Both were the same as used previously.[2]

Methods

The viscosity of PVP solution, the cloud point, and the solubility of PVA–Ac solution were measured as described previously.[1,2] The cloud point of the PVA–Ac solution was determined as the temperature at which the system became cloudy on slow warming.

RESULTS

Figure 1 shows the reduced viscosity of PVP solution in the presence of various alkylammonium chlorides and thiocyanates. Whereas butylammonium, hexylammonium, and octylammonium chlorides increased the reduced viscosity only slightly, the thiocyanates decreased it, and octylammonium thiocyanate (OASCN) precipitated PVP at a concentration of about 0.1 M, and redispersed and dissolved it at concentrations above 0.5 M. It was shown that at room temperature thiocyanate ions cause an increase in viscosity of PVP[5-7] and PVA–Ac.[1] As explained previously regarding the dodecylammonium–PVP system,[2] the decrease in viscosity or coiling of a polymer chain at dilute concentrations is due to cooperative binding of the long-chain cations and thiocyanate ions as pairs to the polymer. Because octylammonium cation is moderately surface-active, the salt was markedly bound to the polymer with increase of concentration. When the polymer chain is fully covered by the pairs, supposedly the binding of the long-chain cations prevails, and as a result the shrunken and precipitated PVP chain is redispersed, uncoiled, and dissolved at higher concentrations. In the case of dodecylammonium thio-
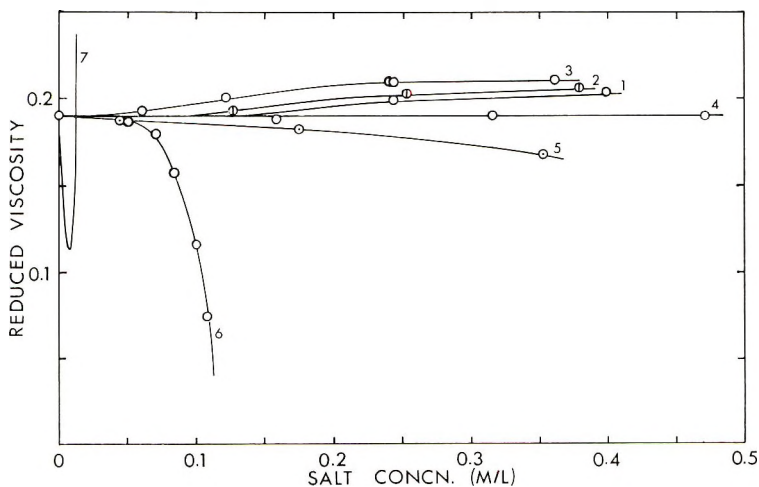
Fig. 1. Reduced viscosity of 1.70 g/l. PVP in various alkylammonium salt solutions plotted as a function of salt concentration at 25°C: (1) butylammonium chloride; (2) hexylammonium chloride; (3) octylammonium chloride; (4) butylammonium thiocyanate; (5) hexylammonium thiocyanate; (6) octylammonium thiocyanate; (7) dodecylammonium thiocyanate (from ref. 2).
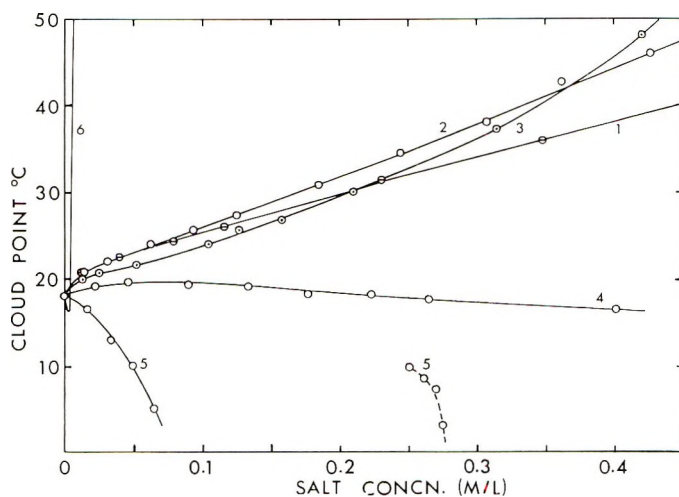
Fig. 2. Cloud point of 0.21% PVA–Ac solution plotted against concentration of various alkylammonium thiocyanates added: (1) NH₄SCN; (2) ethylammonium thiocyanate; (3) butylammonium thiocyanate; (4) hexylammonium thiocyanate; (5) octylammonium thiocyanate (dotted portion; see text); (6) dodecylammonium thiocyanate (from ref. 2).
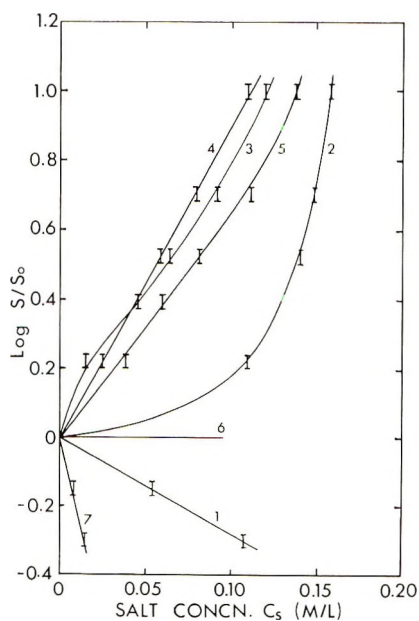
Fig. 3. Plots of $\log S/S_0$ against salt concentration C_s: (1) NH₄Cl; (2) octylammonium chloride; (3) NH₄SCN; (4) ethylammonium thiocyanate; (5) butylammonium thiocyanate; (6) hexylammonium thiocyanate; (7) octylammonium thiocyanate. S_0 (0.042%) and S are solubilities of PVA–Ac in pure water and in salt solution at C_s, respectively, at 25°C.
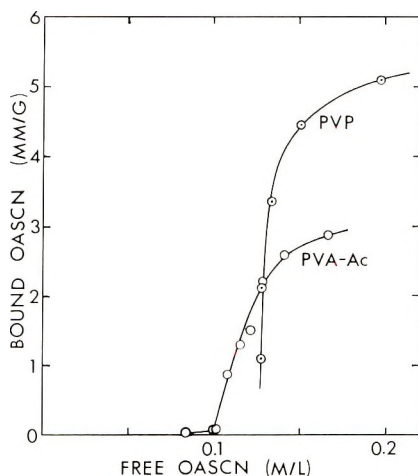
Fig. 4. Amounts of octylammonium thiocyanate (OASCN) bound per gram of precipitated polymers plotted against free OASCN concentration in the mother liquors at 20°C. Initial polymer concentrations before precipitation were 1% in both cases.

cyanate,[2] however, the coiling and uncoiling regions of surfactant concentration were so closed and partly overlapped that only a minimum appeared in the viscosity curve and no precipitation occurred.

The difference in alkylammonium chlorides and thiocyanates in the effect on solution properties of the polymer was shown more systematically and clearly by the cloud point (Fig. 2) and in the solubility at 25°C. (Fig. 3) of the PVA–Ac solution. In Figure 3, log S/S_0 is plotted against salt concentration C_s in the form of the Setschenow equation for the salt effect log $S/S_0 = kC_s$, where $S_0$ and S are the solubilities of PVA–Ac in water (0.042%) and in salt solution at C_s, respectively. As shown previously,[1] NH_4Cl and NH_4SCN exert a salting-out and a salting-in effect, respectively, on the PVA–Ac solution. With increase of alkyl chain length and concentration, addition of alkylammonium chlorides resulted in a steady rise in the cloud point and in the solubility of PVA–Ac,[1] but addition of alkylammonium thiocyanates showed complicated effects. At low concentrations, compared with the reference curve of NH_4SCN, ethylammonium thiocyanate tended to raise the cloud point (Fig. 2) and to increase the solubility at 25°C. (Fig. 3) only a little, but butylammonium thiocyanate lowered them, and with greater increase of the alkyl chain length this tendency became marked. The salting-in action of thiocyanate ions is therefore not only cancelled out by hexylammonium cations, but changes to a salting-out action in the presence of the longer-chain cations. Actually, the effect of OASCN was more powerful than that of a strong salting-out agent such as potassium fluoride. Thus, as the effects of NH_4Cl and NH_4-SCN on PVA–Ac solution are opposite, so the contribution of the alkyl chain of alkylammonium chlorides and that of the thiocyanates are opposite.
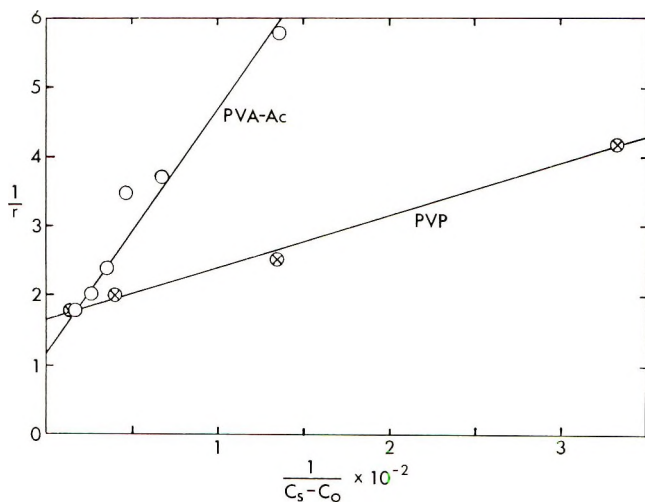
Fig. 5. Plots of $1/r$ against $1/(C_s - C_0)$. C_0 for PVP and PVA–Ac are 0.125 and 0.10 mole/l., respectively.

The PVA–Ac solution became cloudy with increasing temperature. In this case the cloudiness is related to the interaction of water with the hydrophobic acetate parts of the polymer. Above 0.25 M OASCN concentration, however, cloudiness disappeared with elevation of temperature (dotted portion of curve 5 in Fig. 2), and above 0.5 M the precipitates dissolved. Because the acetate parts of PVA–Ac are covered by OASCN as shown subsequently, with a rise of temperature the attraction between the alkyl chains bound to the polymer may be weakened and the precipitates dissolve. For the same reason as mentioned regarding PVP, dodecylammonium thiocyanate produced no precipitation of PVA–Ac but showed a minimum in the cloud point curve.[2]

The amounts OASCN bound per unit weight of the polymers were determined in their precipitated systems at 20°C by measurement of thiocyanate concentration in the equilibrium transparent mother liquors, on the assumption that the mother liquors contained practically no polymer. As shown in Figure 4, the binding increased abruptly at a certain concentration C_0 depending on the polymers (0.125 and 0.10 mole/l. for PVP and PVA–Ac, respectively) and their concentration, and this is a feature of surfactant binding as indicated also in the system sodium dodecylsulfate–PVP.[8] With increase of OASCN concentration C_s above C_0, the binding was enhanced by Langmuir type adsorption, and eventually the precipitates dissolved in the solution. On applying the Klotz equation[9]

$$1/r = (1/nkC) + (1/n)$$

(where r and n are moles of cosolutes bound per unit mole of polymer at free cosolute concentration C and $C \rightarrow \infty$, respectively, and nk is the equilibrium constant of the first binding of the cosolute to the polymer)

to these binding equilibria and putting $C_s - C_0$ instead of C, we obtained the straight lines in $1/r$ versus $1/(C_s - C_0)$ plots shown in Figure 5. Originally, this equation was derived on the assumption that each adsorbate is independent of others. Because the polymers were precipitated by OASCN by its mutual attraction upon binding, the validity of the Klotz equation for the present systems is questionable. Moreover, as OASCN is a surfactant, the concentration in the above equation should be replaced by activity. Accordingly, the linear relationship of the Klotz plots for these systems shown in Figure 5 seems rather fortuitous. Since hydroxyl groups in PVA–Ac are considered not to be related to the binding,[2] r values for the copolymer in Figure 5 were expressed in terms of the acetate residue. The values of nk (133 for pyrrolidone and 29 for acetate) calculated from the slopes are only qualitatively reliable, but a pyrrolidone group clearly has a greater affinity for OASCN than does an acetate group.

By extrapolation of the lines to $1/(C_s - C_0) \to 0$ in Figure 5, the maximum moles n of OASCN bound per mole of pyrrolidone and acetate was estimated to be 0.60 and 0.85, respectively, and this may imply that an acetate group located in the copolymer can afford more space for the binding of the long-chain molecules than a pyrrolidone in its own sequence.

Methylcellulose also was precipitated by OASCN, but poly(vinyl alcohol) (PVA) and poly(ethylene oxide) (PEO) were not. As shown previously,[2] dodecylammonium thiocyanate had hardly any interaction with PVA but weak interaction with PEO. Both polymers were the same as used before.[2] It is plausible that polymers with more hydrophobic groups interact more strongly with both alkyl–chain cations and SCN^-, and therefore, with long-chain alkylammonium thiocyanates.

DISCUSSION

It is known that, following the lyotropic series of inorganic anions, SCN^- is closer than Cl^- not only to uncharged water–air,[10,11] water–low-dielectric substance,[12] and water–mercury[13] interfaces, but also to charged polymers.

In the latter cases, counterions accumulate around the polycations, and SCN^- or I^- is fixed more tightly than Cl^- to the cationic polyelectrolytes[14] by long-range electrostatic forces and also by a specific attraction, and this induces a significant change in the conformation of some polypeptides.[15–17]

The specific behavior of these large, water-structure-breaking anions together with cations having hydrophobic groups may be caused by changes in the arrangement of water molecules around the cation and anion concerned.[18] In a study of aqueous solutions of tetraalkylammonium halides,[19] the fact that the salts of the more water-structure-breaking anion ($I^- > Br^- > Cl^- > F^-$; F^- being water-structure-making) have lower activity coefficients has been explained by the possible mechanism that the more water-structure-breaking anion makes more water molecules

available for the self-salting-in of the water-structure-making tetraalkyl-ammonium cation, this effect outweighing the salting-out effect of the anion by the cation. Thus, in a comparison of the salting-in effect of Pr_4NI and Pr_4NBr on PVA–Ac,[1] for example, supposedly iodide ions drive the cations to the polymer (salting-in), but at the same time the anions also are attracted to the polymer much more tightly than are bromide ions, and therefore the salting-in of the polymer by the cations is lessened by iodide ions, which reduce the effective charge on the polymer. Generally, the activities of a polymeric salt are much lower than those of the mono-meric salt.[20] In this regard, when a single component of a salt is bound to a nonionic polymer forming a high-density charged field, the counterions are much less mobile than those of the unbound ones.

By application of this idea to the present case, it is considered that SCN^- also may promote self-association of the alkylammonium cations, though not in such a characteristic way as in the Pr_4NX compounds. When a hydrophobic polymer is present, SCN^- enhances binding of both cation and itself to the polymer more tightly than does Cl^-. This re-ciprocal attraction encourages binding of the ion-pair to the polymer in the neutral state, which tends to cause mutual intramolecular attraction (the viscosity or solubility depression) between the hydrophobic parts of the salt-bound polymer complex. When the chain of the cations becomes longer, the ion-pair binding to the polymer and the attraction between the bound salts increase, inducing a drastic change to precipitate the poly-mers, particularly by OASCN, whereas the salt itself is highly water-solu-ble. (n-Dodecylammonium thiocyanate might be a more effective pre-cipitant for the polymers at dilute concentration.)

On the other hand, when the counterions are chlorides, since they are less confined to polycations than are thiocyanate ions, the cations may pri-marily be subjected to binding to the nonionic polymers. Thus, on addi-tion of alkylammonium chlorides, the solubility of PVA–Ac and the cloud point of its solution profoundly and steadily increase,[1] and also the reduced viscosity of PVP solution increases, though only slightly (Fig. 1), with an increase of the alkyl chain length. Also, because anions generally have greater influence upon the water structure than do the cations and because sodium ions are water-structure-making,[21] it may be natural that sodium salts of long-chain anions show considerable differences in their mode of interaction with nonionic polymers from chloride and thiocyanate salts of long-chain cations, as already described.[1,22]

References

1. S. Saito, *J. Polym. Sci. A-1*, **7**, 1789 (1969).
2. S. Saito and M. Yukawa, *J. Colloid Interface Sci.*, **30**, 211 (1969).
3. S. Saito and M. Yukawa, *Kolloid-Z. Z. Polym.*, **234**, 1015 (1969).
4. *Handbook of Analytical Chemistry*, The Japan Society for Analytical Chemistry, Ed., Maruzen, Tokyo, 1961, p. 439.
5. J. Eliassaf, F. Eriksson, and F. R. Eirich, *J. Polym. Sci.*, **47**, 193 (1960).
6. P. Molyneux and H. P. Frank, *J. Amer. Chem. Soc.*, **83**, 3169 (1961).

7. J. Goldfarb and S. Rodriguez, *Makromol. Chem.*, **116,** 96 (1968).

8. S. Saito, *Kolloid-Z.*, **154,** 19 (1967).

9. I. M. Klotz, F. A. Walker, and P. R. Pivan, *J. Amer. Chem. Soc.*, **68,** 1486 (1946).

10. J. E. B. Randles, *Discussions Faraday Soc.*, **24,** 194 (1957).

11. N. L. Jarvis and M. A. Scheiman, *J. Phys. Chem.*, **72,** 74 (1968).

12. N. K. Adam, *The Physics and Chemistry of Surfaces*, 2nd Ed., Oxford Univ. Press, London, 1938, p. 360.

13. J. T. Davies and E. K. Rideal, *Interfacial Phenomena*, Academic Press, New York, 1961, p. 98.

14. I. Noda and I. Kagawa, *Kogyo Kagaku Zasshi*, **68,** 987 (1965)

15. S. Makino and S. Sugai, *J. Polymer Sci. A-2*, **5,** 1013 (1967).

16. S. Makino, K. Wakabayashi, and S. Sugai, *Biopolymers*, **6,** 551 (1968).

17. D. Puett, A. Ciferri, E. Bianchi, and J. Hermans, Jr., *J. Phys. Chem.*, **71,** 4126 (1968).

18. R. M. Diamond, *J. Phys. Chem.*, **67,** 2513 (1963).

19. W. Y. Wen, S. Saito, and C. M. Lee, *J. Phys. Chem.*, **70,** 1244 (1966).

20. H. Morawetz, *Macromolecules in Solution*, Interscience, New York, 1965, p. 334.

21. J. L. Kavanau, *Water and Solute-Water Interactions*, Holden-Day, San Francisco, 1964.

22. S. Saito, *Kolloid-Z. Z. Polym.*, **215,** 16 (1967).

NOTES

Photo Polymerization of Vinyl in the Presence of
Tetrachlorides of Group IV Elements

In radical polymerization in the presence of carbon tetrachloride, CCl_4 is a well known chain-transfer agent. In a previous study[1,2] it was found that $SiCl_4$ also acted as chain-transfer agent in radical polymerization.

$SiCl_4$ and $GeCl_4$ do not act as cationic catalysts in benzene, but it was previously observed that when metal halides, for example, $HgCl_2$, are present, they can be cationic catalysts.[3]

$SnCl_4$ is a well known cationic catalyst but styrene does not polymerize in ether with $SnCl_4$.

There are some reports[4,5] that methyl methacrylate and vinyl acetate form complexes with $SnCl_4$ and their radical polymerizability increases.

We carried out the photopolymerizations of methyl methacrylate (MMA, $e = 0.40$, $Q = 0.74$) and vinyl acetate (VAc, $e = -0.22$, $Q = 0.026$) in benzene and styrene (St, $e = -0.80$, $Q = 1.00$) in di-ethyl ether at 30°C in the presence of tetrachlorides of group IV elements.

Photopolymerizations were carried out by the usual sealed tube method at 30°C. The sealed tubes were placed at a constant distance (10 cm) and a SHL-100 UV high-pressure mercury lamp manufactured by the Toshiba Electric Co., Ltd., was used for irradiation.

The effect of tetrachlorides of group IV elements on the rates of polymerizations of methyl methacrylate, vinyl acetate, and styrene are shown in Figures 1, 2, and 3, respectively.

It was found that the rates of polymerization increased with addition of the halides to the polymerization systems and these chlorides acted as photosensitizers.

The effect of the concentration of chlorides on the rates of polymerization was not ascertained, but the activities for St of tetrachlorides of group VI elements in this experiment decreased in the order, $SnCl_4 > GeCl_4 \gtrsim CCl_4 > SiCl_4$. For MMA, the order was $CCl_4 \gtrsim SnCl_4 > GeCl_4 \gtrsim SiCl_4$; for VAc the activity decreased in the order, $CCl_4 > SnCl_4 > GeCl_4 > SiCl_4$.

The differences in the rates of polymerization R_p in the presence of these chlorides seems to be attributable to the differences in the rate of initiation, the increase of the rate of propagation, by the interaction of monomers with the photosensitizers, or the decrease in the rate of the termination.

To clarify these points, the degree of polymerization P_n of St and MMA was determined for the polymers obtained at approximately the same conversion by using eqs. (1) and (2) for St and MMA, respectively.[6,7]

$$P_n = 1770 \, [\eta]^{1.4} \tag{1}$$

$$P_n = 2200 \, [\eta]^{1.43} \tag{2}$$

The rates and the degrees of polymerization are shown in Table I.

The degrees of polymerization of St in the presence of the tetrachlorides decreased in the following order: $SiCl_4 > CCl_4 > GeCl_4 > SnCl_4$. From the relationships between the rates and degrees of polymerization, it was thought that the difference of the rates of

273

Fig. 1. Photopolymerization of MMA in the presence of tetrachlorides of group IV elements: (▽) SnCl$_4$; (□) GeCl$_4$; (△) SiCl$_4$; (○) CCl$_4$; (×) blank, in benzene at 30°C. [MMA] = 4.68 mole/l. (4.68 g); [halide] = 6.24 × 10^{-2} mole/l.

Fig. 2. Photopolymerization of VAc in the presence of tetrachlorides of group IV elements: (□) SnCl$_4$; (×) GeCl$_4$; (△) SiCl$_4$; (▽) CCl$_4$; (○) blank, in benzene at 30°C. [VAC] = 5.44 mole/l. (4.67 g); [halide] = 6.24 × 10^{-2} mole/l.

polymerization depended on the difference of the rates of initiation and was independent of the rates of propagation.   The rate of initiation seems to decrease in the following order: SnCl$_4$ > GeCl$_4$ > CCl$_4$ > SiCl$_4$. This order of the rates of initiation was thought to be dependent on the quantum yield of cleaving these chlorides into radicals or on the difference of the reactivity of radicals formed with St.

On the other hand, the degree of polymerization of MMA in the presence of the tetrachlorides decreased in the following order: CCl$_4$ > SnCl$_4$ > GeCl$_4$ > SiCl$_4$.   In the case of MMA, the degrees of polymerization increased with increasing rates of polymerization. It was considered that the rate of propagation was increased by the complexes formed between MMA and these halides.   It is known that complexes are formed between SnCl$_4$ and MMA or VAc and therefore the rate of polymerization in the presence of SnCl$_4$ increases.   In the present experiments, the increase of the rate of polymerization

TABLE I
Rate of Polymerization R_p and Degree of Polymerization $\bar{P}_n$ of Monomers in the Presence of Halides of Group IV Elements

Halide	MMA[a]			St[b]			VAc,[e]	
	$R_p \times 10^5$, mole/l.-sec	$[\eta]$	$\bar{P}_n$[d]	$R_p \times 10^5$, mole/l.-sec	$[\eta]$	$\bar{P}_n$[e]	$R_p \times 10^5$, mole/l.-sec	$\bar{P}_n$[e]
None	3.75	3.31	8514	0.67	0.93	1605	0.97	
CCl$_4$	2.50	1.67	3920	2.20	0.57	805	3.22	
SiCl$_4$	4.17	1.00	2200	1.39	0.74	1170	1.93	
GeCl$_4$	7.78	1.11	2490	2.22	0.56	788	2.01	
SnCl$_4$	20.0	1.15	2550	2.83	0.33	376	2.86	

[a] [MMA] = 4.68 mole/l., [halide] = 6.24 × 10^{-2} mole/l.; 30°C, in benzene.
[b] [St] = 4.35 mole/l.; [halide] = 6.24 × 10^{-2} mole/l.; 30°C, in Et$_2$O.
[c] [VAc] = 5.44 mole/l.; [halide] = 6.24 × 10^{-2} mole/l.; 30°C, in benzene.
[d] Degree of polymerization obtained by the equation,[7] $\bar{P}_n$ = 2200 $[\eta]^{1.13}$.
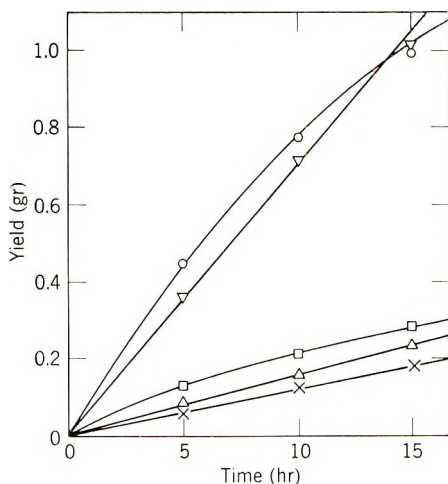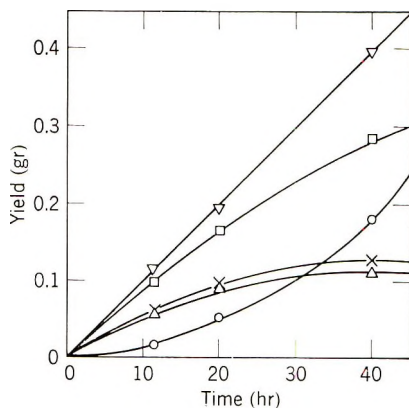[e] Degree of polymerization obtained by the equation,[6] $\bar{P}_n$ = 1770 $[\eta]^{1.4}$.
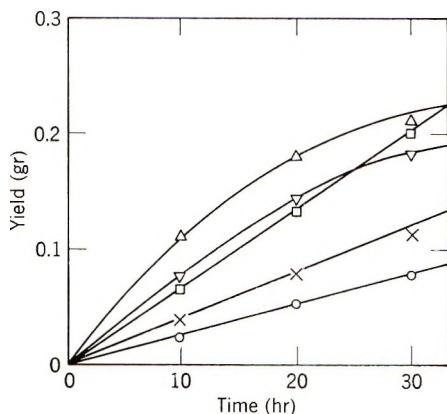
Fig. 3. Photopolymerization of St in the presence of tetrachlorides of group IV elements: (△) SnCl₄; (▽) GeCl₄; (×) SiCl₄; (□) CCl₄; (○) blank, in Et₂O at 30°C. [St] = 4.35 mole/l. (4.52 g); [halide] = 6.24 × 10⁻² mole/l.

seems to be due to the contribution of $SnCl_4$ not only at the initiation stage but also at the propagation stage. Otsu et al.[8,9] have shown similar examples in which the complexes are formed between MMA or VAc with $ZnCl_2$ and the rate of polymerizations is consequently increased.

As mentioned above, the photopolymerizations of MMA and VAc were also accelerated in the presence of $SiCl_4$ and $GeCl_4$. It was considered that radicals formed from highly ionic $SiCl_4$, $GeCl_4$, and $SnCl_4$ as well as CCl_4 on irradiation of ultraviolet light and the rates of propagation increased as a result of formation of complexes of MMA or VAc with these tetrachloride.

These results indicate that halides of group IV elements act as photosensitizers. Further studies of the photopolymerization of vinyl monomers in the presence of various halides are continuing, and full details of the results will be reported at a later date.

References

1. Y. Minoura and Y. Enomoto, *J. Polym. Sci. A-1*, **6**, 13 (1968).

2. Y. Minoura, M. Shundo, and Y. Enomoto, *J. Polym. Sci. A-1*, **6**, 979 (1968).

3. Y. Minoura and H. Toshima, *J. Polym. Sci. A-1*, submitted.

4. S. Makigima, S. Okuno, and E. Hirai, paper presented at 19th Annual Meeting, Japan Chemical Society, 1966.

5. K. Ibonai, paper presented at Nagoya Meeting, Japan Chemical Society, 1964.

6. A. V. Tobolsky, *J. Amer. Chem. Soc.*, **74**, 938 (1952).

7. A. V. Tobolsky and B. Baysal, *J. Polym. Sci.*, **9**, 171 (1952).

8. M. Imoto, T. Otsu, and Y. Harada, *Makromol. Chem.*, **65**, 180 (1963).

9. M. Imoto, T. Otsu, and T. Ito, *Bull. Chem. Soc. Japan*, **36**, 310 (1963).

YUJI MINOURA
HIROYUKI TOSHIMA

Department of Chemistry
Research Institute For Atomic Energy
Osaka City University
Osaka, Japan

Room-Temperature Condensation of N-(Hydroxyalkyl)amine with Carboxylic Acid Ester

INTRODUCTION

It was reported in the previous papers[1-3] that N-(hydroxyethyl)amine reacts rapidly at room temperature with carboxylic acid ester to form an amide compound in the presence of a basic catalyst. Thus, N-(hydroxyethyl)polyamide was obtained from N,N'-(bis-hydroxyethyl)diamine with a carboxylic acid ester in alcohol solution at room temperature.

In this study, the condensation reaction of several N-(hydroxyalkyl)amines with carboxylic acid esters was carried out in order to elucidate the reaction mechanism of the room-temperature condensation reaction.

EXPERIMENTAL

Synthesis of N,N'-(Bishydroxyethyl)alkylenediamines

An aqueous solution of 1 mole of alkylenediamine and 2 moles of ethylene chlorhydrin, each in a concentration of 20% (w/v), was heated at 70°C for 1 hr. The solution was neutralized, and each monomer was then obtained by fractional distillation in vacuum: $HOCH_2CH_2NH(CH_2)_2NHCH_2CH_2OH$, mp 95°C; $HOCH_2CH_2NH(CH_2)_4NHCH_2CH_2$-OH, bp 150°C/3 mm Hg; $HOCH_2CH_2NH(CH_2)_6NHCH_2CH_2OH$, bp 155°C/3 mm Hg.

Polycondensation

N,N'-(Bishydroxyethyl)alkylenediamines and dicarboxylic acid esters were dissolved in ethanol, each in the concentration of 1 mole/l., in the presence of 5 mole-% lithium ethoxide, and the solution was allowed to stand for the desired time of reaction. The white polymer which precipitated from the solution was filtered off, dried, and weighed.

TABLE I

$CH_3(CH_2)_3$-$NH(CH_2)_nOH$	Yield, %	Bp, °C
$n = 2$	48	204–205
$n = 3$	72	218–220
$n = 5$	45	145–150 (16 mm Hg)
$n = 6$	50	155–158 (17 mm Hg)

The ethanol solution was evaporated and the residual polymer was weighed. Solid-phase polycondensation of the alcohol-insoluble polymer was carried out in the presence of 5 mole-% of phosphoric acid at 164°C under vacuum (2 mm Hg). The inherent viscosity of the polymer was determined in concentrated sulfuric acid at 30°C.

Model Reaction of Amide Formation

Several N-(hydroxyalkyl) n-butylamines were synthesized by the reaction of n-butylaldehyde with amino alcohols as shown in eq. (1). The products are summarized in Table I.

$$CH_3(CH_2)_2CHO + NH_2(CH_2)_nOH \rightarrow CH_3(CH_2)_2CH{=}N(CH_2)_nOH \xrightarrow{\text{H}_2}$$
$$CH_3(CH_2)_3NH(CH_2)_nOH \quad (1)$$
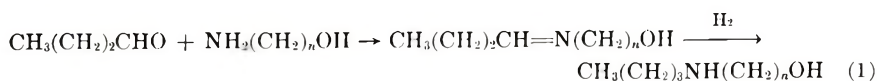
The model reaction of the amide formation between ethyl acetate and N-(hydroxy-alkyl) n-butylamine [eq. (2)], was carried out at 30°C each at a concentration of 1 mole/l., in ethanol in the presence of 5 mole-% lithium ethoxide and the reaction rate was determined by titration in a given period of the reaction.

$$CH_3COOC_2H_5 + n\text{-}BuNH(CH_2)_nOH \rightarrow n\text{-}Bu\overset{\overset{\displaystyle (CH_2)_nOH}{|}}{N}COCH_3 + C_2H_5OH \qquad (2)$$
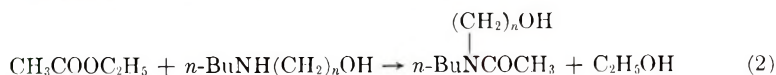
RESULTS AND DISCUSSION

Polycondensation

The polycondensation of N,N'-(bishydroxyethyl)ethylenediamine and ethyl succinate was carried out in ethanol at 0, 30, and 60°C. As shown in Table II, the yield of the polymer was not appreciably affected by temperature, while the polymer of highest inherent viscosity was obtained at 30°C.

TABLE II
Polycondensation of $N,N,'$-(Bishydroxyethyl)ethylene-
diamine and Diethyl Succinate at Various Temperatures[a]

		Alcohol-insoluble polymer	
Temp, °C.	Time, days	Yield, %	η_{inh}, dl/g[b]
0	2	51	0.08
0	4	76	0.08
30	2	49	0.15
30	4	73	0.13
60	2	57	0.13
60	4	77	0.12

[a] Concn., 1 mole/l. in C_2H_5OH; catalyst, C_2H_5OLi, 5 mole-%.
[b] In H_2SO_4 at 30°C.

TABLE III
Polycondensation of N,N'-(Bishydroxyethyl)diamines
and Dicarboxylic Acid Esters[a]

Monomer			Polymer			
Di-amine m	Di-ester n	Catalyst (5 mole-%)	Yield, %		η_{inh}, dl/g[b]	Mp, °C
			Alcohol-soluble	Alcohol-insoluble		
2	2	C_2H_5OLi	—	50	0.13	185–195
2	2	C_2H_5ONa	—	18	0.16	190–195
2	2	C_2H_5OK	—	20	0.18	192–197
2	0	C_2H_5OLi	—	46	0.08	180–190
4	0	C_2H_5OLi	100	0	0.08	Grease
4	2	C_2H_5OLi	100	0	0.08	Grease
6	0	C_2H_5OLi	100	0	0.10	Grease
6	2	C_2H_5OLi	100	0	0.08	Grease
6	4	C_2H_5OLi	100	0	0.06	Grease
6	8	C_2H_5OLi	100	0	0.05	Grease

[a] Concn, 1 mole/l. in C_2H_5OH, 30°C, 65 hr.
[b] In H_2SO_4 at 30°C.

Results of the polycondensation of various N,N'-(bishydroxyethyl)alkylene diamines and dicarboxylic acid esters [eq. (3)] are summarized in Table III, where it is seen that the inherent viscosity of the alcohol-insoluble polymer obtained from the monomer combinations of $m = 2$ and $n = 2$ depends on the catalyst and decreases in the following order: K > Na > Li.

$$CH_2CH_2OH \quad CH_2CH_2OH$$
$$| \qquad\qquad |$$
$$C_2H_5OOC(CH_2)_nCOOC_2H_5 + HN-(CH_2)_m-NH \longrightarrow$$

$$CH_2CH_2OH \quad CH_2CH_2OH$$
$$| \qquad\qquad |$$
$$+CO(CH_2)_nCON-(CH_2)_m-N+ + C_2H_5OH \quad (3)$$
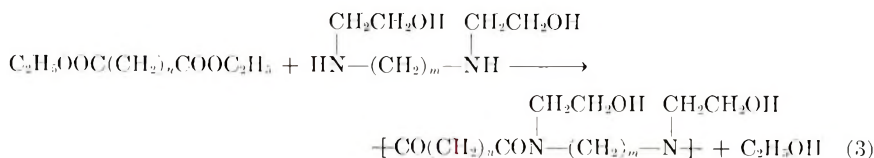
Alkylenediamines with $m = 4$ and $m = 6$ gave only alcohol-soluble and greasy polymers which did not show a distinct melting point.

Solid-Phase Polycondensation

The alcohol-insoluble polymers obtained from N,N'-(bishydroxyethyl)ethylenediamine and dicarboxylic acid esters were heated in the solid phase at 164°C in the presence of 5 mole-% of phosphoric acid under vacuum. Results are shown in Table IV. The prepolymer obtained from N,N'-(bishydroxyethyl)ethylenediamine and methyl succinate gave a high molecular weight polyamide with a melting point of 200–205°C on solid-phase polycondensation. The infrared spectrum of this polyamide is shown in Figure 1.

TABLE IV

$$CH_2CH_2OH \quad CH_2CH_2OH$$
$$| \qquad\qquad |$$
Solid-Phase Polycondensation[a] of $RO+OC(CH_2)_nCON-(CH_2)_2-N+$

	Prepolymer				
R	n	η_{inh}, dl/g[b]	Time (hr.)	η_{inh}, dl/g[b]	Mp (dec), °C
C_2H_5	0	0.08	8	0.10	195–200 (210)
C_2H_5	2	0.13	8	0.16	200–205 (220)
CH_3	2	0.16	4	0.20	200–205 (220)
CH_3	2	0.16	5	0.26	200–205 (220)
CH_3	2	0.16	8	0.30	200–205 (220)
CH_3	2	0.16	17	0.52	200–205 (220)

[a] 164°C/2 mm Hg, catalyst H_3PO_4, 5 mole-%.

[b] In H_2SO_4 at 30°C.

As can be seen in Figure 1, with increasing reaction time, the intensity of the carbonyl absorption at $1720 \ cm^{-1}$ increased and the solubility of the polymer decreased. The polymer did not dissolve, even in concentrated sulfuric acid, after prolonged heating. Therefore, it is presumed that a crosslinking reaction between pendant hydroxyl and end ester groups occurs during the solid-phase polycondensation. All of the polymer decomposed rapidly at temperature above the melting point of the polymer.

Model Reaction of Amide Formation

The rates of the reaction of several N-(hydroxyalkyl)amines with ethyl acetate, each at a concentration of 1 mole/l. were determined at 30°C in ethanol; results are shown in Figure 2.

The reaction rates of N-(hydroxyalkyl)amines with ethyl acetate decreased with increasing number of carbon atoms in the hydroxyalkyl group in the following order: $n = 2 > 3 \gg 5, 6$. The hydroxyl group on the amine nitrogen has an important role in the condensation of amine and ester; particularly N-hydroxyethylated amine underwent condensation with esters at room temperature.
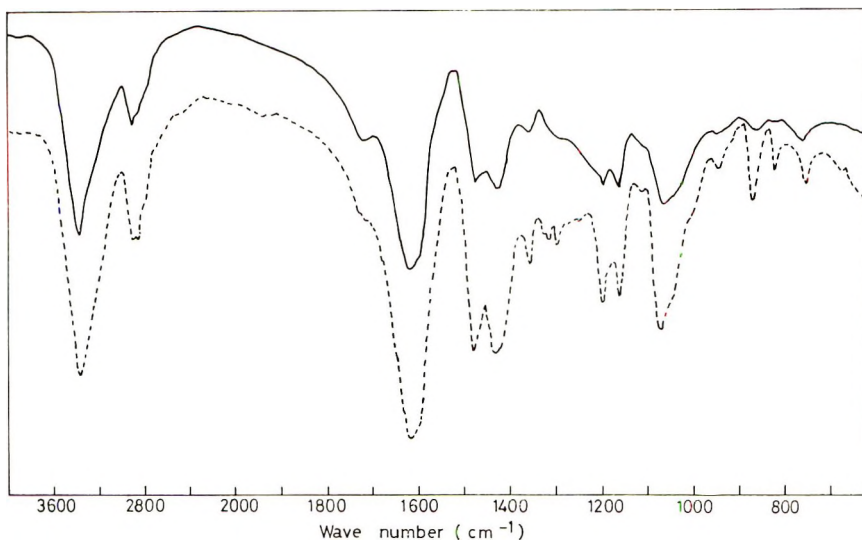
Fig. 1. Infrared spectra of (−) prepolymer and (——) polymer obtained by solid-phase polymerization (H₃PO₄ catalyst, 164°C, 17 hr).
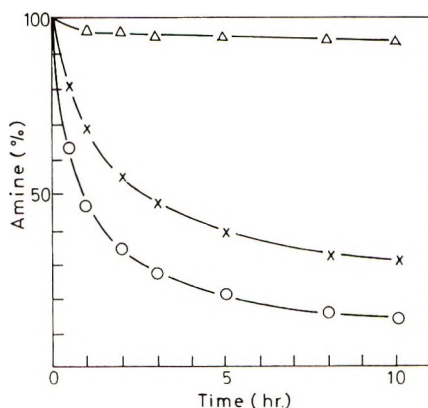
Fig. 2. Reaction of ethyl acetate with various N-(hydroxyalkyl)-n-butylamines: (O) $n = 2$; (×) $n = 3$; (△) $n = 5,6$. Monomer concentrations, 1 mole/l.; in C₂H₅OH at 30°C; catalyst C₂H₅OLi, 5 mole-%.

It is presumed that the room-temperature condensation of N-hydroxyethyl amine with carboxylic acid ester takes place through the reaction scheme (4). Amide formation occurs by an exchange reaction through a cyclic intermediate between N-hydroxyalkyl amine and ester.

$$R-\overset{\overset{\text{O}}{\|}}{\underset{\overset{|}{\text{OR}}}{\text{C}}} + H\overset{\overset{\text{R}'}{|}}{\text{N}}(CH_2)_nOH \xrightarrow{\text{B}^-} R-\overset{\overset{\text{O}}{\|}}{\underset{\overset{|}{\text{OR}}}{\text{C}}} + {}^-O(CH_2)_n\overset{\overset{\text{R}'}{|}}{\text{N}}H \rightarrow$$

$$R-\overset{\overset{\text{O}^-}{|}}{\underset{\overset{|}{\text{OR}}}{\text{C}}}-O(CH_2)_nNHR' \xrightarrow{-RO^-} R-\overset{\overset{\text{OH}}{|}}{\underset{\overset{|}{\text{N}}}{\text{C}}}\underset{\overset{|}{R'}}{\overset{\text{O}}{\diagdown}}(CH_2)_n \rightarrow \quad \underset{R-\overset{\|}{C}-\overset{|}{N}-R'}{O\ (CH_2)_nOH} \tag{4}$$

Termination may occur by an ester-exchange reaction between pendant hydroxyl and ester end groups as shown in eq. (5).

$$\underset{R-NH}{\overset{CH_2CH_2OH}{|}} + R'COOEt \rightarrow \underset{R-NH}{\overset{CH_2CH_2OCOR'}{|}} + EtOH \tag{5}$$

This transformation of the pendant hydroxyl group may disturb the whole reaction, and thus it would be difficult to obtain a high molecular weight polyamide directly by room-temperature polycondensation unless this ester-exchange reaction is completely inhibited by using an appropriate solvent.

References

1. K. Sanui, T. Asahara, and N. Ogata, *J. Polym. Sci. A-1*, **6**, 1195 (1968).
2. K. Sanui and N. Ogata, *Kogyo Kagaku Zasshi*, **70**, 2051 (1967).
3. N. Ogata and K. Sanui, *J. Polym. Sci.*, in press.

K. SANUI
N. OGATA

Department of Chemistry
Sophia University
Chiyoda-Ku
Tokyo, Japan

BOOK REVIEWS

Preparative Methods of Polymer Chemistry, Second Edition. Wayne R. Sorenson and Tod W. Campbell, Eds., Interscience, a division of John Wiley & Sons, Inc., New York, 1968. 504 pp. $15.00.

Polymer synthesis has grown in the past 25 years from a few relatively simple polymer-forming reactions to a large number of quite sophisticated syntheses. The success of these more complex syntheses in terms of molecular weight control, stereo-structure control, and the elimination of side reactions, often depends on subtle changes in reagents and syntheses conditions. The student or chemist wishing to synthesize a polymer was often faced with a lengthy literature search as well as the expenditure of extra time to learn the exact conditions required for successful preparation. The first edition of this book, published in 1961, was a remarkably successful attempt to assemble a number of polymer preparations that had been produced by the authors and their colleagues and friends, and hence were quite reproducible. The second edition has been extensively updated maintaining the quality standards set by the first edition.

Sorenson and Campbell's book interweaves general sections on polymer synthesis and characterization and the scope of the various types of polymer-forming reactions with 434 specific polymer preparations. The general sections give perspective to the preparations. The specific preparations give the directions needed for synthesis of the polymers described as well as giving guidance to the synthesis of homologs. The material is grouped under chapter headings of *Polycondensation and Hydrogen Transfer Polymerization, Addition Polymers from Unsaturated Monomers, Ring Opening Polymerization, Nonclassical Routes to Polymers* and *Crosslinked Synthetic Resins.* This grouping brings together allied polymers so that alternative preparations can be compared. Revisions have been made to each of the chapters. The most extensive revision is to the chapter on *Addition Polymers from Unsaturated Monomers* necessitated by the advances made in coordination and ionic polymerization since the first edition was published. A section on *High Temperature Polymers* has been added and extensive revision of the section on *Block Condensation Elastomers* has been made.

Both students and experienced polymer chemists will find this book a valuable source of polymer preparation information. This reviewer regrets the untimely death of Tod Campbell shortly after this book was completed partly for the reason that polymer chemists cannot look forward to his contributions to a third edition of this book.

J. R. Elliott

Loctite Corporation
705 North Mountain Road
Newington, Conn. 06111

Advances in Polyurethane Technology. J. M. Buist and H. Gudgeon, Eds., John Wiley & Sons, New York, 1969. $12.00.

Advances in Polyurethane Technology is a well organized series of lectures on some of the most important aspects of polyurethane technology. The various chapters are written by a group of British experts from Imperial Chemical Industries Ltd., a company which has played an important role in the early pioneering as well as subsequent technological advances in the field of polyurethanes. Most of the names of the authors, headed by J. M. Buist, are well known for their many technical contributions in this area. The book contains eight chapters: (1) *Isocyanate Reactions: Nature, Control*

and Significance in Manufacture of Polyurethanes, by P. C. Johnson, (2)   *Polyurethane Elastomers* by G. Trappe, (3)   *Relations between Structure and Properties of Polyurethanes* by G. Trappe, (4)   *The Mechanism of Polyurethane Foam Formation* by F. D. Hartley, (5)   *Flexible Foam: Manufacture and Properties* by J. M. Buist, (6)   *Rigid Foams: Manufacture and Properties* by J. M. Buist, R. Hurd, and R. L. Stafford, (7) *The Utilization of Isocyanates in the Surface Coating Industry* by A. Lowe, (8)   *Health Hazards from Isocyanates* by A. Munn.

In addition to references at the close of each chapter, there is a Bibliography at the end of the book listing additional references for various areas of polyurethanes.   In view of the large amount of published literature in the last decade, the number of references are somewhat sparse and this section deserves a better coverage.

As the editors point out in their Preface, the book is not intended to be an all inclusive reference work on all aspects of polyurethanes, but rather aims to stress scientific principles involved in the various branches of polyurethane technology.   Another obvious aim of the editors was to present more recent advances in the respective areas which are covered in the book.

In the opinion of this reviewer both of these goals have admirably been met, and the editors and authors are to be commended in the assemblying and presentation of highly useful and pertinent data in an interesting and clear style.   Of particular value are the structure-property relationships which are treated in several chapters and are well documented by means of numerous experimental data, tables, and figures.   However, it is regrettable that certain important aspects of polyurethane chemistry and technology are not discussed at greater length such as catalysis and more recently developed relationships between chemical structure and flammability characteristics.   At times many of the sections are so short that, although they are well presented, leave the reader avid for additional information on these topics.   There is also an inconsistency with regard to units shown in the various graphs by employing both units of the metric and British systems.

Despite these minor flaws, this reviewer highly recommends this book to any person engaged in research and development of polyurethanes.   It could serve also as a valuable stimulus for future research for investigators in this rapidly growing field of polymers.

<div align="right">*Kurt C. Frisch*</div>

Polymer Institute, University of Detroit
Detroit, Michigan 48221

Carbanions, Living Polymers, and Electron-Transfer Processes.   Michael Szwarc, Interscience Publishers, a division of John Wiley and Sons, Inc., New York, 1968.   695 pp. $25.50.

As in all endeavors, chemistry has its scholars, investigators, craftsmen, prospectors, speculators, adventurers, entrepreneurs, statesmen, and chroniclers whose combined functions give movement and substance to the science.   In the early stages of development of a branch of chemistry occasionally one person integrates some of these activities. But as the field expands, the hard economics of time drive investigators into specialization, both of subject matter and function.   Polymer chemistry, in general, and carbanion chemistry, in particular, are now vast fields with hundreds of practitioners, objectives, techniques, and approaches that range from almost pure physics to synthetic organic chemistry.   Ideally, a monograph possesses enough breadth to encompass a field, enough depth to critically evaluate its current state, and enough insight to anticipate and define the goals of the future.   Ambitious, indeed, is the man who, understanding these things, writes a monograph embracing two vital fields, one of practical and the other of theoretical significance.   Professor Szwarc is such a man, and Carbanions, Living Polymers, and Electron Transfer Processes is such a monograph.   The functions of scholar,

investigator, and chronicler are nicely blended in this book, as are the arts and crafts and theory of physical, organic, and applied polymer chemistry.

Carbon with a partial or full negative charge is the unifying theme, with polymers and their models, the vehicle. The first chapter provides orientation in the general field of anionic addition polymerization and provides a context in which living polymers are placed. The structural, stereochemical, and kinetic problems are stated. The second chapter deals with the environmental factors that control molecular weight and its distribution, and the means by which block and other "tailored" structural features of polymers are generated. Chapter three is concerned with the thermodynamics of carbanion addition and of polymerization. The interplay of techniques and fundamentals is stressed. The next chapter details techniques applicable in kinetic studies of carbanion reactions and most useful from the point of view of extraction of mechanistic information. These four chapters provide a background for discussions of the next several chapters that deal with reaction mechanism. Chapter five is a wide-ranging discussion of ions, ion-pairs, rates of dissociation and association of ions, their structure, their solvation, their reactivities, and their thermodynamic properties. Radical-ions, particularly radical-anions and solvated electrons, are similarly treated in Chapter six, along with electron transfer phenomena. These two chapters build a foundation for the remaining six in which physical-chemical concepts are applied to the anionic polymerization process. Initiation, propagation, copolymerization, and termination are given explicit treatment, as are the special problems encountered with organolithium compounds, both simple and polymeric.

The character of this book springs more from what is found at the paragraph level than in the formal organization. Professor Szwarc is equally conversant with quantum and and molecular models. The concepts and tools of the physical chemist merge with those of the structural organic chemist in many of the chapters. His quest for knowledge of the structure, properties, and reactivities of short-lived ionic species represents a confluence of streams of ideas and techniques to which all the chemical disciplines contribute. Stereochemical and kinetic probes of mechanism stand side by side with spectroscopic and conductivity results obtained on static systems. Equally impressive is the evolutionary flavor that emerges enough times from the print to remind the reader of the historical dimension of chemistry. The enthusiasm of the author for his subject is always in evidence, and his use of words and imagery are pleasing and natural. For example, in discussing changes with temperature of equilibrium constants between contact and solvent-separated ion pairs, the author states: "The same solvent at two different temperatures represents, after all, two different media. For example, tetrahydrofuran at $+25$ and $-70°C$ has different densities, viscosities, dielectric constants, etc. One may say, with some justification, that it is only the label on the bottle that remains the same, but the content is different at different temperatures."

A monograph oriented toward research that draws from so many disciplines must be written by a practitioner of those disciplines, and here the author shines. He knows what he is writing about because he led the way in many of the subjects treated. This is particularly true in his discussions of living polymers and the treatment of ion-pair phenomena. This book should be of value to those investigators who wish to look behind the curtain of empiricism and find the beginnings of a science of anionic polymerization. For creative readers, the book points to many unsolved and intriguing problems. For the scholarly, the book reflects the critical judgment of a talented and seasoned investigator.

Donald J. Cram

Department of Chemistry
University of California
at Los Angeles

Excerpt from Forward of Book entitled, *Carbanions, Living Polymers, and Electron-Transfer Processes.*

Newer Methods of Preparative Organic Chemistry, Volume IV. Ed.,
W. Foerst, Verlag Chemie GmbH, Weinheim/Bergstr., Germany.   1968.
348 pages $15.00.

This volume consists of seven selected reviews written by experts and characterized
by the same high quality and general format as those in the previous volumes.   The
reviews have been brought up to date and expanded, particularly in regard to the num-
ber of detailed experimental procedures, since they first appeared in "Angewandte
Chemie."   Each contribution presents historical material, the scope, limitations and
variations of the synthetic technique, tabular summaries of literature examples, de-
tailed representative procedures, and extensive literature references.   The latter in-
clude pertinent publications up to the period about 1964–67.

The reviews are: (1) α-Additions to Isonitriles.   Triple Additions and Four-Com-
ponent Condensations (I. Ugi).   An illustrative triple addition is the general synthesis
of an α-acyloxy carboxamide *via* the reaction of an isonitrile with a carboxylic acid and
a carbonyl compound (the Passerini Reaction).   The major portion of this review sum-
marizes the "four-component condensation" (or Ugi Reaction)—the condensation of an
isonitrile with an amine derivative, an aldehyde or ketone, and an acid.   Such conden-
sations can be used to generate a variety of product types including amides, thion-
amides and selenomides of α-amino carboxylic acids, 1,5-disubstituted tetrazoles, hydan-
toin and thiohydantoin imides, amides of α-acylamino carboxylic acids, oligopeptide
derivatives, β-lactams, penicillanic acid derivatives, urethanes, diacyl imides, and hy-
drazine derivatives.   (2) Isonitrile Syntheses (I. Ugi, U. Fetzer, U. Eholzer, H. Knup-
fer, and K. Offermann).   Mainly a summary of isonitrile synthesis *via* the dehydration
of N-substituted formamides using phosgene and a tertiary amine.   (3) Reactions of
Sodium Hydrazide with Organic Compounds (T. Kauffmann).   The reagent is a versa-
tile one, affording addition, substitution, reduction or cleavage products with a variety
of substrates.   (4) Ethynation Reactions (W. Ried).   A summary of the addition of
acetylene and terminal alkynes to carbonyl species, particularly quinones.   (5) Syn-
theses with Nascent Quinones (H. W. Wanzlick).   Treatment of hydroquinones with
an oxidizing agent in the presence of a nucleophile affords products viewed as arising
from Michael-type addition of the latter reagent with the quinone produced *in situ.*
(6) Cyclization of Dialdehydes with Nitromethane (F. W. Lichtenthaler).   This con-
tribution describes the syntheses of cyclic nitrodiols and aminodiols *via* the base-cat-
alyzed condensation of nitromethanes with aliphatic, aromatic, and sugar dialdehydes.
(7) The Use of Complex Borohydrides and of Diborane in Organic Chemistry (E. Schen-
ker).   This review, the longest by far in the volume, probably represents the most com-
plete summary of the subject that is currently available.   It covers all aspects of the
subject, has nearly 2 000 literature references, and gives 49 detailed procedures for the
reduction of diverse functional groups and the transformation of organoborane inter-
mediates.

Schenker's review alone makes this volume a particularly valuable reference work for
synthetic organic chemists.

Daniel T. Longone

Department of Chemistry
University of Michigan
Ann Arbor, Michigan 48104

INFORMATION FOR CONTRIBUTORS

This *Journal* Does Not Carry a Page Charge for Contributions

1. Manuscripts should be submitted to H. Mark, Polytechnic Institute of Brooklyn, 333 Jay Street, Brooklyn, New York 11201, or for Part A-1 (Polymer Chemistry) to C. G. Overberger, Department of Chemistry, University of Michigan, Ann Arbor, Michigan 48104, or for Part A-2 (Polymer Physics) to T. G Fox, Mellon Institute, Pittsburgh, Pennsylvania 15213. Address all other correspondence to Periodicals Division, Interscience Publishers, John Wiley & Sons, Inc., 605 Third Avenue, New York, New York 10016.

2. It is the preference of the Editors that papers be published in the English language. However, if the author desires that his paper be published in French or German, it is necessary that a particularly complete and comprehensive English synopsis be furnished.

3. Manuscripts should be submitted in triplicate (one *original*, two carbon copies), typed *double space* throughout and on one side of each sheet only, on a *heavy* grade of paper with margins of at least one inch on all sides.

4. A short synopsis (maximum length 200 words) is required for papers in Parts A-1 and A-2. No synopsis is published for Part B or for "Notes" in Parts A. This synopsis should be carefully prepared, for it is automatically the source of most abstracts. The Synopsis should be a summary of the entire paper; not the conclusions alone.

5. The paper should be reasonably subdivided into sections and, if necessary, subsections. Please refer to any issue of this *Journal* for examples.

6. The references should be numbered consecutively in the order of their appearance and should be complete, including authors' initials and—for unpublished lectures or symposia—the title of the paper, the date, and the name of the sponsoring society. Please compile references on a separate sheet at the end of the manuscript. Abbreviations of journal titles should conform to the practices of *Chemical Abstracts*.

7. Please supply numbers and titles for all tables. All table columns should have an exploratory heading.

8. It is particularly important that all figures be submitted in a form suitable for reproduction. Good glossy photographs are required for halftone reproductions. For line drawings (graphs, etc.), the figures must be drawn clearly with India ink on heavy white paper, Bristol board, drawing linen, or coordinate paper with a very light blue background. The India ink lettering of graphs must be large, clear, and "open" so that letters and numbers do not fill in when reduced for publication. It is the usual practice to submit drawings that are twice the size of the final engravings; the maximum final size of figures for this *Journal* is $4^1/_2 \times 7^1/_2$ inches.

It is the author's responsibility to obtain written permission to reproduce material which has appeared in another publication.

If in doubt about the preparation of illustrations suitable for reproduction, please consult the publisher at the address given above in paragraph 1 and ask for a sample drawing.

9. Please supply legends for all figures and compile these on a separate sheet.

10. Authors are cautioned to type—wherever possible—all mathematical and chemical symbols, equations, and formulas. If these must be handwritten, please print clearly and leave ample space above and below for printer's marks; please use only ink. All Greek or unusual symbols should be identified in the margin the first time they are used. Please distinguish in the margins of the manuscript between capital and small letters of the alphabet wherever confusion may arise (e.g., k, K, κ). Please underline with a wavy line all vector quantities. Use fractional exponents to avoid root signs.

The nomenclature sponsored by the International Union of Chemistry is requested for chemical compounds. Abbreviations should follow the American Chemical Society *Handbook for Authors*. Chemical bonds should be correctly placed, and

double bonds clearly indicated.   Valence is to be indicated by superscript plus and minus signs.

11. Authors will receive 50 reprints of their articles without charge.   Additional reprints can be ordered and purchased by filling out the form attached to the galley proof. Page proofs will not be supplied.

12. No manuscript will be returned following publication unless a request for return is made when the manuscript is originally submitted.

Manuscripts and illustrations not conforming to the style of the *Journal* will be returned to the author for reworking, thus delaying their appearance.

Contents (continued)

BOOK REVIEWS

The *Journal of Polymer Science* publishes results of fundamental research in all areas of high polymer chemistry and physics. The *Journal* is selective in accepting contributions on the basis of merit and originality. It is not intended as a repository for unevaluated data. Preference is given to contributions that offer new or more comprehensive concepts, interpretations, experimental approaches, and results. Part A-1 *Polymer Chemistry* is devoted to studies in general polymer chemistry and physical organic chemistry. Contributions in physics and physical chemistry appear in Part A-2 *Polymer Physics*. Contributions may be submitted as full-length papers or as "Notes." Notes are ordinarily to be considered as complete publications of limited scope.

Three copies of every manuscript are required. They may be submitted directly to the editor: For Part A-1, to C. G. Overberger, Department of Chemistry, University of Michigan, Ann Arbor, Michigan 48104; and for Part A-2, to T. G Fox, Mellon Institute, Pittsburgh, Pennsylvania 15213. Three copies of a short but comprehensive synopsis are required with every paper; no synopsis is needed for notes. Books for review may also be sent to the appropriate editor. Alternatively, manuscripts may be submitted through the Editorial Office, c/o H. Mark, Polytechnic Institute of Brooklyn, 333 Jay Street, Brooklyn, New York 11201. All other correspondence is to be addressed to Periodicals Division, Interscience Publishers, a Division of John Wiley & Sons, Inc., 605 Third Avenue, New York, New York 10016.

Detailed instructions in preparation of manuscripts are given frequently in Parts A-1 and A-2 and may also be obtained from the publisher.